

# *Chapter 1*

## *Introduction*

### **1.1 Eukaryotic cell cycle**

All eukaryotic cells are capable of self-replication in a set of events termed the cell cycle. Non-dividing cells are considered to be in a resting phase termed G<sub>0</sub>. Once a cell is required to duplicate itself, it enters the cell cycle. The cell cycle is composed of four phases: the first growth phase (G<sub>1</sub>), DNA synthesis (S), the second growth phase (G<sub>2</sub>), and mitosis (M), where the newly replicated chromosomes are segregated into two daughter cells (Alberts *et al.*, 2009). Cell cycle progression is driven by sequential activation of cyclins and their cognate kinases (cyclin-dependent kinases - Cdks) in a precise order (Woo and Poon, 2003). Therefore, cell cycle progression comprises a series of critical events that involve complex regulatory mechanisms to ensure duplication and segregation of the genome.

## 1.2 DNA damage

DNA contains the vital genetic information in all living cells. Therefore, its integrity and stability are essential to life. However, it is inevitably vulnerable to damage due to a wide range of endogenous and exogenous agents (Kaufmann and Paules, 1996 ; Clancy, 2008). Exogenous agents, such as ultra-violet (UV) radiation cause the formation of cyclobutane pyrimidine dimers (CPD) and 6-4 photoproducts (PPs) which distort the DNA double helix. This restricts the binding of regulatory proteins to the affected DNA with an impact on replication and transcription (Sinha and Hader, 2002). CPDs and 6-4 PPs are both repaired through a process known as nucleotide excision repair (NER) (Branze and Foiani, 2008).

Moreover, ionizing radiation, including gamma rays and X-rays introduce highly damaging and mutagenic double-strand DNA breaks which also interfere with replication and transcription. Double-strand breaks (DSB) are repaired through one of two mechanisms: non-homologous end joining (NHEJ) or homologous recombination repair (HRR) (Branze and Foiani, 2008). Many chemical agents also damage DNA. For example, chemotherapeutic alkylating agents such as cyclophosphamide and temozolomide result in C·G→T·A transitions that

cause mutations at methylated CpGs dinucleotides during replication (Helleday *et al.*, 2014).

Endogenous agents, free radical species such as reactive oxygen species (ROS) or nitrogen oxide species are generated as by-products of normal cellular metabolism (Hussain *et al.*, 2003). They induce base oxidation and DNA breaks which cause DNA mismatches and replication fork collapse, again resulting in DNA strand breaks (Sancar *et al.*, 2004).

Under attack from endogenous and exogenous agents, cells must be capable of preventing loss or transmission of incorrect genetic information, as errors can and will cause developmental abnormalities, and can result in tumorigenesis.

### **1.3 Replication stress**

Replication stress is defined as the slowing or stalling of replication fork progression and/or DNA synthesis (Zeman and Cimprich, 2014). Replication stress results in loss of genomic integrity arising from a failure to replicate specific regions of DNA, as well as DNA damage resulting from replication fork abandonment.

Replication stress can be generated by obstacles such as a limited supply of replication components (Zeman and Cimprich, 2014).

However, both endogenous (such as spontaneous or enzymatic conversions) or exogenous sources (such as ultra-violet (UV) radiation) also constantly pose a threat to chromosomal stability, resulting in replication progression arrest (Mazouzi *et al.*, 2014). Experimentally, replication stress can be induced by chemical agents such as hydroxyurea (HU). HU inhibits ribonucleotide reductase, the enzyme responsible for catalysing the formation of deoxyribonucleotides from ribonucleotides, which limits the cellular nucleotide pool used in the DNA synthesis (Elledge *et al.*, 1992).

Replication stress usually results in the formation of excess single-stranded DNA (ssDNA) after replication forks have stalled/slowed while the replicative helicase continues to unwind the parental DNA. In the case of destabilised stalled forks, the replication fork can collapse, which results in the formation of double-stranded breaks (DSB) and a DNA damage response (Pacek and Walter, 2004 ; Zeman and Cimprich, 2014).

## **1.4 Cell cycle checkpoint**

Cell cycle checkpoints are surveillance mechanisms to ensure that later events in a cell cycle are not initiated if earlier stages are not completed. In effect they operate to create additional time within a cell cycle phase to enable relevant cellular responses to be completed.

DNA damage and replication stress causes cell cycle arrest via G1/S, intra-S and G2/M phase checkpoints. The nature of the checkpoint effector response depends on the point in the cell cycle at which the checkpoint is activated (Segurado and Tercero, 2009) (Figure 1.1). Importantly, the core of the cell-cycle control system comprises a series of cyclin-Cdk complexes. Cyclin-dependent kinases (Cdks) are serine/threonine protein kinases the enzymatic activity of which is regulated both by post-translational modification, principally phosphorylation, as well as by association with a cognate cyclin. During the cell cycle, the level of any specific Cdk protein normally remains relatively constant, whereas the levels of the relevant cyclin binding partner changes. Therefore, formation of each cyclin-Cdk complex is essential for bringing about the appropriate phase transition during cell cycle progression (Figure 1.2).

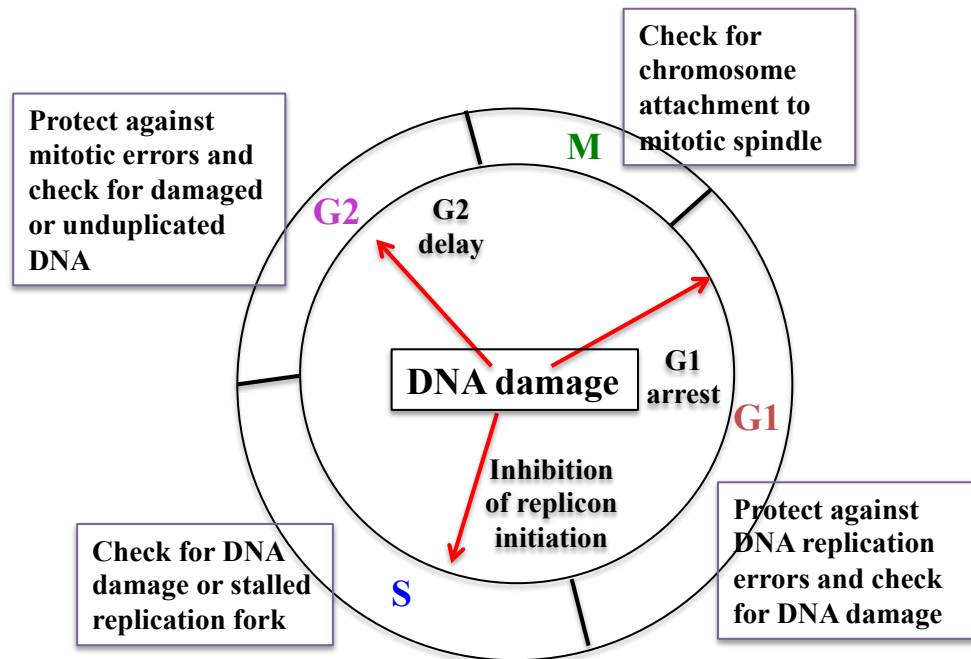


**Figure 1.1** DNA damage-responsive cell cycle checkpoint.

In eukaryotic cells, interphase checkpoints may become activated by the presence of DNA damage at discrete points within the cycle, namely at the G1/S transition, during S phase and the G2/M transition (Kaufmann and Paules, 1996). The first checkpoint operates in late G1 (G1/S checkpoint) to ensure the absence of DNA damage before the cell proceeds into S phase. The intra-S phase checkpoint operates to resolve DNA damage and/or DNA replication errors as they arise within S phase, if necessary slowing the rate of initiation of new replicons (sites of replication initiation), and stabilising stalled replication forks. The third, G2/M checkpoints ensures the absence of any unresolved DNA damage that would prevent successful DNA segregation during

mitosis. If DNA damage is encountered at any point in the cell cycle, the checkpoint machinery overrides the normal cell-cycle system controlling progression. For example, if DNA damage is detected S phase, the G2/M checkpoint will arrest the cell cycle at the G2/M transition until the problem is resolved (Albert *et al.*, 2008).



**Figure 1.2** Cyclin-Cdk complexes of the cell-cycle control system (figure modified from Alberts *et al.*, 2008 ; Hochegger *et al.*, 2008).

Cell-cycle progression is regulated by the sequential activation of cyclin-Cdk complexes, followed by the destruction of the cyclin component. This ensures transition from one phase to another while ensuring directionality of the cycle. The accumulation of specific cyclin-Cdk complexes bring about the transitions at each of the four phases of cell

cycle. Cyclin D-Cdk4 or Cdk6 is the cyclin/Cdk pair controlling G1 progression past the restriction point. Cyclin E-Cdk2 is required to initiate S phase, whereas cyclin A-Cdk1 or Cdk2 is responsible for the beginning of S phase until mitosis. Cyclin B-Cdk1 triggers the early events of mitosis. Each cyclin-Cdk complex phosphorylates a different set of substrate proteins to bring about distinct structural and functional changes required for each cell cycle phase.

#### **1.4.1 G1/S phase checkpoint**

In eukaryotic cells, the transition from G1 into S phase involves passage through the restriction point, after which point the cells are committed to complete one round of replication or, in appropriate circumstances, undergo apoptosis. If unfavourable conditions such as DNA damage, arising either from ionising radiation or UV, or nutrient limitation, the G1/S phase checkpoint arrests cell cycle in G1 phase. G1 arrest is largely dependent on the presence of a functional p53. In the case of DNA damage arising in G1, stabilisation of p53 principally occurs as a consequence of its phosphorylation by members of the PIKK family of protein kinases (ATR, ATM, Chk1 and Chk2) depending on the nature of the genotoxic stress (Appella and Anderson, 2001). p53 acts as a transcription factor to induce the expression of p21<sup>Cip1</sup>,

which is a member of the CKI family of cyclin-dependent kinase inhibitors.

Under normal circumstances, the restriction point is traversed as a consequence of a cyclin E-Cdk2 mediated phosphorylation of Rb, which releases the S phase specific transcription factor E2F, thus allowing the transcription of S phase genes (Bartek and Lukas, 2001). However, in response to DNA damage, p53-mediated accumulation of p21<sup>Cip1</sup> results in the latter binding to, as well as, inhibiting and activating the degradation of cyclin D1, (Agami and Bernards, 2000). The degradation of cyclin D1 leads to a release of p21<sup>Cip1</sup> from Cdk4 and its subsequent binding to, and inhibition of, Cdk2 associated with cyclin E (Poon *et al.*, 1996). This in turn results in the retinoblastoma gene product Rb remaining in a hypophosphorylated state, in which it remains bound to and inhibitory for, the S phase specific transcription factor E2F.

#### **1.4.2 Intra-S phase checkpoint**

This checkpoint operates in cells that are actively undertaking DNA replication. To avoid confusion, I have used this term to define checkpoint responses to genotoxic stress induced DSB and replication arrest during DNA synthesis. The key components of this checkpoint include the ataxia telangiectasia mutated (ATM) signalling cascade,

the single stranded DNA binding protein, replication protein A (RPA), the ataxia-telangiectasia and RAD3 related (ATR) kinase and ATR-interacting protein (ATRIP) complex, the mediator protein claspin, and RAD17 together with the RAD9-RAD1-HUS1 (9-1-1) complex (Bartek *et al.*, 2004 ; Merrick *et al.*, 2004) (Figure 1.3). Targets of the intra-S phase checkpoint include unfired replication origins (thus ensuring that additional replication stress may be avoided), as well as stalled or arrested replication forks (Figure 1.4) Cells lack a functional of intra-S phase checkpoint fail to suppress late origin firing either in response to replication stress or ionising radiation induced DNA damage. In addition, cells fail to stabilise arrested replication forks giving rise to elevated levels of replication fork abandonment (Karnani and Dutta, 2011).



**Figure 1.3** The components of checkpoint sensors involved with ATM and ATR-directed cellular activities (diagram was redrawn from Kastan and Bartek, 2004).

This diagram shows multiple proteins (MDC1, 53BP1, MRN, BRCA1) known to be involved in sensing double strand DNA breaks resulting in conversion of ATM dimers to monomers which are active as kinases. The detection of excess single-stranded DNA induced by replication fork arrest requires Claspin, RAD17 and the 9-1-1 complex for ATR activation. Each pathway leads to cell cycle arrest as well as the specific activation of relevant DNA repair pathways via selective substrate phosphorylation.

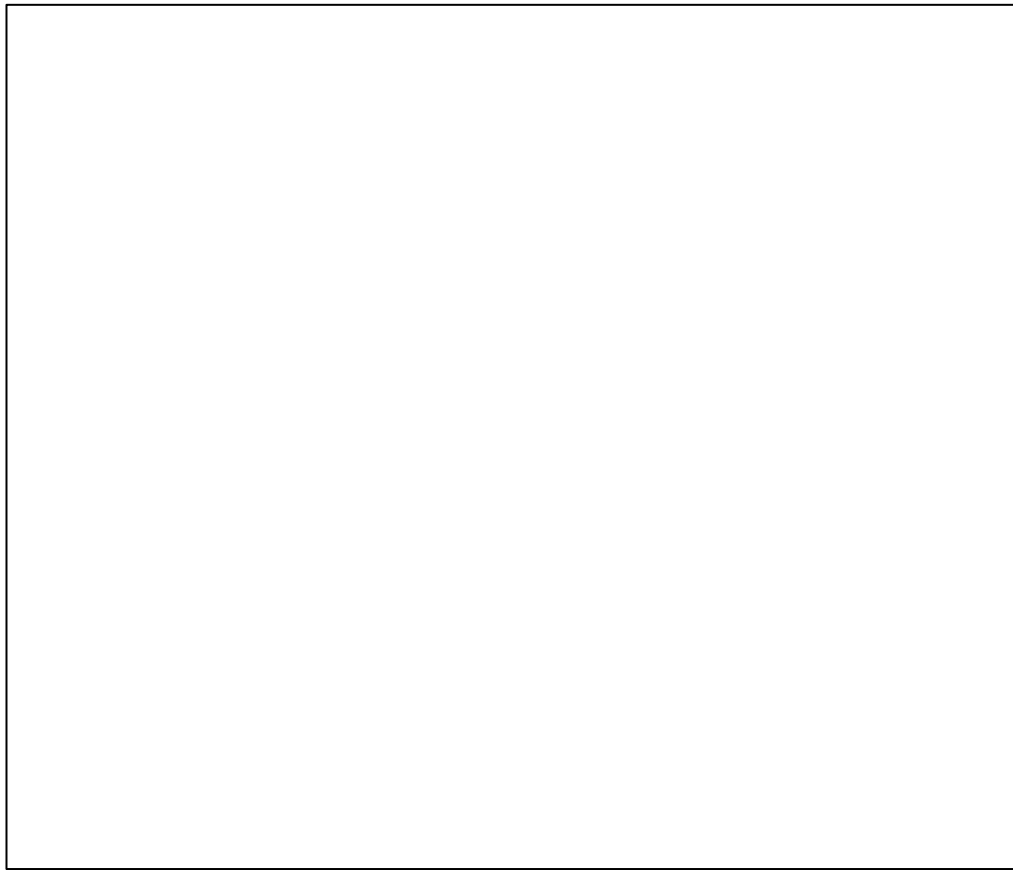


**Figure 1.4** Intra-S phase checkpoint (diagram was modified from Kastan and Bartek, 2004).

The signal pathways ATM/ATR-Chk2/Chk1 also control the checkpoint network in response to DNA damage and replication arrest within S phase. There are two branches of this checkpoint. One of these operates through the faster-operating Cdc25A pathway (Kastan and Bartek, 2004). The ATR/Chk1 modulates the phosphorylation of Cdc25A to maintain the appropriate abundance of Cdc25 in the normal function of unperturbed cells (Bartek *et al.*, 2004). In response to DNA damage and replication arrest, the activity of the Chk1 increases, leading directly to effective down-regulation of Cdc25A and consequently to the inhibition of cyclin E-Cdk2 complexes (Bartek *et al.*, 2004 ; Kastan and

Bartek, 2004). Inhibition of Cdk2 activity prevents the loading of Cdc45 onto chromatin which blocks the initiation of new origin firing (Bartek *et al.*, 2004 ; Kastan and Bartek, 2004). The second intra-S phase checkpoint branch involves ATM-mediated phosphorylation of NBS1 (Nijmegen breakage syndrome 1) (component of MRN complex), and a cohesin protein SMC1 (structure maintenance of chromosome) to prevent replication origin firing (Zhang *et al.*, 2006 ; Saito *et al.*, 2013).

### **1.4.3 G2/M phase checkpoint**

This checkpoint ensures that cells do not initiate mitosis before genome duplication is complete and any arising DNA damage repaired. Failure of this checkpoint results in mitotic catastrophe in which cells that have incompletely replicated DNA attempt mitosis (Bartek *et al.*, 2004). The key target of this checkpoint is the activity of cyclin B-cyclin dependent kinase 1 (Cdk1) complex (Nurse, 1990).

## **1.5 DNA damage response (DDR)**

Interphase checkpoints respond to DNA damage that considered a elements of the cellular DNA damage response (DDR). In theory, there are three component types that comprise interphase checkpoints (Figure 1.5). In reality, the pathways are proving to be more complex (Zhou and Elledge, 2000 ; McGowan and Russell, 2004 ; Polo and Jackson, 2011) with some components having multiple roles within the theoretical framework. The component types are:

1. Sensors that detect aberrant DNA structures
2. Transducers or mediators capable of creating and amplifying a checkpoint signal
3. Effectors or targets that are modified by transducers thus leading to cell cycle arrest, transcriptional induction, DNA repair, senescence, histone mRNA decay or apoptosis.



**Figure 1.5** Schematic outlining the principles of an integrated cellular response to DNA damage or replication stress (figure was modified from Zhou and Elledge, 2000).

Both DNA damage or replication stress generate structures that recruit sensors (such as MDC1, 53BP1, BRCA1), transducers (such as ATM/ATR) and effectors (such as Chk1 and Chk2). The precise combination of activated protein species determines the effector outcomes of the cell as shown in blue boxes. Importantly, while all of the 4 left-most responses are part of a survival response, prolonged activation of checkpoint signalling results in apoptosis.

The pathway by which DNA replication stress induced histone induced histone mRNA decay is still unknown. However, the published observation by Kaygun and Marzluff (2005a) and Smythe group (2007) proposed that members of the phosphatidylinositol 3'-kinase-like kinase (PIKK) family (ATM, ATR and DNA-PK) are involved in the regulation of histone mRNA decay during replication stress (Figure 1.6).

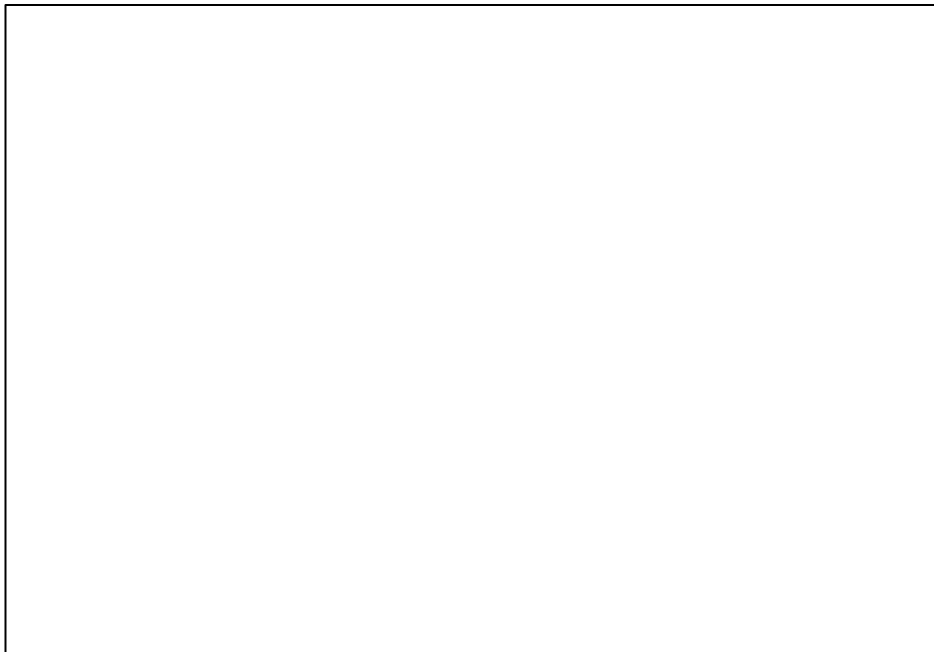


**Figure 1.6** The proposed model for the coordinated regulation of DNA damage and replication arrest-induced histone mRNA decay (figure was redrawn from Muller *et al.*, 2007).

Replication stress activates ATR and Chk1 results in stalled and slowed replication fork via a pathway involving homologous recombination (HR). However, when a replication fork encounters a DNA damage

complex and checkpoint failure, replication fork collapse may occur, generating DNA double-strand breaks. The system that operates to repair such breaks involves ATM-dependent homologous recombination-induced replication restart or via non-homologous end joining (NHEJ) mediated by DNA-PK. The regulation of histone mRNA decay induced by replication stress via ATM/ATR and DNA-PK ensures that there is enough histone production meets the requirement for supply for newly synthesised DNA. Consistent with this model, histone mRNA is destabilised during replication stress. Moreover, the DNA/RNA helicase Upf1, known to be involved in histone mRNA decay (Kaygun and Marzluff, 2005a) may act as an effector of ATR/DNA-PK signalling during the process of histone mRNA decay.

### **1.5.1 DNA damage sensors**

These are proteins that detect the abnormal/aberrant DNA structures and initiate the DDR. In addition to the proteins discussed above, sensors include the PIKKs protein kinases ATM and ATR may also be considered as sensors in addition to their effector role which involves in the C-terminal kinase domain only. These are central components of the checkpoint mechanism that signal the presence of damaged DNA and stalled replication forks respectively.

PIKKs phosphorylate multiple substrates that regulate cell cycle progression, and activate DNA repair pathways (Abraham, 2001). Moreover, the PIKK phosphorylate and activate a pair of downstream checkpoint kinases, Chk1 (in response to ATR) and (Chk2 in response to ATM), that further amplify the initial DDR signalling and diversify the cellular response.

### **1.5.2 Sensing and signalling by ATM**

ATM is required for the cellular response to DNA double strand breaks (DSBs) in response to agents such as ionizing radiation (IR). Mre11-Rad50-Nbs1 (MRN) mediator complex acts as a primary damage sensor and then recruits and activates ATM (Lee and Paull, 2005 ; Berkovich *et al.*, 2007). Phosphorylation of the specific histone H2AX by ATM occurs at DSBs enabling additional mediator protein binding to the DSB-flanking chromatin such as mediator of DNA damage checkpoint (MDC1), p53-binding protein1 (53BP1) and breast cancer type 1 susceptibility protein (BRCA1) (Lee and Paull, 2005 ; Lavin, 2007). In addition to phosphorylation of downstream targets, ATM undergoes autophosphorylation. Moreover, autophosphorylation of ATM occurs in response not only to DSBs but also other forms of chromatin-associated stress. For example, cells exposed to mildly hypotonic buffers

or to chromatin-modifying drugs do not acquire DSBs but nonetheless such treatments lead to rapid autophosphorylation of ATM, suggesting that a change in chromatin structure also stimulates ATM phosphorylation (Bakkenist *et al.*, 2003). The ability of ATM to phosphorylate the downstream kinase Chk2, depends on certain proteins and the region around the damage (Bakkenist *et al.*, 2003). The actual strength and duration of the damage response signal depend on ATM and the continuing presence of damaged DNA (McGowan and Russell, 2004).

### **1.5.3 Sensing and signalling by ATR**

ATR is the principle initiator of the signalling aspect of the DDR in response to stalled replication forks, which arise when cells are exposed to replication inhibitors such as hydroxyurea (HU) or aphidicolin (Feijoo *et al.*, 2002). However, it is also needed for the response to DNA damage, for example, it is required for IR-induced G2 arrest (Cortez *et al.*, 2001). ATR and its molecular partner ATRIP co-function in the activation of downstream checkpoint kinases, mediators and several proteins involved in repair. Both ATR and ATRIP are DNA binding proteins associated with the single-strand binding protein complex, replication protein A (RPA), and do so at sites of

damage or stalled replication forks containing a region of ssDNA (Zou and Elledge, 2003). The ssDNA-RPA complex also recruits and activates the Rad17 clamp loader which then loads the PCNA-related 911 (Rad9-Rad1-Hus1) complex onto DNA (Yang and Zou, 2006). ATR phosphorylates Rad17 and 911, which activates the cascade of downstream responses (Yang and Zou, 2006). In addition, topoisomerase-binding protein1 (TopBP1) also has a role in DNA replication and checkpoint signalling. TopBP1 also binds to the 911 complex and stimulates ATR kinase activity (Kumagai *et al.*, 2006). Claspin is also a mediator protein which coordinates with ATR to effect the efficient activation of Chk1 (Lee *et al.*, 2003). It is noted that ATR activation in response to DSBs appears to require ATM (Myers and Cortez, 2006).

#### **1.5.4 Transducers or mediators**

Transducers are a group of proteins that act directly downstream of the ATM and ATR kinases. They recruit additional substrates to assemble complexes and signal to downstream effectors. To date, multiple transducers such as MDC1, 53BP1, Claspin and BRCA1 (Harper and Elledge, 2007) have been identified (Figure 1.3) Phosphorylation of H2AX on Ser139 by ATM, ATR or DNA-PK

directly recruits MDC1 (Rogakou *et al.*, 1998). MDC1 and H2AX allow the recruitment of many additional factors to sites of damage leading to the generation of IR-induced foci (IRIF). 53BP1 has a role in recombination which coordinates with MDC1 phosphorylation to facilitate the ubiquitination of H2AX at sites of DSBs (Harper and Elledge, 2007).

### **1.5.5 Effectors**

They are the downstream targets regulated by protein kinases to function in cellular processes such as cell cycle arrest, DNA repair, transcription, histone mRNA decay, and apoptosis, thereby preventing genome instability (Zhou and Elledge, 2000). Identified ATM/Chk2 and ATR/Chk1 substrates are not restricted to transducers but also a wide range of proteins involved in multiple DNA repair pathways such as mismatch repair, homologous recombination (HR) and global excision repair (Matsuoka *et al.*, 2007). For example, Chk1 phosphorylation of Rad51 is important for homologous recombination (HR). Thus, checkpoint signalling components have roles in the direct regulation of genomic stability beyond their function in controlling cell cycle. Latterly, a wide range of cellular pathways have been identified to participate in the DDR, including nonsense-mediated decay (NMD),

RNA splicing, spindle checkpoints and histone mRNA decay which point to a much broader role for the DDR in cellular biochemistry and physiology (Figure 1.7) (Harper and Elledge, 2007).

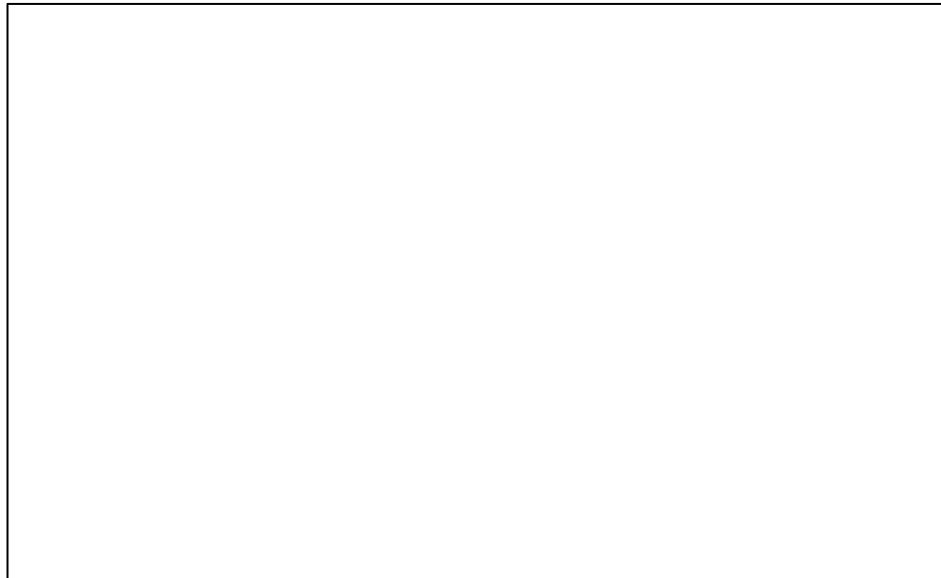


**Figure 1.7** DDR impacts on multiple elements of biochemistry and physiology (figure was redrawn from Harper and Elledge, 2007)

This diagram shows known and newly emerging connections between DDR surveillance systems and normal aging involving cell cycle, DNA repair, apoptosis and senescence. However, histone mRNA decay may be an additional pathway linked to the DDR. This is suggested on the basis of the findings that many DDR response components were found associated with the histone RNA processing machinery. In addition, this study identified changes in the phosphorylation state of a key histone mRNA decay component in response to replication stress. The

identification of the relevant kinase may provide new physiological insights into the links between the DDR and events required to avoid genetic diseases and cancer, while ensuring healthy aging, and development.

## **1.6 Two major repair pathways of DSBs**

### **1.6.1 Homologous recombination (HR)**

HR occurs in S and G2 phases to allow accurate repair of post-replicative DSBs and involves the use of a sister chromatid to provide the templating information to repair DSBs (San Filippo *et al.*, 2008 ; Moynahan and Jasin, 2010). The MRN complex acts as a primary damage sensor which then recruits and activates ATM. Phosphorylation of H2AX by ATM occurs around DSBs which initiates the sequential recruitment of a series of factors starting with MDC1. This triggers the recruitment of chromatin remodelling and modification complexes, which allow the association of downstream factors, such as 53BP1 and BRCA1 (Chapman and Jackson, 2008 ; Spycher *et al.*, 2008). 5'-to-3' nucleolytic processing of DNA ends (resection) is undertaken by the MRN complex (Rupnik *et al.*, 2010) together with other factors such as CtIP, RECQ family helicases and the nucleases Exo1 and Dna2 (Zou and Elledge, 2003 ; Bernstein and Rothstein, 2009). The resulting ssDNA

overhangs are then coated by the ssDNA-binding complex replication protein A (RPA), which consequently recruits ATR. The recombination factors RAD51 and RAD52, ATR kinase and its interacting partners ATRIP, and the DNA-clamp proteins RAD17 and RAD9 then load around the DSBs, (Bekker-Jensen, 2006). Finally, repairing interstrand cross-links takes place. This is especially found at the sites of stalled DNA replication. Then it is the actions of DNA polymerases and DNA end ligation by ligase I following DNA helicases and enzymes for cleavage and repaired DNA molecule.

### **1.6.2 Non-homologous end-joining (NHEJ)**

This system operates at the sites of DNA damage throughout the cell cycle, without the need for a DNA template to ensure accurate re-establishment of genomic integrity. It functions by inducing the direct ligation of broken DNA ends. DNA ends are bound by the Ku70/Ku80 heterodimer, which recruits and activates the DNA-dependent protein kinase catalytic subunits (DNA-PKcs) to form the DNA-PK holoenzyme (Gottlieb and Jackson, 1993).

DNA-PKcs is thought to participate in end bridging during mammalian NHEJ. End processing involves removal of damaged or mismatched nucleotides by nucleases and resynthesis by DNA

polymerases where appropriate. This step is not necessary if the ends have compatibility and have 3' hydroxyl and 5' phosphate termini. DNA ligase IV and its cofactor XRCC4 perform the ligation step of repair. XLF is also required for NHEJ. While the precise role of this protein remains unclear, it interacts with the XRCC4/DNA ligase IV complex and likely participates in the ligation step.

### **1.6.3 Single-strand break repair (SSBR)**

Mostly, SSBs are sensed by poly (ADP-ribose) polymerase 1 (PARP1) which then bind to DNA breaks triggering poly-(ADP-ribosyl)ation of nuclear proteins (Zhou and Elledge, 2000). Downstream of SSB sensing, XRCC1 protein is activated and promotes end-processing, gap filling and ligation (Polo and Jackson, 2011). One of the consequences of this is that it leads to a block in DNA replication and transcription.

After I review cellular responses to SSBs and DSBs in eukaryotic cells, next I will explain how cellular responses to DNA breaks are relevant in a physiological context.

## 1.7 Responses to DNA breaks in a physiological context

When DNA breaks occur, several protein factors and complexes are involved in signalling, the nature, and implications of the aberration, as well as to the relevant repair system. For example, ATM has been reported to mediate local inhibition of both RNA polymerase I- and II-dependent transcription at sites of DNA breaks in human cells (Kruhlak *et al.*, 2007 ; Shanbhag *et al.*, 2010). However, some proteins such as those involved in the transcription machinery are excluded from DDR signalling. Therefore, protein dynamics at DNA breaks during DNA damage and replication arrest operate in both directions: recruited to or dissociating from the sites of DNA breaks (Figure 1.8) (Polo and Jackson, 2011).

The physiological substrate for the DDR machinery in the cell nucleus is chromatin: DNA condensed, protected, and regulated by histone proteins. Although, chromatin acts as a physical barrier to the detection and repair of DNA lesions, there are modifications of chromatin organization that occur in the DDR such as DNA methylation (Kulis and Esteller, 2010), incorporation of histone variants ( $\gamma$ -H2AX) (Bernstein and Hake, 2006), histone post-translational modifications (Kouzarides, 2007) and nucleosome remodelling complexes (Clapier and Cairns, 2009). As a consequence, there are chromatin-associated proteins

which are mobilized to and from sites of DNA breaks, for example, histone deacetylase, HDAC1 and HDAC2, which are recruited to damaged chromatin in response to DNA breaks (Miller *et al.*, 2010) (for review, see Polo and Jackson, 2011).

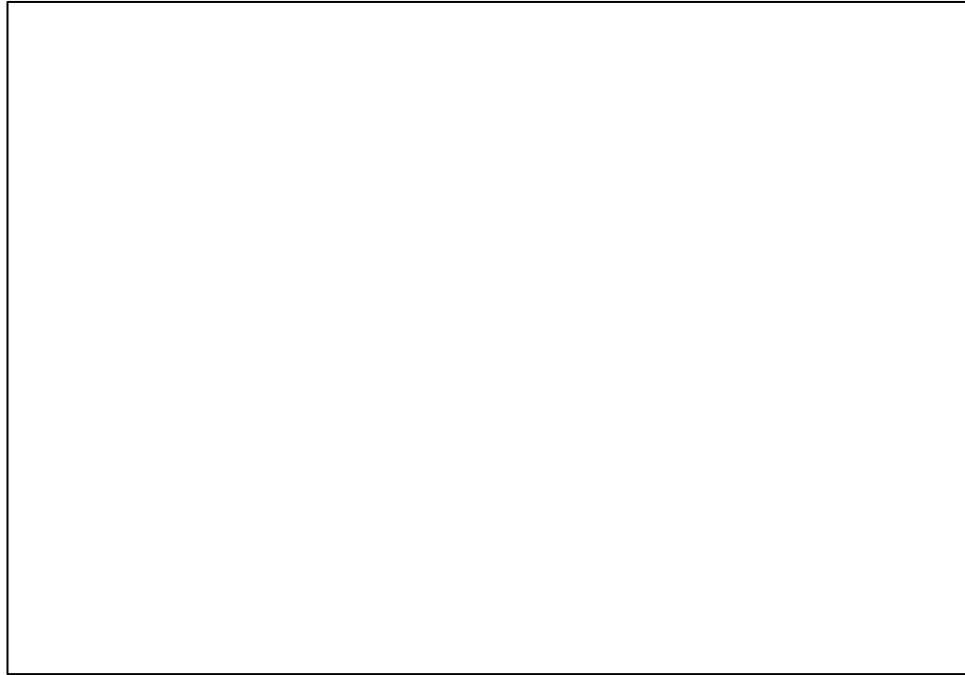


**Figure 1.8** Protein dynamics respond to DNA breaks (picture was redrawn from Polo and Jackson, 2011).

DNA damage checkpoint and repair factors and modulators of chromatin are recruited (red arrows) to DNA breaks (SSB and DSB), while transcription machineries are excluded from DDR foci (green arrow), and the dynamics of structural chromatin components operate in both (pink arrow).

## 1.8 Histones

Histones are basic proteins which are essential for the assembly of chromatin. Newly replicated DNA is wrapped around an octamer of histone molecules to facilitate packaging into chromatin to structure chromosomes in the nucleus during S phase of the cell cycle in all eukaryotes. Unsurprisingly, histones are essential for viability and regulate access to the genetic information contained within the DNA. There are four cores of histone types-H2A, H2B, H3 and H4 with linker histone H1. The structure of histones of H3 and H4 are highly conserved between animal and plant kingdoms ((Maxson *et al.*, 1983 ; Osley, 1991 ; Sarma and Reinberg, 2005). In metazoans, there are multiple copies of histone genes, however, they are categorised into two classes of histone genes.

### 1. Replication-dependent histone genes

These genes encode for the major histone proteins (called replication-dependent histones or canonical histones or histones): H2A, H2B, H3, H4 and H1. The canonical histone genes are clustered in tandemly repeated gene sets, with the repeat unit containing one copy of each of the five histone genes (Marzluff *et al.*, 2008). They are expressed during S phase of the cell cycle to package the newly synthesised DNA into chromosome in nucleus (Kamakaka and Biggins, 2005). Table 1 is a

list of human histone genes (Marzluff *et al.*, 2002 ; <https://en.wikipedia.org/wiki/Histone>)

## 2. Replication-independent histone genes

These genes are known as orphan genes which encode for histone variants. These genes are not restricted in their expression to the S phase but are expressed throughout the cell cycle (Kamakaka and Biggins, 2005 ; Skene and Henikoff, 2013). Therefore, histone variants are expressed and incorporated into chromatin throughout the cell cycle in a replication-independent manner or with special functions/or in a tissue-specific manner (Sarma and Reinberg, 2005). Histone variants can be classified into homomorphous and heteromorphous families depending on the extent of their amino acid sequence which differs from the main canonical histones (Ausio, 2006). Homomorphous variants involve only a few amino acid changes (i.e. H2A.1 and H2A.2; H3.1, H3.2 and H3.3) (Ausio, 2006). Heteromorphous variants involve large changes of the histone molecule (i.e. H2A.X, H2A.Z, macroH2A (mH2A), H2A Barr body-deficient (H2A.Bbd) and centromeric protein A (CENP-A)) (Ausio, 2006). The classification data of histone variants specific features can be found in HistoneDB 2.0 - Variants database (Draizen *et al.*, 2016).

The canonical histone genes lack introns and as expressed contain a unique 3' end of the mRNA which, instead of a poly(A) tail, contains a 26 nucleotide sequence (includes the 5 nucleotides before the stem-loop, the 16 nucleotide stem-loop and the 4-5 nucleotides after the stem-loop) that forms a hairpin structure recognized by stem-loop binding protein (Dominski and Marzluff, 1999 ; Whitfield *et al.*, 2000 ; Marzluff *et al.*, 2008). In mammals, there are approximately 75 distinct canonical histone mRNAs (Marzluff *et al.*, 2002). By contrast, histone variant genes are typically found in single or low copy number. The variant genes contain introns and the transcripts are often polyadenylated (Kamakaka and Biggins, 2005).

**Table 1.1** List of human histone genes.

<b>Histones</b>	<b>Genes</b>
H1	H1F0, H1FNT, H1FOO, H1FX, HIST1H1A, HIST1H1B, HIST1H1C, HIST1H1D, HIST1H1E, HIST1H1T
H2A	H2AFB1, H2AFB2, H2AFB3, H2AFJ, H2AFV, H2AFX, H2AFY, H2AFY2, H2AFZ, HIST1H2AA, HIST1H2AB, HIST1H2AC, HIST1H2AD, HIST1H2AE, HIST1H2AG, HIST1H2AI, HIST1H2AJ, HIST1H2AK, HIST1H2AL, HIST1H2AM, HIST2H2AA3, HIST2H2AC
H2B	H2BFM, H2BFS, H2BFWT, HIST1H2BA, HIST1H2BB, HIST1H2BC, HIST1H2BD, HIST1H2BE, HIST1H2BF, HIST1H2BG, HIST1H2BH, HIST1H2BI, HIST1H2BJ, HIST1H2BK, HIST1H2BL, HIST1H2BM, HIST1H2BN, HIST1H2BO, HIST2H2BE
H3	HIST1H3A, HIST1H3B, HIST1H3C, HIST1H3D, HIST1H3E, HIST1H3F, HIST1H3G, HIST1H3H, HIST1H3I, HIST1H3J, HIST2H3C, HIST3H3
H4	HIST1H4A, HIST1H4B, HIST1H4C, HIST1H4D, HIST1H4E, HIST1H4F, HIST1H4G, HIST1H4H, HIST1H4I, HIST1H4J, HIST1H4K, HIST1H4L, HIST4H4

Histones form complexes with DNA in an invariant 1:1 mass ratio termed nucleosomes. The nucleosome basic structure consists of an octameric core of 4 types of histones (H2A, H2B, H3 and H4) which are presented in equimolar quantities, together with a linker histone H1 which is present at half the stoichiometry of each core histone - around which 147 bp of DNA is wrapped (for review, see Maxson *et al.*, 1983 ; Luger 2003; Khorasanizadeh 2004 ; Sarma and Reinberg, 2005). These histones are assembled into the nucleosome during S phase to compact a newly synthesised DNA into the nucleus (Fransz and de Jong H, 2011). However, histone variants deposition occurs outside of S phase (Kamakaka and Biggins, 2005). Histone variants also forms an octameric core and together with the linker histone, assemble into chromatin. However, the actual variant histones that are assembled and inserted into DNA vary from canonical histones depending on their functional requirements (Kamakaka and Biggins, 2005 ; Ausio, 2006). Core histone variants are the variants of histones H2A, H2B, H3 and H4 (i.e. H2A.1, H2A.2, H3.1, H3.2, H2A.Z, H2A.X, macroH2A, H3.3, CENP-A). The linker histone variants are also variants of histone H1 (i.e. often referred to as histone H1 microheterogeneity) (Brown, 2001 ; Ausio, 2006 ). The main function associated with variants histones is modulation of the chromatin function via post-translational modification

of histone variants, or via alteration of the position and structure of the nucleosomes in order to facilitate various cellular processes (Iizuka and Smith 2003 ; Kamakaka and Biggins, 2005). For example, there are one to two of H2A.X molecules every ten nucleosomes distributed throughout the genome (Ausio, 2006). Upon DSB damage, phosphorylation of H2AX plays a key role in DDR which is required for the assembly of DNA repair proteins at the sites containing damaged chromatin and for activation of checkpoint proteins to arrest the cell cycle progression (Podhorecka *et al.*, 2010).

In my study, I have focused on replication-dependent histones which are vital proteins during DNA replication. Therefore, DNA synthesis is tightly coordinated with histone synthesis either under normal conditions or in circumstances of DNA damage. Accordingly, the regulation of histone genes is required to co-ordinate histone production with ongoing DNA replication. Inhibition of DNA synthesis results in a rapid repression of histone gene expression and down regulation of histone mRNA levels (Zhao, 2004).

Cells operate a surveillance mechanism called histone mRNA decay (HD). HD is regulated to prevent harmful effects of inappropriate levels of histone accumulation. Excess histone accumulation leads to

increased DNA damage and genomic instability which are associated eventually with malignancy (Osley, 1991 ; Muller and Schumperli, 1997 ; Dominski and Marzluff, 1999).

## **1.9 Histone gene regulation during the cell cycle**

As indicated previously, histone production is largely restricted within S phase coupled to the period of DNA synthesis. Increased histone synthesis in S phase is a consequence of the regulatory mechanisms controlling histone gene expression at both transcriptional and posttranscriptional levels. The transcription of histone genes occur within the nucleus in the histone locus body (HLB), a subnuclear organelle containing factors required for histone pre-mRNA processing (Ma *et al.*, 2015).

The expression of multiple histone genes on S phase entry is regulated by phosphorylation of nuclear protein ataxia-telangiectasia locus (NPAT or p220) by cyclin E/cdk2 (Ma *et al.*, 2000 ; Zhao *et al.*, 2000 ; Zhao, 2004). After cyclin E/cdk2 activity has reached its peak in early S phase, it decreases due to the degradation of the cyclin E component, preventing further activation of NPAT until cyclin E re-accumulates in the next cell cycle.

Histone gene transcription increases three to fivefold as cells enter S phase (late G1) and decreases by the end of S phase or when DNA replication is arrested (Nelson *et al.*, 2002). The half-life of histone gene transcripts has been estimated as 40-60 min., but it dramatically decreases to ~10 min. at the end of S phase, and DNA replication is arrested (Ewen, 2000).

### **1.10 Histone mRNAs**

The rate of histone synthesis is largely regulated by the level of histone mRNAs. Histone mRNAs are encoded by replication-dependent histone genes which lack introns and end in a conserved 26 nucleotide sequence structure (Dominski and Marzluff, 1999). Endonucleolytic cleavage of pre-mRNA is the only process that produces unique mature replication-dependent histone mRNAs with no poly (A) tails, ending in a conserved stem-loop structure in their 3' untranslated (UTR) region (Sanchez and Marzluff, 2002) (Figure 1.9). It is likely that the stem-loop operates as the functional homologue of a poly (A) tails for nuclear export, translation, and stability of mRNA.

The sole protein that binds, in a highly specific interaction, to the conserved 16 nucleotide sequence of stem-loop histone mRNA, is the histone binding protein/stem-loop binding protein (HBP/SLBP)

(Marzluff and Duronio, 2002). Importantly, HBP/SLBP is involved in every steps of histone mRNA metabolism: histone transcription, pre-mRNA processing (Dominski *et al.*, 1999), nucleo-cytoplasmic transport (Sullivan *et al.*, 2009), translation (Sanchez and Marzluff, 2002) and histone mRNA degradation (Townley-Tilson *et al.*, 2006).

At the beginning of S-phase, the level of histone mRNA rapidly increases with half-life of approximately 40 min. By the end of S-phase it decreases to a half-life of ~10 min (Harris *et al.*, 1991). The coupling of histone synthesis with DNA replication regulated via steady state histone mRNA concentrations occurs via the regulation of HBP/SLBP (hereinafter referred to as SLBP).

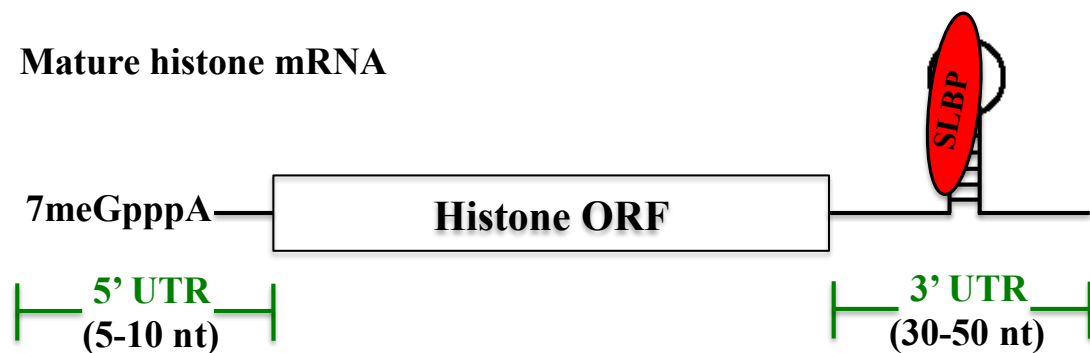


**Figure 1.9** Structure of histone mRNA

Histone mRNA has short 5' and 3' UTRs. At the 3' UTR, it contains 30-50 nucleotide sequence with the conserved 26 nucleotide sequence that includes the 5 nucleotides before the stem-loop, the 16 nucleotides stem-loop and the 4-5 nucleotides after the stem-loop.

## **1.11 Histone binding protein (HBP) or Stem-loop binding protein (SLBP)**

### **1.11.1 Human SLBP**

The human SLBP (hSLBP) gene (NM\_006527) is composed of eight exons on the short (p) arm of chromosome 4 at region 1 band 6. It encodes a protein of 270 amino acids (Q14493) with molecular mass 31 kDa (Martin *et al.*, 1997). This is in contradiction to the estimated molecular mass obtained by SDS-PAGE involved mobility shift assay (Wang *et al.*, 1996). Two bands of 40 and 45 kDa are observed in both nuclear and polyribosome enriched fractions (Wang *et al.*, 1996). It is possible that there are two forms of SLBP that could result either from post-translational modification or from proteolysis. This is consistent with the observations associated with mobility shift analyses in which doublets are regularly observed (Wang *et al.*, 1996).

The protein SLBP consists of three important regions: N-terminal TAD domain, the central RNA-binding domain (RBD)/L-motif and C-terminal domain (Martin *et al.*, 2000 ; Jaeger *et al.*, 2004 ; Jaeger *et al.*, 2005) (Figure 1.10).

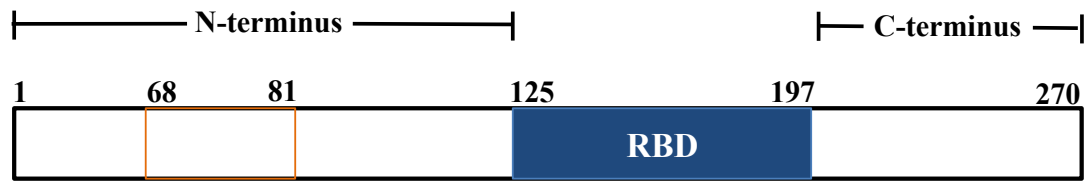


**Figure 1.10** Structure of human SLBP.

Two important domains are the RNA binding domain (RBD) at C-terminus and translation activation domain (TAD) at N-terminus.

The N-terminal region contains a short segment of ~14 amino acid residues. This transactivation domain (TAD) at amino acids 68-81 is essential for the activation of histone mRNA translation, and includes a highly conserved motif, DWX3VEE (Cakmakci *et al.*, 2008). The TAD is located near known N-terminal phosphorylation sites (von Moeller *et al.*, 2013). Importantly, SLIP1 or MIF4G (SLBP-binding protein 1 or middle domain of initiation factor 4G) interacts with this highly conserved motif (Cakmakci *et al.*, 2008). The activation of SLIP1 interacts with SLBP may form a bridge to cooperates, either directly or indirectly, with the eIF3 or eIF4G translation initiation complex (Gorgoni *et al.*, 2005 ; Cakmakci *et al.*, 2008 ; Neusiedler *et al.*, 2012 ; von Moeller *et al.*, 2013).

The RNA binding domain (RBD) of SLBP (amino acid 125-197) is the only region of SLBP conserved among diverse metazoans (Caenorhabditis elegans, Drosophila, and vertebrates) (Wang *et al.*, 1996 ; Pettitt *et al.*, 2002). Previous structural studies found that the RBD region of SLBP folds on binding the histone RNA stem-loop with a highly stable complex and the SLBP-histone mRNA complex functions as an integral unit (Zhang *et al.*, 2012 ; Thapar, 2014). The first stem loop binding site involves Glu129-Val158 and second binding site Arg180 and Pro200 which are bound to the stem-loop structure of histone mRNA, regulated by threonine phosphorylation and proline isomerization in a conserved TPNK sequence that lies between the two binding sites (Zhang *et al.*, 2012). The phosphorylation of the motif TPNK of both the human and Drosophila SLBP RBD is proposed to increase the stability and proper folding of the SLBP-histone mRNA complex (Zhang *et al.*, 2014). However, the C-terminal region is flexible in the protein:RNA complex and does not contact the RNA (Zhang *et al.*, 2014). This is consistent with in solution NMR studies, which found that SLBP RBD is intrinsically disordered in the absence of RNA in solution (Zhang *et al.*, 2012 ; Thapar, 2014). Importantly, SLBP is natively unfolded in the free state (Thapar *et al.*, 2004). The RBD and

the C-terminal regions of SLBP are involved in 3' end processing (Dominski and Marzluff, 2001).

The crystal structure of hSLBP in complex with other proteins has been determined by Tan and colleagues (2013) who reported that SLBP RBD forms a ternary complex with histone mRNA stem-loop and 3'-5' exonuclease (3'hExo/Eri-1) also binding to histone mRNA stem-loop which is required for histone mRNA degradation. However, there is no direct contact between SLBP and 3'hExo in the ternary complex. It is likely that both proteins help each other to induce structural changes in the loop so as to bind with other proteins (Tan *et al.*, 2013 ; Zhang *et al.*, 2014).

SLBP is an RNA binding protein that is regulated within the cell cycle by both translational and post-translational mechanisms (Whitfield *et al.*, 2000 ; Zheng *et al.*, 2003). SLBP is synthesized just before the entry into S phase and is imported into the nucleus by the importin  $\alpha$ -importin  $\beta$  transport factors (Erkman *et al.*, 2005). SLBP is present both in nucleus, and in the cytoplasm on the polyribosomes (Martin *et al.*, 1997; Whitfield *et al.*, 2004 ; Hanson *et al.*, 1996). SLBP binds to the stem loop at the 3' end of histone mRNA which coordinates the histone biosynthesis and cell cycle (Marzluff, 1992).

The disruption of the interaction between the SLBP-histone mRNA complex by stem-loop mutations causes mRNA retention in the nucleus, and a decrease in processing efficiency both *in vivo* and *in vitro* (Sun *et al.*, 1992 ; Pandey *et al.*, 1994 ; Williams *et al.*, 1994 ; Dominski *et al.*, 1999). Therefore, the formation of the SLBP-histone mRNA complex plays a pivotal role in maintaining cell-cycle regulation of histone levels in eukaryotic cells.

Taken together, the data obtained from structural and functional analysis have shown that SLBP is a key protein binding to histone mRNA stem-loop for histone mRNA metabolism including histone transcription, pre-mRNA processing, nucleo-cytoplasmic transport, translation and histone mRNA degradation.

### **1.11.2 SLBP and replication-dependent histone mRNA metabolism**

#### **1.11.2.1 Transcription**

The initiation of histone gene expression is activated by the phosphorylation of transcription factor p220<sup>NPAT</sup> (NPAT) by cyclin E/Cdk2 prior to entry into S phase, as well as the initiation of DNA replication by cyclin E/cdk2 activating cdc6 (Ma *et al.*, 2000 ; Zhao *et al.*, 2000 ; Ye *et al.*, 2003 ; Koseoglu *et al.*, 2010 ; Lunn *et al.*, 2010).

Cyclin E/Cdk2 is an essential cyclin-dependent kinase that coordinates multiple aspects of the transition from G1 to S phase. These aspects include activation of E2F1, which is a major S phase transcription factor and required for expression of many S phase genes expression. The components of replication-dependent histone gene expression are regulated in histone locus body (HLB) by concentrating the required protein complexes and RNA components at the histone gene locus (Nizami *et al.*, 2010 ; Morimoto and Boerkoel, 2013).

#### **1.11.2.2 Pre-mRNA processing**

The regulatory properties at the histone mRNA 3' end impact the rate of histone protein synthesis, histone stoichiometry, and the timing of histone synthesis during the cell cycle. At late G1, the histone mRNA processing efficiency increases 10-fold (Harris *et al.*, 1991). Changes in 3' end affect histone mRNA metabolism including mRNA processing, localization or translation, that lead to alterations in histone protein abundance. Therefore, eukaryotic cells must tightly regulate the balance between the amounts of newly synthesised DNA and the rates of histone protein synthesis so as to regulate proper chromatin assembly during the cell cycle (Marzluff and Duronio, 2002 ; Marzluff *et al.*, 2008). Taken together, posttranscriptional regulation of histone gene expression

is a critical element in coupling to DNA replication and involves pre-mRNA processing, translation and mRNA stability control.

Formation of the histone mRNA 3' end required two *cis*-acting elements in the pre-mRNA. One is the 26 nucleotide stem-loop sequence in the 3' untranslated region (3'UTR) of histone mRNA, which remains part of the mature mRNA after pre-mRNA processing. The second element is a purine-rich downstream element (HDE) located 3' to the cleavage site, which is cleaved during the processing (Marzluff, 1992). Each of these sequences recruits factors that produce the single endonucleotic cleavage between stem-loop and HDE required for mature histone mRNAs (Dominski and Marzluff, 2007) (Figure 1.11).

The *trans*-acting factors are the small ribonucleoprotein particle (U7 snRNP), SLBP and a heat-labile processing factor (HLF) (Schaufele *et al.*, 1986 ; Gick *et al.*, 1987 ; Bond *et al.*, 1991 ; Wang *et al.*, 1996 ; Martin *et al.*, 1997 ; Walther *et al.*, 1998). The small ribonucleoprotein particle (U7 snRNP), containing U7 snRNA and a heptameric ring of Sm, Lsm10 and Lsm11 proteins, interacts with the histone pre-mRNA by hybridisation via base pairing between the HDE and the 5' end of U7 snRNA (Bond *et al.*, 1991 ; Dominski *et al.*, 1999 ; Pillai *et al.*, 2001 ; Azzouz *et al.*, 2005 ; Pillai *et al.*, 2003). HLF and novel zinc finger protein (hZFP100) interacts with the U7 snRNP (Dominski *et al.*, 2002 ;

Azzouz *et al.*, 2005 ; Wagner *et al.*, 2006) and SLBP binds to stem-loop histone mRNAs (Wang *et al.*, 1996 ; Martin *et al.*, 1997).

Importantly, histone genes lack introns. Therefore, the processing of histone pre-mRNA requires only endonucleolytic cleavage which occurs at the end of a conserved ACCCA sequence following the stem-loop (Gick *et al.*, 1986). Following processing, the downstream cleavage product is degraded by 5'-3' exonuclease activity (Walther *et al.*, 1998). The N-terminal region of Lsm11 interacts with the N-terminal region of FLICE-associated huge protein (FLASH) which recruits the histone pre-mRNA cleavage complex (HCC) including CPSF73 (and its homologue CPSF100) and the scaffolding protein symplekin (a key component of HLF) to form the cleavage complex involved in histone mRNA 3' end processing (Dominski *et al.*, 2005 ; Kolev and Steitz, 2005 ; Sullivan *et al.*, 2009 ; Yang *et al.*, 2009). Recently, the splicesomal U2 snRNP has been identified in the processing of the intronless histone mRNAs by stimulating U7-dependent histone pre-mRNA processing (Friend *et al.*, 2007). After processing, only SLBP remains bound to the stem-loop (Dominski *et al.*, 1995) (Figure 1.12).

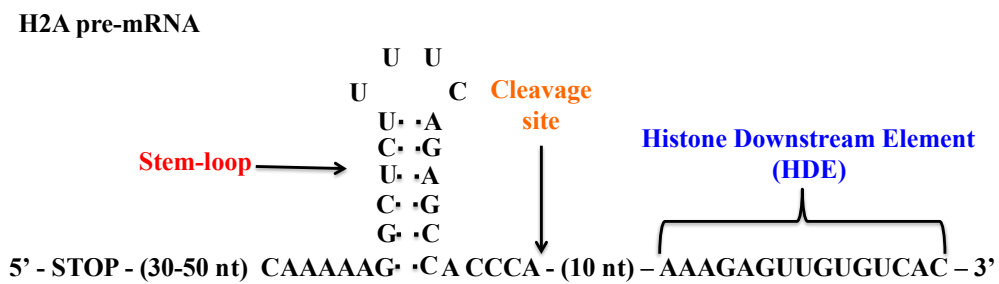


**Figure 1.11** Structure of histone pre-mRNA

The structure of histone pre-mRNA contains the conserved stem-loop sequence, the cleavage site and HDE. For the formation of a mature histone mRNA, it requires only endonucleolytic cleavage is required. This occurs at the cleavage site in the 3' untranslated region between two conserved cis-acting elements, the highly conserved hairpin structure and the purine-rich spacer element in order to form a mature histone mRNA.

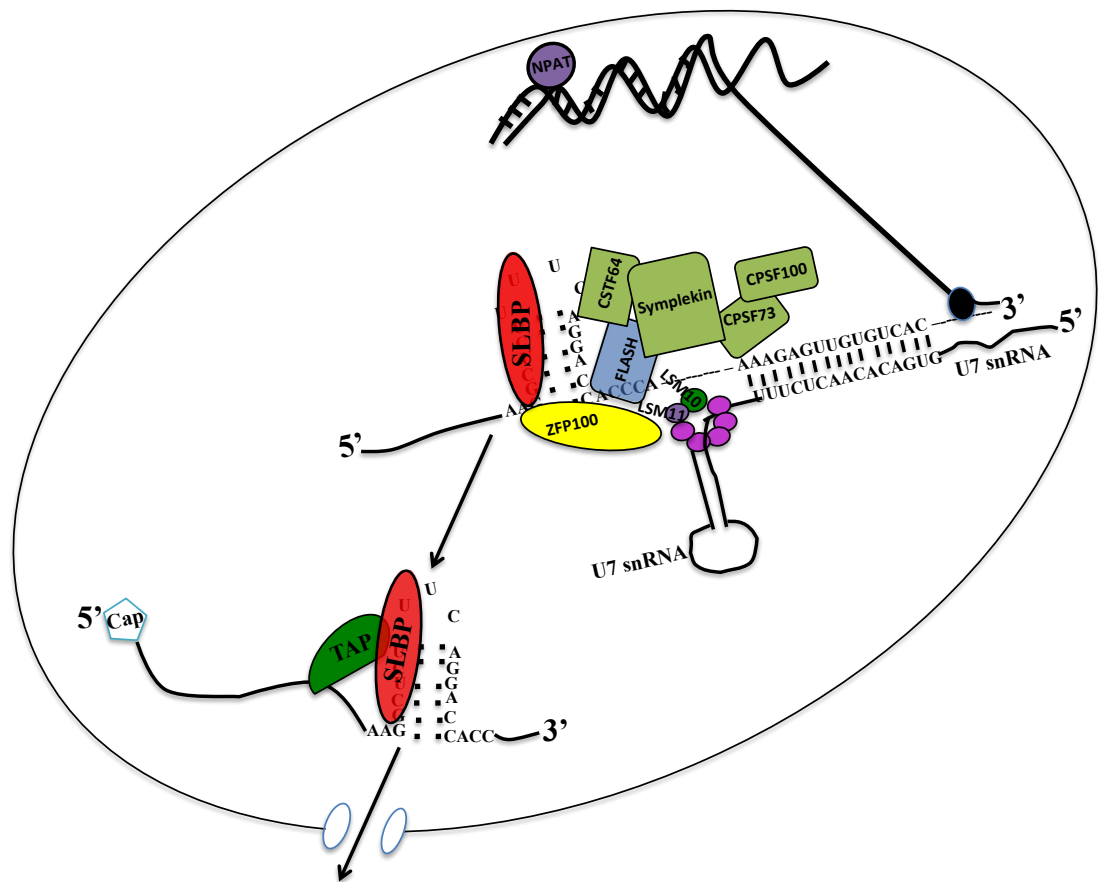


**Figure 1.12** Histone mRNA metabolism

Histone mRNAs are up-regulated at the G1/S boundary as a result of phosphorylation of NPAT by CyclinE/Cdk2. A cleavage complex containing CPSF73, CPSF100, symplekin and CSTF64 is recruited to cleave the pre-mRNA. Within this complex, endonucleolytic cleavage by CPSF73 as directed by the U7 snRNP produces the mature histone mRNA. The U7 snRNP contains a heptameric ring of five Sm proteins and two U7 snRNP-specific Sm-like proteins, LSM10 and LSM11. LSM11 contacts ZFP100 and FLASH, which also interacts with the

SLBP-stem-loop complex. Export from the nucleus to the cytoplasm occurs in a TAP dependent manner.

### **1.11.2.3 Export**

SLBP is imported into the nucleus by the importin  $\alpha$ - importin  $\beta$ -transport factors (Erkman *et al.*, 2005). The mature histone mRNP with bound SLBP is rapidly exported to the cytoplasm via the canonical mRNA transport factor TAP (Erkman *et al.*, 2005 ; Huang *et al.*, 2003). However, it was reported that nuclear cap binding complex (CBC) (two main subunits CBC20 and CBC80) links to the 5' end of intronless transcripts connecting SLBP for mRNA export (Muller-McNicoll and Neugebauer, 2013).

### **1.11.2.4 Translation**

Accumulation of histone mRNA is a result of an increase in the rate of histone gene transcription and the efficiency of histone pre-mRNA processing. SLBP is also required for the regulation of histone mRNA translation and is found on polysomes in the presence of an intact stem-loop (Sanchez and Marzluff, 2002 ; Gorgoni *et al.*, 2005). The protein accompanies the mature mRNA to the cytoplasm as a component of the histone messenger ribonucleoprotein particle (mRNP), where

it plays a role in translation of the mRNA (Sanchez and Mazluff, 2002).

Histone mRNA stem-loop is necessary for translation efficiency as well as the stability of the mRNA, and like the poly (A) tails which use to stimulate translation *in vivo* (Gallie *et al.*, 1996). This function is mediated by SLBP, which stimulates cap-dependent translation initiation factors: the CBP80/20-dependent translation initiation factor (CTIF), CBC with translation initiation factors, eIF4F, eIF4E eIF4G and eIF3 (Ling *et al.*, 2002 ; Lejeune *et al.*, 2004). The cap structure of histone mRNAs is bound by either CBC or eIF4E (Maquat *et al.*, 2010 ; Choe *et al.*, 2013). Moreover, the CTIF, which is localised in cytoplasmic side of nuclear envelope, binds to CBP80 in the mRNA being exported (Kim *et al.*, 2009). The CBP80-CTIF complex then recruits eIF3 which, in turn, recruits the small subunit of ribosome (40S) to initiate the first round of translation in the cytoplasm (Ishigaki *et al.*, 2001).

Recently, SLBP Interacting Protein 1 (SLIP1) has been shown to be a histone mRNA-specific translation initiation factor (Cakmakci *et al.*, 2008). The SLBP-SLIP1 complex assembles on the 3'UTR region of histone mRNA to regulate its translation by bridging the 5' and 3' ends of histone mRNA bound by eIF4E/eIF4G and SLBP leading histone mRNA to a closed-loop configuration (Ling *et al.*, 2002 ; Gorgoni *et al.*, 2005 ; Nicholson and Muller, 2008 ; Neusiedler *et al.*, 2012).

The resultant multicomponent complex includes the SLBP-SLIP1-histone mRNA ternary complex is exported to the cytoplasm where it stimulates translation of histone mRNAs. In the cytoplasm, SLBP is an inactive unphosphorylated form due to the formation of an SLBP-SLIP1 heterotetramer complex that cannot bind other histone mRNAs. It is thought that the assembly of the SLBP-SLIP1 complex facilitates SLIP1's protection of SLBP from proteolytic degradation machinery in the cell (Bansal *et al.*, 2013). At the end of S phase, SLBP needs to be in an inactive form that involves removal of SLBP from the histone 3'UTR. This is achieved by dephosphorylation at T171 in the highly conserved TPNK sequence by phosphatase PP2A acting in concert with the prolyl isomerase Pin1 and, resulting in dissociating of the SLBP-SLIP1 heterotetramer to the SLBP-SLIP1 heterodimer (Krishnan *et al.*, 2012). SLBP dissociates from the histone mRNA prior to histone mRNA degradation in the cytoplasm by the exosome-mediated degradation. The phosphorylation of Thr171 is required for efficient import of SLBP into the nucleus (Krishnan *et al.*, 2012). SLBP is eventually phosphorylated at Thr60 and Thr61 by cyclin A/Cdk1 to trigger SLBP degradation by the ubiquitin proteasome system at the end of the S phase as well as histone mRNAs are degraded (Zheng *et al.*, 2003 ; Koseoglu *et al.*, 2008 ; Krishnan *et al.*, 2012). The control of SLBP polyubiquitination is

required Pin1 which may regulate SLBP phosphorylation at the N-terminus at Ser20 and Ser23 (Krishnan *et al.*, 2012).

## **1.12 Regulation of histone mRNA during the mammalian cell cycle**

Cell cycle progression is driven by a class of protein kinases, the cyclin-dependent kinases (Cdks), which are involved at different stages of cell cycle transition. The initiation of DNA replication requires the activation of Cyclin E/cdk2 (Sanchez and Dynlacht, 2005). Cyclin A/Cdk2 activity is required for continued progression through S phase (Yam *et al.*, 2002). The progression through mitosis requires the activation of Cyclin B/cdk1 which induce nuclear envelope breakdown resulting in chromosome condensation (Hara *et al.*, 2012).

The replication of DNA is coupled to histone synthesis in order to provide enough histones to newly replicated DNA. When DNA replication is complete, the accumulation of histone protein must stop quickly. The biosynthesis of histone is started with the up-regulation of histone gene transcription. This is activated by the phosphorylation of the transcription factor p220<sup>NPAT</sup> (NPAT) by cyclin E/Cdk2 prior to entry into S phase, as well as the initiation of DNA replication by cyclin E/cdk2 activating cdc6 (Ma *et al.*, 2000 ; Zhao *et al.*, 2000 ; Ye *et al.*,

2003 ; Koseoglu *et al.*, 2010). The level of histone mRNA concentration is rapidly increased at the beginning of S phase with half-life approximately 40 min and fall down at the end of S phase with a short half-life 10 min (Harris *et al.*, 1991) (Figure 1.13).

The function of SLBP results in the formation of mature histone mRNAs. It is unsurprising therefore that cell cycle controls signal to regulate SLBP levels appropriately. SLBP is kept low in G1 phase to limit histone mRNA processing and histone mRNA production (Whitfield *et al.*, 2000 ; Zheng *et al.*, 2003) which is controlled by simultaneous synthesis and degradation at G1-phase involving two mechanisms:

(1) low translational efficiency of SLBP mRNA (Whitfield *et al.*, 2000)

(2) proteasome mediated degradation (independent of S/G2 degradation mechanism) of SLBP in G1-phase (Djakbarova *et al.*, 2013).

At late G1/beginning of S phase, the levels of SLBP increase 10- to 20-fold after induction of cyclin E (Marzluff and Duronio, 2002 ; Marzluff *et al.*, 2008). This is proposed to be the main reason for the increase in transcription of replication dependent histone genes, increase in histone mRNA processing efficiency and finally accumulation of

histone mRNAs in S-phase (Harris *et al.*, 1991 ; Whitfield *et al.*, 2000 ; Zheng *et al.*, 2003 ; Marzluff *et al.*, 2008). However, the level of SLBP mRNA does not significantly change throughout the cell cycle (Whitfield *et al.*, 2002). At the end of S phase, SLBP is rapidly degraded as it is targeted for proteasomal destruction following phosphorylation of Thr61 by cyclin A/cdk1. This primes the phosphorylation of Thr60 by CK2 to stop histone mRNA processing, resulting in a rapid decrease in histone mRNA levels (Whitfield *et al.*, 2000 ; Zheng *et al.*, 2003 ; Koseoglu *et al.*, 2008 ; Koseoglu *et al.*, 2010).

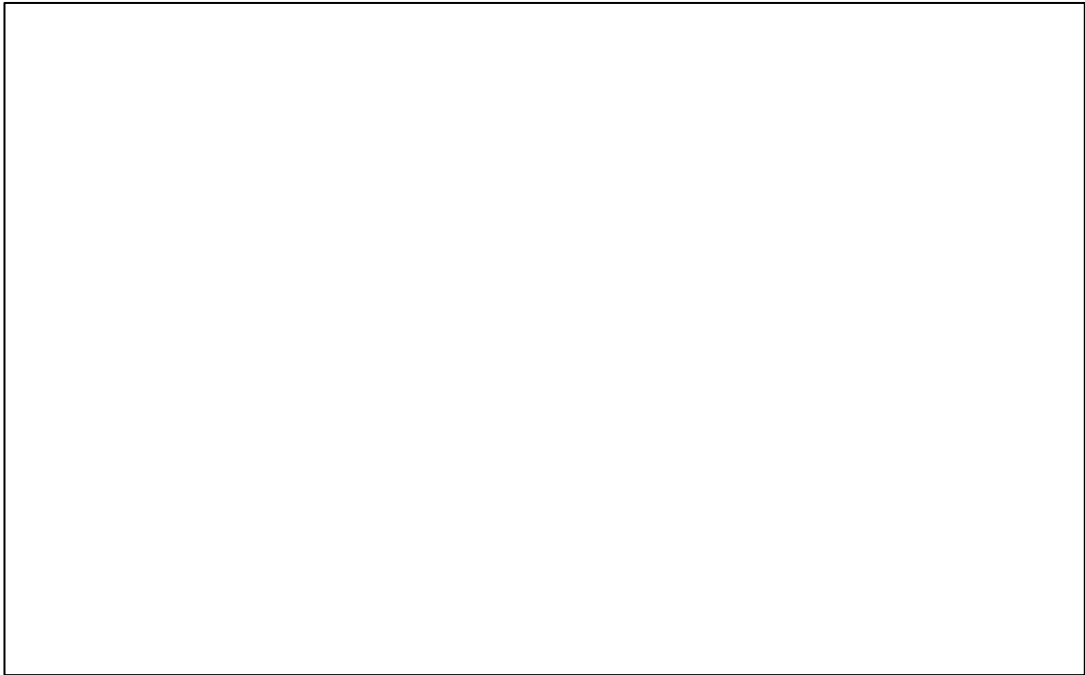


**Figure 1.13** Schematic diagram for the regulation of histone mRNA and SLBP throughout cell cycle (picture was redrawn from Marzluff *et al.*, 2008).

The changes in levels of histone mRNA, SLBP and SLBP mRNA during the cell cycle. CyclinE/Cdk2 activation leads to phosphorylation of NPAT and likely translation of SLBP mRNA, resulting in histone mRNA accumulation. At the end of S phase, histone mRNA and SLBP are degraded. However, under DNA synthesis inhibition, only histone mRNA decay happens but SLBP is still stable.

### **1.13 Histone mRNA decay**

Histone mRNA decay is the key regulation step operated by a system to monitor histone accumulation and eventually promote the degradation of histone mRNA at the end of S phase. Therefore, histone mRNA decay is likely to be a surveillance mechanism during S phase of cell cycle.

Most cellular mRNA decay is effected by a multi-protein complex termed the exosome, which brings about 3'-5' exonucleolytic degradation. Histone mRNA decay is a translation-dependent process and requires 3' oligouridylation, decapping of the mRNA and both 5'-3' and 3'-5' nucleases that include exosome components (Mullen and Marzluff, 2008).

Histone mRNA decay also occurs when DNA synthesis is inhibited, resulting in a rapid repression of histone gene expression (Marzluff *et al.*, 2008) and S phase arrest (Nelson *et al.*, 2002). Histone gene expression appears to be one target of the intra S phase checkpoint. In support of this notion, replication stress-induced histone mRNA decay is blocked in the presence of inhibitors of checkpoint signalling (Kaygun and Mazluff, 2005a ; Muller *et al.*, 2007). However, replication stress does not induce histone mRNA decay via destabilisation and proteolytic destruction of SLBP, because the protein SLBP remains to be detected

after prolonged periods of replication stress (Kaygun and Mazluff, 2005c).

To date, there are two models have been proposed to explain how histone mRNA degradation occurs under DNA damage and replication stress.

The first model suggests the binding of Up-frameshift protein 1 (Upf1) to histone mRNP or the ribosome is the critical step in triggering histone mRNA degradation (Kaygun and Marzluff, 2005b). The phosphorylation of Upf1 and/or SLBP by specific replication stress or double-strand breaks activated transducer Ataxia telangiectasis and Rad3 related (ATR) or DNA-dependent protein kinase (DNA-PK) (Muller *et al.*, 2007 ; Kaygun and Marzluff, 2005a), results in (1). Upf1 binds to histone mRNP via SLBP or (2). Upf1 binds to the stalled ribosome due to the alteration of histone mRNP and modification of SLBP and/or translation release factors (eRFs).

Moreover, there are two ways to initiate histone mRNA degradation

(1). Upf1 binds to the decapping complex (Dcp1/Dcp2) and the Xrn1 5'-3' exoribonuclease, which are involved in degrading mRNA from its 5' end (Kaygun and Marzluff, 2005b).

(2). The recruitment of Upf1 stimulates the specific recruitment of the terminal uridylyl transferases (TUTases) which oligouridylate to 3' mRNA end. The Lsm 1-7 complex binds this tails and recruits decapping complex (Dcp1/Dcp2) to remove the 5' cap of the mRNA (Coller *et al.*, 2001). Then mRNA is degraded from 5' - 3' by the Xrn1 exoribonuclease or degraded from 3' - 5' exonuclease by exosome components (Mitchell *et al.*, 1997). Moreover, recent data finds that 3'hExo selectively degrades oligouridylated histone mRNAs (Dominski *et al.*, 2003 ; Mullen and Marzluff, 2008 ; Hoefig *et al.*, 2013).

The second model (Figure 1.14) proposes that direct interacting of cap-associated initiation proteins (CBC or CBP80/20) with SLBP is the critical step in triggering histone mRNA decay (Choe *et al.*, 2013). In eukaryotic translation, CBC-bound mRNAs are precursors of eIF4E-bound mRNAs in cytoplasm (Lejeune *et al.*, 2002 ; Maquat *et al.*, 2010). In the nucleus, the cap structure of newly synthesised mRNAs-bound CBC is exported from the nucleus to cytoplasm. During or after mRNA export with the action of importin  $\alpha/\beta$  in a translation-independent manner, the CBC is replaced by eIF4E in cytoplasm (Sato and Maquat, 2009). The pioneer round of translation of CBC-bound mRNAs begins with the cap-bound CBC recruits CTIF by direct interaction, then CBP80-CTIF at the 5' end of mRNA recruits the eIF3

complex and the small subunit of ribosome (40S) is recruited to that complex (Ishigaki *et al.*, 2001 ; Kim *et al.*, 2009 ; Maquat *et al.*, 2010). However, the recruitment of CTIF towards the 5' end of mRNA by CBC may occur in the nucleus or during mRNA export.

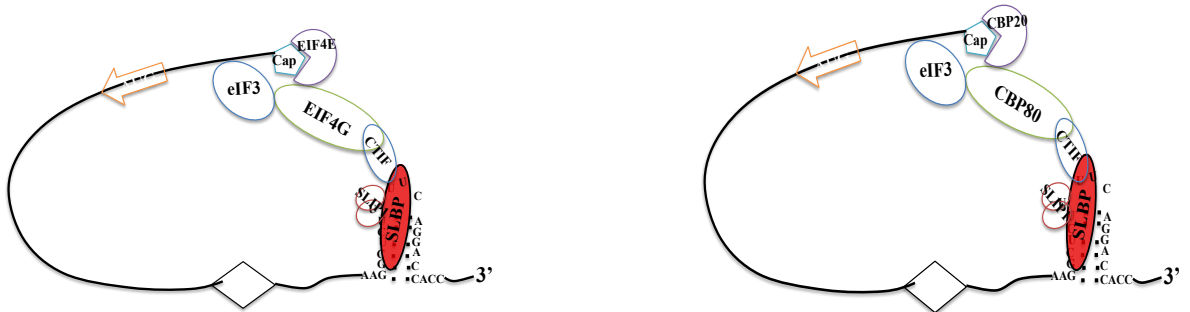
Under replication stress, the replication-dependent histone mRNP switch from an actively translating mode to an mRNA degrading mode. SLBP is likely to interact with CBP80/20-dependent translation (CT) complex as a CT initiation factor (CTIF)-interacting protein, but not with the eIF4E-dependent translation (ET) complex. The translational function of SLBP normally requires eIF4E, eIF4G and eIF3 (Ling *et al.*, 2002). When cells encounter DNA damage or replication stress, remodelling of histone mRNP to CT complex results in weak interaction of SLBP-eIF4GI/II or SLIP1-eIF4GI/II. The role of the 3'hExo may only decrease the stimulation of translation but it is not involved in histone mRNA degradation in mammalian cells (Mullen and Marzluff, 2008) or *Drosophila* (Kupsco *et al.* 2006).

Moreover, there is the competition between CTIF and Upf1 for SLBP binding which Upf1 interacts with SLBP more strongly upon the inhibition of DNA synthesis, promoting the release of CTIF and eIF3 from SLBP containing histone mRNP (Choe *et al.*, 2014). In addition, hyperphosphorylation of Upf1 recruits PNRC2 and SMG5 to trigger

decapping and then the histone mRNA degradation by 5'-to-3' degradation (Choe *et al.*, 2014).

However, the molecular details and signalling pathway which cause the remodelling of CBP80/20-bound histone mRNP to trigger histone mRNA degradation are currently unknown.

**A. eIF4E-dependent translation (ET)    B. CBP80/20-dependent translation (CT)**



**C. The recruitment of Upf1**

**D. Histone mRNA degradation**

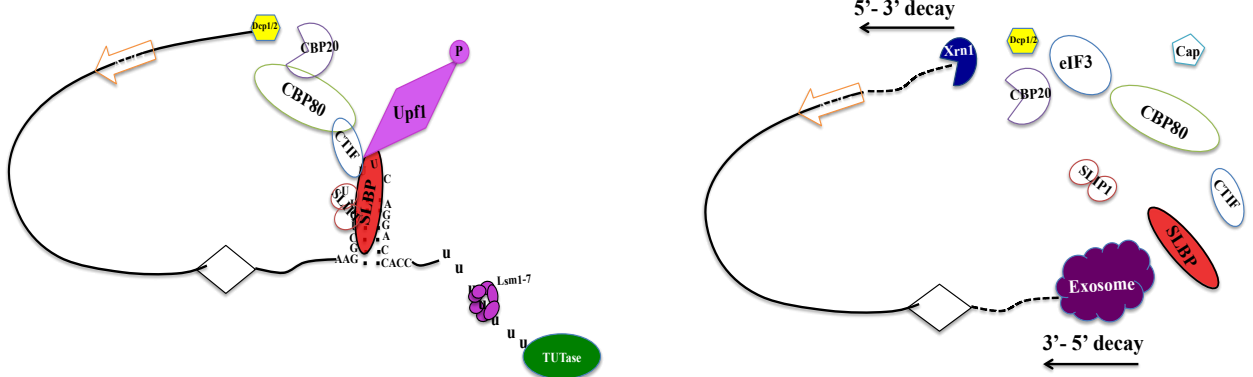


**Figure 1.14** Proposed model of histone mRNA degradation and possible pathways for initiate histone mRNA degradation under DNA damage and replication stress.

Histone mRNA degradation normally occurs on (A) mRNA undergoing eIF4E-dependent translation, but under DNA damage and replication arrest, translation largely occurs would be replaced by CBP80/20 (B) CBP80/20-dependent translation. (C) The initiation of histone

mRNA degradation involved the recruitment of a Upf1 and oligouridylation of the 3' end of histone mRNA. Lsm1-7 binds to the oligo (U) tail, promoted by Lsm4 binding to the SLBP and 3'hExo. **(D)** Subsequently the histone mRNA can be degraded both directions, 3' to 5' or 5' to 3' degradation.

### **1.14 Connection between histone mRNA degradation and the cell cycle checkpoints**

Histone mRNA degradation is a regulatory step to ensure proper histone mRNA levels at the end of S phase and after the inhibition of DNA synthesis.

Muller and colleagues (2007) reported that the phosphorylation activity of ATR and DNA-PK but not ATM is required for histone mRNA degradation after DNA replication arrested.

Phosphorylation of Upf1 is thought to be a crucial step in histone mRNA degradation through the interaction with SLBP. The serine/glutamine motifs (SQ motifs) and threonine/glutamine motifs (TQ motifs) of Upf1 are phosphorylated by phosphatidylinositol-3-kinase-related protein kinase (PIKK) family (Yamashita *et al.*, 2001). However, the relative important of this pathway is unknown.

### **1.15 SLBP phosphorylation and known functions** (Figure 1.15)

The expression of histone gene begins at Histone Locus Body (HLB) which contains factors required for processing histone mRNAs (Nizami *et al.*, 2010). Phosphorylation of T171 is necessary for recruitment of SLBP to the stem-loop to the site of histone pre-mRNA processing in the nucleus. During S phase, SLBP remains phosphorylated at T171 and accompanies the histone mRNP to the cytoplasm for histone mRNA translation. At the end of S phase, dephosphorylation of SLBP in its RNA binding domain by Pin1 and a phosphatase remove SLBP from the 3' UTR, resulting in histone mRNA decay via exosome-mediated mRNA degradation and subsequent ubiquitination proteasomal degradation of SLBP. The degradation of SLBP at the end of S phase is mediated by phosphorylation at Thr60 and Thr61 by cyclinA/Cdk1 (Zheng *et al.*, 2003). The released SLBP in the cytoplasm may return to the nucleus for recycling or degradation. Additionally, the phosphorylation of Ser 20 and Ser 23 may be control SLBP polyubiquitination by proteasomal degradation acting as a phosphodegron (by exposing amino acids, Ser 20 and Ser 23, this phosphorylation may reveal important portions of SLBP sequence that participates in, regulation of SLBP degradation rates) during S phase.

Importantly, the kinases that phosphorylate SLBP at Ser 20, Ser 23 and Thr 171 remain unknown (Krishnan *et al.*, 2012).

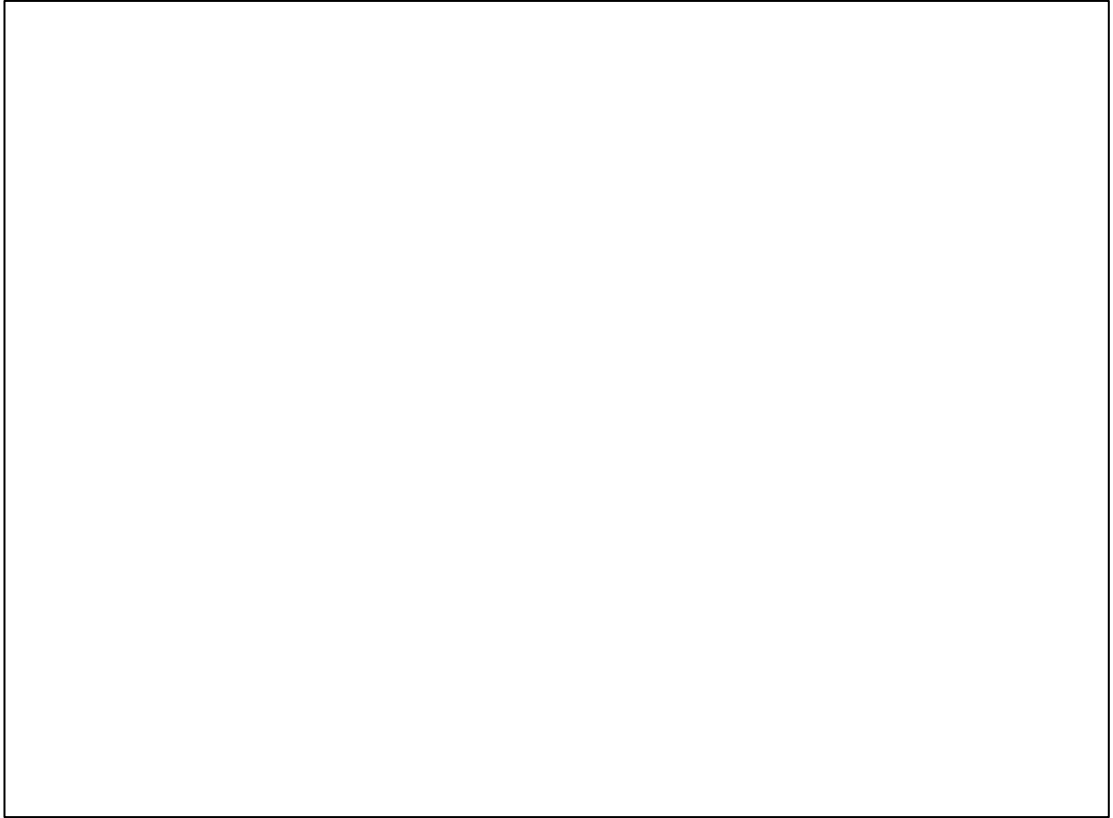


**Figure 1.15** The model between SLBP and histone mRNA decay during S phase and at the end of S-phase (figure was redrawn from Krishnan *et al.*, 2012).

## **1.16 Mass spectrometry(MS)-based quantitative proteomics using stable isotope labelling by amino acids in cell culture (SILAC)**

Mass spectrometry (MS) has increasingly become the method of choice for study of complex protein samples especially MS-based quantitative proteomics for analysis of protein-protein interactions, post-translational modification (PTM) and protein profiling etc. (Aebersold and Mann, 2003 ; Dephoure *et al.*, 2012).

Applying proteomics to protein interactions has advantages compared to two-hybrid and chip-based approaches. The protein or modified protein itself can serve as a bait to isolate its binding partners as multicomponent complexes in the native environment and cellular location using affinity-purification approach followed by MS (Aebersold and Mann, 2003 ; Dunham *et al.*, 2012). However, the purification step is important to allow specific isolation of the protein of interest and its partners and the concomitant reduction in complexity is less challenging for MS analysis (Dunham *et al.*, 2012).

So far, MS-based quantitative proteomics using SILAC develop the study of stable or transient protein interactions and its partners using accurate quantification of SILAC analysed by MaxQuant computational

platform (Cox *et al.*, 2009). The stable-isotope ratios distinguish between the protein composition of two or more protein complexes (Bantscheff *et al.*, 2007 ; Ong and Mann, 2007 ; Boulon, 2012). For example, in the case of a sample containing a complex and a control, the method can distinguish between true complex and nonspecific components or in the case of complexes isolated from cells at different conditions/states, the method can identify the dynamic changes in the composition of protein complexes at that conditions/states (Aebersold and Mann, 2003 ; Park *et al.*, 2012).

There have been many studies looking for RNA-RNA and RNA-protein interactions in different biological targets such as RNA nuclear exosome complex (Lubas *et al.*, 2011), mRNA export (Gebhardt *et al.*, 2015) and nucleolar dynamics under stress conditions. However, the study of histone mRNA degradation focusing on SLBP under DNA damage and replication arrest has not previously been elucidated.

## 1.17 References

- Abraham, R.T. 2001. Cell cycle checkpoint signalling through the ATM and ATR kinases. *Gene Dev.* 15: 2177-2196.
- Aebersold, R. and Mann, M. 2003. Mass spectrometry-based proteomics. *Nature.* 422(6928): 198-207.
- Agami, R. and Bernards, R. 2000. Distinct initiation and maintenance mechanisms cooperate to induce G1 cell cycle arrest in response to DNA damage. *Cell.* 102(1): 55-66.
- Alberts, B., Johnson, A., Bray, D., Hopkin, K., Johnson, A.D., Lewis, J., Raff, M., Roberts, K. and Walter, P. 2009. The Cell Cycle. In *Essential Cell Biology*. 3rd ed. New York: Garland Science, Taylor and Francis Group, LLC. 609-612.
- Alberts, B., Johnson, A., Lewis, J., Raff, M., Roberts, K. and Walter, P. 2008. The Cell Cycle. *Molecular biology of the cell*. 5rd ed. New York: Garland Science, Taylor and Francis Group, LLC. 1053-1114.
- Appella, E. and Anderson, C.W. 2001. Post-translational modifications and activation of p53 by genotoxic stresses. *Eur J Biochem.* 268(10): 2764-2772.
- Ausió, J. 2006. Histone variants—the structure behind the function. *Brief Funct Genomics.* 5 (3): 228-243.

- Azzouz, T.N., Gruber, A. and Schumperli, D. 2005. U7 snRNP-specific Lsm11 protein: Dual binding contacts with the 100 kDa zinc finger processing factor (ZFP100) and a ZFP100-independent function in histone RNA 3'end processing. *Nucleic Acids Res.* 33: 2106-2117.
- Bakkenist, C.J., Kastan, M.B. 2003. DNA damage activates ATM through intermolecular autophosphorylation and dimer dissociation. *Nature.* 421: 499-506.
- Bansal, N., Zhang, M., Bhaskar, A., Itotia, P., Lee, E., Shlyakhtenko, L.S., Lam, T.T., Fritz, A., Berezney, R., Lyubchenko, Y.L., Stafford, W.F. and Thapar, R. 2013. Assembly of the SLIP1-SLBP complex on histone mRNA requires heterodimerization and sequential binding of slbp followed by SLIP1. *Biochemistry,* 52(3): 520-536.
- Bantscheff, M., & Schirle, M., Sweetman, G., Rick, J. and Kuster, B. 2007. Quantitative mass spectrometry in proteomics: a critical review. *Anal Bioanal Chem.* 389: 1017-1031.
- Bartek, J., Lukas, C. and Lukas, J. 2004. Checking on DNA damage in phase. *Nat Rev Mol Cell Biol.* 5(10): 792-804.

- Battle, D.J. and Doudna, J.A. 2001. The stem-loop binding protein forms a highly stable and specific complex with the 3' stem-loop of histone mRNAs. *RNA*. 7: 123-132.
- Bekker-Jensen, S., Lukas, C., Kitagawa, R., Melander, F., Kastan, M.B., Bartek, J. and Lukas, J. 2006. Spatial organization of the mammalian genome surveillance machinery in response to DNA strand breaks. *J. Cell Biol.* 173: 195-206.
- Berkovich, E., Monnat, R.J. Jr and Kastan, M.B. 2007. Roles of ATM and NBS1 in chromatin structure modulation and DNA double-strand break repair. *Nat Cell Biol.* 9: 683-690.
- Bernstein, E and Hake, S.B. 2006. The nucleosome: a little variation goes a long way. *Biochem Cell Biol.* 84(4): 505-517.
- Bernstein, K.A. and Rothstein, R. 2009. At loose ends: resecting a double-strand break. *Cell.* 137(5): 807-810.
- Bond, U., Yario, T.A. and Steitz, J.A. 1991. Multiple processing defective mutations in a mammalian histone messenger RNA are suppressed by compensatory changes in U7 RNA both in vivo and in vitro. *Genes & Dev.* 5: 1709-1722.

- Borchers, C.H., Thapar, R., Petrotchenko, E.V., Torres, M.P., Speir, J.P., Easterling, M., Dominski, Z., Marzluff, W.F. 2006. Combined top-down and bottom-up proteomics identifies a phosphorylation site in stem-loop-binding proteins that contributes to high-affinity RNA binding. *Proc. Natl. Acad. Sci. U.S.A.* 103(9): 3094-3099.
- Boulon, S. 2012. Dynamics of Protein Complexes Tracked by Quantitative Proteomics, Integrative Proteomics. InTech, available from:<http://www.intechopen.com/books/integrative-proteomics/dynamics-of-protein-complexes-tracked-by-quantitative-proteomics>.
- Branzei, D. and Foiani, M. 2008. Regulation of DNA repair throughout the cell cycle. *Nat Rev Mol Cell Biol.* 9(4): 297-308.
- Brown, D.T. 2001. Histone variants: are they functionally heterogeneous? *Genome Biol.* 2(7): REVIEWS0006.
- Cakmakci, N.G., Lerner, R.S., Wagner, E.J., Zheng, L. and Marzluff W.F. 2008. SLIP1, a factor required for activation of histone mRNA translation by the stem-loop binding protein. *Mol. Cell. Biol.* 28: 1182-1194.
- Chapman, J. R. and Jackson, S. P. 2008. Phospho-dependent interactions between NBS1 and MDC1 mediate chromatin retention of the MRN complex at sites of DNA damage. *EMBO Rep.* 9: 795-801.

- Choe, J., Kim, K. M., Park, S., Lee, Y. K., Song, O. K., Kim, M. K., Lee, B. G., Song, H. K. and Kim, Y. K. 2013. Rapid degradation of replication-dependent histone mRNAs largely occurs on mRNAs bound by nuclear cap-binding proteins 80 and 20. *Nucleic Acids Res.* 41: 1307-1318.
- Choe, J., Ahn, S.H. and Kim, Y.K. 2014. The mRNP remodeling mediated by UPF1 promotes rapid degradation of replication-dependent histone mRNA. *Nucleic Acids Res.* 42(14): 9334-9349.
- Clancy, S. 2008. DNA damage & repair: mechanisms for maintaining DNA integrity. *Nature Education* 1(1): 103.
- Clapier, C.R. and Cairns, B.R. 2009. The biology of chromatin remodeling complexes. *Annu Rev Biochem.* 78: 273-304.
- Coller, J.M., Tucker, M., Sheth, U., Valencia-Sanchez, M.A. and Parker, R. 2001. The DEAD box helicase, Dhh1p, functions in mRNA decapping and interacts with both the decapping and deadenylase complexes. *RNA* 7: 1717-1727.
- Cortez, D., Guntuku, S., Qin, J., and Elledge, S.J. 2001. ATR and ATRIP: Partners in checkpoint signaling. *Science.* 294: 1713-1716.

- Cox, J., Matic, I., Hilger, M., Nagaraj, N., Selbach, M., Olsen, J.V. and Mann, M. 2009. A practical guide to the MaxQuant computational platform for SILAC-based quantitative proteomics. *Mol Cell Proteomics* 4(5): 698-705.
- Dephoure, N., Gould, K.L., Gygi, S.P. and Kellogg, D.R. 2013. Mapping and analysis of phosphorylation sites: a quick guide for cell biologists. *Mol Biol Cell* 24(5): 535-542.
- Djakbarova, U., Marzluff, W.F. and Köseoglu, M.M. 2014. Translation regulation and proteasome mediated degradation cooperate to keep Stem-loop binding protein, a major player in histone mRNA metabolism, low in G1-phase. *J Cell Biochem* 115(3): 523-530.
- Dominski, Z., Erkmann, J.A., Yang, Y.X., Sánchez, R. and Marzluff, W.F. 2002. A novel zinc finger protein is associated with U7 snRNP and interacts with the stem-loop binding protein in the histone pre-mRNP to stimulate 3'-end processing. *Genes Dev* 16(1): 58-71.
- Dominski, Z. and Marzluff, W.F. 1999. Formation of the 3' end of histone mRNA. *Gene* 239(1): 1-14.
- Dominski, Z., and Marzluff, W.F. 2001. Three-hybrid screens for RNA-binding proteins: Proteins binding the 3'- end of histone mRNA. *Methods Mol. Biol.* 177: 291-318.

- Dominski, Z. and Marzluff, W.F. 2007. Formation of the 3' end of histone mRNA: getting closer to the end. *Gene*. 396(2): 373-390.
- Dominski, Z., Sumerel, J., Hanson, R.J., and Marzluff, W.F. 1995. The polyribosomal protein bound to the 3' end of histone mRNA can function in histone pre-mRNA processing. *RNA* 1: 915-923.
- Dominski, Z., Yang, X., Kaygun, H., and Marzluff, W.F. 2003. A 3' exonuclease that specifically interacts with the 3' end of histone mRNA. *Mol. Cell* 12: 295-305.
- Dominski, Z., Yang, X.C. and Marzluff, W.F. 2005. The polyadenylation factor CPSF-73 is involved in histone-pre-mRNA processing. *Cell*. 123: 37-48.
- Dominski, Z., Zheng, L.X., Sanchez, R., Marzluff, W.F. 1999. Stem-loop binding protein facilitates 3'-end formation by stabilizing U7 snRNP binding to histone pre-mRNA. *Mol. Cell. Biol.* 19: 3561-3570.
- Draizen, E.J., Shaytan, A.K., Marino-Ramirez, L., Talbert, P.B., Landsman, D. and Panchenko, A.R. 2016. HistoneDB 2.0: a histone database with variants-an integrated resource to explore histones and their variants. *Database (Oxford)*, 1-10.

- Dunham, W.H., Mullin, M. and Gingras, A.C. 2012. Affinity-purification coupled to mass spectrometry: basic principles and strategies. *Proteomics*. 12: 1576-1590.
- Eckner, R., Ellmeier W. and Birnstiel, M. 1991. Mature mRNA 3' end formation stimulates RNA export from the nucleus. *EMBO J.* 10, 3513-3522.
- Elledge, S.J., Zhou, Z., and Allen, J.B. 1992. Ribonucleotide reductase: regulation, regulation, regulation. *Trends Biochem. Sci.* 17 (3): 119-123.
- Erkman, J.A., Wagner, E.J., Dong, J., Zhang, Y., Kutay, U. and Marzluff, W.F. 2005. Nuclear Import of the Stem-Loop Binding Protein and Localization during the Cell Cycle. *Mol Biol Cell*. 16(6): 2960-2971.
- Ewen, M.E. 2000. Where the cell cycle and histones meet. *Genes & Dev.* 14: 2265-2270.
- Fransz, P. and de Jong, H. 2011. From nucleosome to chromosome: a dynamic organization of genetic information. *Plant J.* 66: 4-17.
- Friend, K., Lovejoy, A.F. and Steitz, J.A. 2007. U2 snRNP binds intronless histone pre-mRNAs to facilitate U7-snRNP-dependent 3' end formation. *Mol. Cell*. 28(2): 240-252.

- Gallie, D. R., Lewis, N. J., and Marzluff, W. F. 1996. The histone 3'-terminal stem-loop is necessary for translation in Chinese hamster ovary cells. *Nucleic Acids Res.* 24: 1954-1962.
- Gebhardt, A., Habjan, M., Benda, C., Meiler, A., Haas, D.A., Hein, M.Y., Mann, A., Mann, M., Habermann, B. and Pichlmair, A. 2015. mRNA export through an additional cap-binding complex consisting of NCBP1 and NCBP3. *Nat. Commun.* 6: 1-13.
- Gick, O., Krämer, A., Keller, W. and Birnstiel, M.L. 1986. Generation of histone mRNA 3' ends by endonucleolytic cleavage of the pre-mRNA in a snRNP-dependent in vitro reaction. *EMBO J.* 5(6): 1319-1326.
- Gorgoni, B., Andrews, S., Schaller, A., Schumperli, D., Gray, N.K., and Muller, B. 2005. The stem-loop binding protein stimulates histone translation at an early step in the initiation pathway. *RNA* 11: 1030-1042.
- Gottlieb, T.M. and Jackson, S.P. 1993. The DNA-dependent protein kinase: requirement for DNA ends and association with Ku antigen. *Cell.* 72(1): 131-142.

- Hanson, R.J., Sun, J., Willis, D.G. and Marzluff, W.F. 1996. Efficient extraction and partial purification of the polyribosome-associated stem-loop binding protein bound to the 3' end of histone mRNA. *Biochemistry*. 35: 2146-2156.
- Hara, M., Abe, Y., Tanaka, T., Yamamoto, T., Okumura, E. and Kishimoto, T. 2012. Greatwall kinase and cyclin B-Cdk1 are both critical constituents of M-phase-promoting factor. *Nat. Commun.* 3: 1059.
- Harper, J.W. and Elledge, S.J. 2007. The DNA damage response: ten years after. *Mol. Cell*. 28: 739-745.
- Harris, M.E., Bohni, R., Scheniderman, M.H., Ramamurthy, L., Schumperli, D. and Marzluff, W.F. 1991. Regulation of histone mRNAs in the unperturbed cell cycle: evidence suggesting control at two posttranscriptional steps. *Mol. Cell. Biol.* 11(5): 2416-2424.
- Helleday, T., Eshtad, S. and Nik-Zainal, S. 2014. Mechanisms underlying mutational signatures in human cancers. *Nat Rev Genet* 15: 585-598.
- Hochegger, H., Takeda, S. and Hunt, T. 2008. Cyclin-dependent kinases and cell-cycle transitions: does one fit all? *Nat. Rev. Cell. Mol Biol.* 9: 910-916.

Hoefig, K.P., Rath, N., Heinz, G.A., Wolf, C., Dameris, J., Schepers, A., Kremmer, E., Ansel, K.M. and Heissmeyer, V. 2013. Eri1 degrades the stem-loop of oligouridylated histone mRNAs to induce replication-dependent decay. *Nat Struct Mol Biol.* 20: 73-81.

<https://en.wikipedia.org/wiki/Histone>

Huang, Y., Gattoni, R., Stevenin, J., and Steitz, J.A. 2003. SR splicing factors serve as adapter proteins for TAP-dependent mRNA export. *Mol. Cell.* 11: 837-843.

Hussain, S. P., Hofseth, L. J. and Harris, C. C. 2003. Radical causes of cancer. *Nature Rev. Cancer* 3: 276-285.

Iizuka, M. and Smith, M.M. 2003. Functional consequences of histone modifications. *Curr. Opin. Genet Dev.* 13: 154-160.

Ishigaki, Y., Li, X., Serin, G. and Maquat, L.E. 2001. Evidence for a pioneer round of mRNA translation: mRNAs subject to nonsense-mediated decay in mammalian cells are bound by CBP80 and CBP20. *Cell.* 106: 607-617.

- Jaeger, S., Eriani, G. and Martin, F. 2004. Critical residues for RNA discrimination of the histone hairpin binding protein (HBP) investigated by the yeast three-hybrid system. *FEBS Lett.* 556(1-3): 265-70.
- Jaeger, A., Barends, S., Giege, R., Eriani, G. and Martin, F. 2005. Expression of metazoan replication-dependent histone genes. *Biochimie.* 87: 827-834.
- Kamakaka, R.T. and Biggins, S. 2005. Histone variants: deviants? *Genes & Dev.* 19: 295-316.
- Karnani, N. and Dutta, A. 2011. The effect of the intra-S-phase checkpoint on origins of replication in human cells. *Genes and Dev.* 25: 621-633.
- Kaufmann, W.K. and Paules, R.S. 1996. DNA damage and cell cycle checkpoints. *Faseb J.* 10: 238-247.
- Kaygun, H. and Marzluff, W.F. 2005a. Regulated degradation of replication-dependent histone mRNAs requires both ATR and Upf1. *Nat. Struct. Mol. Biol.* 12(9): 794-800.
- Kaygun, H. and Marzluff, W.F. 2005b. Upf1 regulates mammalian histone mRNA decay. *RNA.* 1(7): 567-574.

- Kaygun, H. and Marzluff, W.F. 2005c. Translation termination is involved in histone mRNAs degradation when DNA replication is inhibited. *Mol. Cell. Biol.* 25: 6879-6888.
- Khorasanizadeh, S. 2004. The nucleosome: From genomic organization to genomic regulation. *Cell.* 116: 259-272.
- Kim, K.M., Cho, H., Choi, K., Kim, J., Kim, B.W., Ko, Y.G., Jang, S.K. and Kim, Y.K. 2009. A new MIF4G domain-containing protein, CTIF, directs nuclear cap-binding protein CBP80/20-dependent translation. *Genes. Dev.* 23: 2033-2045.
- Kolev, N.G. and Steitz, J.A. 2005. Symplekin and multiple other polyadenylation factors participate in 3'-end maturation of histone mRNAs. *Genes & Dev.* 19: 2583–2592.
- Koseoglu, M.M., Dong, J. and William F Marzluff. 2010. Coordinate regulation of histone mRNA metabolism and DNA replication. *Cell Cycle.* 9(19): 3857-3863.
- Koseoglu, M.M., Graves, L.M. and Marzluff, W.F. 2008. Phosphorylation of threonine 61 by cyclin a/Cdk1 triggers degradation of stem-loop binding protein at the end of S phase. *Molecular and cellular biology.* 28: 4469-4479.
- Kouzarides, T. 2007. Chromatin modifications and their function. *Cell.* 128(4): 693-705.

- Krishnan, N., Lam, T.T., Fritz, A., Rempinski, D., O'Loughlin, K., Minderman, H., Berezney, R., Marzluff, W.F. and Thapar, R. 2012. The prolyl isomerase Pin1 targets stem-loop binding protein (SLBP) to dissociate the SLBP-histone mRNA complex linking histone mRNA decay with SLBP ubiquitination. *Mol Cell Biol.* 32(21): 4306-22.
- Kruhlak, M., Crouch, E.E., Orlov, M., Montañó, C., Gorski, S.A., Nussenzweig, A., Misteli, T., Phair, R.D. and Casellas R. 2007. The ATM repair pathway inhibits RNA polymerase I transcription in response to chromosome breaks. *447(7145): 730-734.*
- Kulis, M. and Esteller, M. 2010. DNA methylation and cancer. *Adv Genet.* 70: 27-56.
- Kumagai, A., Lee, J., Yoo, H.Y. and Dunphy, W.G. 2006. TopBP1 activates the ATR-ATRIP complex. *Cell.* 124: 943-955.
- Kupsco, J.M., Wu, M.-J., Marzluff, W.F., Thapar, R., Duronio, R.J. 2006. Genetic and biochemical characterization of *Drosophila* sniper: A promiscuous member of the metazoan 3' hExo/ERI-1 family of 3' to 5' exonucleases. *RNA.* 12: 2103-2117.
- Maquat, L.E., Tarn, W.Y. and Isken, O. 2010. The pioneer round of translation: features and functions. *Cell.* 142: 368-374.

- Lavin, M.F. 2007. ATM and the Mre11 complex combine to recognize and signal DNA double-strand breaks. *Oncogene*. 26: 7749-7758.
- Lee, J., Kumagai, A. and Dunphy, W.G. 2003. Claspin, a Chk1-regulatory protein, monitors DNA replication on chromatin independently of RPA, ATR, and Rad17. *Mol Cell*. 11(2): 329-340.
- Lee, J.H. and Paull, T.T. 2005. ATM activation by DNA double-strand breaks through the Mre11-Rad50-Nbs1 complex. *Science*. 308(5721): 551-554.
- Lejeune, F., Ishigaki, Y., Li, X. and Maquat, L.E. 2002. The exon junction complex is detected on CBP80-bound but not eIF4E-bound mRNA in mammalian cells: dynamics of mRNP remodelling. *EMBO J*. 21: 3536-3545.
- Lejeune, F., Ranganathan, A.C. and Maquat, L.E. 2004. eIF4G is required for the pioneer round of translation in mammalian cells. *Nat Struct Mol Biol*. 11: 992-1000.
- Ling, J., Morley, S.J., Pain, V.M., Marzluff, W.F., and Gallie, D.R. 2002. The histone 3'-terminal stem-loop-binding protein enhances translation through a functional and physical interaction with eukaryotic initiation factor 4G (eIF4G) and eIF3. *Mol. Cell. Biol*. 22: 7853-7867.

- Lubas, M., Christensen, M.S., Kristiansen, M.S., Domanski, M., Falkenby, L.G., Lykke-Andersen, S., Andersen, J.S., Dziembowski, A. and Jensen, T.H. 2011. Interaction profiling identifies the human nuclear exosome targeting complex. *Mol Cell*. 43(4): 624-637.
- Luger, K. 2003. Structure and dynamic behavior of nucleosomes. *Curr. Opin. Genet. Dev.* 13: 127-135.
- Lunn, C.L., Chrivia, J.C. and Baldassare, J.J. 2010. Activation of Cdk2/Cyclin E complexes is dependent on the origin of replication licensing factor Cdc6 in mammalian cells. *Cell Cycle*. 9: 4533-4541.
- Ma, T., Van Tine, B.A., Wei, Y., Garrett, M.D., Nelson, D., Adams, P.D., Wang, J., Qin, J., Chow, L.T. and Harper, J.W. 2000. Cell cycle-regulated phosphorylation of p220(NPAT) by cyclin E/Cdk2 in Cajal bodies promotes histone gene transcription. *Genes Dev.* 14: 2298-2313.
- Ma, Y., Kanakousaki, K. and Buttitta, L. 2015. How the cell cycle impacts chromatin architecture and influences cell fate. *Front. Genet.* 6(19): 1-18.

- Martin, F., Michel, F., Zenklusen, D., Müller, B. and Schümperli, D. 2000. Positive and negative mutant selection in the human histone hairpin-binding protein using the yeast three-hybrid system. *Nucleic Acids Res.* 28: 1594-1603.
- Martin, F., Schaller, A., Eglite, S., Schumperli, D. and Muller, B. 1997. The gene for histone RNA hairpin binding protein is located on human chromosome 4 and encodes a novel type of RNA binding protein. *EMBO J.* 16: 769-778.
- Marzluff, W.F. 1992. Histone 3' ends: essential and regulatory functions. *Gene Expr.* 2(2): 93-97.
- Marzluff, W.F. and Duronio, R.J. 2002. Histone mRNAs expression: multiple levels of cell cycle regulation and important developmental consequences. *Curr. Opin. Cell Biol.* 14: 692-699.
- Marzluff, W.F., Gongidi, P., Woods, K.R., Jin, J. and Maltais, L.J. 2002. The human and mouse replication-dependent histone genes. *Genomics.* 80(5): 487-498.
- Marzluff, W.F., Wagner, E.J. and Duronio, R.J. 2008. Metabolism and regulation of canonical histone mRNAs: life without a poly (A) tail. *Nat. Rev. Genet.* 9: 843-854.

- Matsuoka, S., Ballif, B.A., Smogorzewska, A., McDonald, E.R., Hurov, K.E., Luo, J., Bakalarski, C.E., Zhao, Z., Solimini, N., Lerenthal, Y., Shiloh, Y., Gygi, S.P. and Elledge, S.J. 2007. ATM and ATR substrate analysis reveals extensive protein networks responsive to DNA damage. *Science*. 316(5828): 1160-1166.
- Maxson, R., Cohn, R., Kedes, L. and Mohun, T. 1983. Expression and organization of histone genes. *Annu. Rev. Genet.* 17: 239-277.
- Mazouzi, A., Velimezi, G. and Loizou, J.I. 2014. DNA replication stress: Causes, resolution and disease. *Exp. Cell. Res.* 329(1): 85-93.
- McGowan, C.H. and Russell, P. 2004. The DNA damage response: sensing and signaling. *Curr Opin Cell Biol.* 16(6): 629-633.
- Merrick, C. J., Jackson, D. A. and Diffley, J. 2004. Visualization of altered replication dynamics after DNA damage in human cells. *J. Biol. Chem.* 279: 20067-20075.
- Miller, K.M, Tjeertes, J.V., Coates, J., Legube, G., Polo, S.E., Britton, S. and Jackson, S.P. 2010. Human HDAC1 and HDAC2 function in the DNA-damage response to promote DNA nonhomologous end-joining. *Nat Struct Mol Biol.* 17(9): 1144-1151.

- Mitchell, P., Petfalski, E., Shevchenko, A., Mann, M. and Tollervey, D. 1997. The exosome: A conserved eukaryotic RNA processing complex containing multiple 3'→5' exoribonuclease activities. *Cell*. 91: 457–466.
- Morimoto, M. and Boerkoel, C.F. 2013. The role of nuclear bodies in gene expression and disease. *Biology (Basel)*. 2(3): 976-1033.
- Moynahan, M.E. and Jasin. M. 2010. Mitotic homologous recombination maintains genomic stability and suppresses tumorigenesis. *Nat Rev Mol Cell Biol*. 11(3): 196-207.
- Mullen, T.E. and Marzluff, W.F. 2008. Degradation of histone mRNA requires oligouridylation followed by decapping and simultaneous degradation of the mRNA both 5' to 3' and 3' to 5'. *Genes Dev*. 22: 50-65.
- Müller, B., Blackburn, L., Feijoo, C., Zhao, X. and Smythe, C. 2007. DNA-activated protein kinase functions in a newly observed S phase checkpoint that links histone mRNAs abundance with DNA replication. *JCB*. 179(7): 1385-1398.
- Müller, B. and Schümperli, D. 1997. The U7 snRNP and the hairpin-binding protein: key players in histone mRNA metabolism. *Semin. Cell Dev. Biol*. 8: 567-576.

- Müller-McNicoll, M. and Neugebauer, K.M. 2013. How cells get the message: dynamic assembly and function of mRNA–protein complexes. *Nature Rev Genet.* 14: 275-287.
- Myers, J.S. and Cortez, D. 2006. Rapid activation of ATR by ionizing radiation requires ATM and Mre11. *J. Biol. Chem.* 281: 9346-9350.
- Nelson, D.M., Ye, X., Hall, C., Santos, H., Ma, T., Kao, G.D., Yen, T.J., Harper, J.W. and Adams, P.D 2002. Coupling of DNA synthesis and histone synthesis in S phase independent of cyclin/cdk2 activity. *Mol Cell Biol* 22: 7459-7472.
- Neusiedler, J., Mocquet, V., Limousin, T., Ohlmann, T., Morris, C. and Jalinot, P. 2012. INT6 interacts with MIF4GD/SLIP1 and is necessary for efficient histone mRNA translation. *RNA.* 18: 1163-1177.
- Nicholson, P. and Müller, B. 2008. Post-transcriptional control of animal histone gene expression-not so different after all. *Mol BioSystems,* 4: 721-725.
- Nizami, Z., Deryusheva, S. and Gall, J. G. 2010. The Cajal body and histone locus body. *Cold Spring Harb. Perspect. Biol.* 2:a000653.
- Nurse, P. 1990. Universal control mechanism regulating onset of M-phase. *Nature.* 344: 503-508.

- Ong, S-E and Mann, M. 2007. A practical recipe for stable isotope labeling by amino acids in cell culture (SILAC). *Nat. Protoc.* 1: 2650- 2660.
- Osley, M.A. 1991. The regulation of histone synthesis in the cell cycle. *Annu Rev Biochem.* 60: 827-861.
- Pacek, M. and Walter, J.C. 2004. A requirement for MCM7 and Cdc45 in chromosome unwinding during eukaryotic DNA replication. *EMBO J.* 23: 3667-3676.
- Pandey, N.B. and Marzluff, W.F. 1987. The stem-loop structure at the 3' end of histone mRNAs is necessary and sufficient for regulation of histone mRNA stability. *Mol. Cell. Biol.* 7: 4557-4559.
- Pandey, N.B., Sun, J-H. and Marzluff, W.F. 1991. Different complexes are formed on the 3' end of histone mRNA in nuclear and polysomal extracts. *Nucleic Acids Res.* 19: 5653-5659.
- Pandey, N.B., Williams, A.S., Sun, J.-H., Brown, V.D., Bond, U. and Marzluff, W.F. 1994. Point mutations in the stem-loop at the 3' end of mouse histone mRNA reduce expression by reducing the efficiency of 3' end formation. *Mol. Cell. Biol.* 14: 1709-1720.

- Park, S-S., Wu, W.W., Zhou, Y., Shen, R-F. Martin, B and Maudsley, S. 2012. Effective correction of experiment errors in quantitative proteomics using stable isotope labelling by amino acids in cell culture (SILAC). *J Proteomics*. 75(12): 3720-3732.
- Pettitt, J., Crombie, C., Schumperli, D. and Muller, B. 2002. The *Caenorhabditis elegans* histone hairpin-binding protein is required for core histone gene expression and is essential for embryonic and postembryonic cell division. *J. Cell Sci.* 115: 857-866.
- Pillai, R.A., Grimmmler, M., Meister, G., Will, C.L., Lührmann, R., Fischer, U. and Schümperli, D. 2003. Unique Sm core structure of U7 snRNPs: assembly by a specialized SMN complex and the role of a new component, Lsm11, in histone RNA processing. *Genes Dev.* 17(18): 2321-2333.
- Pillai, R.S., Will, C.L., Lührmann, R., Schümperli, D., and Müller, B. 2001. Purified U7 snRNPs lack the Sm proteins D1 and D2 but contain Lsm10, a new 14 kDa Sm D1-like protein. *EMBO J.* 20: 5470-5479.
- Podhorecka, M., Skladanowski, A. and Bozko, P. 2010. H2AX Phosphorylation: Its Role in DNA Damage Response and Cancer Therapy. *J Nucleic Acids.* 1-9.

- Polo, S.E. and Jackson, S.P. 2011. Dynamics of DNA damage response proteins at DNA breaks: a focus on protein modifications. *Genes Dev.* 25(5): 409-433.
- Poon, R.Y.C., Jiang, W., Toyoshima, H. and Hunter, T. 1996. Cyclin-dependent Kinases Are Inactivated by a Combination of p21 and Thr-14/Tyr-15 Phosphorylation after UV-induced DNA Damage. *J. Biol. Chem.* 271(22): 13283-13291.
- Rogakou, E.P., Pilch, D.R., Orr, A.H., Ivanova, V.S. and Bonner, W.M. 1998. DNA double-stranded breaks induce histone H2AX phosphorylation on serine 139. *J. Biol. Chem.* 273: 5858-5868.
- Rupnik, A., Lowndes N.F. and Grenon, M. 2010. MRN and the race to the break. *Chromosoma.* 119: 115-135.
- Saito, Y., Fujimoto, H. and Kobayashi, J. 2013. Role of NBS1 in DNA damage response and its relationship with cancer development. *Transl Cancer Res.* 2(3): 178-189.
- Sancar, A., Lindsey-Boltz, L. A., Unsal-Kacmaz, K. and Linn, S. 2004. Molecular mechanisms of mammalian DNA repair and the DNA damage checkpoints. *Annu. Rev. Biochem.* 73: 39-85.
- Sanchez, I., and Dynlacht, B.D. 2005. New insights into cyclins, CDKs, and cell cycle control. *Semin. Cell Dev. Biol.* 16: 311-321.

- Sánchez, R. and Marzluff, W.F. 2002. The stem-loop binding protein is required for efficient translation of histone mRNA in vivo and in vitro. *Mol Cell Biol.* 22(20): 7093-7104.
- San Filippo, J., Sung, J. and Klein, H. 2008. Mechanism of Eukaryotic Homologous Recombination. *Annu. Rev. Biochem.* 77: 229-225.
- Sarma, K. and Reinberg, D. 2005. Histone variants meet their match. *Nat Rev Mol Cell Biol.* 6(2): 139-149.
- Sato, H. and Maquat, L.E. 2009. Remodeling of the pioneer translation initiation complex involves translation and the karyopherin importin beta. *Genes Dev.* 23: 2537-2550.
- Schaufele, F., Gilmartin, G.M., Bannwarth, W. and Birnstiel, M.L. 1986. Compensatory mutations suggest that base-pairing with a small nuclear RNA is required to form the 3' end of H3 messenger RNA. *Nature.* 323: 777-781.
- Segurado, M. and Tercero, J.A. 2009. The S-phase checkpoint: targeting the replication fork. *Biol Cell.* 101(11): 617-627.
- Shanbhag, N.M., Rafalska-Metcalf, I.U., Balane-Bolivar, C., Janicki, S.M. and Greenberg, R.A. 2010. ATM-dependent chromatin changes silence transcription in cis to DNA double-strand breaks. *Cell* 141: 970-981.

- Sinha, R. P., and Häder, D. P. 2002. UV-induced DNA damage and repair: A review. *Photochemical and Photobiological. Sciences.* 1: 225-236.
- Spycher, C., Miller, E.S., Townsend, K., Pavic, L., Morrice, N.A., Janscak, P., Stewart, G.S. and Stucki, M. 2008. Constitutive phosphorylation of MDC1 physically links the MRE11–RAD50–NBS1 complex to damaged chromatin. *J. Cell Biol.* 181: 227-240.
- Sullivan, K.D., Mullen, T.E., Marzluff, W.F. and Wagner, E.J. 2009. Knockdown of SLBP results in nuclear retention of histone mRNA. *RNA.* 15: 459-472.
- Sun, J.-H., Pilch, D. R. and Marzluff, W. F. 1992. The histone mRNA 3'-end is required for localization of histone mRNA to polyribosomes. *Nucleic Acids Res.* 20: 6057-6066.
- Tan, D., Marzluff, W.F., Dominski, Z. and Tong, L. 2013. Structure of histone mRNA stem-loop, human stem-loop binding protein and 3'hExo ternary complex. *Science.* 339(6117): 318-321.
- Thapar, R., Denmon, A. P. and Nikonowicz, E. P. 2014. Recognition modes of RNA tetraloops and tetraloop-like motifs by RNA-binding proteins. *Wiley Interdiscip. Rev. RNA* 5: 49-67.

- Thapar, R., Marzluff, W.F. and Redinbo, M.R. 2004. Electrostatic Contribution of Serine Phosphorylation to the Drosophila SLBP-Histone mRNA Complex. *Biochemistry*. 43: 9401-9412.
- Townley-Tilson, W.H., Pendergrass, S.A., Marzluff, W.F. and Whitfield, M.L. 2006. Genome-wide analysis of mRNAs bound to the histone stem-loop binding protein. *RNA*. 12: 1853-1867.
- von Moeller, H., Lerner, R., Ricciardi, A., Basquin, C., Marzluff, W.F. and Conti, E. 2013. Structural and biochemical studies of SLIP1-SLBP identify DBP5 and eIF3g as SLIP1-binding proteins. *Nucleic Acids Res.* 41(16): 7960-7971.
- Walther, T.N., Koning, T.H.W., Schumperli, D. and Muller, B. 1998. A 5'-3' exonuclease activity involved in forming the 3' products of histone pre-mRNA processing in vitro. *RNA*. 4(9): 1034-1046.
- Wagner, E.J., Berkow, A. and Marzluff, W.F. 2005. Expression of an RNAi-resistant SLBP restores proper S-phase progression. *Biochem. Soc. Trans.* 33: 471-473.
- Wagner, E.J., Ospina, J.K., Hu, Y., Dundr, M., Matera, A.G and Marzluff, W.F. 2006. Conserved zinc fingers mediate multiple functions of ZFP100, a U7snRNP associated protein. *RNA*. 12: 1206-1218.

- Wang, Z. F., Ingledue, T. C., Dominski, Z., Sanchez, R., and Marzluff, W. F. 1999. Two *Xenopus* proteins that bind the 3' end of histone mRNA: implications for translational control of histone synthesis during oogenesis. *Mol. Cell. Biol.* 19: 835-845.
- Wang, Z. F., Whitfield, M.L., Ingledue, T. I., Dominski, Z. and Marzluff, W. F. 1996. The protein which binds the 3' end of histone mRNA: implications for translational control of histone synthesis during oogenesis. *Mol. Cell. Biol.* 19: 835-845.
- Whitfield, M.L., Zheng, L.-X., Baldwin, A., Ohta, T., Hurt, M. and Marzluff, W.F. 2000. Stem-loop binding protein, the protein that binds the 3' end of histone mRNA, is cell cycle regulated by both translational and posttranslational mechanisms. *Mol. Cell Biol.* 20: 4188-4198.
- Whitfield, M.L., Kaygun, H., Erkmann, J.A., Townley-Tilson, W.H., Dominski, Z. and Marzluff, W.F. 2004. SLBP is associated with histone mRNA on polyribosomes as a component of the histone mRNP. *Nucleic Acids Res.* 32(16): 4833-4842.
- Williams, A.S., Ingledue III, T.C., Kay, B.K., and Marzluff, W.F. 1994. Changes in the stem-loop at the 3'terminus of histone mRNA affects its nucleocytoplasmic transport and cytoplasmic regulation. *Nucleic Acids Res.* 22: 4660-4666.

- Woo, R.A. and Poon, R.Y. 2003. Cyclin-dependent kinases and S phase control in mammalian cells. *Cell Cycle*. 2(4): 316-324.
- Yam, C. H., Fung, T.K. and Poon, R.Y. 2002. Cyclin A in cell cycle control and cancer. *Cell Mol. Life Sci*. 59: 1317-1326.
- Yamashita, A., Ohnishi, T. Kashima, I., Taya, Y. and Ohno, S.2001. Human SMG-1, a novel phosphatidylinositol 3-kinase-related protein kinase, associates with components of the mRNA surveillance complex and is involved in the regulation of nonsense-mediated mRNA decay. *Genes Dev*. 15: 2215-2228.
- Yang, X.C., Burch, B.D., Yan, Y., Marzluff, W.F. and Dominski, Z. 2009. FLASH, a proapoptotic protein involved in activation of caspase-8, is essential for 3'end processing of histone pre-mRNAs. *Mol Cell* 36: 267-278.
- Yang, X.H. and Zou, L. 2006. Checkpoint and coordinated cellular responses to DNA damage. *Results Probl. Cell Differ*. 42: 65-92.
- Ye, X., Wei, Y., Nalepa, G. and Harper, J.W. 2003. The cyclin E/Cdk2 substrate p220(NPAT) is required for S-phase entry, histone gene expression, and Cajal body maintenance in human somatic cells. *Mol Cell Biol*. 23: 8586-8600.
- Zeman, M.K. and Cimprich, K.A. 2014. Causes and consequences of replication stress. *Nat Cell Biol*. 16(1): 2-9.

- Zheng, L., Dominski, Z., Yang, X.C., Elms, P., Raska, C.S., Borchers, C.H., and Marzluff, W.F. 2003. Phosphorylation of stem-loop binding protein (SLBP) on two threonines triggers degradation of SLBP, the sole cell cycle-regulated factor required for regulation of histone mRNA processing, at the end of S phase. *Mol. Cell. Biol.* 23: 1590-1601.
- Zhang, M., Lam, T. T., Tonelli, M., Marzluff, W. F. and Thapar, R. 2012. Interaction of the histone mRNA hairpin with stem-loop binding protein (SLBP) and regulation of the SLBP-RNA complex by phosphorylation and proline isomerization. *Biochemistry* 51: 3215-3231.
- Zhang, J., Tan, D., DeRose, E.F., Perera, L., Dominski, Z., Marzluff, W.F., Tong, L. Hall, T.M.T. 2014. Molecular mechanisms for the regulation of histone mRNA stem-loop-binding protein by phosphorylation. *PNAS*. 111(29): 1-10.
- Zhang, Y., Zhou, J. and Lim, C.UK. 2006. The role of NBS1 in DNA double strand break repair, telomere stability, and cell cycle checkpoint control. *Cell Res.* 16: 45-54.

- Zhao, J., Kennedy, B.K., Lawrence, B.D., Barbie, D.A., Matera, A.G., Fletcher, J.A. and Harlow, E. 2000. NPAT links cyclin E-Cdk2 to the regulation of replication-dependent histone gene transcription. *Genes Dev.* 14: 2283-2297.
- Zhao, J. 2004. Coordination of DNA synthesis and histone gene expression during normal cell cycle progression and after DNA damage. *Cell Cycle.* 3(6): 695-697.
- Zheng, L.-X., Dominski, Z., Yang, X., Elms, P., Raska, C.S., Borchers, C.H., and Marzluff, W.F. 2003. Phosphorylation of SLBP on two threonines triggers degradation of SLBP, the sole cell- cycle regulated factor required for regulation of histone mRNA processing, at the end of S-phase. *Mol.Cell Biol.* 23: 1590-1601.
- Zhou, B-B.S., and Elledge, S.J. 2000. The DNA damage response: putting checkpoints in perspective. *Nature.* 408: 433-439.
- Zou, L. and Elledge, S.J. 2003. Sensing DNA damage through ATRIP recognition of RPA-ssDNA complexes. *Science.* 300: 1542-1548.

## **1.18 Aim**

When cells are exposed to replication stress, one cellular response is the rapid induction of histone mRNA decay, the purpose of which is to ensure the co-ordination of histone protein production with the synthesis of newly produced DNA. The precise mechanism by which replication stress signals to the histone mRNA homeostatic machinery is not well understood. The aim of this work is to establish a cell model for the analysis of SLBP, a key protein component of histone mRNA homeostasis, and to use mass spectrometry approaches to investigate SLBP status including post-translational modifications and interacting components, to identify and characterize molecular events and interacting proteins associated with SLBP-mediated histone mRNA degradation as a consequence of replication stress.

# *Chapter 2*

## *Materials and Methods*

### **2.1 Materials**

All of the formulation of the solutions, the sequences of primers, the characteristics of the plasmids and the antibodies used in the study are described in the corresponding Appendices. (Appendix A: Solution recipes, Appendix B: List of antibodies, Appendix C: List of oligonucleotides, Appendix D: List of plasmids, Appendix E: Flag-tagged SLBP protein sequence, Appendix F: Flag-tagged SLBP cDNA sequence, Appendix G: HA-tagged SLBP cDNA sequence).

### **2.2 Methods**

#### **2.2.1 Molecular Biology Techniques**

##### **2.2.1.1 cDNA synthesis**

The human SLBP cDNA was generated by Omniscript reverse transcription (QIAGEN) of HeLa cell total RNA. The specific PCR product of SLBP was amplified from SLBP cDNA using the Phusion<sup>®</sup>

high-fidelity DNA polymerase (NEB) following amplification conditions.

The cycling parameters were as follow.

<b>Segment</b>	<b>Cycle</b>	<b>Temperature</b>	<b>Time</b>
1	1	98 °C	30 sec
2	30	98 °C	10 sec
		50-60 °C	15 sec
		72 °C	15 sec
3	1	72 °C	5 min

#### **2.2.1.2 Plasmid construction**

For untagged expression, the relevant SLBP PCR product was directionally cloned into pCI-neo following digestion with *EcoRI/NotI*. For the Flag-tagged vector, pCMV-Tag 2A, the relevant SLBP PCR product and parent plasmid was digested with *EcoRI/XhoI*. The using of standard cloning procedures was performed as described in section 2.22 and verified by DNA sequencing.

### 2.2.1.3 pcDNA/FRT/TO/CAT-Flag-SLBP construction

A single N-terminal flag was added by PCR to pcDNA/FRT/TO/CAT-Flag-SLBP using the Phusion High-fidelity DNA polymerase (NEB) (see appendix D and F). The digestion was performed with *XmaII/NotI*.

### 2.2.1.4 Introduction of siRNA resistance mutation into SLBP

Two silent mutations (A327G and A330C) (Figure 2.1) conferring resistance to a specific SLBP siRNA were generated using the Quickchange mutagenesis kit (Stratagene) to generate Flag-SLBP<sup>res</sup> (see mutagenesis section for conditions).

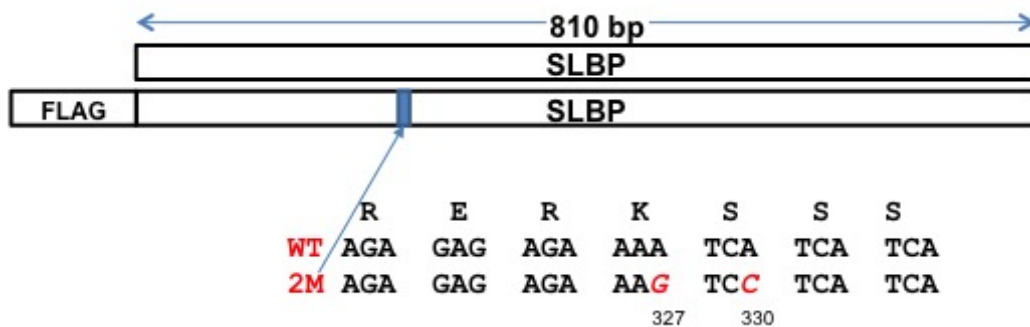


**Figure 2.1** Schematic representation of the Flag-SLBP<sup>res</sup>. The SLBP-siRNA target sequence is indicated by capital letters. Red bold/italic letters are mutations.

### **2.2.1.5 pcDNA/FRT/TO/CAT-Flag-SLBP<sup>res</sup> construction**

A single N-terminal flag was added by PCR to pcDNA/FRT/TO/CAT-Flag-SLBP<sup>res</sup> using the Phusion High-fidelity DNA polymerase (NEB) (see appendix D and F). The digestion was performed with *AfIII/XhoI*.

### **2.2.1.6 Alanine and glutamic acid substitution of SLBP S182 generation**

The appropriate primers were used to amplify S182A and S182E. Alanine and glutamic substitution mutagenesis was performed using the Quickchange mutagenesis kit (Stratagene).

### **2.2.1.7 DNA digestion with restriction enzymes**

DNA digestion was performed by using miniprep DNA or maxiprep DNA (QIAGEN). Analytical digests were performed in a maximum volume 60 µl using 10 unit of restriction enzyme per microgram of DNA, appropriate enzyme buffer and milliQ H<sub>2</sub>O. 10% of total digest reaction mix was used to confirm digest by agarose gel electrophoresis.

### **2.2.1.8 DNA ligation**

The parental plasmid and the digested DNA were ligated using T4 DNA ligase (NEB). The amount of the digested vector and DNA were varied from 1:1 to 6:1 ratios. The reaction was incubated overnight at room temperature. Control reactions including plasmid-only ligation reactions and T4 DNA ligase-free reactions were also set up.

### **2.2.1.9 Electrophoretic analysis of DNA**

The electrophoresis apparatus was prepared and the electrophoresis tank was filled with 1x TAE buffer (see appendix A) to cover the agarose gel. The appropriate amount of agarose was transferred to a flask with 100 ml of 1x TAE. The slurry was heated until the agarose dissolved and allowed to cool to 60 °C before adding ethidium bromide to a final concentration of 1 µg/ml. The agarose was poured into the gel mould and then the comb was positioned. After the gel was completely set, the comb was removed and the gel mould was moved in the electrophoresis tank. The DNA samples were mixed with 1x loading buffer and loaded into the wells using a pipette. The molecular weight marker set DNA hyperladder I (NEB) was also loaded into the wells as reference. The tank lid was closed and the electric current was applied across the gel (typically 100 V, 400 mA for 45-60

min) so that the DNA migrates toward the anode. After electrophoresis, the gel was examined under UV light at 312 nm, photographed and analysed with Uvitech UviProchemi camera system.

#### **2.2.1.10 Purification of DNA (QIAquick PCR purification kit) from reaction mixtures**

DNA was purified using a kit from Qiagen according to the manufacturer's instructions. The kit was used to purify DNA fragments generated by PCR or following other enzymatic reactions. Briefly, 5x volumes of Qiagen buffer PB were added to 1 volume of the solution to be purified and mixed. The sample was added to a spin column placed in a collection tube and centrifuged for 1 min. at 13,000 rpm to bind DNA. The flow-through was discarded and the column washed with 0.75 ml Qiagen buffer PE by centrifugation for 1 min at 13,000 rpm. Then the flow-through was discarded again. The column was placed back in the same collection tube and re-centrifuged to remove traces of the washing buffer. The column was then placed in a clean 1.5 ml microcentrifuge tube and 50 µl of Qiagen buffer EB was added and allowed to stand for 1 min. DNA was eluted by centrifuge at 13,000 rpm for 1 min DNA was stored at -20 °C.

### **2.2.1.11 DNA extraction and purification from agarose gels (QIAquick gel extraction kit)**

DNA was extracted from agarose gel and purified using a kit from Qiagen according to the manufacturer's instructions. For agarose gel extraction, SYBR Safe (Invitrogen) were used to stain DNA gel that can be visualised by blue-light. A gel slice containing the DNA was excised with a clean, sharp scalpel and weighed. The buffer QG 3 volumes were added to 1 volume of weighed agarose gel and incubated for 10 min at 50 °C. After the gel slice had dissolved, 1 volume of isopropanol was added and the solution was mixed. The solution was transferred to a QIAquick column and centrifuged for 1 min at 13,000 rpm. The flow-through was discarded and added 0.75 ml Qiagen buffer PE to the column. The column was centrifuged for 1 min and re-centrifuged to remove residual wash buffer. DNA was eluted in either 50 µl (for plasmids) or 30 µl (PCR product) of Qiagen buffer EB into a clean 1.5 ml eppendorf tube by centrifugation for 1 min at 13,000 rpm.

### 2.2.1.12 Site-directed mutagenesis

Site-directed mutagenesis was performed using the QuickChange kit (Stratagene) according to the manufacturer's instructions. Each reaction contained 10x Pfu ultra buffer (5 $\mu$ l), double-stranded DNA template (10 ng), 5' primer (125 ng), 3' primer (125 ng), dNTP (1  $\mu$ L of 100 mM mix (25 mM each of dATP, dGTP, dCTP, dTTP)), Quicksolution (3  $\mu$ l) in a final volume of 49  $\mu$ l. 1  $\mu$ l of Pfu ultra HF DNA polymerase (Stratagene) was added to the reaction and mixed gently. The cycling parameters were as follow.

Segment	Cycle	Temperature	Time
1	1	95 °C	2 min
2	30	95 °C	30 sec
		60 °C	1 min
		68 °C	3 min
3	1	68 °C	5 min

Subsequently, the template plasmid was digested by adding 1  $\mu$ l of Dpn1 restriction enzyme and incubating at 37 °C for 1 h. The remaining DNA (mutated) was then transformed into XL-10 Gold ultra-competent *E. coli* cells, as described in section 2.2.2.3 below.

### **2.2.1.13 DNA sequencing**

All DNA sequencing reactions were performed by staff of the Genetic Core facility at the Medical school, University of Sheffield using Applied Biosystems 3730 DNA Analyser. The manufacturer's standard protocol was 10 µl of 100 ng/µl DNA and 10 µl of 1 pmol/µl primers per sequence reaction. DNA sequences were verified by the visual inspection of raw sequence data using the 4peak program and analysed using the DNA Strider program and BLAST online software.

## **2.2.2 Bacterial techniques**

### **2.2.2.1 Antibiotic solutions and agar plates preparation**

The antibiotics were routinely used. Stock solutions of antibiotics and following concentrations in LB (Luria-Bertani) liquid medium and LB agar plates were prepared as described. Kanamycin stock solution was 10 mg/ml and used at 50 µg/ml. Ampicillin stock solution was 100 mg/ml and used at 100 µg/ml. The Antibiotic agar plates were generated by adding the appropriate amount of stock antibiotic after partial cooling of the media, and once set, agar plates were stored at 4 °C.

## **2.2.2.2 Transformation of competent bacteria with plasmid DNA**

### **2.2.2.2.1 Routine cloning**

DH5 $\alpha$  competent cells were produced in Smythe Lab by D.Sutton using the described method (Sambrook and Russel, 2001). Cells were thawed on ice and 10% of each ligation reaction added to 20  $\mu$ l cells and gently swirled to mix. The cells were incubated on ice for 30 min. Bacterial cells and DNA mixtures were heat shocked at 42  $^{\circ}$ C for 30 sec and then placed on ice for 5 min. 200  $\mu$ l of pre-warmed super optimal broth with catabolite repression (SOC) media was added and cells were incubated at 37  $^{\circ}$ C for 1 h with shaking at 225 rpm. The cells were then plated on the appropriate antibiotic agar medium and incubated at 37  $^{\circ}$ C overnight. Control transformations lacking, added DNA, or inserted were also performed in parallel.

### **2.2.2.2.2 Cloning following site-directed mutagenesis**

XL-10 gold ultra competent cells (obtained from Agilent Technologies) were thawed slowly on ice. 45  $\mu$ l of competent cells were placed in pre-chilled 14 ml BD Falcon polypropylene round bottom tubes. 2  $\mu$ l of  $\beta$ -mercaptoethanol was added and the cells were incubated on ice and swirled gently every 2 min for 10 min. 2  $\mu$ l of Dpn1-treated

DNA was added and incubated on ice for a further 30 min. The cells were heat shocked at 42 °C for 30 sec and then placed on ice for 2 min. 500 µl of pre-warmed NZY+ broth was added and incubated at 37 °C at 225 rpm for 1 h. 200 µl of the transformation was plated on the appropriate antibiotic agar medium and incubated overnight at 37 °C.

### **2.2.2.3 Isolation of plasmid DNA from bacteria using QIAquick spin miniprep kit**

DNA was purified using a kit from QIAGEN according to the manufacturer's instructions. A single bacterial colony was transferred into 4 ml of LB media containing 100 µg/ml ampicillin and incubated overnight at 37 °C with shaking at 225 rpm. 1.5 ml of this culture was transferred to an eppendorf tube and centrifuged at 13,000 rpm for 1 min. The media was removed and the process repeated to give a bacterial pellet representative of 3 ml of culture. The pellet was then resuspended in 250 µl of Qiagen buffer P1, 250 µl of Qiagen buffer P2 was added and mixed by inversion until the solution became viscous and slightly clear. 350 µl of Qiagen buffer N3 was added and the sample inverted until the solution became cloudy. The sample was centrifuged at 13,000 rpm for 10 min and the resulting supernatant was applied to a QIAprep spin column placed in a collection tube. After centrifugation for 1 min at

13,000 rpm, the flow-through was discarded. The column was washed by adding 750  $\mu$ l of Qiagen buffer PE and centrifuging at 13,000 rpm for 1 min. The flow-through was discarded and QIAprep column was re-centrifuged at 13,000 rpm for an additional 1 min to remove residual wash buffer. Finally, the column was transferred to a clean 1.5 ml eppendorf tube, 50  $\mu$ l of Qiagen buffer EB was added and let it stand for 1 min. prior to elution of the DNA by centrifugation at 13,000 rpm for 1 min. DNA obtained by this method was firstly used for DNA sequencing, transfection, molecular biology experiment. DNA was stored at -20 °C.

#### **2.2.2.4 Isolation of plasmid DNA from bacteria using a PureLink<sup>®</sup> HiPure Maxiprep kit**

DNA was purified using a kit from Invitrogen according to the manufacturer's instructions. A single bacterial colony was transferred into 3 ml of LB media containing 100  $\mu$ g/ml ampicillin and incubated at 37 °C in an orbital shaker rotating at 225 rpm for 6 h. This culture was then transferred to 500 ml of LB media containing 100  $\mu$ g/ml ampicillin and incubated at 37 °C overnight in an orbital shaker rotating at 225 rpm. The culture was centrifuged at 4000 rpm for 10 min at 4 °C using a Beckman Avanti J-26XP (JLA 8.1 rotor) centrifuge and media

discarded. A maxi column was equilibrated by adding 30 ml of buffer EQ1 and allowed to flow through. The bacterial pellet was resuspended in 10 ml of buffer R3 (containing RNase A 20 µg/ml) and further diluted with 10 ml of lysis buffer L7, mixed and left at room temperature for 5 min. DNA was precipitated by adding 10 ml of buffer N3 and sample transferred to the equilibrated maxi column. Lysate filtered through the column by gravity flow and was washed with 50 ml of buffer W8. The flow through was discarded. A sterile 50 ml centrifuge tube was used to collect eluted DNA after adding 15 ml of elution buffer E4. 10.5 ml of isopropanol was added to the eluted DNA and centrifuged at 12,000 rpm for 30 min at 4 °C, discarding the supernatant. DNA pellet was washed with 5 ml of 70% absolute ethanol and centrifuged at 12,000 rpm for 5 min at 4 °C. Pellet was allowed to air dry before resuspending in 500 µl of TE buffer. DNA was stored at -20 °C.

#### **2.2.2.5 Glycerol stocks of transformed bacterial cells**

Single colonies were picked from an agar plate and grown overnight at 37 °C in an orbital shaker at 225 rpm in 4 ml of LB media with the required selective antibiotic. 700 µl of cell culture was mixed with 300 µl of sterile 50% glycerol. Cells were then stored at -80 °C.

## **2.2.3 Tissue culture techniques**

### **2.2.3.1 Mammalian cell culture**

HeLa cells were cultured in DMEM with 4,500 mg/L glucose, L-glutamine, and sodium bicarbonate (Sigma-Aldrich) supplemented with 10% FBS (Sigma-Aldrich). Cells were incubated at 37 °C with 5% CO<sub>2</sub>. Cells were trypsinised by 1x trypsin (Gibco, Life Technologies) and subcultured 1:4 to 1:8 every 2-4 days.

### **2.2.3.2 Flp-IN cell lines**

Stable cell lines were created by using Flp-In<sup>TM</sup> T-REx<sup>TM</sup> Core kit according to the manufacturer's manual (Invitrogen) in order to integrate Flag-SLBP, HA-SLBP and mutants structures into the Flp-In<sup>TM</sup> TRex<sup>TM</sup> host HeLa cell line. T-Rex stage HeLa cells containing a single integrated Flp recombination target (FRT) site has been acquired by the Smythe lab. The line was generated by transfecting HeLa cells with the pFRT/lacZeo vector that expresses a lacZ-Zeocin fusion gene controlled by the early SV40 promoter that contains a single FRT site and maintained in DMEM supplemented with 10% FBS, 4 µg/ml Blasticidin S hydrochloride (Fisher Scientific) and 50 µg/ml Zeocin (Invitrogen, Life Technologies).

To generate Flp-In stable cell lines, 100 mm dishes were seeded with  $1.6 \times 10^6$  T-Rex HeLa cells the day before transfection in media containing 4  $\mu\text{g/ml}$  Blasticidin S hydrochloride and 50  $\mu\text{g/ml}$  Zeocin. The following day, the plasmids PCDNA5/FRT/TO/CAT-Flag-SLBP and pOG44 were co-transfected in a 1:9 ratio using Polyfect reagent (Qiagen) (as described in section 2.2.3.4.1). Transfected cells were maintained in DMEM supplemented with 10% FBS and 4  $\mu\text{g/ml}$  Blasticidin S hydrochloride for 24 h and then media was replaced with fresh media containing 10% FBS and 4  $\mu\text{g/ml}$  Blasticidin S hydrochloride for additional 24 h. After 48 h of transfection, cells were removed and transferred into T25 flasks at a range of densities (10-40% confluent) and then incubated for 4 h. After that the medium was replaced with DMEM supplemented with 10% FBS, 4  $\mu\text{g/ml}$  Blasticidin S hydrochloride and 20  $\mu\text{g/ml}$  Hygromycin B (Invitrogen, Life Technologies) and was changed every 2-3 days until isolated colonies of proliferating cells were observed. Then, these colonies expanded were expanded to produce Flp-In stable cell lines. This process was repeated for all plasmids used in this study.

### **2.2.3.3 Doxycycline (Dox) treatment of Flp-In cells**

The expression of Flag-SLBP in Flp-In HeLa cell lines was induced through the addition of a 0.1-1 µg/ml in the media for the required length of time.

### **2.2.3.4 Mammalian cell transfection technique**

#### **2.2.3.4.1 Neon<sup>TM</sup> Transfection System**

Cells were transfected with siRNA using Neon<sup>TM</sup> Transfection System (Invitrogen) using the supplied protocol. FlpIn HeLa cells were grown in a flask for one to two days prior to electroporation. On the day of the experiment, the cells are 70-90% confluent. For 6.0 cm dishes, the number of cells were  $4 \times 10^5$  cells per each 100 µl Neon<sup>TM</sup> tip. Cells were trypsinised, re-suspended and transferred to 15 ml conical tube. The cells were counted to determine the cell density. Cells were centrifuged at 225 rpm for 5 min at room temperature. The supernatant was discarded and washed the cells with PBS and re-centrifuged three times. Finally, the cells were re-suspended in Resuspension Buffer R at a final density of  $2 \times 10^6$  cells/ml and were gently pipetted to obtain a single cell suspension. Before electroporation step, 6.0 cm dishes were prepared by filling the dishes with 3 ml of DMEM with 0.5 µg/ml doxycycline and pre-incubated dishes in a humidified 37 °C / 5 % CO<sub>2</sub> incubator.

For electroporation step, 3 ml of Invitrogen Electrolyte buffer E was filled in the plastic neon tube and inserted a tube into the Neon pipette station. The Neon machine was set to the desired Pulse parameters. For FlpIn HeLa cells in 100  $\mu$ l were set the following: Pulse voltage 1,400 / Pulse width (ms) 20 / Pulse number 1. 110  $\mu$ l of cells in Resuspension Buffer R were transferred to the eppendorf tube containing 200 nM siRNA. The Neon pipette was pressed down to open the pipette clamp, then insert the 100  $\mu$ l Neon tip onto the Neon pipette pushing down firmly. The cells/siRNA mixture were mixed by pipette up and down and sucked up on the Neon pipette. The pipette and tip were inserted into the tube filled with electrolyte buffer on the Neon pipette station. It was ready to press "Start" on the Neon machine. The bubbles that appeared around the tip demonstrate that electroporation was working. The pipette was removed from the station and gently expelled the cell/siRNA mixture by pressing the push-button down to the first stop into a tissue culture dish containing pre-warmed media with doxycycline (Dox). The final step was ejected tip by pressing to second stop.

### **2.2.3.5 Cryo-preservation of cells**

Cell lines were pelleted at 2,500 rpm for 5 min in a Biofuge Primo Heraeus bench top centrifuge (Heraeus #7591 rotor) and resuspended in cell freezing medium. Cells were slowly frozen using a Mr. Frosty cell freezing chamber (Invitrogen) at -80 °C for one week before being transferred to liquid nitrogen for long-term storage.

## **2.2.4 Protein techniques**

### **2.2.4.1 Whole cell extract preparation**

For preparation of whole cell extracts for analysis by Western blotting, dishes or plates containing HeLa cells were cooled on ice for a few minutes. The media was aspirated and cells were washed twice with ice-cold PBS. Cells were lysed by the addition of lysis buffer. The cells were scraped and transferred to eppendorf tubes. The lysates were snap-frozen on dry ice and subjected to three freeze-thaw cycles. The lysates were then centrifuged at 13,000 rpm for 15 min at 4 °C and the supernatants were transferred to new eppendorf tubes and stored at -20 °C.

#### **2.2.4.2 Bradford assay**

Protein concentration was determined using Bio-Rad Protein assay reagent based on the protein dye binding method of Bradford (1976). The protein sample being measured was mixed with Bradford reagent and milli-Q H<sub>2</sub>O at the dilution 1:5. The absorbance was measured at OD<sub>595</sub> and determined the concentration of protein by using known BSA standard curve.

#### **2.2.4.3 SDS-polyacrylamide gel electrophoresis (SDS-PAGE)**

Polyacrylamide gel electrophoresis was carried out under denaturing condition using mini-gels (82 mm x 102 mm) according to the method of Laemmli (1970). In my study, 12% polyacrylamide gels were used. Water was added to protein samples to make up the total volume of each sample equal with an appropriate volume of 5x sample loading buffer. Prior to loading, protein samples were boiled at 95 °C for 5 min. Polymerised gels were assembled into the Bio-Rad Mini-PROTEAN II apparatus, before the inner and outer reservoirs were filled with 1x gel running buffer and current applied to run protein samples through the gel under typical electrophoresis conditions (120 V, 400 mA for 3 h).

#### **2.2.4.4 Western blotting**

Polyacrylamide gels were removed from their retaining plates, and transferred to nitrocellulose membrane that sandwiched between 4 sheets of Whatman paper at 100 V, 400 mA for 75 min using the Bio-Rad Mini-PROTEAN II apparatus. The nitrocellulose membrane was blocked with either 5% milk or 5% BSA in TBS for 1 h at room temperature. The membrane was incubated with primary antibody against the protein of interest at a dilution between 1:500 and 1:5,000 in either 5% milk or 5% BSA in TBS at 4 °C overnight. Membranes were then washed in TBS five times for min. The blots were then incubated with HRP-conjugated secondary antibody at a dilution 1:5,000 in 5% milk in TBS for 1 h at room temperature. Membranes were washed five times for 5 min in TBS and Amersham ECL Western Blotting Detection Reagent (GE Healthcare) was added for 5 min. Bands were detected by exposing the membranes to photographic film (Fuji film RX NIF) which was developed using an Optimax 2010 X-ray film processor. Images were quantified by using Image J software to determine the optical density. To re-probe the membrane with a different antibody, it was stripped by rotating on a rocker for 30 min in a stripping buffer. The membrane was washed five times for 5 min in TBS, re-blocked for 1 h at room

temperature and probed with new primary and secondary antibodies, respectively.

#### **2.2.4.5 Colloidal Coomassie blue staining of SDS-PAGE**

Gels were stained in colloidal Coomassie blue staining solution for at least 30 min before being de-stained in a solution of 40% methanol and 10% acetic acid. Gels were dried on Whatmann 3MM papers using a gel dryer (Gel Master<sup>TM</sup>, Welch, Rietschle Thomas).

#### **2.2.5 Flow cytometry**

Flp-IN cells were seeded in 35 mm, 60 mm or 100 mm dishes at a density of  $0.5 \times 10^5$ - $1 \times 10^6$  cells/cm<sup>2</sup>, depending on the experiment. For bivariate flow cytometry, the medium was aspirated and replaced with medium containing 25  $\mu$ M BrDu and the cells were incubated at 37 °C for 30 min. prior to fixation. The cells were washed twice with PBS and detached from the surface of the dish by incubating with 0.05% trypsin-EDTA in PBS (Gibco) for 5 min. A IFA buffer was added to a total volume 10 ml. The cells were transferred to a falcon tube and centrifuged at 1,000 rpm for 5 min at room temperature. The supernatant was aspirated, leaving 0.5 ml behind in which the cells were resuspended. 4.5 ml of ice-cold 70% ethanol was added dropwise while

shaking at a low speed using a vortexer. The cells were incubated on ice for 30 min and the centrifuged at 1,000 rpm for 5 min at 4 °C. Again, the supernatant was removed, leaving 0.5 ml behind in which the cells were resuspended. 4.5 ml of ice-cold 70% ethanol was added dropwise while shaking and the cells were incubated on ice for a further 30 min. Cells were stored at -20 °C if the flow cytometry was to be carried out on a different day. Before analysis by flow cytometry, the fixed cells were warmed to 4 °C if frozen. For univariate flow cytometry, the cells were washed once with ice-cold PBS, resuspended in 1 ml of PI staining solution and incubated at room temperature for a minimum of 30 min. For bivariate flow cytometry, the cells were washed once with ice-cold PBS, resuspended in 1 ml of ice-cold wash buffer and transferred to an eppendorf tube. The cells were centrifuged at 2,200 rpm for 5 min at 4 °C. The supernatant was aspirated and the cells were resuspended in 1 ml of 2M HCl. After incubating at room temperature for 20 min, the cells were washed twice with ice-cold wash buffer by centrifuging at 2,200 rpm between washes and resuspended in 0.5 ml of 0.1 M sodium borate at pH 8.5 in order to neutralise any residual acid for 2-3 min. The cells were washed once with ice-cold wash buffer and resuspended in 100 µl of ice-cold dilution buffer. Rat monoclonal anti-BrdU primary antibody (Abcam) was added at a 1:50 dilution and the cells were

incubated at room temperature for 30 min and then at 4 °C for 30 min with occasional mixing. The cells were washed three times with ice-cold wash buffer by centrifuging at 2,200 rpm between washes and resuspended in 1 ml of ice-cold dilution buffer. Alexa Fluor<sup>®</sup> 488 goat anti-rat secondary antibody (Invitrogen) was added at a 1:50 dilution. The cells were protected from light and incubated at 4 °C for 1 h with occasional mixing. The cells were washed three times with ice-cold wash buffer by centrifuging at 2,200 rpm between washes. Finally, 1 ml of PI stain was added to cells and incubated at room temperature for a minimum of 30 min. Samples were analysed using a BD Bioscience LSR II flow cytometer at the Medical school and Stem cell facility, Department of Biomedical Science, University of Sheffield. The data analysis was performed using Flowjo software. Cells were irradiated with a blue laser and the emission measured at 660 nm for PI and 530 nm for Alexa Fluor<sup>®</sup> 488.

### **2.2.6 Immuno-isolation (I-i) of Flag-tagged SLBP**

Immuno-isolation of Flag-tagged SLBP using ANTI-FLAG<sup>®</sup> M2 Affinity resin (Sigma-Aldrich). This is a monoclonal antibody covalently attached to agarose resin (Technical bulletin, Sigma-Aldrich, product number A2220). Lysates were generated from Flp-In-HeLa cells stably transfected with Flag-tagged SLBP grown in the presence of doxycycline (15 cm dish) (70% confluent) treated or untreated with 5 mM HU (to induce replication stress) for 20 min. 1 mg lysate in a total volume of 1 ml lysis buffer was incubated with 40 µl anti-FLAG M2 Affinity Gel for each I-i experiment. The samples were rotated at 4 °C overnight. After protein binding, the supernatant was retained as “depleted lysates” and the resin was washed three times with 0.5 ml TBS. Bound protein can elute with 3X FLAG peptide, 0.1 M glycine HCl, pH 3.5 or SDS-PAGE Sample Buffer, depending on the experiment. For 3X FLAG peptide elution, 100 µl of 3X FLAG elution solution (300 ng/µl final concentration was diluted from 25 µg/µl of 3X FLAG stock solution) was added to each sample. The sample was incubated with gentle shaking for 1 h at 4 °C. The resin was centrifuged for 30 sec at 8,000 rpm and then the supernatant was transferred to fresh tubes. For 0.1 M glycine HCl, pH 3.5 elution, 100 µl of 0.1 M glycine

HCl, pH 3.5 was added to each sample. The sample was incubated with gentle shaking for 5 min at room temperature. The supernatant was removed after centrifugation at 8,000 rpm for 30 sec at 4 °C and the pH returned to neutral by transferring the supernatant to fresh tubes containing 10 µl of 0.5M Tris HCL, pH 7.4. For SDS-PAGE Sample Buffer elution, 20 µl of 2x gel loading buffer was added to each sample. The sample was boiled for 5 min and spined down for 30 sec at 4 °C. Then, the supernatant was transferred to fresh tubes. All supernatant were stored at -20 °C until further analysis by SDS-PAGE, western blotting or mass spectrometry.

## **2.2.7 Protein purification**

### **2.2.7.1 Preparation of recombinant GST-SLBP-6xHis**

The modified pGEX-6P-1 plasmid (termed pGEX6SLBPHIS) encoding the GST-SLBP-6xHis fusion protein was transformed into *E. coli* strain BL21 DE3 pLysS. 5 ml of LB medium containing 100 µg/ml ampicillin was inoculated with a single colony of transforming bacteria. The bacteria were then incubated overnight at 37°C with shaking at 225 rpm before being transferred to 100 ml of LB/ampicillin until the culture reached an  $OD_{600} = 0.4$ . Recombinant protein expression was induced with 1 mM IPTG with cultures maintained either at 30 °C

or 37 °C until each culture reached  $OD_{600} = 1.2$ . For a pilot 100 ml of culture, bacteria were harvested by centrifuging at 3,000 rpm for 3 min. The supernatant was discarded. The pellet was re-suspended in 25 ml of 0.9% NaCl and re-centrifuged again. The bacteria cells were re-suspended in 10 ml of buffer A and were left on ice for 30 min. The suspension was diluted with 1 ml of buffer B and was kept on ice for 1 h. The suspension was then added 0.1% (by weight) sodium deoxycholate, 10 mM  $MgCl_2$  and 25  $\mu$ l DnaseI (stock 2,000 U/ml) and was also kept on ice for 15 min until suspension was no longer viscous. The lysate was clarified by centrifugation at 13,000 rpm for 30 min. The supernatant was aspirated (~1.5 ml). 80  $\mu$ l of packed glutathione agarose beads were added to the lysate and incubated 45 min. at 4°C on a rotating wheel. To isolate GST-tagged protein, the washed glutathione agarose beads were washed five times with buffer C and then GST-SLBP-6xHis was eluted three times with buffer C containing 5 mM glutathione, pH 8.0.

For large scale, 4 litres of culture was added 3 ml of packed glutathione agarose and the washed glutathione agarose beads were added to the clarified lysate and incubated for 1 h at 4 °C on a rotating wheel.

## **2.2.8 RNA techniques**

### **2.2.8.1 Phenol-chloroform RNA extraction**

Cells were washed twice in PBS before addition of 1 ml of TRI reagent (Sigma) and incubated for 5 min. Cells were detached by pipetting up and down and transferred to new eppendorf tube. 0.2 ml of chloroform was added to eppendorf tube, vortexed for 20 sec and then centrifuged at 12,000 rpm for 15 min at 4 °C. The colourless upper aqueous phase was taken to a clean eppendorf tube and 0.5 ml of isopropanol added. The mixture was inverted for a few times, incubated for 10 min at room temperature and then centrifuged at 12,000 rpm for 10 min at 4 °C. The supernatant was aspirated. The RNA pellet was washed with 70% ethanol and centrifuged at 8,000 rpm for 5 min at 4 °C. The supernatant was aspirated again and the RNA pellet was air-dried in fume hood. 20 µl of Rnase-free water was added to the dried RNA pellet. RNA concentration was determined by absorbance measurement at 260 nm using a NanoDrop ND-1000 spectrophotometer and samples were stored at -20 °C.

### **2.2.8.2 Reverse transcription**

For the analysis of histone mRNA decay, RNA (2 µg per reaction) was reverse transcribed using the High Capacity RNA-to-cDNA Kit (Applied Biosystems). The total reaction volume was made up to 20 µl with RNase-free water. The mixture was incubated at 37 °C for 1 h and then 95 °C for 5 min. cDNA was quantified using a NanoDrop ND-1000 spectrophotometer and samples were stored at -20 °C.

### **2.2.8.3 Quantitative real-time PCR (qPCR)**

qPCR was carried out using Bio-Rad C1000 Touch thermal cycler with a CFX96 real-time PCR detection system. The master mix reaction containing 5 µl of SYBR Green JumpStart Taq ReadyMix (Sigma-Aldrich), 0.1 µl (100 µM stock solution) of forward and reverse primers (Invitrogen) and water to a total volume of 9 µl were added each to the wells of a 96-well qPCR plate. 10 µg of cDNA was diluted with water to a concentration of 100 ng/µl and 1 µl of the 100 ng/µl solution was added to the wells. The plates were sealed with StarSeal polyolefin film (STARLAB). The target cDNA was amplified using a program consisting of 40 cycles. The cycling parameters were as follow.

Segment	Cycles	Temperature	Time
1	1	94 °C	2 min
2	39	94 °C	15 sec
		64 °C	30 sec

Each sample was analysed in triplicate. The results were quantified by comparison to a standard curve made by combining cDNA from all samples and analysing serial dilutions on the qPCR plate. A well containing no template was included to check for contamination and the formation of primer-dimers. Control targets (GAPDH) were amplified to allow for variations in plate loading. The data was analysed using Microsoft Excel, Prism and Bio-Rad CFX manager softwares.

#### **2.2.8.4 Analysis of alternative mRNA splicing**

The analysis of alternative splicing by PCR amplification using cDNA as a template, primers as shown in Rattray *et al.* (2013). The PCR components contained final concentration; 0.5 µM of forward and reverse primers, 1x Phusion<sup>®</sup> buffer contained and Phusion<sup>®</sup> High-Fidelity DNA Polymerase (NEB) and 100 ng cDNA template. PCR reaction was performed for 30 sec at 98°C, followed by 35 cycles of 10

sec at 98°C, 30 sec at 64°C and 1 min 72°C, followed by a final 10 min at 72°C. The PCR products were electrophoresed on 1.5% agarose gel.

## **2.2.9 The Wee1 kinase assay**

### **2.2.9.1 Isolation of the substrate**

The immuno-isolation of Flag-SLBP<sup>res</sup> (SLBPwt) and Flag-SLBP<sup>resS182E</sup> were performed as described in section 2.2.6. However, the lysis buffer was prepared in the absence of phosphatase inhibitors. After overnight incubation with ANTI-FLAG<sup>®</sup> M2 Affinity resin, the mixture was treated with 5 µl of lambda phosphatase in 1x lambda phosphatase buffer at 30 °C 10 min with mild shaking. The beads were washed with lysis buffer containing phosphatase inhibitor before eluting with kinase assay buffer without phosphatase inhibitors and 3X FLAG peptide.

### **2.2.9.2 Kinase assay**

Before the experiment, 1 mM ATP (containing radioactive (gamma-32P) ATP at 10<sup>6</sup> cpm per nmol) was prepared, the WEE1 and kinase assay buffer were added into 1.5 ml microcentrifuge tube. The reactions were started by adding 2 µl of 10 mM Mg acetate and 1 mM ATP (containing radioactive (gamma-32P) ATP at 10<sup>6</sup> cpm per nmol).

The tubes were incubated at 30 °C for 30 min. The reactions were stopped by adding 5 µl of 5x SDS loading buffer and run out on the SDS-polyacrylamide gel electrophoresis as described in section 2.2.4.3. The gel was dried on a Whatman 3.0 paper, and the the dry gel was exposed to an autoradiogram. The cassette was kept at -80 °C for overnight or the desired time.

## **2.2.10 Proteomic techniques**

### **2.2.10.1 InstantBlue™ staining compatible with mass spectrometry**

After SDS-polyacrylamide gel electrophoresis, gels were directly stained for 2 h or overnight with InstantBlue™ staining (Expedeon). Following this, gels were left in Milli-Q water until further processed.

### **2.2.10.2 In-gel Digestion**

#### **2.2.10.2.1 Band excision and destaining**

The bands of interest were excised into pieces with a clean scalpel and transferred the gel pieces into Sterilin™ 1.5 ml microcentrifuge tubes. The gel pieces were washed with 200 µl of solution 1 and incubated at 37 °C for 30 min. The supernatants were discarded and this

step was repeated again. The gel pieces were dried down in vacuum concentrator for 30 min.

#### **2.2.10.2.2 Reduction and alkylation of protein**

(see Appendix A for the component of solution)

In this step, gels were reduced with freshly prepared of 1mM DTT in solution 2. The gels were incubated at 56 °C for 1 h. The supernatants were regarded. The gels were alkylated with 2 mM IAA in solution 2 at room temperature for 30 min in the dark. Then the gels were washed twice with 200 µl of solution 2 for 15 min. 200 µl of solution 3 was used to wash gels at 37 °C for 15 min. The liquid was removed by centrifugation at 13,000 rpm for 10 sec. Once the liquid was discarded the gel slices were dried down in vacuum concentrator for 30 min.

#### **2.2.10.2.3 Enzymatic digestion**

Before digestion, enzymes were prepared working stock at a concentration of 0.02 µg/ml trypsin (NEB), 0.025 µg/ml chymotrypsin (NEB) and 0.02 µg/ml elastase (NEB). To perform digestion, dried gel slices were incubated with enzymes at a final concentration of 1 ng/µl in solution 4 at 37 °C overnight.

#### **2.2.10.2.4 Peptide extraction from gel slices**

Next day, the gels were centrifuged at 13,000 rpm for 10 sec. The supernatants were collected into new Sterilin™ 1.5 ml microcentrifuge tubes. Further extraction of peptides was performed by incubating the gel slices with 20 µl of solution 5 at 37 °C for 15 min. 50 µl of solution 6 was added to the gel pieces and incubated at 37 °C for 15 min. The supernatants were collected into the same tubes as stated before. This step was repeated once. After a further repetition of this step, gel slices were incubated with 50 µl of solution 7 at 37 °C for 30 min followed by the collection of supernatants into the tubes. Extracted peptides were dried down using a SpeedVac concentrator overnight on low heat and then stored at -20 °C. Before the analysis by LC-MS/MS the peptides were resuspended in 0.5% formic acid at room temperature for 10 min. with gentle shaking.

#### **2.2.10.3 HLBP-mass spectrometry setting**

Resuspended peptides were injected by using a Dionex Ultimate 3000 uHPLC onto a PepMap100 C18 2 cm x 75 µm I.D. trap column (ThermoFisher Scientific) at 5µl/min in 0.1% formic acid, 2% acetonitrile and 45 °C in the column oven and 6 °C in the autosampler. The sample was separated over a 60-minute gradient of increasing

acetonitrile from 2.4% up to 72%, in 0.1% formic acid, using a 15 cm PepMap100 C18 analytical column (2  $\mu\text{m}$  particle size, 100  $\text{\AA}$  pore size 75  $\mu\text{m}$  I.D.) (ThermoFisher Scientific) at 300 nl/min and 45  $^{\circ}\text{C}$ .

The mass spectrometer analyzer used was an ETD (electron transfer dissociation) enabled ThermoFisher-Scientific Orbitrap Elite, equipped with a Nanospray Flex Ion ESI source (ThermoFisher Scientific). Nanospray ionization was carried out at 2.3 kV, with the ion transfer capillary at 250  $^{\circ}\text{C}$ , and S-lens setting of 60%. MS1 spectra were acquired at a resolving power of 60,000 with an AGC (automatic gain control) target value of  $1 \times 10^6$  ions by the Orbitrap detector, with a range of 350-1850 m/z. Following MS1 analysis the top 10 or top 15 (depend on experiment) most abundant precursors were selected for data dependant activation (MS2 analysis) using CID (collision induced dissociation), with a 10 ms activation time, and an AGC setting of 10,000 ions in the dual cell linear ion trap on normal scan rate resolution. Precursor ions of single charge were rejected, and a 30 second dynamic exclusion window setting was used after a single occurrence of an ion.

#### **2.2.10.4 Data analysis**

Data analysis was performed using different software analysis because a new staff was positioned during my study.

Proteome Discoverer (PD) version 1.4.1.14 with Mascot search engine was used to identify peptides that contain phosphorylated residues (Brosch *et al.*, 2009) including serine/threonine (ST) phosphorylation with high mass accuracy (within 100 ppm) in Chapters 4 and 5. For peptide-spectrum matches (PSM) scoring, false discovery rates (FDRs) for peptides medium-confidence peptide hits (actual relaxed) was set at 0.05 and for peptides high-confidence peptide hits (actual strict) was set at 0.01.

MaxQuant (MQ) version 1.5.5.1 was used to analyse SILAC proteomic analysis. For protein identification, false discovery rates (FDRs) at both the protein and peptide levels were set at 1% by decoy database searching. Proteins with 3 valid intensity values in the Flag-tagged SLBP immuno-isolation were considered for quantification. The statistical analysis was then performed by t-testing with correction for multiple hypothesis testing at two thresholds, 0.05 (5% FDR) and 0.01 (1% FDR). Proteins required a minimum of two peptides or above in order to be reported. Perseus version 1.5.5.3 was used to analysed the statistical significant among 3 independent experiments.

## **2.3 References**

- Bradford, M.M. 1976. A Rapid and Sensitive Method for the Quantitation of Microgram Quantities of Protein Utilizing the Principle of Protein-Dye Binding. *Anal. Biochem.* 72: 248-254.
- Laemmli, U.K. 1970. Cleavage of Structural Proteins during the Assembly of the Head of Bacteriophage T4. *Nature.* 227(5259): 680-685.
- Sambrook, J. and Russell, D. 2001. *Molecular Cloning: A Laboratory Manual*, 3rd edn. Cold Spring Harbor, NY: Cold Spring Harbor Laboratory Press.

# *Chapter 3*

## *Development of a model system for analysis of SLBP in a model cell line*

### **3.1 Introduction**

In order to achieve the aims of this project, it was necessary to develop a tractable model system to investigate SLBP function. I initially used a transient transfection approach to determine levels of transient expression of untagged and tagged forms of SLBP. I therefore created SLBP expression construct in two distinct vectors. pCI-neo and pCMV-Tag 2A plasmids were used to express untagged and Flag-tagged SLBP proteins, respectively. Each plasmid containing SLBP was transiently transfected in HeLa cells and I found that unlike untagged SLBP, expression levels of tagged SLBP were low and could not be directly compared with endogenous levels. Due to the limitations of transient SLBP expression, I subsequently decided to establish a stable transfection Flag- and HA-tagged SLBP in HeLa cells by using the Flp-In™ T-Rex™ system. This system provides the means for the

generation of isogenic, stable expression and inducible stable cell lines with a rapid and efficient expression

([https://tools.thermofisher.com/content/sfs/manuals/flpinsystem\\_man.pdf](https://tools.thermofisher.com/content/sfs/manuals/flpinsystem_man.pdf)).

In the experiment described in this chapter therefore, I have set out to (i) determine whether inducible expression of tagged siRNA-resistant SLBP affected cell cycle progression (ii) establish that the induced form was resistant to siRNA targeting the wild-type mRNA and (iii) investigate SLBP mediated cellular function in cells solely expressing tagged siRNA resistant SLBP, specially the application of DNA replication stress, histone mRNA degradation and alternative mRNA splicing of SLBP.

Here, I demonstrate the construction and validation of that stable transfection Flp-In system and establish it has significant advantages over the use of transient transfection. Furthermore, I show that the inducible Flag- and HA-tagged SLBP protein is expressed in a manner similar to that of endogenous SLBP throughout cell cycle progression. Importantly, although both tagged versions showed slightly different profiles of degradation, the time required to observed degradation of SLBP was similar in both cases (~12 h). Therefore, only Flag-tagged

SLBP was subsequently used in this study, due to time limits unless otherwise stated.

## **3.2 Results**

### **3.2.1 Transient transfection of untagged and Flag-tagged SLBP in HeLa cells**

In order to construct SLBP expression vectors, cDNA was generated by reverse transcription of HeLa cell total RNA as described in section 2.2.1.1. This was used as a template for PCR amplification of wild-type SLBP cDNA. SLBP cDNA was generated following optimization of PCR amplification by utilising a range of annealing temperature between 60 °C and 70 °C as described in section 2.2.1.1. The optimal annealing temperature at 61°C showed an appropriate size of SLBP product, suggesting that optimised PCR conditions generated products consistent with the predicted size of full length SLBP cDNA (813 bp) (Figure 3.1). Annealing temperatures higher than 61 °C resulted in amplification of multiple PCR products with sizes inconsistent with the predicted for the expected specific product (data not shown). Figure 3.1 shows both PCR products obtained after gel electrophoresis using PCR primers designed to be compatible with each vector, the sequences of which were described in Appendices C and D. Each PCR

product was purified, and sub-cloned into pCI-neo and pCMV-Tag 2A plasmids as described in section 2.2.1. Each plasmid was verified by DNA sequencing (data not shown).

Transient transfection of untagged and Flag-tagged SLBP constructs was undertaken in HeLa cells, and expression of SLBP was analysed by western blotting of lysates as described in section 2.2.4.4 derived from transfected cells. The results indicated in Figure 3.2 showed that SLBP expression was detected following transfection with either plasmids as a band of the expected molecular weight (~30 kDa), although the levels of expression of the untagged form appeared to be far greater than that of the tagged protein. Detection of the endogenous protein was not observed under these conditions, presumably because the endogenous levels of SLBP expression are considerably lower than the levels observed following transient transfection of either constructs. However, the reason for the difference in expression levels is not known. The lower level of Flag-tagged SLBP could be a result of increased instability of the tagged protein, due to steric hindrance affecting protein folding or variation in expression arising from site of plasmid integration. An important concern was that utilising transient transfection for further study might generate large differences in

expression level among the individual cells within a population, which might interfere with the overall analysis.

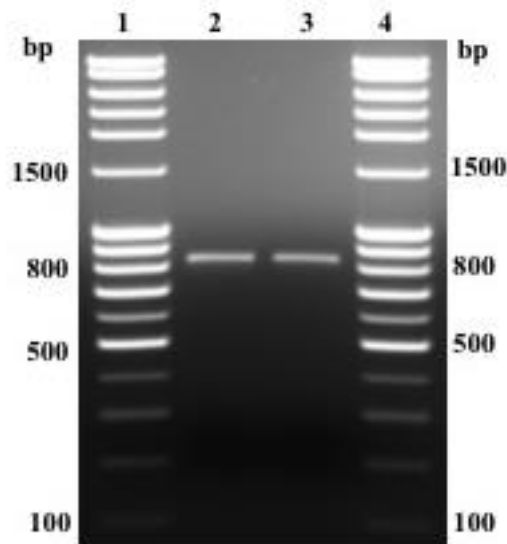
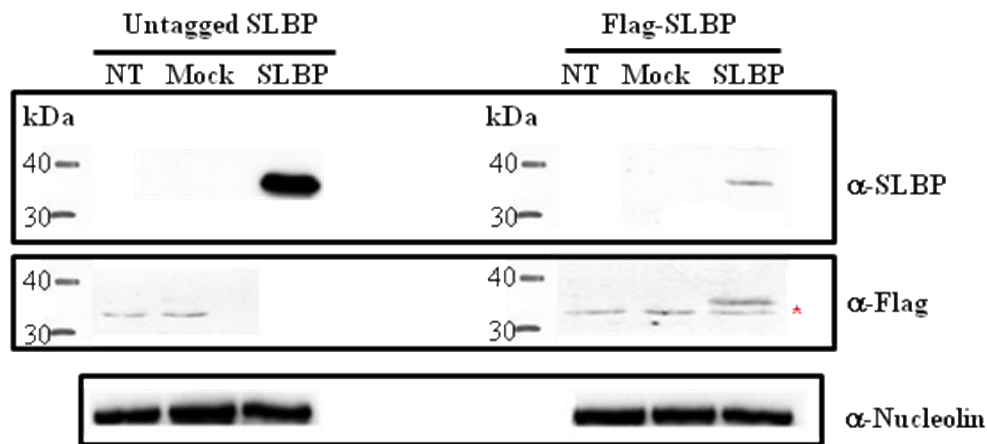


**Figure 3.1** DNA gel electrophoresis of SLBP PCR products.

PCR products obtained using annealing temperature ( $T_m$ ) at 61°C for both untagged vector (lane 2) and Flag-tagged vector (lane 3) were electrophoresed on a 1.5% agarose gel and visualised under UV light using a photographed and analysed with Uvitech UviProchemi camera system (as described in section 2.2.1.9). Lanes 1 and 5 contained DNA molecular size ladder (Norgen FullRanger 100 bp DNA ladder, Norgen Biotek Corp.).



**NT : non-transfected**

**Mock : cells transfected with empty plasmid**

**Figure 3.2** Western blot detection of untagged SLBP, and Flag-tagged SLBP proteins expressed in HeLa cells after transient transfection of pCI-Neo-SLBP (left hand side) and pCMV-Tag2a-SLBP (right hand side) for 24 h.

Cell lysates (50  $\mu$ g of protein) were subjected to 12% SDS-PAGE and analysed by western blotting with anti-SLBP (top panel), anti-Flag (middle panel), and anti-nucleolin antibody (bottom panel) as loading control. NT, non-transfected; M, mock (cells transfected with empty plasmid); SLBP, lysates from cells transfected with appropriate recombinant plasmid (\* = non-specific bands).

Consequently, I decided to create stable cell lines expressing physiologically relevant levels of SLBP, expressing Flag- and HA-tagged SLBP using FLP recombinase technology that allows the stable integration of any given gene into a single site in the genome (O'Gorman *et al.*, 1991).

### **3.2.2 Developing a stable cell line model for inducible siRNA-resistant expression of Flag- and HA-tagged SLBP in HeLa cells using the Flp-In<sup>TM</sup> T-Rex<sup>TM</sup> system**

The generation of a Flp-In<sup>TM</sup> T-Rex<sup>TM</sup> expression cell line requires the integration of two plasmids, one (pOG44) containing a *Flp* Recombination Target (FRT) site and the other (pcDNA<sup>TM</sup>5/FRT/TO) expression vector into which the gene of interest is cloned under the control of the human cytomegalovirus (CMV) immediate-early promoter (Figure 3.3). A HeLa cell line containing a single integrated FRT site was kindly provided by Dr. P. Eyers (University of Liverpool). The line was generated by transfecting HeLa cells with the pFRT/*lacZeo* vector and pcDNA6/TR plasmid. The pFRT/*lacZeo* vector expresses a *lacZ*-Zeocin fusion gene controlled by the early SV40 promoter, and containing a single FRT site (O'Gorman *et al.*, 1991). The Zeocin-

resistant clones were screened by the Evers lab to identify one containing a single integrated FRT site. The pcDNA6/TR plasmid constitutively expresses the Tet repressor (tetR) under the control of the human CMV promoter. However, upon the addition of doxycycline (Dox), derivative of tetracycline, Tet repressor is inactive and Tet operator (TetO2) is active which allow the induction of Flag-SLBP transcription (Figure 3.4). The Flp-In cell system allows one to generate isogenic, stable cell lines inducibly expressing a gene of interest under the control of a doxycycline-dependent promoter. Therefore, protein expression, once expression is induced, is constant across a population of cells. This system has a significant advantage over the use of transient transfection, in terms of opportunities for experimental manipulation and reproducibility of expression levels. The Flag- and HA-tagged SLBP DNA sequence (Appendix C) was integrated into a single genomic site in HeLa cells to generate a Flp-In stable cell line as described in section 2.2.3.2.

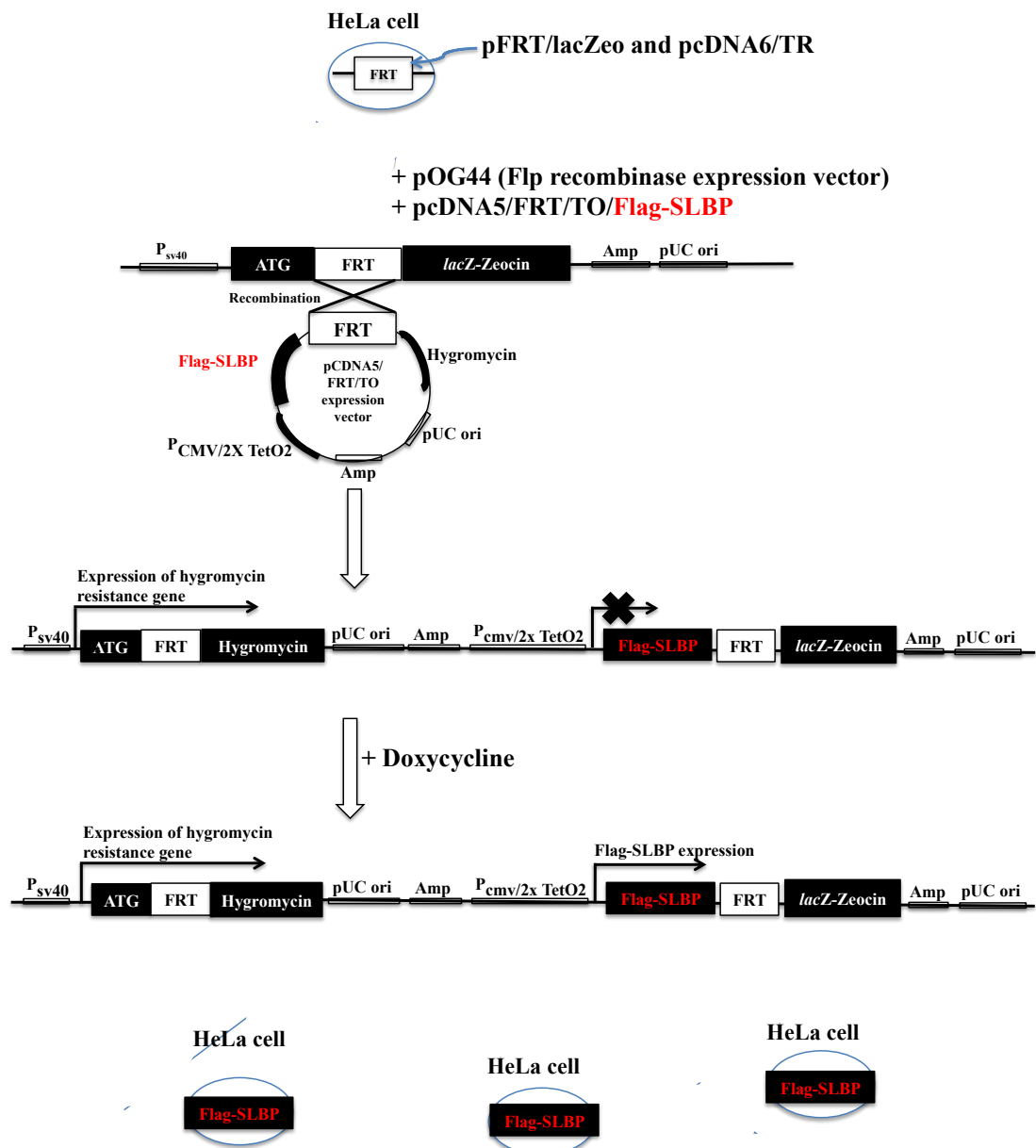


**Figure 3.3** Schematic diagram for the preparing of Flag-tagged SLBP HeLa stable cell lines by using Flp-In system (picture was adapted from [https://tools.thermofisher.com/content/sfs/manuals/flpinsystem\\_man.pdf](https://tools.thermofisher.com/content/sfs/manuals/flpinsystem_man.pdf)).

The Flp-In<sup>TM</sup> T-Rex<sup>TM</sup>-HeLa cell line (host cell) contains a single integrated FRT site and stably expresses the Tet repressor from the co-expression of pFRT/*lacZeo* and pcDNA6/TR. This cell line is used to generate the Flp-In<sup>TM</sup> T-Rex<sup>TM</sup>-HeLa expression cell line. The generation of a Flp-In<sup>TM</sup> T-Rex<sup>TM</sup> expression cell line requires the integration of two plasmids, one (pOG44) containing a *Flp* Recombination Target (FRT) site and the other (pcDNA5/FRT/TO) expression vector containing the gene of interest (Flag-SLBP). The Flp recombinase expressed from pOG44 catalyse a homologous recombination event between the FRT sites in the host cells and the pcDNA5/FRT/TO expression vector. The expression of Flag-SLBP is under the control of a tetracycline-regulated, hybrid human cytomegalovirus (CMV)/TetO<sub>2</sub> promoter. The selection of stable cell lines is selected by a hygromycin resistance gene. The expression of Flag-SLBP is repressed by the Tet repressor (TetR) which expresses from pcDNA6/TR. The addition of doxycycline induces Flag-SLBP expression by inactivation of the structure of TetR which allows the Tet operator to become active.

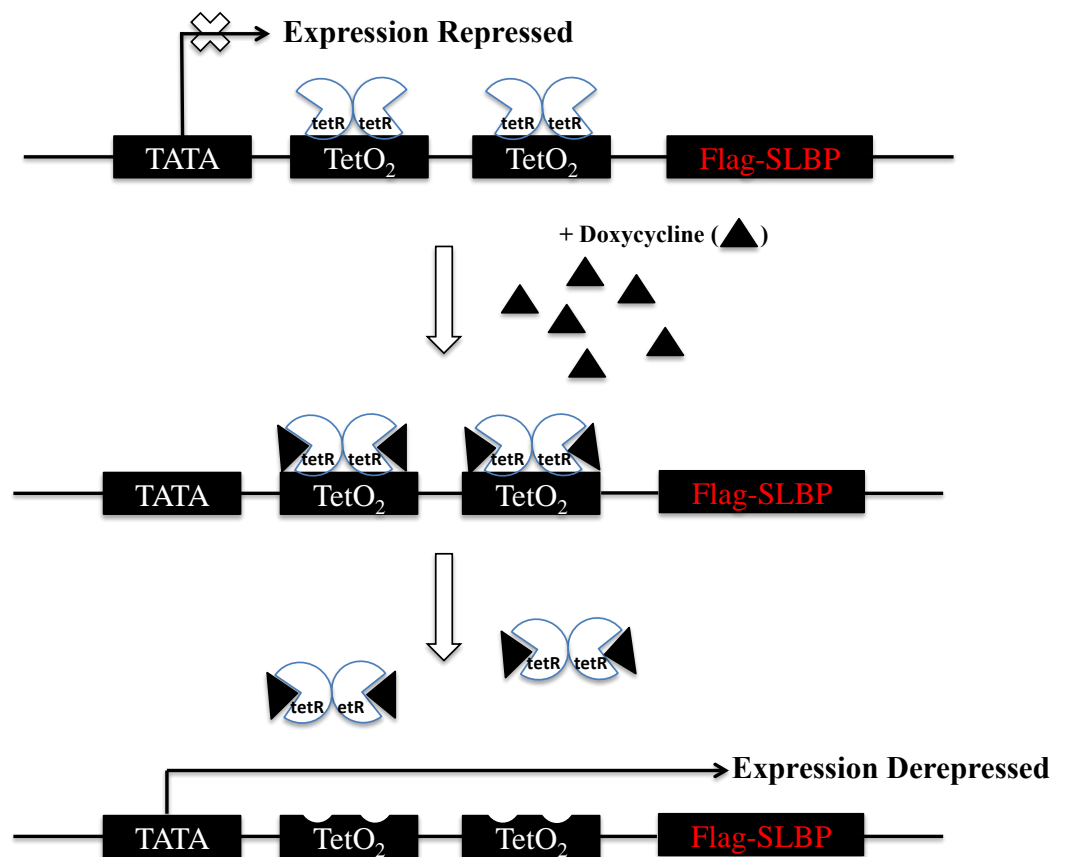


**Figure 3.4** Schematic diagram of doxycycline-mediated regulation of Flag-tagged SLBP in the Flp-In™ T-Rex™ system (picture was redrawn from [https://tools.thermofisher.com/content/sfs/manuals/flpinsystem\\_man.pdf](https://tools.thermofisher.com/content/sfs/manuals/flpinsystem_man.pdf)).

The Tet repressor is expressed from pcDNA6/TR plasmid which is under the control of the human CMV promoter. However, the homologous recombination event between the FRT sites in the Flp-In™ T-Rex™ HeLa host cell line and the pcDNA5/FRT/TO which contain the *tet*

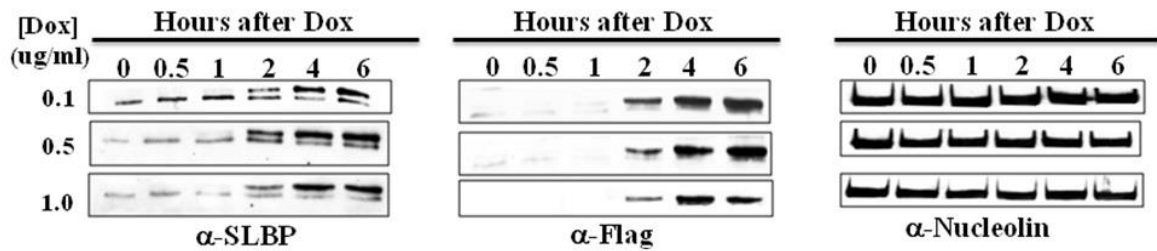
operator2 (TetO<sub>2</sub>) confers regulation by tetracyclin or doxycycline on the CMV promoter. In the Tet repressor-operator system, the tetracycline repressor protein (TetR) binds to the Tet operator sequence (TetO) and inhibits transcription of downstream elements. Addition of doxycycline (Dox), a tetracycline derivative, which is more stable than tetracycline in cell culture, allows a conformational change in the repressor structure. This releases complexes from the promoter and allows the transcription of Flag- tagged SLBP or HA-tagged SLBP.

### **3.2.3 Optimization conditions for doxycycline-induced expression of Flag- and HA-tagged SLBP**

The aim of this part of the work was to determine conditions under which the level of Flag- and HA-tagged SLBP expression was similar to that of the endogenous expressed protein. Moreover, it was also to determine the similarities and differences between the level of Flag- and HA-tagged SLBP expression. To do this, I analysed Flag- and HA-tagged SLBP expression levels in cell lysates by western blotting, after cells were treated with either a range of Dox concentrations ranging from 0.1 to 1.0 µg/ml, and for varying lengths of time up to 72 h. Then cells were harvested, lysates prepared and analysed by western blotting

(Figure 3.5 and 3.6). Dox treatment resulted in detectable amounts of HA-tagged and Flag-tagged protein after 1 h and 2 h, respectively. Over the 10-fold range of concentration of Dox used, there was little difference in the overall level of inducible expression of both forms of tagged protein. Both forms were expressed at slightly higher levels than the endogenous protein at all Dox concentrations tested after 2-6 h incubation (Figure 3.5A and 3.6A). The doublet bands reflect endogenous and tagged SLBP expression (Figure 3.5A). However, only tagged SLBP was detected after 8 h, probably due to the low expression level of endogenous SLBP. It is possible that cells respond to Dox treatment differently depending on the cell confluence or quiescent state. One example of such a circumstance would be contact inhibition which might affect expression pattern of cells (Abercrombie, 1970). After 24-72 h exposure to Dox, Flag- and HA-tagged SLBP level were reduced (Figure 3.5B and 3.6B). Importantly, this result confirms that there is no significant difference in Dox-inducible SLBP expression between either Flag- and HA-tags. In the subsequent experiments, induction of tagged SLBP was undertaken using 0.5  $\mu\text{g/ml}$  Dox for 5-6 h, unless otherwise stated. Where relevant, cells used either contain one integrated copy of either Flag-tagged SLBP (designated HeLa<sup>wtFlag-SLBP</sup>) or HA-tagged SLBP (HeLa<sup>wtHA-SLBP</sup>).

**A.**



**B.**

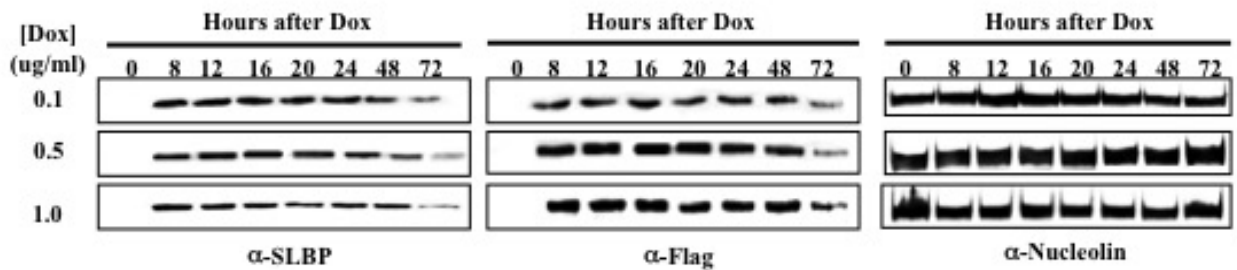


**Figure 3.5** Induction of the expression for Flag-tagged SLBP stably transfected in Flp-In-HeLa cells under control of the tetracycline regulatory system ( $Tet_{on}$ ). Cells treated with (A) 0-6 h and (B) 0-72 h Dox with different doses. The concentration of Dox and induction times varied from 0.1 to 1 µg/ml. Cell lysate samples (50 µg of protein) were subject to 12% SDS-PAGE and analyzed by immunoblotting with anti-SLBP and anti-Flag antibodies. Anti-nucleolin was used as loading control.

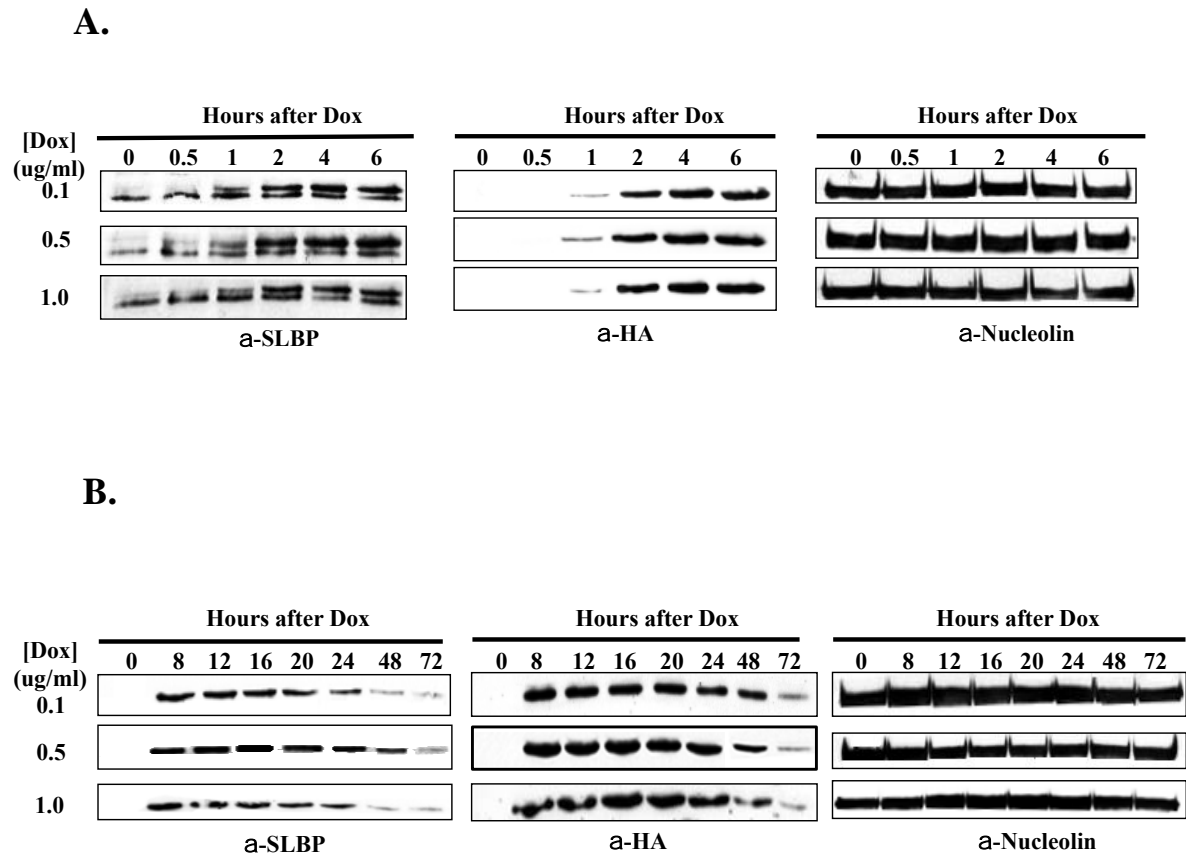


**Figure 3.6** Induction of the expression for HA-tagged SLBP stably transfected in Flp-In-HeLa cells under control of the tetracycline regulatory system ( $Tet_{on}$ ). Cells treated with (A) 0-6 h and (B) 0-72 h Dox with different doses. The concentration of Dox and induction times varied from 0.1 to 1 µg/ml. Cell lysate samples (50 µg of protein) were subject to 12% SDS-PAGE and analyzed by immunoblotting with anti-SLBP and anti-HA antibodies. Anti-nucleolin was used as loading control.

### **3.2.4 The effect of inducible expression of Flag- and HA-tagged SLBP on cell cycle progression**

In unmodified cells, SLBP expression is limited to S-phase and the protein is rapidly degraded at the end of S phase (Whitefield *et al.*, 2000). I wished to investigate whether up-regulation of Flag- or HA-tagged SLBP was restricted to the G1/S transition and also whether it was degraded at the end of S-phase. Additionally, it was important to determine whether inducible expression of either tag affected normal cell cycle progression and the expression levels of each as a function of cell cycle progression.

In order to synchronise the Flp-In HeLa cells, cells growing in asynchronous culture were treated with 40 ng/ $\mu$ l nocodazole (Noc) for 12 h and mitotic cells were isolated by shake-off (Figure 3.7, red line). Cells were then re-plated and exposed to either Dox-containing fresh medium or fresh medium without Dox for 5 h. At the times indicated in Figure 3.7A, cells were harvested and lysates were prepared and analysed by western blotting.

Strikingly, the expression of Flag-tagged SLBP protein coincided closely with the endogenous protein (Figure 3.8 right-hand panel and Figure 3.9). Significant up-regulation of protein levels coincided with cyclin A expression corresponding to the beginning of S-phase, with a

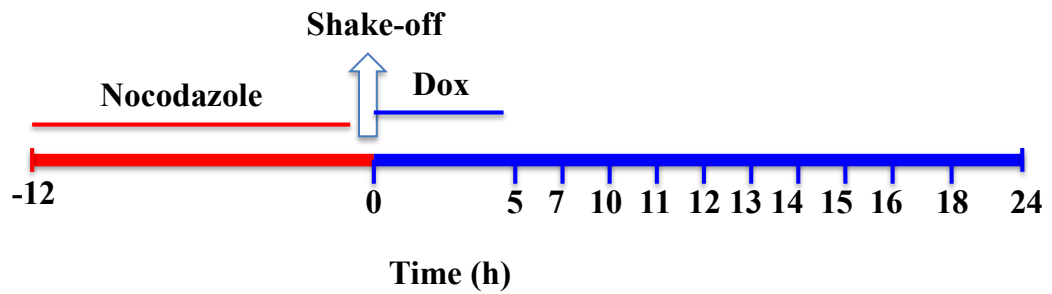
peak of expression just before 13 h after mitotic release. In addition, HA-tagged SLBP protein also coincided closely with the endogenous protein (Figure 3.11 right-hand panel and Figure 3.12), with a peak of expression after 13 h. However, both of the inducible tagged-SLBPs were gradually degraded ~16-18 h after release from Noc arrest.

In order to determine whether expression of either Flag- or HA-tagged SLBP affects cell cycle progression, samples of the synchronised cells were also analysed by flow cytometry following propidium iodide staining (Figure 3.10 and 3.13). The results showed that after cells were released from Noc-induced mitotic arrest, cells expressing either tagged version of SLBP progress through cell cycle at a similar rate to cells to which no Dox was added, suggesting that the ectopic expression of Flag- or HA-tagged SLBP do not affect cell cycle progression.

The cell cycle progression using fluorescence-activated cell sorter (FACS) analysis of both HeLa<sup>wtFlag-SLBP</sup> and HeLa<sup>wtHA-SLBP</sup> cells were similar to non-expressing cells. Taken together with the data reported above, these results indicate that the regulated timing of both the translation and the destruction of the Flag- and HA-tagged SLBP occurs normally in these cell line models. Additionally, although both tagged versions showed slightly different profiles of degradation, the time

required to observed degradation of SLBP was similar in both cases (~12 h) (Figure 3.14).

**A.**



**B.**

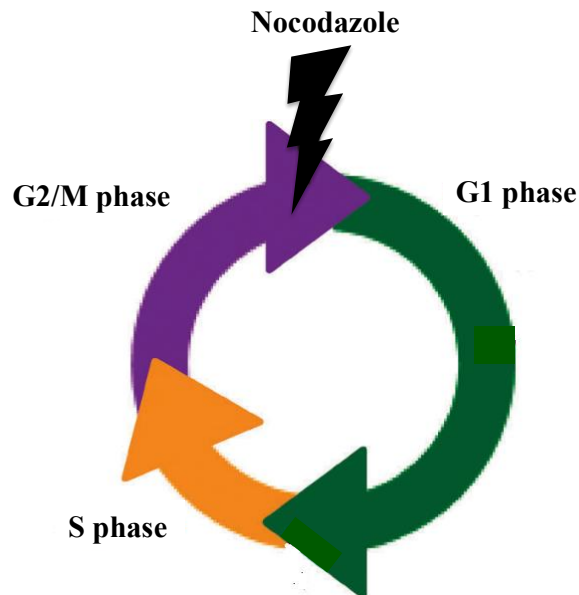


**Figure 3.7** Experimental timeline for cell synchronization and inducible expression of Flag-tagged SLBP (A) time indication of cell synchronisation with nocodazole (Noc) and Dox treatment (B) Cell cycle phase shows Noc treatment with synchronises cells in M phase.

When shake-off, cells start undergoing in M/G1 and early S phase which is consistent with the increase of SLBP level at the beginning of S phase.

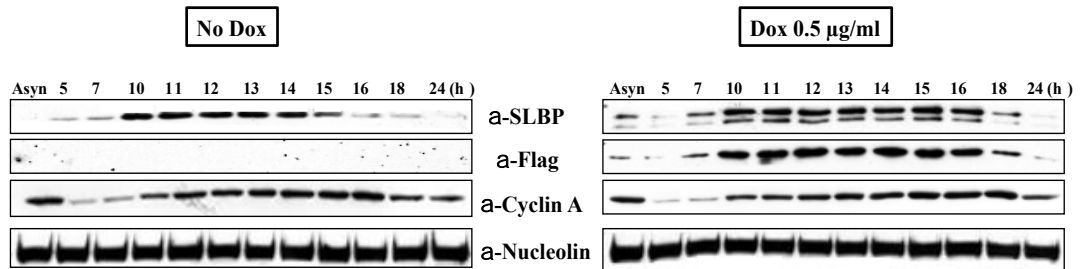


**Figure 3.8** Expression of Flag-tagged SLBP cells with and without Dox. Flag-tagged SLBP cells growing in asynchronous (Asyn) culture were treated with 40 ng/ $\mu$ l Noc for 12 h, mitotic cells were isolated by shake off (time = 0 h) and cells were replated with no Dox or 0.5  $\mu$ g/ml Dox for 5 h, and allowed to progress through the cell cycle for the indicated times. Lysates were subjected to 12% SDS-PAGE and analysed by western blotting followed by probing with the indicated antibodies.

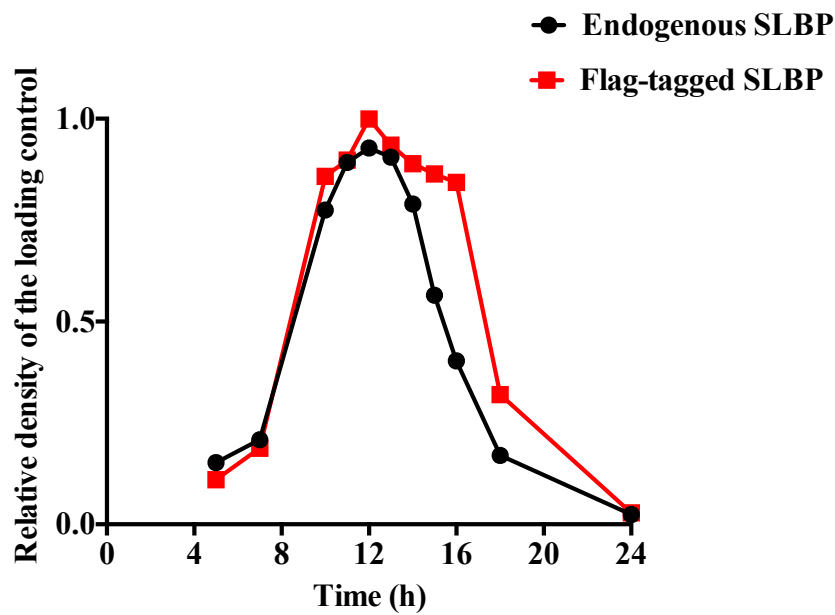


**Figure 3.9** Quantification of the expression of endogenous SLBP (black line) compared to Flag-tagged SLBP (red line) using ImageJ software. Protein levels are expressed relative to the density of the loading control.

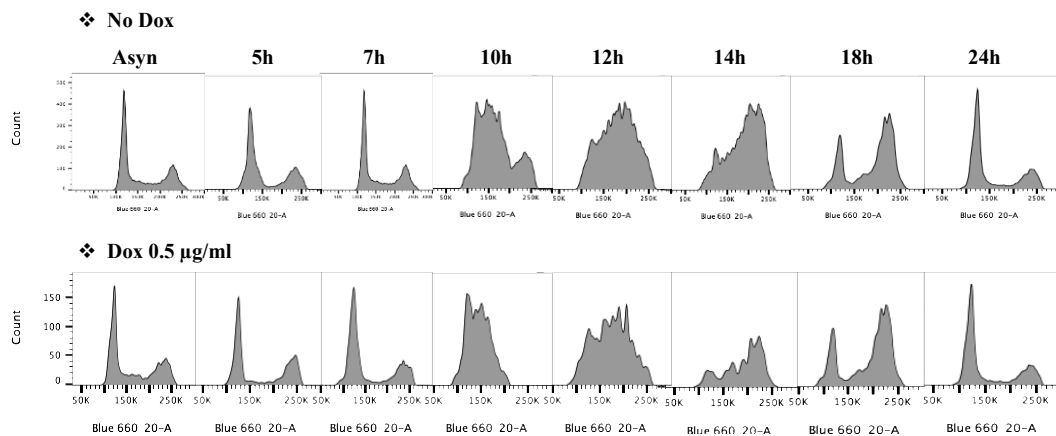


**Figure 3.10** FACS profiles of inducible Flag-tagged SLBP cells without Dox (top panel) and Dox-treated (lower panel) stained with PI at the indicated times after release from Noc arrest.

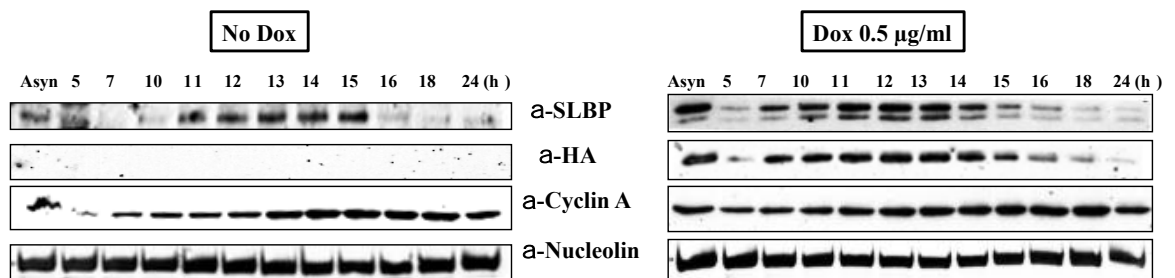


**Figure 3.11** Expression of HA-tagged SLBP cells with and without Dox. HA-tagged SLBP cells growing in Asyn culture were treated with 40 ng/ $\mu$ l Noc for 12 h, mitotic cells were isolated by shake off and cells were replated with no Dox or 0.5  $\mu$ g/ml Dox for 5 h, and allowed to progress through the cell cycle for the indicated times. Lysates were subjected to 12% SDS-PAGE and analysed by western blotting followed by probing with the indicated antibodies.

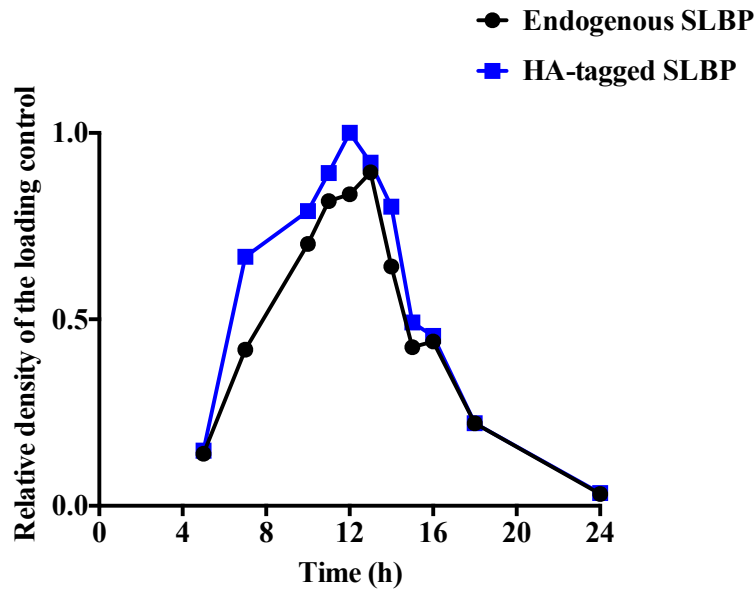


**Figure 3.12** Quantification of the expression of endogenous SLBP (black line) compared to HA-tagged SLBP (blue line) using ImageJ software. Protein levels are expressed relative to the density of the loading control. In a correlation analysis, the expression of endogenous SLBP showed a strong association ( $r = 0.97$ ) between Flag-tagged SLBP and HA-tagged SLBP during 24 h. The figure shows data from only one experiment.

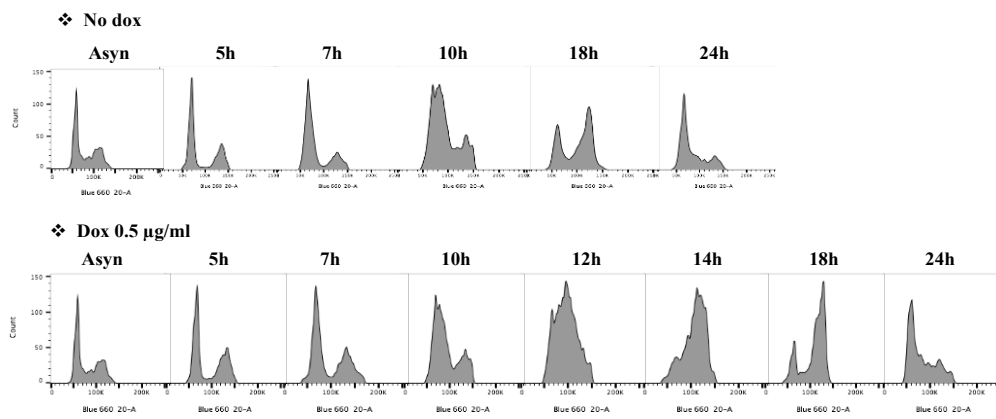


**Figure 3.13** FACS profiles of inducible HA-tagged SLBP cells without Dox (top panel) and Dox-treated (lower panel) stained with propidium iodide (PI) at the indicated times after release from Noc arrest.

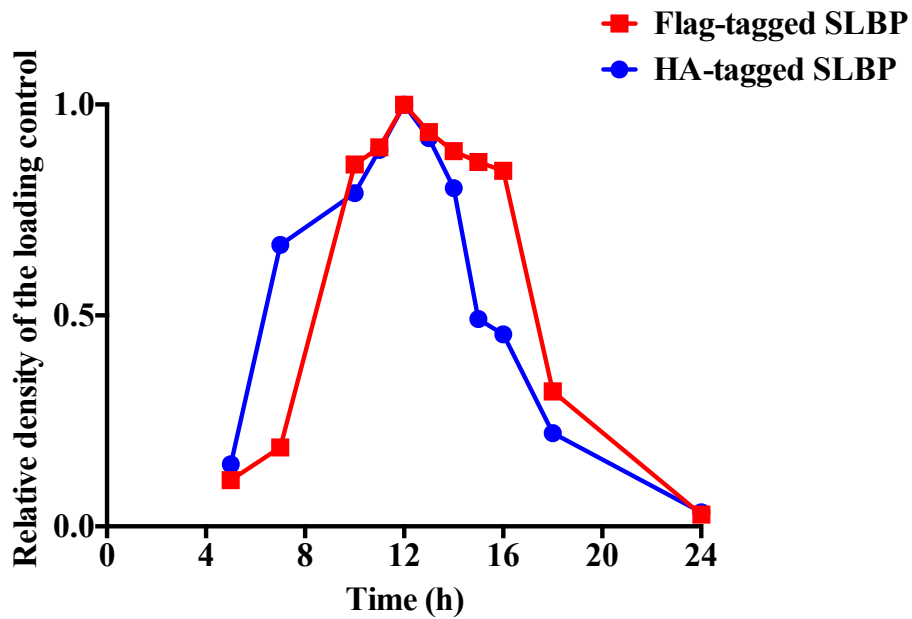


**Figure 3.14** Quantification of the expression of Flag-tagged SLBP (red line) compared to HA-tagged SLBP (blue line) using ImageJ software. Protein levels are expressed relative to the density of the loading control. In a correlation analysis, the expression of exogenous SLBP showed a strong association ( $r = 0.8$ ) between Flag-tagged SLBP and HA-tagged SLBP during 24 h. The picture shows data from only one experiment.

### **3.2.5 Ectopic expression of SLBP containing silent mutations is resistant to knockdown of endogenous protein using siRNAs directed against wild-type sequence**

In order to investigate the ability of the Flag- and HA-tagged SLBP to rescue cells lacking endogenous SLBP with siRNA-mediated knockdown, a Flp-In cell line inducibly expressing Flag-tagged SLBP and HA-tagged SLBP were established using a form of the SLBP gene containing two silent mutations (2M) in the sequence corresponding to that targeted by siRNA knockdown (Erkman *et al.*, 2005), referred to hereafter as Flag-SLBP<sup>res</sup> and HA-SLBP<sup>res</sup>, respectively (Figure 3.15).

In both the Flag-SLBP and Flag-SLBP<sup>res</sup> cell lines, together with HA-SLBP and HA-SLBP<sup>res</sup> cell lines, siRNA-mediated knockdown of endogenous SLBP were observed (Figure 3.16A and 3.16C, lanes 3-6). Following Dox induction, reduced expression of both tagged proteins was also observed in cells containing tagged wild-type SLBP sequence, but not in cells containing Flag-SLBP<sup>res</sup> and HA-SLBP<sup>res</sup> sequences (Figure 3.16A and C, compare upper band in lanes 4 and 6) which was consistent with the quantification of SLBP expression shown in Figure 3.16B and C. These demonstrate that the tagged version of Flag-SLBP<sup>res</sup> and HA-SLBP<sup>res</sup> are resistant to siRNA-induced knockdown of endogenous protein.

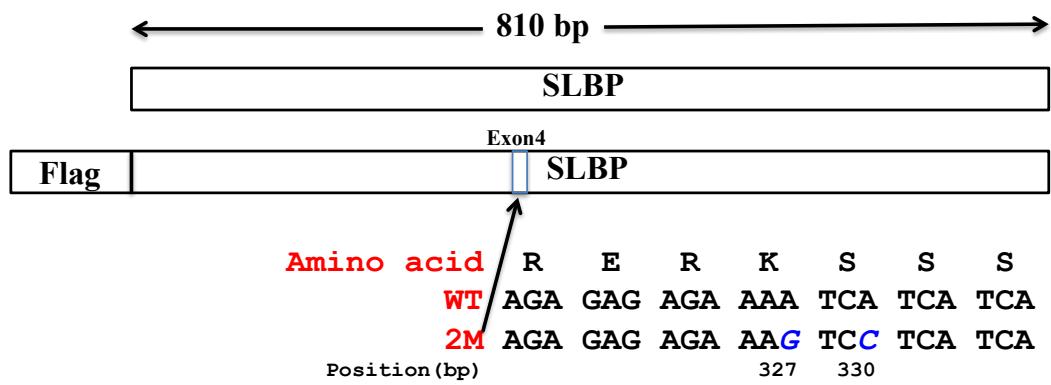


**Figure 3.15** Schematic representation of the Flag-SLBP<sup>res</sup>. The SLBP-siRNA target sequence is shown. Red/italic letters are mutated.

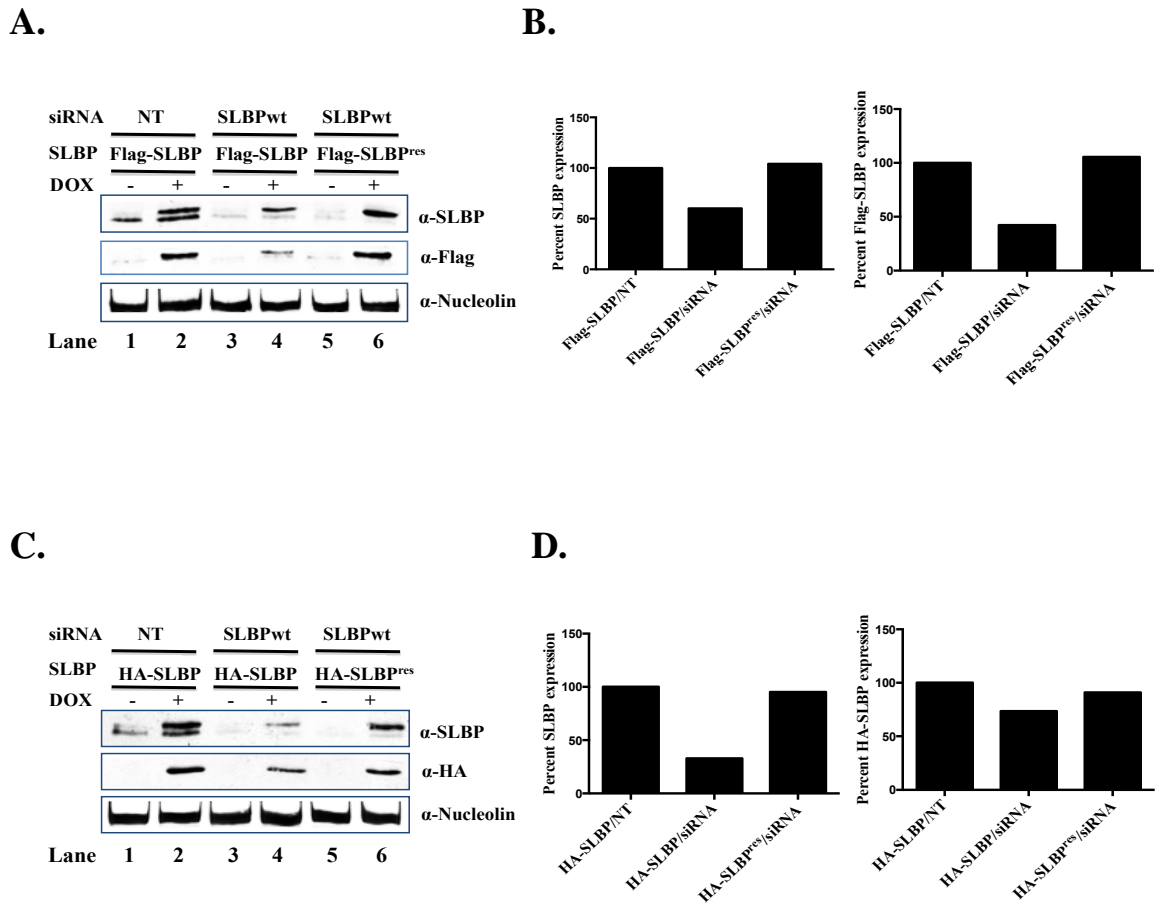


**Figure 3.16** Flag-SLBP<sup>res</sup> and HA-SLBP<sup>res</sup> resistant to siRNA-induced knockdown of endogenous protein.

The (A) Flag-SLBP and Flag-SLBP<sup>res</sup> expression and (C) HA-SLBP and HA-SLBP<sup>res</sup> expression (either wild-type (WT) or containing silent mutations (2M) in the SLBP sequence) treated with 200 nM non-targeting (NT) or SLBP siRNA for 24 h in the absence (-) or presence (+) of 0.5  $\mu$ g/ml Dox. Cell lysate (50  $\mu$ g of protein) were subjected to 12% SDS-PAGE and analyzed by western blotting with anti-SLBP and anti-Flag antibodies. Anti-nucleolin was used as a loading control. Quantification of SLBP expression with anti-SLBP and anti-Flag

antibodies correspond to lanes 2, 4 and 6 of **(B)** Flag-SLBP and **(D)** HA-SLBP.

Previous work has shown that small interfering RNA-induced knockdown of SLBP results in a delay in progression through S phase (Zhao *et al.*, 2004 ; Wagner *et al.*, 2005). In order to determine whether tagged SLBP constructs were sufficient to rescue SLBP function, progression through S-phase was monitored by FACS analysis in control, and Dox treated HA-SLBP<sup>res</sup> cells treated with SLBP siRNA for 72 h, and synchronized as before (Table 3.1). These data is consistent with the notion that expression of a siRNA-resistant SLBP restores S phase progression after knocking down endogenous SLBP as expected (Wagner *et al.*, 2005).

**Table 3.1** Cells loss of SLBP progress more slowly through S phase.

Shown in the percentage of cells with S phase DNA content.

<b>Time (hours)</b>	<b>Conditions</b>	<b>Percentage of cells in S phase</b>
4	siRNA/no Dox	56.78
	siRNA/Dox	62.13
10	siRNA/no Dox	68.78
	siRNA/Dox	62.27
12	siRNA/no Dox	68.24
	siRNA/Dox	69.53
14	siRNA/no Dox	80.18
	siRNA/Dox	50.92

HA-SLBP and HA-SLBP<sup>res</sup> cells were synchronized using a previously established protocol with Noc for 12 h, following siRNA knock down for 24 h and subsequently released as described in section 2.2.3.4.1. Cells were harvested at the indicated time and stained with PI.

### **3.2.6 An alternative endogenously expressed SLBP splice form is targeted by SLBP siRNA**

Previous work has demonstrated that HeLa cells up-regulated alternatively spliced forms of SLBP, lacking exons 2 and/or 3 which accumulate under the condition of replication stress (Rattray *et al.*, 2013). One possibility is that these forms of SLBP play an important role in the initial cellular response to replication stress, and could be rate limiting for the rapid destruction of histone mRNA following replication stress. If this was the case, then tagged-SLBP<sup>res</sup> cells might be expected NOT to function efficiently in replication stress-induced histone mRNA decay following siRNA-induced knockdown of the endogenous proteins. This is because these cells are predicted to express full-length tagged-SLBP protein only, as the Flag-SLBP DNA sequence lacks introns and thus will not be subject to the alternative splicing reported previously. Considering this, I wished to confirm that whether or not the condition of siRNA knock-down removed the presence of alternatively spliced SLBP mRNA in Flp-In-HeLa cells model.

Flag-SLBP and Flag-SLBP<sup>res</sup> cell lines were transfected with NT or siRNA targeting SLBP, respectively for 24 h in the presence of Dox. Cells were treated with 5 mM hydroxyurea (HU) up to 3 h. HU is an inhibitor of ribonucleotide reductase, which causes DNA polymerase to

stall at replication forks, resulted in DNA synthesis being blocked (Adams and Lindsay, 1967). RNA extract was prepared using phenol-chloroform RNA extraction and reverse transcription from RNA to cDNA as described in section 2.2.8. For analysis of alternative splicing, PCR amplification was undertaken using cDNA as a template, utilising primers as shown in Rattray *et al.* (2013) and Phusion<sup>®</sup> High-Fidelity DNA Polymerase (NEB). PCR reaction was performed as described in section 2.2.8.4. Finally, the PCR products were electrophoresed on 1.5% agarose gel.

Full-length SLBP transcripts are predicted to generate a PCR product of 752 bp with these primers (Rattray *et al.*, 2013). Products of this size were detected in both Flag-SLBP cells treated with NT, and Flag-SLBP<sup>res</sup> cells-expressing siRNA-resistant Flag-SLBP treated with siRNA. Addition of HU for up to 3 h had no effect in either cell line on the expression of the PCR product corresponding to full-length transcript (Figure 3.17, Lanes 2-5 and 6-9). A PCR product of ~700 bp was also observed in Flag-SLBP cells treated with NT siRNA, which is presumed to correspond to SLBP $\Delta$ E2 as described (Rattray *et al.*, 2013). Here, there appeared little change in the level of this product following HU treatment (Figure 3.17, Lanes 2-5). Importantly, however, Flag-SLBP<sup>res</sup> cells which had been treated with siRNA targeting endogenous

SLBP did not have detectable levels of this PCR product, either in asynchronously growing cells or cells treated with HU for up to 3 h. These data are consistent with the notion that at least one alternatively spliced form of SLBP are present in the HeLa cells used in this study, and that they are also knocked down by the SLBP targeted siRNA in exon 4 used in these experiments. This finding indicates that in the siRNA-treated Flag-SLBP<sup>res</sup> cell line system, addition of Dox results in the expression of one SLBP isoform, corresponding to the full-length protein, following DNA replication stress.

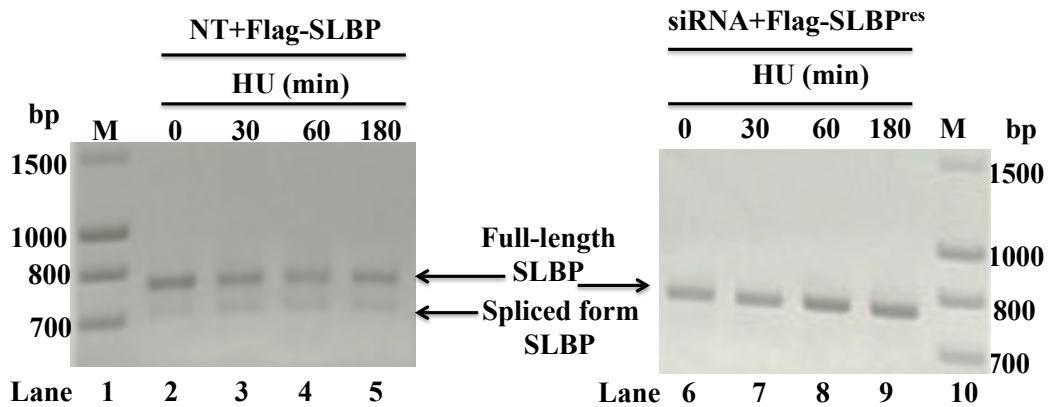


**Figure 3.17** Alternative splicing of Flp-In Flag-SLBP and Flag-SLBP<sup>res</sup> HeLa cell lines when the latter is exposed to SLBP siRNA.

In cells expressing wild-type SLBP, at least one additional splice form (~700 bp) may be detected following exposure to replication stress, consistent with Rattray *et al.*, 2013 (left-hand figure). In siRNA-treated cells expressing Flag-SLBP<sup>res</sup>, the presence of the cognate sequence corresponding to the siRNA in all splice forms, means that, following addition of siRNA, all are knocked down (with the exception of mRNA from SLBP<sup>res</sup>). This analysis allows us to test whether the splice variants alone are required for replication stress induced histone mRNA decay. Flp-In Flag-SLBP and Flag-SLBP<sup>res</sup> HeLa cell lines were transfected with NT or siRNA with Dox for 24 h and untreated or treated with 5 mM HU before cell harvesting. The analysis of splicing using cDNA prepared from total RNA, followed by PCR amplification and agarose

gel electrophoresis on a 1.5% agarose gel (M = DNA molecular size ladder; Norgen FullRanger 100 bp DNA ladder, Norgen Biotek Corp.)

### **3.2.7 Ectopic expression of SLBP containing silent mutation facilitates histone mRNA decay following replication stress**

In order to determine whether or not Flag-SLBP<sup>res</sup> was capable of carrying out established functions of SLBP in histone mRNA decay following replication stress, quantitative real-time PCR (qPCR) was used to measure the amount of histone mRNA in cells.

I used two pairs of qPCR primers (see primer sequences in Appendix C) to quantify transcripts from the histone and GAPDH genes, respectively. The primers were designed to amplify cDNA generated from reverse transcription of total RNA from Flag-SLBP<sup>res</sup> cells. The histone primers were designed to target the Hist1H3B gene. GAPDH (which encodes glyceraldehyde-3-phosphate dehydrogenase) was a reference gene for the total amount of mRNA.

To optimize the annealing temperature of histone and GAPDH primers, I initially used a PCR reaction with a gradient annealing temperature (T<sub>m</sub>), with a range from 46 to 65 °C. Importantly, DNase treated RNA was added in small PCR tube before adding PCR reaction. Agarose gel electrophoresis (Figure 3.18) showed that all temperatures

in the range 46-65 °C give specific PCR products of the correct size for both histone and GAPDH cDNA (91 bp and 106 bp, respectively). However, this experiment lacks negative control which has no PCR reaction.

Next, qPCR reactions were carried out for both histone and GAPDH, using an annealing temperature of 65 °C and the melt curves were analysed (Figure 3.19). Both melt curves had a single peak, indicating that primer dimers were not forming. Therefore, an annealing temperature of 65 °C was used subsequently throughout this study.

To validate the qPCR reaction, the PCR efficiency was investigated. qPCR reactions of 10-fold dilutions of the positive control (cDNA of Flag-SLBP cells) were carried out for each pair of primers, using  $T_m$  65 °C, to create a standard curve. An example of the standard curve obtained with each set of primers is shown in Figure 3.20. The accepted range of correlation coefficient is 90-100% (Schmittgen and Livak, 2008). In my study, the correlation coefficient was 99% which is in the accepted range.

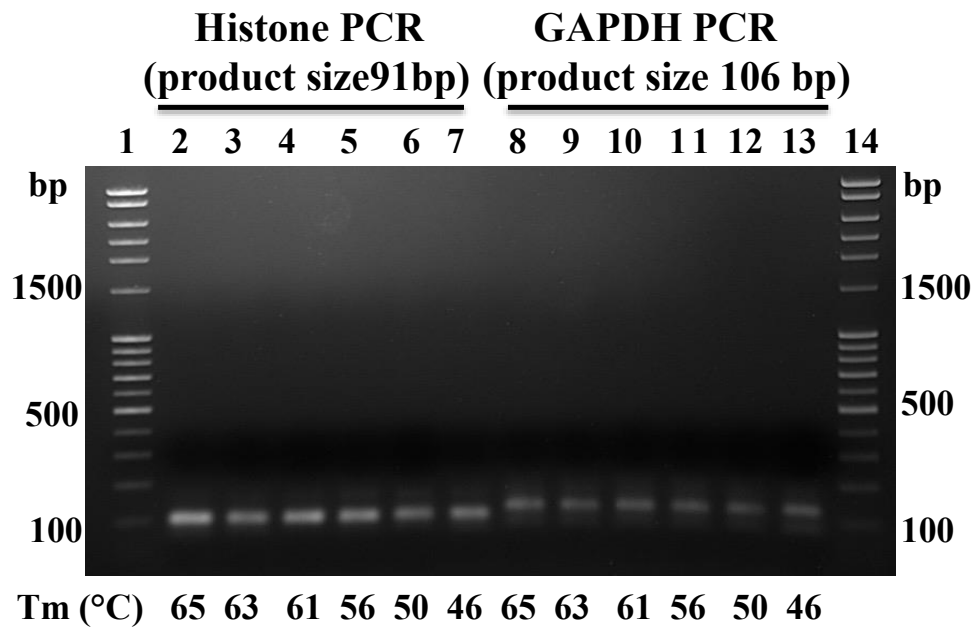


**Figure 3.18** Optimal annealing temperature

Agarose gel electrophoresis of PCR products following a gradient PCR reaction using cDNA from Flag-SLBP. The annealing temperature ( $T_m$ ) range was 46-65 °C. PCR products were electrophoresed on a 1.5% agarose gel. Lanes 1 and 14 contained DNA molecular size ladder (Norgen FullRanger 100 bp DNA ladder, Norgen Biotek Corp.)

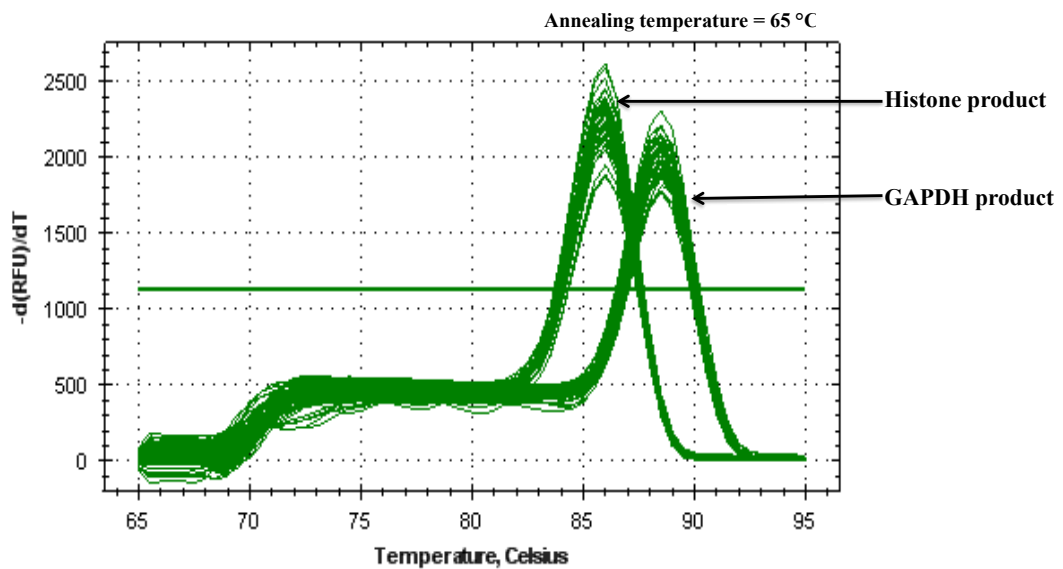


**Figure 3.19** Melt curves of Histone and GAPDH products. Temperature ( $^{\circ}\text{C}$ ) (X-axis) is plotted against the first negative derivative of the fluorescence with respect to temperature ( $-dF/dT$ ) (Y-axis). qPCR reaction for both sets of primers were performed using a  $65^{\circ}\text{C}$  annealing temperature. This graph shows a single peak of both histone and GAPDH products which mean that PCR reaction of histone and GAPDH products only generate one amplicon.

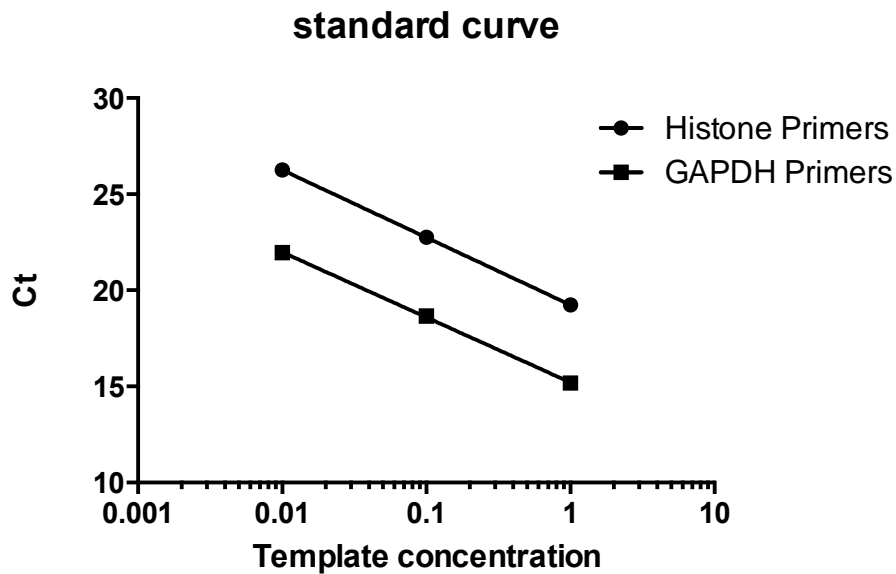


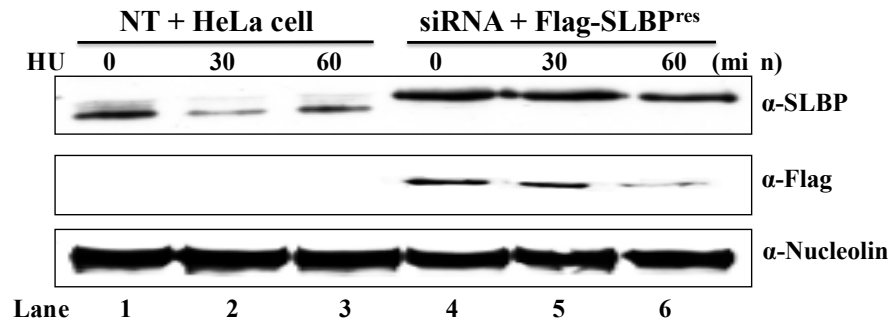
**Figure 3.20** Example of standard curves obtained using Histone and GAPDH primers (correlation coefficient ( $R^2$ ) =0.99). Threshold cycle (Y-axis) is plotted against log DNA concentration (X-axis).

I next examined the ability of Flag-SLBP<sup>res</sup> to undergo histone mRNA decay following replication stress. Normal HeLa cells were treated for 24 h with a control non-targeting siRNA (NT) and Dox-treated HeLa Flag-SLBP<sup>res</sup> cells were treated for 24 h with siRNA targeting SLBP (Figure 3.21). Figure 3.21A clearly shows that knockdown efficiency was more than 90% compared to HeLa cells (compare lane 4-6 with 1-3 of top panel).

Both sets of cells were exposed to HU. Cells lacking endogenous SLBP and expressing Flag-SLBP<sup>res</sup> degraded histone mRNA to the same extent, and with the same kinetic as control cells in response to HU

treatment (Figure 3.21B). This result confirms that Flag-SLBP<sup>res</sup> is capable of facilitating histone mRNA decay after the inhibition of DNA replication.

**A.**



**B.**

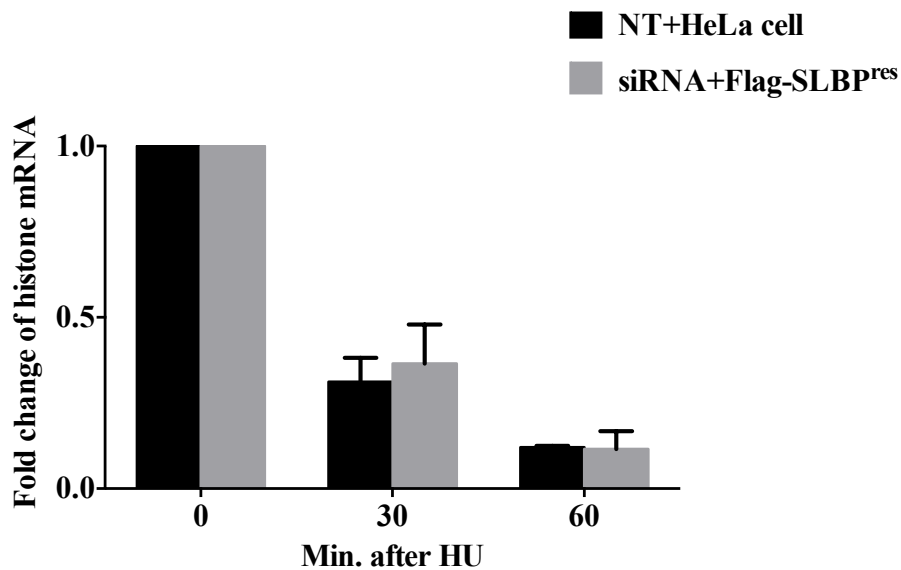


**Figure 3.21** The effect of Flag-SLBP<sup>res</sup> expression on histone mRNA decay following replication stress. Error bars show the standard error in the mean obtained from three independent experiments. The data shows that no significant difference was observed when cells lacking

endogenous SLBP and expressing Flag-SLBP<sup>res</sup> degraded histone mRNA in response to HU treatment.

Normal HeLa cells were transfected with NT. Flp-In HeLa cells expressing Flag-SLBP<sup>res</sup> were transfected with siRNA and treated with doxycycline for 24 h. RNA and protein extracts were prepared before HU treatment and after the addition of 5 mM HU for 30 and 60 min. (A) SLBP levels were assessed by western blotting with anti-SLBP and anti-Flag antibodies. Anti-nucleolin was used as a loading control. (B) Fold change of histone mRNA levels measured using qPCR. GAPDH was used as an internal reference. The data was calculated by delta CT method which normalises the target (histone) with reference (GAPDH) value. The relative fold change in each minute after HU treatment was normalised with the untreated (no HU) condition (0 min).

### **3.3 Discussion**

In this chapter, the objective was to develop a tracable model system to investigate SLBP function. Transient transfection using Polyfect (QIAGEN) were initially used to overexpress SLBP following a 24 h transfection protocol. At 24 h post transfection, SLBP was detected at a molecular mass  $> 31$  kDa which is in agreement with the calculated molecular mass ( $M_r$ ) which is slightly over 31 kDa (Martin *et al.*, 1997).

#### **3.3.1 Mammalian cells transfection: transient versus stable transfections**

There are several aspects of transient transfection technology that may have resulted in the low expression of Flag-tagged SLBP compared to untagged SLBP. For examples, transiently transfection gives rise to cells expressing genes that are not integrated into the host genome and may only be expressed for a limited period of time (Kim and Eberwine, 2010). Additionally, the backbone of the Flag vector could differentially interfere non-specifically with the mechanism of Flag-tagged SLBP expression. Finally, the efficiency of transfection can be variable in transient experiments, and thus there may have been a difference between the extent of transfection between the two constructs.

Therefore, a stable transfection approach was used to overcome the low level of Flag-tagged SLBP expression obtained using transient expression. I began to generate a stable cell line system for the inducible expression of Flag-tagged SLBP in HeLa cells using the FLP-IN cell system, that utilises FLP recombinase technology. There are several advantages in generating stable Flag-tagged SLBP cell lines using this system. Firstly, the gene of interest (Flag-tagged SLBP) and any mutant derivatives are integrated into a single specific site on the genome, which minimises the risk that any observed differences are a consequence of differences in gene dosage, chromosomal location effects, differential expression. Secondly, the generation of an isogenic stable cell line permits for the efficient and rapid production of expressed protein. Thirdly, utilization of the Flp-In<sup>TM</sup> T-Rex<sup>TM</sup> expression system, allows for expression to be controlled by a Dox-inducible promoter, enabling the design of experiment where the timing of expression may be critical. However, inducible expression by Dox was used instead of tetracycline because of its long half-life (Gossen *et al.*, 1995). The level of Flag-tagged SLBP expression varied subtly as a function of the different concentrations of Dox. At the concentration of 0.5 ug/ml of Dox, the maximal level of Flag-tagged SLBP expression was observed. Maximal expression levels of SLBP were obtained after 24-48 h and decreased

subsequently (by 72 h). One possible explanation for this is it may be due to progressive reduction in the fraction of cells undertaking S-phase (where SLBP levels are presumed maximal) as cells approach confluency.

As mentioned above, the endogenous SLBP could not be detected in experiments where transient expression was attempted. In contrast, endogenous SLBP could be detected using the inducible stable expression system. Expression of endogenous SLBP is restricted to S-phase (Marzluff *et al.*, 2008) and experimental limitations precluded an analysis to establish whether SLBP expression from the expression constructs was appropriately regulated. Because transiently transfected cells may contain multiple copies of transfected plasmid, it is possible that the level of ectopic expression was far higher than that of the endogenous protein, precluding the detection of the latter. As discussed above, it is also possible that the number of cells in S-phase under transient transfection conditions were very limited. Overall, these results suggested that the utility of the Flp-In system for inducible stable expression of Flag-tagged SLBP has significant advantages over the use of transient transfection, in terms of opportunities for experimental manipulation and likely reproducibility of expression levels.

### **3.3.2 Model system for analysis of SLBP in a model cell line**

In order to investigate the effect of inducible expression of Flag-tagged SLBP and also the regulation of SLBP on cell cycle progression, I analysed the expression of Flag-tagged SLBP throughout the cell cycle. Flag-tagged SLBP cells, synchronised using mitotic shake-off, showed expression of Flag-tagged SLBP as a function of cell cycle progression. The mitotic shake-off method involves the addition of Noc to Flag-tagged SLBP cells for an extended period. Noc is a drug blocking cells at metaphase by destabilizing the microtubule structure (Vasquez *et al.*, 1997 ; Xu *et al.*, 2002). Cells round up during M-phase and may be detached from the culture plate by shaking them off. By shaking-off cells, Flag-tagged SLBP cells expression started through G1/S phases of cell cycle. In my study, after mitotic shake off, Flag-tagged SLBP cells were released into fresh medium in the presence or absence of Dox for 5h, and the medium was replaced again. Time zero corresponded to the point at which cells were placed in Noc-free medium. Flag-tagged SLBP cells progressed to S-phase by 7 h after replating. Interestingly, the expression of Flag-tagged SLBP cells was up-regulated at the same time expression of control cyclin A which resides in nucleus during S phase (Lim and Kaldis, 2013).

The expression of SLBP is cell cycle-regulated (Whitfield *et al.*, 2000 ; Zheng *et al.*, 2003). In asynchronous cells, Dox induced tagged-SLBP expression levels were approximately twofold higher than those of endogenous protein. This raised a concern that the level of tagged-SLBP expression might overwhelm the cellular regulatory systems that control both the upper regulation and down-regulation of SLBP protein levels. However, the results obtained using synchronized cells showed that the temporal regulation of both tagged forms of SLBP corresponded closely to that observed for the endogenous protein, with very similar kinetics. Overall, the findings are consistent with the previous studies have shown that the level of SLBP increases at the late G1/beginning of S phase, remains constant throughout S phase and rapidly decreases at the end of S-phase (Whitfield *et al.*, 2000). Interestingly, in the experimental protocol developed here, cells were exposed to Dox for five hours only, after release from the Noc arrest. Subsequent FACS analysis confirmed that this corresponded to early G1 phase. During this period, almost no tagged protein could be detected, and it follows that the high levels of both Flag- and HA-tagged observed subsequently must have been synthesized using mRNA synthesized during the previous G1 phase. These data strongly support the notion that the translation of SLBP mRNA and/or SLBP protein stability is regulated by a cell cycle

regulation mechanism between G1 and S phase, as has been suggested (Whitfield *et al.*, 2000 ; Zheng *et al.*, 2003). Much of the previous work on SLBP protein has involved the use of a double thymidine block to synchronise cells for analysis (Whitfield *et al.*, 2000 ; Zheng *et al.*, 2003). While those reports suggest that this synchronization approach arrests cells at the boundary prior to S phase, this is not correct and thymidine treated cells are already in S phase (Feijoo *et al.*, 2001), complicating interpretation of the regulation of SLBP. The work discussed here used synchronisation from mitosis, which allows a more careful analysis of events at the G1-S transition (Whitfield *et al.*, 2000 ; Zheng *et al.*, 2003). While this work was in progress, Djakbarova and colleagues reported that SLBP protein levels are indeed regulated both by translational mechanism as well as regulation of proteasomal mediated destruction (Djakbarova *et al.*, 2014).

FACS analysis was used to monitor the effect of tagged protein expression on cell growth and progression through the cell cycle. The result showed that both Flag- and HA-tagged SLBP expressing cells normally progressed from G1 phase through S and G2 phases of the cell cycle, compared to normal cells expressing endogenous SLBP. After Noc treatment, most cells recovered completely and entered the subsequent G1 and S phase in a highly synchronous pattern, although a

small proportion of cells failed to progress. The reasons for this are unknown. Taken together, these observations confirmed the evidence that SLBP protein expression is cell cycle-regulated, and that the regulated expression of tagged-SLBP reflects the state of endogenous protein with reasonable accuracy.

In order to confirm that tagged SLBP was indeed functional, I examined the ability of tagged SLBP to rescue the reported delay in S-phase progression resulting from loss of SLBP expression. siRNA targeting SLBP induced significant knockdown of SLBP protein in synchronized cells (Figure 3.16) and had a modest effect on S phase progression which was reduced by expression of HA-SLBP (Table 3.1), again supporting the notion that tagged SLBP function in a HeLa cell model.

### **3.3.3 Use of the model system for analysis of aspect of histone mRNA decay in response to DNA replication stress**

An important function of SLBP is that this protein is required for histone mRNA decay both at the end of S-phase as well as when DNA synthesis is inhibited (Kaygun and Marzluff, 2005c). While this project was underway, Rattray and colleagues (2013) reported that HeLa cells contain alternative spliced forms of SLBP mRNA that lack either exons

2 and 3 (HBP/SLBP $\Delta$ E2 and HBP/SLBP $\Delta$ E3, respectively), in addition to a form that lacks both exons 2 and 3 (HBP/SLBP $\Delta$ E2+ $\Delta$ E3). Replication stress induces elevated expression of these SLBP splice variants over a period of 18 h (Rattray *et al.*, 2013). Because it was conceivable that truncated forms of SLBP might be essential for replication stress-induced histone mRNA decay, it was important to investigate the efficiency of histone mRNA decay in the presence and absence of mRNA capable of inducing expression of these splice forms. The results shown in Figure 3.17 show that a PCR product corresponding to the largest SLBP splice variant could be detected in control Flag-SLBP cells exposed to a non-targeting siRNA, but that this form was undetectable in cells (Flag-SLBP<sup>res</sup>) exposed to an siRNA targeting exon 4 of SLBP. These results suggested that resultant proteins derived from the splice variants are likely to be knocked down as a consequence of specific siRNA treatment. The other splice variants were not detected in the experiments described here. Although the reason for this is unclear, it may be that the experimental timeframe in which cells were exposed to replication stress here was insufficient to allow sufficient accumulation of variants whose expression was reported to be induced by replication stress (Rattray *et al.*, 2013).

Therefore, I tested whether siRNA treated cells (which effectively lack endogenous full-length and presumably lower MW splice variants) expressing full length Flag-tagged SLBP alone are able to undertake efficient histone mRNA decay in response to replication stress. The experiment was to knock down endogenous SLBP forms using siRNA targeting exon 4, while inducing the expression of full-length Flag-tagged SLBP using Dox and compare the rate and extent of HU-induced histone mRNA decay using qPCR, to the rate and extent in HeLa cells capable of expressing all variants of endogenous SLBP. The data in Figure 3.21B showed that no significant difference was observed in the kinetic of HU-induced histone mRNA decay. These data suggest that the full-length protein is predominantly the form of SLBP involved in acute replication stress-induced histone mRNA decay. Additionally, the amount of histone mRNA remaining after HU treatment up to 60 min were different in the study using Human bone osteosarcoma epithelial (U2OS) cells compared to HeLa cells (Sullivan *et al.*, 2009). Histone mRNA degradation was slower in U2OS cells than in HeLa cells. However, both cells showed the reduced rate pattern of histone mRNA degradation at 30 and 60 min after HU treatment. The factors involved in their differences might depend on cell type, transfection efficiency, time frame of knocking down and the level of SLBP expression etc. The low

levels of SLBP expression reflect the inefficient translation of histone mRNA resulting in the decrease of histone mRNA degradation and vice versa (Sullivan *et al.*, 2009).

In summary, the stable transfection of Flag- and HA-tagged SLBP in HeLa cells by using Flp-In™ T-Rex™ system is a successful model which composed of (1) inducible expression of Flag- and HA-tagged SLBP progressed normally on cell cycle. (2) the tagged version of Flag-SLBP<sup>res</sup> and HA-SLBP<sup>res</sup> are resistant to siRNA-induced knockdown of endogenous protein. (3) HA-SLBP<sup>res</sup> cells restores S-phase progression after knocking down endogenous SLBP. (4) in the siRNA-treated Flag-SLBP<sup>res</sup> cell line system, addition of Dox results in the expression of one SLBP isoform, corresponding to the full-length protein, following DNA replication stress and this form of SLBP involved in acute replication stress-induced histone mRNA decay. Thus, Flag-tagged SLBP expressing cells will utilize for further study SLBP post-translation modification and its interaction complex using mass spectrometry.

### 3.4 References

- Abercrombie, M. 1970. Contact inhibition in tissue culture. *In Vitro*. 6 (2): 128-142.
- Adams, R.L. and Lindsay, J.G. 1967. Hydroxyurea reversal of inhibition and use as a cell-synchronizing agent. *J Biol Chem*. 242(6): 1314-1317.
- Djakbarova, U., Marzluff, W.F. and Köseoğlu, M.M. 2014. Translation regulation and proteasome mediated degradation cooperate to keep Stem-loop binding protein, a major player in histone mRNA metabolism, low in G1-phase. *J Cell Biochem*. 115(3): 523-530.
- Erkman, J.A., Wagner, E.J., Dong, J., Zhang, Y., Kutay, U. and Marzluff, W.F. 2005. Nuclear Import of the Stem-Loop Binding Protein and Localization during the Cell Cycle. *Mol Biol Cell*. 16(6): 2960-2971.
- Feijoo, C., Hall-Jackson, C., Wu, R., Jenkins, D., Leitch, J., Gilbert, D.M. and Smythe, C. 2001. Activation of mammalian Chk1 during DNA replication arrest: a role for Chk1 in the intra-S phase checkpoint monitoring replication origin firing. *J. Cell Biol*. 154(5): 913-923.

Gossen, M., Freundlieb, S., Bender, G., Müller, G., Hillen, W., Bujard, H. 1995. Transcriptional activation by tetracyclines in mammalian cells. *Science*. 268: 1766-1769.

[https://tools.thermofisher.com/content/sfs/manuals/flpinsystem\\_man.pdf](https://tools.thermofisher.com/content/sfs/manuals/flpinsystem_man.pdf)

Kaygun, H. and Marzluff, W.F. 2005c. Translation termination is involved in histone mRNA degradation when DNA replication is inhibited. *Mol. Cell. Biol.* 25: 6879-6888.

Kim, T.K. and Eberwine, J.H. 2010. Mammalian cell transfection: the present and the future. *Anal Bioanal Chem.* 397: 3173-3178.

Lim, S. and Kaldis, P. 2013. Cdks, cyclins and CKIs: roles beyond cell cycle regulation. *Development* 140: 3079-3093.

Martin, F., Schaller, A., Eglite, S., Schümperli, D., and Müller, B. 1997. The gene for histone RNA hairpin binding protein is located on human chromosome 4 and encodes a novel type of RNA binding protein. *EMBO J.* 16: 769-778.

Marzluff, W.F., Wagner, E.J. and Duronio, R.J. 2008. Metabolism and regulation of canonical histone mRNAs: life without a poly(A) tail. *Nat. Rev. Genet.* 9: 843-854.

- O'Gorman, S., Fox, D.T. and Wahl, G.M. Recombinase-Mediated Gene Activation and Site-Specific Integration in Mammalian Cells. *Science*. 251(1999): 1351-1355.
- Pandey, N.B., Sun, J.H. and Marzluff, W.F. 1991. Different complexes are formed on the 3' end of histone mRNA with nuclear and polysomal proteins. *Nucleic Acids Res.* 19: 5653-5659.
- Rattray, A.M.J., Nicholson, P. and Müller, B. 2013. Replication stress-induced alternative mRNA splicing alters properties of the histone RNA-binding protein HBP/SLBP: a key factor in the control of histone gene expression. *Biosci Rep.* 33(5): e00066.
- Schmittgen, T.D. and Livak, K.J. 2008. Analysing real-time PCR data by the comparative C(T) method. *Nature protocols.* 3: 1101-1108.
- Sullivan, K.D., Mullen, T.E., Marzluff, W.F. and Wagner, E.J. 2009. Knockdown of SLBP results in nuclear retention of histone mRNA. *RNA.* 15: 459-472.
- Vasquez, R.J., Howell, B., Yvon, A.M., Wadsworth, P. and Cassimeris, L. 1997. Nanomolar concentrations of nocodazole alter microtubule dynamic instability in vivo and in vitro. *Mol Biol Cell.* 8(6): 973-985.

- Wagner, E.J., Berkow, A. and Marzluff, W.F. 2005. Expression of an RNAi-resistant SLBP restores proper S-phase progression. *Biochem Soc Trans.* 33(Pt 3): 471-473.
- Whitfield, M.L., Zheng, L.-X., Baldwin, A., Ohta, T., Hurt, M. and Marzluff, W.F. 2000. Stem-loop binding protein, the protein that binds the 3' end of histone mRNA, is cell cycle regulated by both translational and posttranslational mechanisms. *Mol. Cell Biol.* 20: 4188-4198.
- Xu, K., Schwarz, P.M. and Ludueña, R.F. 2002. Interaction of Nocodazole With Tubulin Isotypes. *Drug dev res.* 55: 91-96.
- Zhao, J. 2004. Coordination of DNA synthesis and histone gene expression during normal cell cycle progression and after DNA damage. *Cell Cycle.* 3(6): 695-697.
- Zheng, L., Dominski, Z., Yang, X.C., Elms, P., Raska, C.S., Borchers, C.H., and Marzluff, W.F. 2003. Phosphorylation of stem-loop binding protein (SLBP) on two threonines triggers degradation of SLBP, the sole cell cycle-regulated factor required for regulation of histone mRNA processing, at the end of S phase. *Mol. Cell Biol.* 23: 1590-1601.

# *Chapter 4*

## *Establishment of an approach for immunoisolation (I-i) of Flag-tagged SLBP for mass spectrometry*

### **4.1 Introduction**

Having developed and undertaken a preliminary characterisation of my model cell line for SLBP analysis, as discussed in Chapter 3. I wished to study SLBP post-translational modifications as a function of replication stress, together with an analysis of SLBP interacting proteins in my model tissue culture cell line exposed to replication stress-induced histone mRNA decay. Advanced of peptide-based mass spectrometry (MS) together with the sequencing of the human genome has become incredibly for identifying protein-protein interactions. In MS-based proteomics coupled immuno-isolation allows for the isolation of SLBP protein isolate its interacting partners prior to determining Flag-tagged SLBP in association with its interacting partners, prior to determining SLBP interacting proteins by MS. In order to do this, I began with

identification of conditions for immuno-isolation of Flag-tagged SLBP to facilitate its analysis by MS.

Immuno-isolation could be attempted, using a target protein specific antibody, that is in this case anti-SLBP antibody. However, there are a number of challenges associated with this approach, including limitations in the availability and/or cost of reagents (anti-SLBP antibodies), as well as the possibility that antibodies selectively bind specific sub-populations of SLBP involved in some but not all of SLBP-associated functions. Consequently, I choose to use an ANTI-FLAG<sup>®</sup> M2 affinity resin for successful immuno-isolation. In principle, using this approach, a multicomponent complex can be isolated in a single step.

The experiments undertaken and discussed in Chapter 3 provided evidence that Flag-tagged SLBP expression rescued defects in cell cycle progression and replication stress-induced histone mRNA decay brought about by siRNA mediated knockdown of the endogenous gene product. Such data support the notion that the addition of a small tag at the N-terminus of the protein has little effect on its biological function, and suggest that analysis of the Flag-tagged SLBP is likely to be a relevant proxy to understand SLBP function *in vivo*.

Therefore, scoping experiments were undertaken to determine an appropriate ratio of affinity matrix to protein lysate to achieve efficient depletion of expressed SLBP. In addition, an estimate of efficiency of recovery of bound SLBP, by elution with 3X FLAG peptide, was determined by western blotting. Batch and micro-column methods of depletion and recovery have been compared, and batch methodology found to be more reliable. Matrix stability was found to be an issue during various stages of the procedure, with evidence of antibody dissociation produced. This was largely eliminated by removal of reducing agents in buffers used in the isolation procedure.

Following scale-up, initial MS analysis following tryptic in-gel digestion failed to detect any peptides derived from immuno-isolated Flag-tagged SLBP. Therefore, in order to establish conditions for proteolytic digestion of SLBP to maximize the number of SLBP peptides that could be detected by MS, a strategy for SLBP expression in, and purification from, *E.coli*, was developed. This facilitated comparison of proteolytic approaches (using trypsin, chymotrypsin and elastase) for identification of SLBP-derived peptides by MS. Finally, conditions were established for the identification and analysis of Flag-tagged SLBP immuno-isolated from S-phase synchronized HeLa cells.

## **4.2 Results**

### **4.2.1 Optimisation of conditions for I-i of Flag-tagged SLBP from HeLa cells expressing functional, tagged SLBP**

The aim of the work described in this section was to attempt to optimise conditions for the isolation of Flag-tagged SLBP and potential interacting proteins in the tissue culture cell line model described in Chapter 3. The longer term aim of these experiments was to establish conditions which would allow subsequent investigation into changes in SLBP post-translational status, in presence and absence of replication stress, with the objective of utilizing the immuno-isolated SLBP and consequent mass spectrometry, for molecular analysis of differences in macro-molecular complex composition following exposure to replication stress.

Immuno-isolation experiments were undertaken using ANTI-FLAG<sup>®</sup> M2 affinity resin (packed resin) (Sigma-Aldrich). The latter is a monoclonal antibody covalently attached to agarose resin (Technical bulletin, Sigma-Aldrich, product number A2220). To do this, cells stably transfected with Flag-tagged SLBP (as described in Chapter 3) were grown in the presence of optimal concentrations of

doxycycline (Dox), as determined previously (as described in section 3.2.4).

Cell lysate (typically 1 mg protein in 1x lysis buffer), produced from 100 mm dish of asynchronously growing cells (confluency approx. 80%) was used per I-i experiment, and was incubated with indicated volumes of packed resin overnight. The packed resin volume required to maximise recovery of tagged SLBP was first optimised by analysis of the extent of depletion of cell lysate obtained using either 10  $\mu$ l and 20  $\mu$ l of packed resin. The I-i material was isolated by micro-centrifugation (8,000 rpm for 30 sec), the supernatant removed (designated flow-through below) and, after washing with 600  $\mu$ l of TBS, beads were eluted using 3X FLAG peptide dissolved in TBS (50 mM Tris-HCL and 150 mM NaCl) and then sample loading buffer. All samples were subjected to SDS-PAGE, and western blotting as described in section 2.2.4.4. The membrane was probed with mouse monoclonal  $\alpha$ -SLBP and  $\alpha$ -Flag antibodies, as described in section 2.2.6 in order to establish the efficiency of I-i.

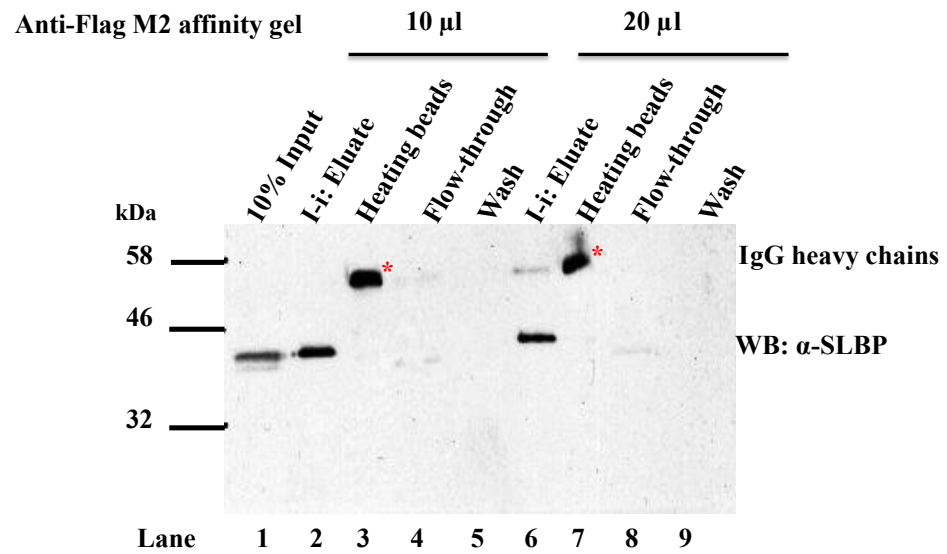
In all cases, bands of expected molecular mass (approximate (approx.) 38 kDa) for SLBP were detected using both  $\alpha$ -SLBP and  $\alpha$ -Flag antibodies (Figure 4.1A and B). Comparison of input material to

immuno-depleted lysate indicated significant depletion of SLBP from the lysate (compare lanes 4 and 8 with lane 1 in Figure 4.1A and B). Depleted material was recovered almost exclusively by 3X FLAG peptide elution (Figure 4.1A and B, lanes 2 and 6). However, the recovery of SLBP in the eluate was approximately only 35% and 29% in lanes 2 and 6, respectively as judged by densitometry (data not shown). The extent of recovery did not appear to improve using 20  $\mu$ l of packed resin volume compared to 10  $\mu$ l, suggesting that the apparent reduced recovery was not simply a consequence of limited resin capacity for the amount of SLBP present in the lysate. However, low level of SLBP cross reacting material remained in the flow-through even when 20  $\mu$ l of packed resin was used, suggesting that the procedure did not completely deplete all SLBP present. It is possible that this represents endogenous untagged SLBP, as it was not detected in the equivalent sample blotted using anti-Flag antibody. The apparent recovery of Flag-tagged SLBP from 20  $\mu$ l of packed resin appeared to be less than that obtained using 10  $\mu$ l. This contrasts with the result obtained with anti-SLBP antibody (compare lanes 2 and 6 in Figure 4.1B and A). The reason for this discrepancy is unknown.

Using heated sample loading buffer for elution resulted in elution of 50 kDa bands consistent in size with IgG heavy chains, suggesting

that covalent crosslinking of Flag antibody was not complete. Other Flag epitope cross-reacting proteins were present in both eluated samples (Figure 4.1B, lanes 2 and 6). As corresponding bands were not present in the blot using anti-SLBP antibody, these do not correspond to any novel SLBP species but presumably arises from non-specific binding, and enrichment from the total cell lysate, of Flag antibody cross-reacting proteins.

**A.**



**B.**

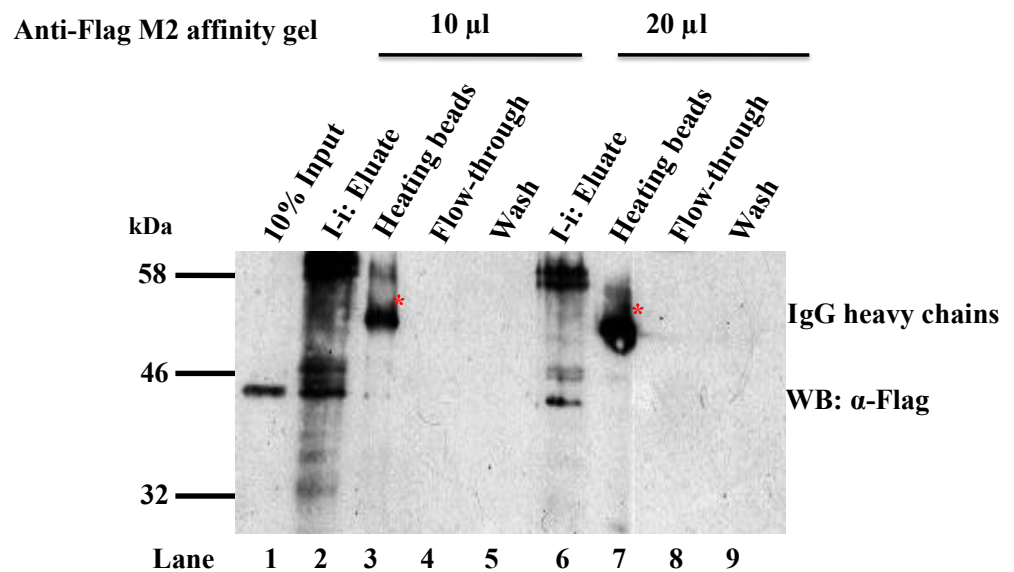


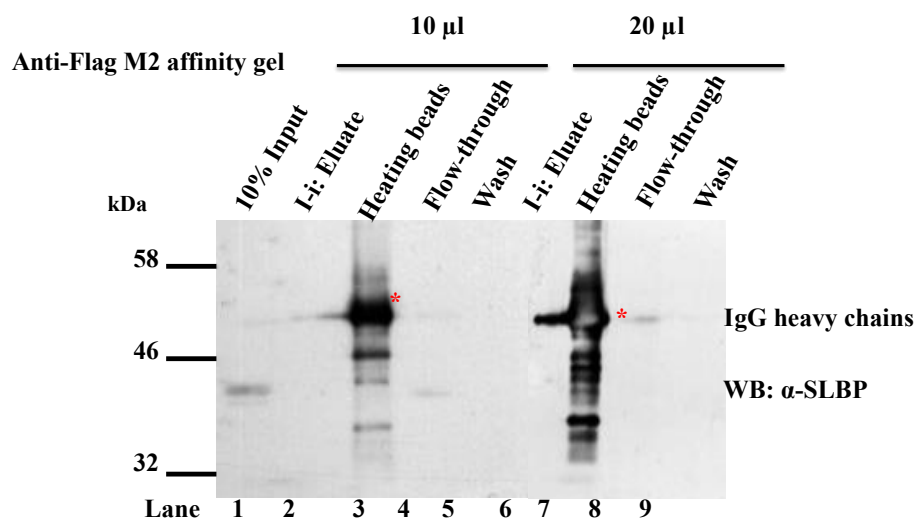
**Figure 4.1** I-i analysis of FLAG-tagged SLBP isolated from Flp-In-HeLa cell lysate. In each experiment, 1 mg of cell lysate was incubated overnight with indicated volume of packed resin (added as 50% (v/v)

slurry in TBS) at 4 °C with repeated agitation prior to washing with 500 µl of TBS and elution, initially using 100 µl of 300 ng/µl final concentration of 3X FLAG peptide in TBS, followed by 8 µl of sample loading buffer (beads heated at 100 °C for 5 min). Flag-tagged SLBP in samples was detected using (A) anti-SLBP antibody and (B) anti-Flag antibody. Lane1, 10% of total input (I used 1 mg protein so I will load lysate 100 µg. I calculated the corresponding volume of 100 ug lysate from the stock of that lysate), Lanes 2 and 6, 30% of 3X FLAG peptide eluate, Lanes 3 and 7, 30% of sample loading buffer eluate, Lanes 4 and 8, 12.5% of flow-through, and Lanes 5 and 9, 5% of wash samples. Red asterisks indicate putative IgG heavy chains.

In order to investigate whether the use of the cell-packed top tip micro-column (Glysci) might improve recovery of Flag-tagged SLBP from ANTI-FLAG<sup>®</sup> M2 affinity resin compared to the batch procedure as described above, the experiment was repeated using resin packed into a small column (P200 size tip). Cell lysate was applied to column by gravity feed and following washing with 200 µl of TBS, eluted with 50 µl of TBS containing 3X FLAG peptide as before. Surprisingly, no SLBP was recovered from the eluate as judged by detection of an

appropriate size band by western blotting with either the anti-SLBP and anti-Flag antibodies. Some SLBP could be detected in the flow-through in each experiment (Figure 4.2B, lanes 4 and 8) although the relative recoveries as judged by band intensity with each antibody were inconsistent. The reason for this is unknown. Some SLBP may have been eluted following treatment of the resin with heated sample loading buffer, and additional lower molecular weight bands were recovered, which might reflect proteolytic or fissile peptide bond breakdown products (Figure 4.2 A and B, lanes 3 and 7). Moreover, the signals of SLBP and Flag-tagged SLBP were also indicated in flow-through. As the levels of SLBP recovered in this experiment were very low, it is difficult to interpret these results. However, they are not inconsistent with the possibility that both binding to, and elution from Flag antibody is relative slow, and thus efficiency is enhanced by using the batch procedure undertake in Figure 4.1.

**A.**



**B.**

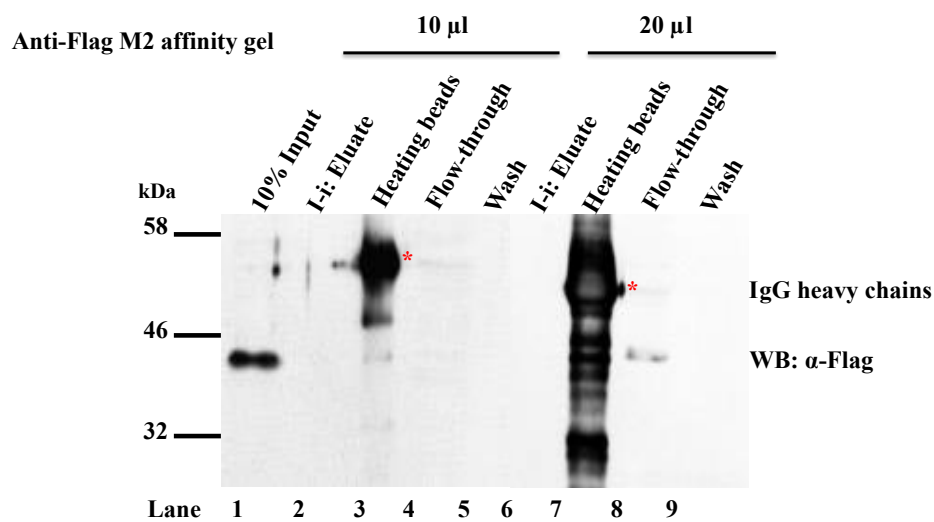


**Figure 4.2** I-i micro-coloumn of Flag-tagged SLBP isolated from Flp-In-HeLa cell lysate. In each experiment, 1 mg of cell lysate was applied to a

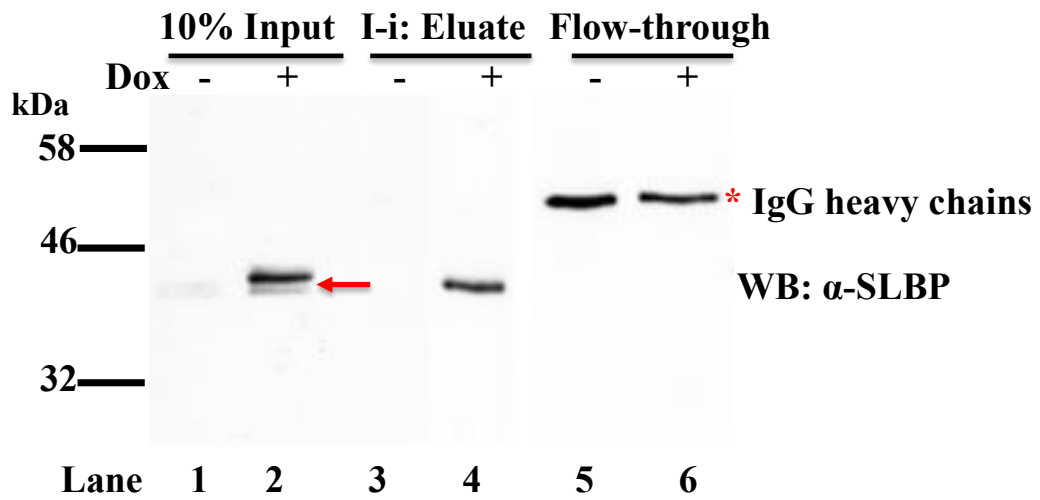
P200 size tip column containing either 10 or 20  $\mu$ l of packed resin at 25 °C, washed with 200  $\mu$ l of TBS, prior to elution with 50  $\mu$ l of TBS containing 300 ng/ $\mu$ l final concentration of 3X FLAG peptide, followed by 8  $\mu$ l of sample loading buffer (beads heated at 100 °C for 5 min). Flag-tagged SLBP in samples was detected using (A) anti-SLBP antibody and (B) anti-Flag antibody. Lane1, 10% of total input, Lanes 2 and 6, 30% of 3X FLAG peptide eluate, Lanes 3 and 7, 30% of sample loading buffer eluate, Lanes 4 and 8, 12.5% of flow-through, and Lanes 5 and 9, 5% of wash samples. Red asterisks indicate putative IgG heavy chains.

One possible explanation for the relatively poor yield of SLBP would be that association of the protein specifically with anti-Flag antibody was relative low affinity, and that the efficiency of binding was thus low under condition used. Thus, in a further attempt to improve recovery of Flag-tagged SLBP was undertaken. In addition because of concerns about the fate of endogenous, untagged SLBP in the initial experiment obtained in Figure 4.1, the experiment was repeated using lysates from cells grown in the absence or presence of 0.5  $\mu$ g/ml of dox for 14 h, prior to lysate preparation. Using batch procedure, 1 mg of cell

lysate in each case was incubated overnight at 4 °C with ANTI-FLAG<sup>®</sup> M2 affinity resin (10 µl final packed resin volume) as before and, following washing in 500 µl of TBS, eluted with altered elution buffer (10 mM Tris-HCl pH 7.4 and 30 mM NaCl) containing 300 ng/µl final concentration of 3X FLAG peptide (Figure 4.3A and B). Under these conditions, Flag-tagged SLBP expression level was significant higher than the endogenous protein (Figure 4.3A, compare lanes 1 and 2) which was barely detectable under these exposure conditions, and which migrated at a position corresponding to a slightly lower molecular mass (red arrow). Efficient depletion of Flag-tagged SLBP was observed as judged by western blotting with either  $\alpha$ -SLBP or  $\alpha$ -Flag antibodies (Figure 4.3A and B, compare lanes 2 and 6). Specific elution using the 3X FLAG peptide resulted in recovery of Flag-tagged SLBP with loss of the band presumed to correspond to the endogenous, untagged protein, suggesting that there is no interaction between polypeptides. Unexpectedly, the endogenous protein could not be detected in the depleted lysate (“flow-through”, Figure 4.3A and B, lanes 5 and 6), possibly because the slight dilution of the extract resulted in the endogenous protein below the threshold for detection. The results showed that the immuno-isolated protein was recovered on specific

elution using the 3X FLAG peptide under modified conditions. However, again, there was variation in the intensity of the band, depending on which antibody (anti-SLBP or anti-Flag) was used; on this occasion, (in contrast to the data in Figure 4.1) an apparent higher recovery was observed using the  $\alpha$ -Flag antibody as judged by the intensity of band. Cross-reacting bands at approx. 50 kDa were observed in this experiment in the depleted lysate fraction in both western blottings. As discussed above, these are likely to be immunoglobulin heavy chains derived from the affinity resin, and suggest that the efficiency of antibody cross-linking to the commercial resin may be less than 100% (Figure 4.3A and, lanes 5 and 6). The reason why they were not observed in this fraction in previous experiments is not known. However, this may relate to use of distinct batches of resin, or altered sensitivity of reducing agents.

A.



B.

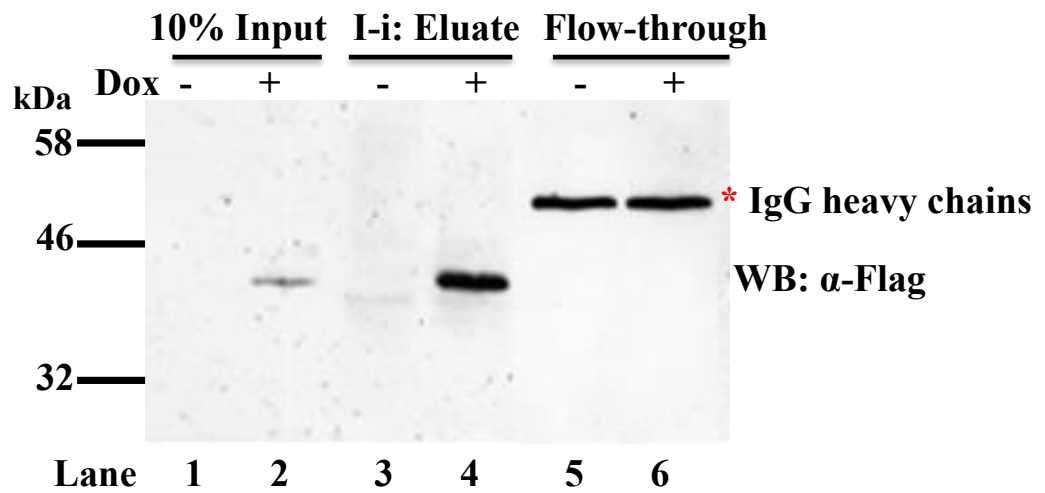


**Figure 4.3** I-i analysis of Flag-tagged SLBP isolated from Flp-In-HeLa cell lysate. Cells previously treated without (-) or with (+) 0.5  $\mu$ g/ml of

dox were lysed as above. In each experiment, 1 mg of cell lysate was incubated overnight with indicated volume of packed resin (added as 50% (v/v) slurry in TBS) at 4 °C with repeated agitation, the depleted lysate removed (flow-through) prior to washing with 500 µl of TBS before elution using 100 µl of 300 ng/µl final concentration of 3X FLAG peptide in TBS. Flag-tagged SLBP in samples was detected using **(A)** anti-SLBP antibody and **(B)** anti-Flag antibody. Lane 1 and 2, 10% of total input), Lanes 3 and 4, 30% of 3X FLAG peptide eluate containing altered elution buffer (10 mM Tris-HCl pH 7.4 and 30 mM NaCl), and Lanes 5 and 6, 12.5% of flow-through. Red arrow indicates endogenous SLBP and red asterisks indicate putative IgG heavy chains.

#### **4.2.2 Mass spectrometric analysis of immuno-isolated SLBP**

Having established conditions for the isolation of Flag-tagged SLBP from cell lysates, the next step was to undertake the isolation on a larger scale to facilitate the analysis of SLBP under normal S-phase and replication stress conditions, and to identify SLBP-associated polypeptides, using mass spectrometry. In this section, Flag-tagged SLBP was isolated by I-i using ANTI-FLAG<sup>®</sup> M2 affinity resin from 37.5 mg of cell lysate protein, subjected to SDS-PAGE and polypeptides visualized by colloidal Coomassie blue staining. Bands were excised, digested in situ and analysed by liquid chromatography-tandem mass spectrometry (LC-MS/MS).

I performed a large-scale, I-i of Flag-tagged SLBP (37.5 mg protein derived from dox-treated Flag-tagged SLBP expressing cells in total volume 7.5 ml and applied to 3 ml of packed resin volume) and eluted with 3X FLAG peptide. The eluate (7.5 ml) was concentrated to final volume 230  $\mu$ l using a Vivaspin 500 (GE Healthcare) and samples derived from the input and recovered material were run subjected by western blotting, prior to further analysis, to confirm enrichment and recovery of Flag-tagged SLBP (Figure 4.4A).

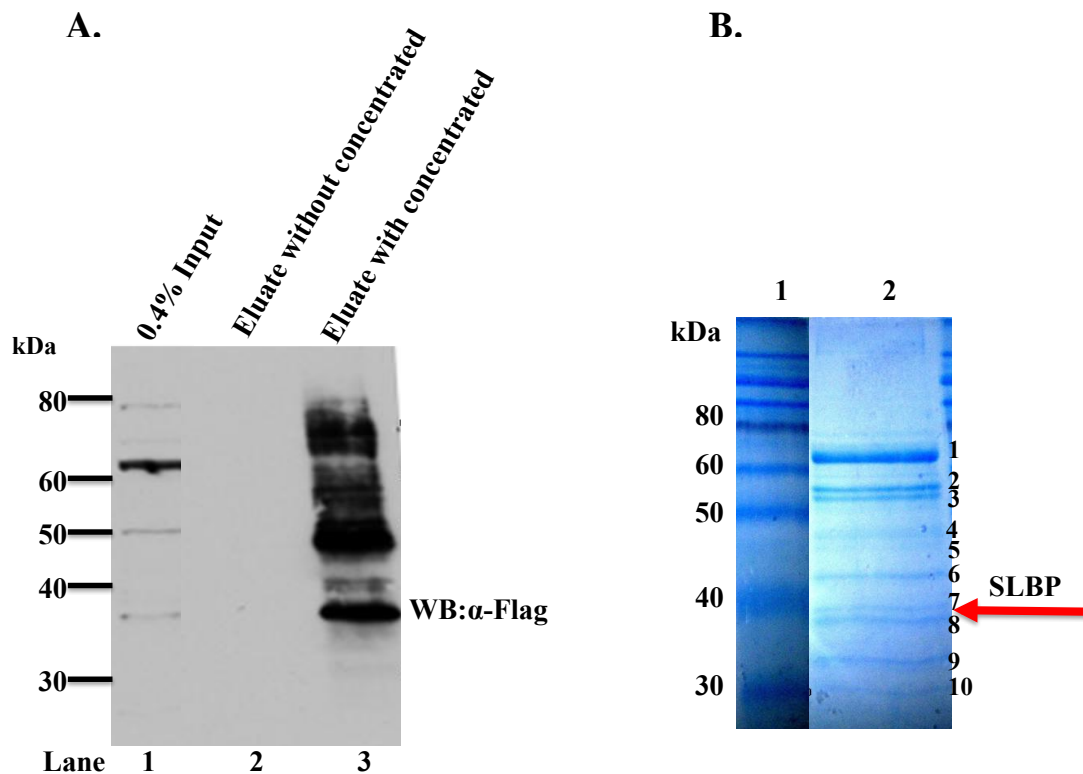


**Figure 4.4** Western blotting analysis of Flag-tagged SLBP content following Flag antibody I-i. **(A)** The packed resin was eluted with 3X FLAG peptide. Eluate and input material were analysed by western blotting using  $\alpha$ -Flag antibody. Lane 1, Input (0.4% of total; (150  $\mu$ g in 30  $\mu$ l lysate), Lane 2 (Eluate prior to concentration (0.4% of total 30  $\mu$ l, out of 7.5 ml total elution volume), Lane 3, Eluate following 32-fold concentration (30  $\mu$ l out of 230  $\mu$ l total of elution volume). **(B)** Concentrated eluate (100  $\mu$ l) was analysed by electrophoresis using a 12% SDS-PAGE gel followed by colloidal Coomassie blue staining. The gel was aligned to its corresponding western blotting and indicated bands

(number 1-10), corresponding to positive signals in western blotting, were removed and subjected to in-gel digestion with trypsin.

In this experiment, western blotting of the cell lysate containing expressed Flag-tagged SLBP identified showed a faint band of the correct MW (approx. 38 kDa), in addition to a number of higher MW proteins. Protein band approx. 38 kDa in addition to a number of MW polypeptides was observed in the eluted fraction although significant concentration was required to observe this (Figure 4.4A, compare lanes 2 and 3). The remaining fraction of the eluted concentrate was subjected to 12% SDS-PAGE and stained with colloidal Coomassie blue staining. All bands (Figure 4.4B, number 1-10) were excised, digested with trypsin and peptides recovered were subjected to LC-MS/MS.

The Sequest search algorithm was used with Swissprot/Uniprot databases to analyse mass spectral data acquired following chromatographic peptide separation of material derived from bands number 1-10. No peptides derived from SLBP were observed in any samples obtained from excised bands shown in Figure 4.4B. The name of proteins identified by a large scale of I-i Flag-tagged SLBP by ANTI-FLAG<sup>®</sup> M2 affinity resin was shown in Appendix H, Table 1H). Most of them (highlighted by yellow colour) were common contaminants which

has been previously listed in immunoprecipitation by Flag antibody and ANTI-FLAG<sup>®</sup> M2 affinity resin from whole cell lysate of HeLa and U2OS cells, respectively (Guo *et al.*, 2009 ; Mellacheruvu *et al.*, 2013). As expected, Ig heavy chain was also found in a list (Appendix H, Table 1H , highlighted by green colour).

The data in Figure 4.4A suggested that Flag-tagged SLBP was indeed present in the eluted sample, although it is clear that the recovery of Flag-tagged SLBP was poor (I did not measure the protein concentration of eluate before concentrated so I lacked of data to show % recovery of samples after concentrated). Again it is unclear why SLBP was not detected in this experiment.

The most likely explanation for the presence of a 50 kDa cross-reacting protein in eluate that was exposed to packed resin is that this band corresponds to some Ig heavy chain, at least one polypeptide of which is covalently attached to the resin. However, the monoclonal used to bind Flag-tagged has been reported to sensitive to reducing agents, such as dithiothreitol (DTT) and 2-mercaptoethanol present in lysis buffer and its covalent attachment to the resin is via a di-thio hydrazide linkage, which may be hydrolysed by reducing agents (Technical bulletin, Sigma-Aldrich, product number A2220). However, in this experiment, a 50 kDa cross-reacting protein was presented in input

material of lysate (Figure 4.4, lane 1) which was not observed in input of lysate in previous experiment. Again, the reason for this difference is not known. However, using a secondary antibody as a probe, it could be shown that this cross-reacting band corresponded to 50 kDa immunoglobulin heavy chain (data not shown) presumably arrived from incomplete cross-linking of anti-Flag antibody to the matrix.

This suggests that this affinity matrix may be unstable under conditions of the experiment as the buffers used in the preparation of expressed proteins contain reducing agent, 2-mercaptoethanol. Given the presence of detectable and relative high levels of contaminating proteins, together with the presence of IgG, identified by LC-MS/MS, it was conceivable that relative low levels of SLBP-derived peptides might not be detect using the Top10 methodology used in this analysis of peptides. In order to address this, it would necessary to generate an inclusion list (Domon and Aebersold, 2006 ; Jaffe *et al.*, 2008) of accurately defined peptide masses derived from the digestion of SLBP with a specific protease.

Therefore, I decided to establish an independent method for the optimisation of SLBP digestion conditions and to establish accurate parameters for the identification of SLBP-derived peptides using mass spectrometry. To do this, SLBP expression was undertaken in *Eschericia*

*coli* (*E. coli*) as a tagged fusion (GST-His tag) protein to facilitate affinity chromatography and thus obtain pure protein for subsequent proteolytic analysis and mass spectrometry.

### **4.2.3 Expression of recombinant GST-SLBP-6xHis protein in *E. coli***

#### **4.2.3.1 Preparation of SLBP PCR product**

To do this, I utilized PCR to amplify the SLBP coding sequence using a forward primer containing a 5' *Xma*I restriction site, a reverse primer containing a 3' *Not*I restriction site, and additional reverse complimentary sequence to generate a 6xHis tag at the C-terminus of the putative gene product. The template used for a plasmid pcDNA5/FRT/TO/CAT/Flag-SLBP (as described in section 2.2.1.3). A range of annealing temperatures was tested (Figure 4.5). In all cases, a strong band corresponding to the predicted size (852bp) was observed. However, the optimal calculated a recommended custom annealing temperature of 64 °C was used subsequently.

The PCR was purified from agarose gel using QIAquick gel extraction kit (as described in section 2.2.1.11), and following digestion of both plasmid backbone and putative insert with restriction enzymes *Xma*I and *Not*I, introduced into the bacterial expression vector, pGEX-6P-1 (Figure 4.6) using restriction sites *Xma*I and *Not*I, with subsequent

ligation, transformation and plasmid preparation. The putative recombinant plasmids were screened by restriction digestion with *XmaI* or *NotI* and subsequently verified by DNA sequencing.

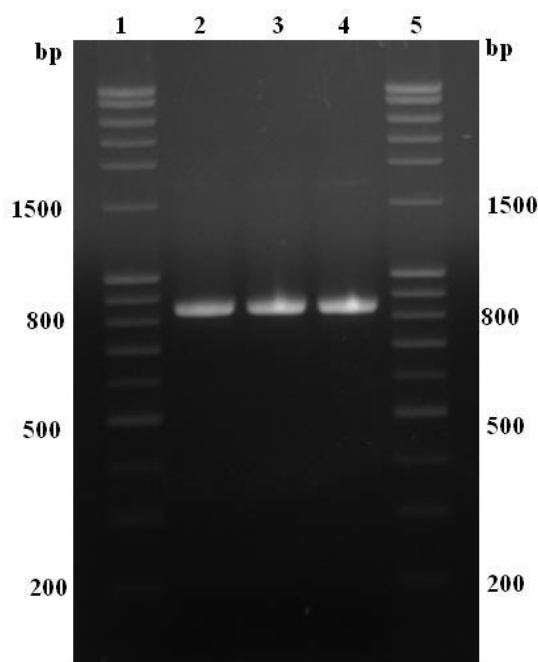


**Figure 4.5** DNA gel electrophoresis of SLBP-6xHis PCR product.

PCR amplification was undertaken utilizing the forward and reverse primers (listed in Appendix C), with the plasmid pcDNA5/FRT/TO/CAT/F-SLBP as template, and Pfu DNA polymerase, using an annealing  $T_m$  of 64°C (Lane 2), 67 °C (Lane 3) or 70 °C (Lane 4), extension  $T_m$  of 68 °C and 20 cycles of amplification. The products were electrophoresed on a 1.5% agarose gel, stained with ethidium bromide and imaged using gel documentation software (UVIprochemi,



#### **4.2.3.2 Expression of GST-SLBP-6xHis in E.Coli**

The modified pGEX-6P-1 plasmid (termed pGEX6SLBPHIS) encoding the GST-SLBP-His fusion protein was transformed into *E. coli* strain BL21 DE3 pLysS. The GST fusion system of pGEX-6P-1 is a versatile system for the expression and purification of fusion proteins produced in *E. coli* where the induced protein accumulates in the cell's cytoplasm. Expression of the GST fusion protein is under the control of the *lac* promoter, which is induced by the lactose analogue isopropyl b-D thiogalactoside (IPTG). pGEX-6P-1 has been engineered with an internal *lacIq* gene (*lac* repressor) to repress gene expression under the *lac* promoter. Addition of IPTG removes the repressor and thus allows protein expression.

#### **4.2.3.3 Optimal temperature of induction**

In order to optimise temperature of induction, two induction conditions were performed in parallel. Cultures 100 ml were grown at either 30 °C or 37 °C in LB medium until the absorbance of each at 600 nm ( $OD_{600}$ ) reached 0.4, and then 1 mM IPTG was added to each of culture media. After the addition of IPTG to the culture, both incubations were continued until the  $OD_{600}$  reached 1.2. Bacteria were harvested by centrifugation and subjected to hypotonic buffer (as described in section

2.2.7) prior to electrophoresis and either protein staining (Figure 4.7A and B) or western blotting (Figure 4.8A and B).

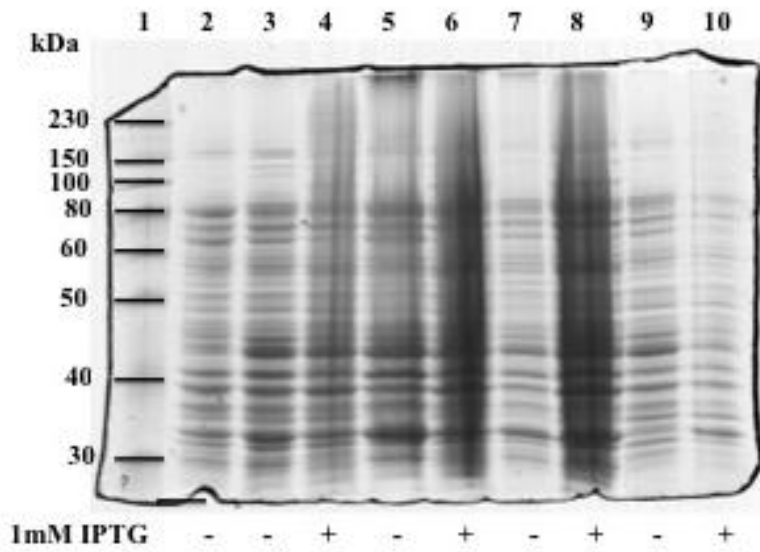
The data showed that following induction at either temperature detectable levels of GST-SLBP-6xHis (approx. 57 kDa) by colloidal Coomassie blue were not observed after induction with IPTG (Figure 4.7A and B). However, analysis of the samples by western blotting with  $\alpha$ -SLBP antibody indicated that IPTG treatment did induce GST-SLBP-6xHis expression (Figure 4.8A and B, compare lanes 2 and 3).

These pilot cultures were subjected to affinity purification using glutathione (GSH) agarose beads. 1.5 ml of lysate was incubated with 80  $\mu$ l of GSH beads for 45 min at 4 °C. Beads were subjected to 4 x 300  $\mu$ l washes with wash buffer C (10 mM Hepes pH 8.0, 1mM DTT, protease inhibitors) and sequentially eluted using 3 x 75  $\mu$ l of wash buffer C containing 5 mM glutathione pH 8.0.

Surprisingly, although both temperatures used for induction resulted in expression of apparently soluble fusion protein as judged by the presence of IPTG-inducible cross-reacting material in the supernatant following centrifugation of lysate at 13,000 rpm for 30 min (as described in section 2.2.7), elution with glutathione generated very little GST-SLBP-6xHis (Figure 4.8A and B). Specific elution of GST-SLBP-6xHis was observed only from bacterial cultures where recombinant protein

expression was induced at 30°C (compare Figure 4.8 A and B, lanes 7-9). At both induction temperatures, either all (37 °C) or the majority (30 °C) of GST-SLBP-6xHis produced remained in the supernatant following incubation of lysate with affinity resin, as judged by the approximate estimates of recovery following GSH-agarose affinity chromatography. However, the recovery of GST-SLBP-6xHis was very low. It is possible that apparently soluble GST-SLBP-6xHis fusion protein may be misfolded, thus preventing glutathione agarose binding. However, small amounts of correctly folded GST moiety was obtained at the lower temperature, and was eluted specifically using glutathione (Figure 4.8 A).

A. Temperature 30 °C



B. Temperature 37 °C

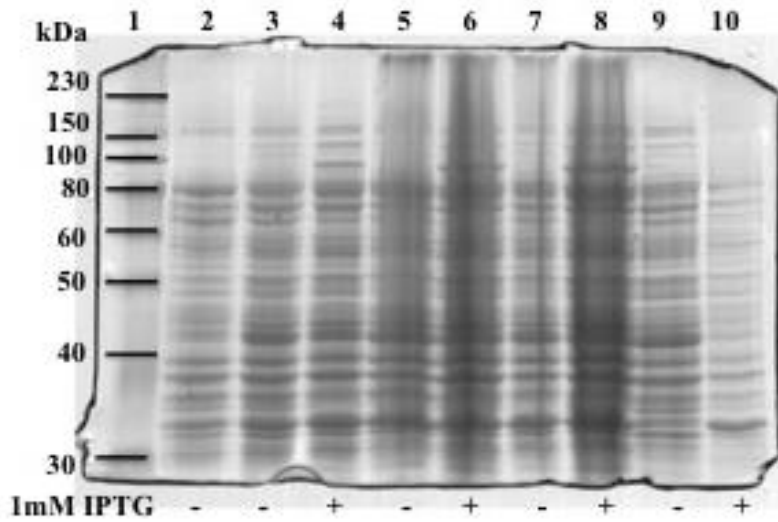
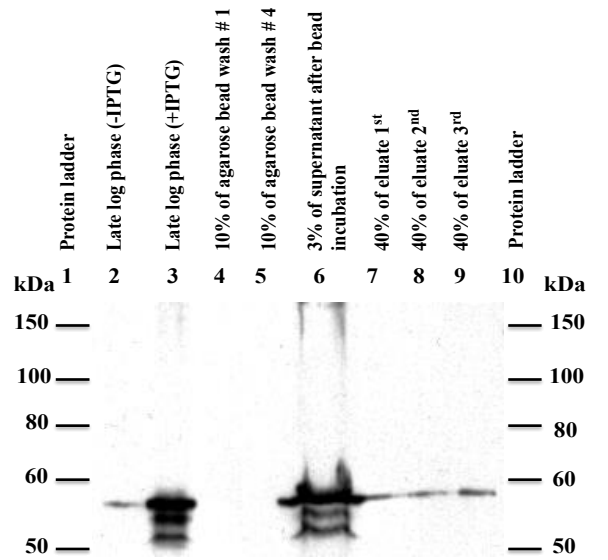


**Figure 4.7** Analysis of GST-SLBP-6xHis protein expression in *E.coli* by SDS-PAGE.

Bacteria growing in log phase ( $OD_{600} = 0.4$ ) were untreated (-) or treated (+) with 1.0 mM IPTG until each culture reached an optical density of  $OD_{600} = 1.2$ , **(A)** at 30 °C or **(B)** 37 °C. Cells were lysed and lysates clarified by centrifugation at 13,000 rpm for 30 min generating a soluble fraction (supernatant) and insoluble pellet. Equivalent amounts of proteins from all fractions were electrophoresed and the gel stained using colloidal Coomassie blue staining. Lane 1: Protein ladder (NEB), Lane 2: lysate  $OD_{600} 0.4$ , Lane 3: lysate  $OD_{600} 1.2$  (-IPTG), Lane 4: lysate  $OD_{600} 1.2$  (+IPTG), Lane 5: lysate before centrifugation (-IPTG), Lane 6: lysate before centrifugation (+IPTG), Lane 7: pellet after centrifugation (-IPTG), Lane 8: pellet after centrifugation (+IPTG), Lane 9: supernatant after centrifugation (-IPTG), Lane 10: supernatant after centrifugation (+IPTG).

### A. Temperature 30 °C



### B. Temperature 37 °C

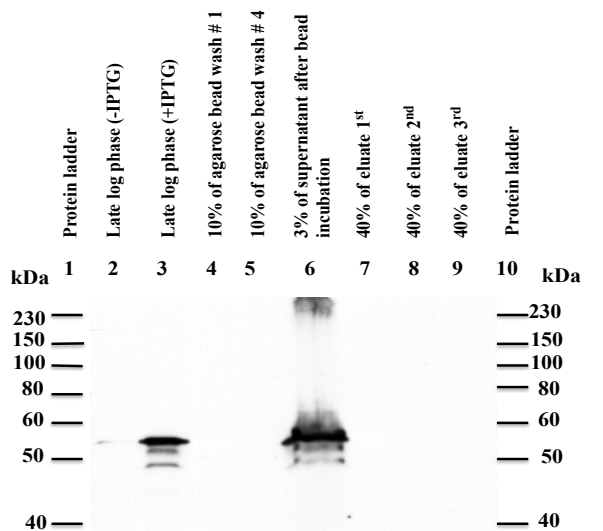


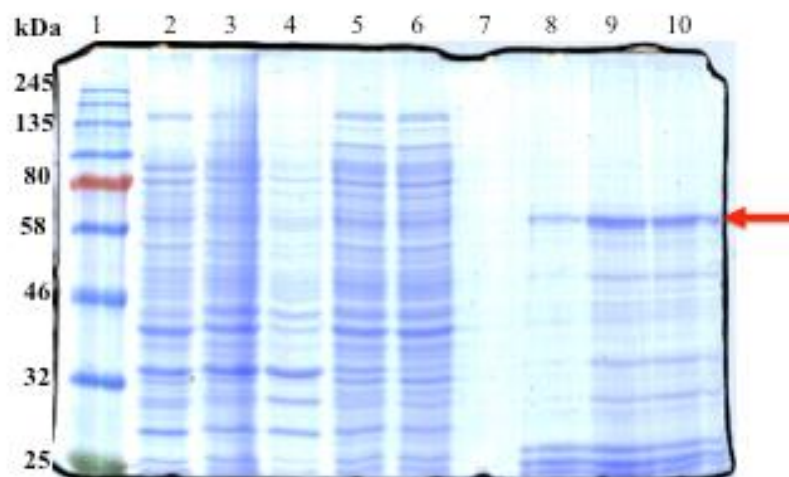
**Figure 4.8** Glutathione agarose affinity purification of GST-SLBP-6xHis.

Protein after IPTG-mediated induction (**A**) at 30 °C and (**B**) 37 °C. Samples were analysed by western blotting using  $\alpha$ -SLBP antibody. 1.5 ml of sample lysate, with 80  $\mu$ l of GSH agarose beads was used for affinity purification. Lane 1: protein ladder (NEB) Lane 2: Late log phase (- IPTG), Lane 3: Late log phase +IPTG, Lane 4: 10% of agarose bead wash #1, Lane 5: 10% of agarose bead wash #4, Lane 6: 3% of supernatant after bead incubation, Lane 7-9: 40% of Eluate 1<sup>st</sup>, 2<sup>nd</sup> and 3<sup>rd</sup>, respectively.

These results suggested that it is possible that reducing the culture temperature during induction might improve GST-SLBP-6xHis expression levels and recovery of soluble protein following affinity purification. Donovan *et al* (1996) found that using an *E.coli* expression system, reducing the induction temperature in some cases improve both yield and/or solubility of the recombinant protein product by decreasing unwanted metabolic responses to the synthesis of a foreign protein and facilitating alternative folding pathways. Therefore, IPTG induction of GST-SLBP-6xHis expression was analysed following IPTG addition (final 1mM to 1 litres of culture) at 15 °C which was fractionated as before. Material in each fraction was analysed by SDS-PAGE and western blotting (Figure 4.9A and B).

In this experiment, approximately 50% of total SLBP as judged by western blotting with  $\alpha$ -SLBP antibody was present in the insoluble pellet (Figure 4.9, compare lanes 4 and 5), and that a significant proportion of apparently soluble SLBP (Figure 4.9, lane 5) did not bind the glutathione affinity resin (Figure 4.9, compare lanes 5 and 6). However, after washing of the beads (Figure 4.9, lane 7), repeated rounds of specific elution with glutathione indicated that some protein had been specifically bound to the column and was recovered using this protocol (Figure 4.9, Lanes 8-10). Analysis of the same material by colloidal Coomassie blue staining indicated that, in addition to material whose MW suggest that it corresponds to full length SLBP (arrow, Figure 4.9A and B), these fractions contained a range of smaller polypeptides, some of which cross-reacted with the SLBP antibody. These data are consistent with the notion that in addition to full-length fusion protein, a range of incompletely synthesized, or partially proteolysed GST-SLBP-6xHis fusion polypeptides were recovered in this experimental protocol.

**A.** Temperature 15 °C



**B.**

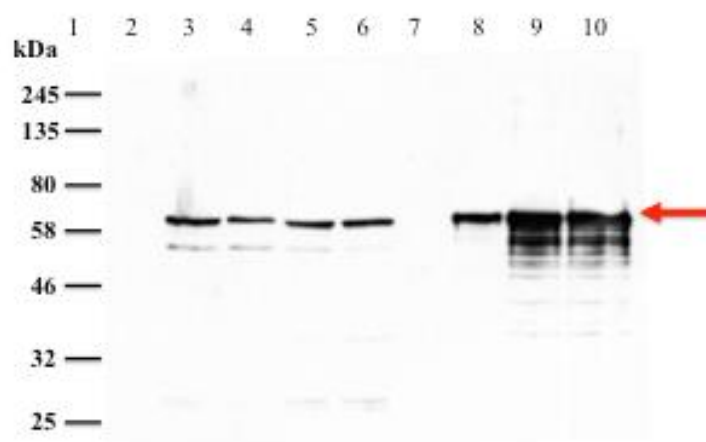


**Figure 4.9** Analysis of GST-SLBP-6xHis protein expression in *E. coli* and glutathione agarose affinity purification by (A) SDS-PAGE (B) western blotting.

Bacteria growing in log phase ( $OD_{600} = 0.4$ ) were untreated (-) or treated (+) with IPTG until each culture reached  $OD_{600} = 1.2$ , at 15 °C. Cells were lysed and lysates clarified by centrifugation generating a soluble fraction (supernatant) and insoluble pellet. Equivalent amounts of protein from all fractions were electrophoresed and the gel stained using colloidal Coomassie blue staining for (A) SDS-PAGE and using  $\alpha$ -SLBP antibody for (B) Western blotting. The equal volume of samples was applied to the gel in A and B. 1.5 ml of sample lysate, with 80  $\mu$ l of GSH beads was used for affinity purification Lane 1: Protein ladder (NEB), Lane 2: lysate  $OD_{600} 1.2$  (-IPTG), Lane 3: lysate  $OD_{600} 1.2$  (+IPTG), Lane 4: pellet before bead incubation (+IPTG), Lane 5: supernatant before bead incubation (+IPTG), Lane 6: supernatant after bead incubation (+IPTG), Lane 7: agarose bead wash #5, Lane 8-10: Eluate 1<sup>st</sup>, 2<sup>nd</sup> and 3<sup>rd</sup>, respectively. The arrows indicate the expected position of GST-SLBP-6xHis.

#### **4.2.4 Bacterial expression system provides SLBP profile by mass spectrometry**

In previous section, I successfully purified small amount (30 µg of protein from 100 ml of bacteria) of GST-SLBP-6xHis by using culture temperature at 15 °C. In order to obtain sufficient quantities of recombinant protein to optimise proteolytic digestion conditions for mass-spectrometry related analyses, large-scale expression was performed. Briefly, 4 litres of LB medium were inoculated with overnight culture of *E. coli* strain BL21 DE3 pLysS containing the pGEX6SLBPHIS expression plasmid and recombinant protein expression induced under the conditions identified above (1 mM IPTG for 12 h at 15 °C). Cells were lysed as before, lysates clarified by centrifugation at 5,000 rpm for 15 min and the solution fraction incubated with 3 ml of GSH agarose beads for 1 h at 4 °C. After repeated washing with 15 ml of wash buffer C, the affinity resin was eluted with 3 x 3 ml of 5 mM glutathione pH 8.0 in wash buffer C. Then, 2 ml of the purified GST-SLBP-6xHis fractions were concentrated using a Vivaspin 500 concentrator (with 10,000 MWCO PES membrane) to a final volume 50 µl containing 175 µg protein, which was stored at -80 °C until required.

In order to determine appropriate conditions for digestion, 5  $\mu$ l aliquots of concentrated eluate was subjected to SDS-PAGE (comprising approximately 18  $\mu$ g of the purified fraction containing recombinant GST-SLBP-6xHis fusion protein) (Figure 4.10A, lanes 5, 6 and 7). In addition to a sample of concentrated eluate 1  $\mu$ l (3.5  $\mu$ g of protein) (Figure 4.10A, lane 3) and a sample of unconcentrated eluate (Figure 4.10A, lane 2) were subjected to SDS-PAGE along with concentrated eluate (corresponding to 4  $\mu$ g of protein). In the case of lanes 5-7, the regions corresponding to full-length GST-SLBP-6xHis were excised and stained with colloidal Coomassie blue prior to processing for enzymatic digestion. In order to confirm that the relevant section of the gel containing GST-SLBP-6xHis had been correctly excised, the remaining gel, after excision of bands, was subjected to western blotting using  $\alpha$ -SLBP antibody (Figure 4.10A, lanes 5-7) compared to uncut bands (Figure 4.10A, lanes 2 and 3). These data confirmed that the largest cross-reacting band corresponding to GST-SLBP-6xHis had been excised.

Excised gel slices were prepared for in-gel proteolytic digestion (as described in section 2.2.10.1). Enzymatic digestion and subsequent extraction of peptides for mass spectrometry was performed. Briefly, each gel slice was resuspended in 200  $\mu$ l of buffer solution 1 containing

200 mM ABC and 40% ACN, and then incubated in 1 mM DTT and 2 mM IAA in buffer solution 2 (50 mM ABC) to bring about reduction and alkylation of protein prior to proteolytic digest. Slices were subsequently incubated at 37 °C overnight in 50 µl of buffer solution 4 (40 mM ABC and 9% ACN) containing 0.02 µg/ml trypsin (NEB), 0.025 µg/ml chymotrypsin (NEB) and 0.02 µg/ml elastase (NEB).

Resuspended peptides were injected by using a Dionex Ultimate 3000 uHPLC onto a PepMap100 C18 2 cm x 75 µm I.D. trap column (ThermoFisher Scientific) at 5µl/min in 0.1% formic acid, 2% acetonitrile and 45 °C in the column oven and 6 °C in the autosampler. The sample was separated over a 60-minute gradient of increasing acetonitrile from 2.4% up to 72%, in 0.1% formic acid, using a 15 cm PepMap100 C18 analytical column (2 µm particle size, 100 Å pore size 75 µm I.D.) (ThermoFisher Scientific) at 300 nl/min and 45 °C.

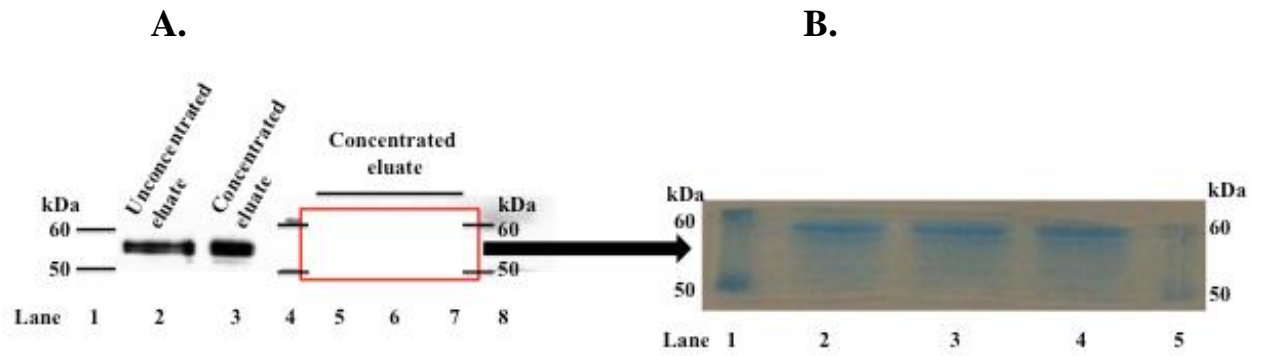


**Figure 4.10** The regions corresponding to full-length GST-SLBP-6xHis were excised (red square) (in parallel to detection by western blotting) and stained with colloidal Coomassie blue for enzymatic digestion prior to mass spectrometry analysis.

Glutathione agarose affinity purification of GST-SLBP-6xHis protein (A) unconcentrated eluate (30  $\mu$ l, 4  $\mu$ g of protein) (Lane 2) and concentrated eluate (1  $\mu$ l, 3.6  $\mu$ g of protein) (Lane 3). Concentrated eluates (Lanes 5-7) were cut in order to stain with colloidal Coomassie blue before blotting with  $\alpha$ -SLBP antibody. All samples were subjected to 12% SDS-PAGE and analyzed by western blotting with  $\alpha$ -SLBP antibody. (B) Concentrated eluate (5  $\mu$ l, 18  $\mu$ g of protein) was analysed by electrophoresis using a 12% SDS-PAGE gel followed by colloidal Coomassie blue staining prior to proteolytic digestion with trypsin, chymotrypsin and elastase, respectively. SLBP-derived peptides

extraction from gel slices was subsequently identified by mass spectrometry.

Mass spectrometry analysis and subsequent database queries using the MASCOT search engine resulted in the successful identification of SLBP-derived peptides as identified in Figure 4.11 and Table 4.1. These data showed that digestion with trypsin produced twelve MS-detectable peptides giving the highest percentage coverage of SLBP of the three proteases tested. In contrast, only 2 peptides were detected using elastase. Chymotrypsin digestion, while not providing as extensive coverage of SLBP as trypsin, nonetheless generated peptides from regions not identified using trypsin in the protein were not detected in this experiment (Table 4.1, highlighted by green colours).

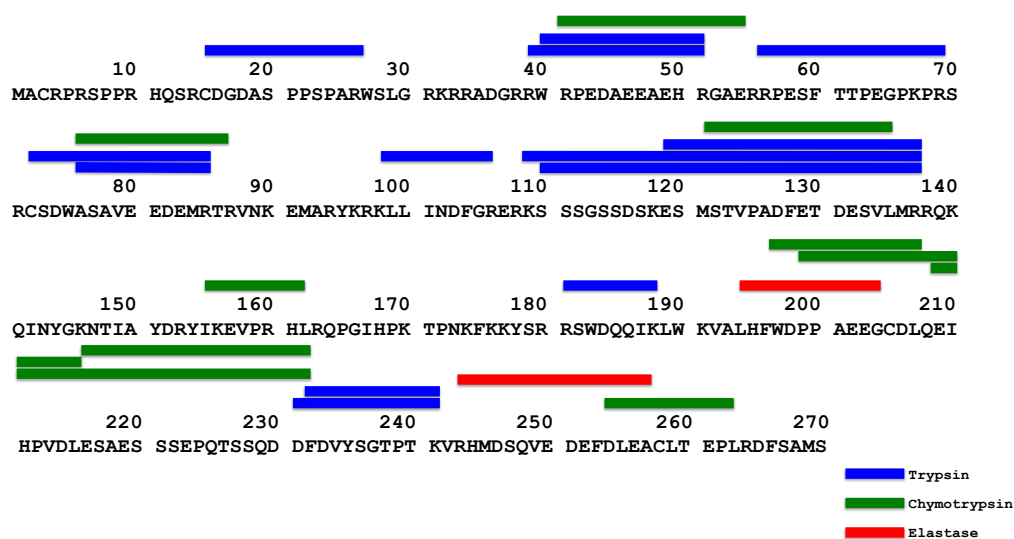


**Figure 4.11** Comparison of SLBP sequence coverage following individual protease digestion of recombinant SLBP analysed by LC-MS/MS from bacterial cell lysate; trypsin (blue), chymotrypsin (green) and elastase (red), respectively.

**Table 4.1** Identification of GST-SLBP-6xHis derived peptide sequences using three protease enzymes: trypsin, chymotrypsin and elastase, respectively (Highlighted by green colours were peptides from region not identified by trypsin).

Peptide position		Peptide sequences	Charge	MS mass	Retention time	Intensity
Start	End		(z)	m/z (Da)	(min)	
<b>Trypsin</b>						
15	26	cdGDASPPSPAR	+2	615.26465	13.77	67892.88281
39	51	RWRPEDAEEAEHR	+2	840.89594	18.31	54978.32813
40	51	WRPEDAEEAEHR	+2	762.84662	18.06	29771.9375
41	51	RPEDAEEAEHR	+2	669.80521	6.94	6325.673014
56	69	RPEFTTPEGPKPR	+2	799.91846	17.75	261507.1406
72	85	cSDWASAVEEDEmR	+2	850.83014	23.81	39410.38281
72	85	cSDWASAVEEDEMR	+2	842.8335	26.01	152696.7188
76	85	ASAVEEDEMR	+2	568.74799	15.67	98462.75781
98	106	KLLINDFGR	+2	538.31683	25.16	3631424.75
109	138	KSSSGSSDSKESmSTVPADFETDESVMR	+3	1042.79712	25.27	31676.28516
110	137	SSSGSSDSKESmSTVPADFETDESVMR	+3	994.76672	27.33	99068.90625
110	137	SSSGSSDSKESmSTVPADFETDESVMr	+3	1000.09766	25.78	137585.1563
119	137	ESMSTVPADFETDESVMR	+2	1072.48071	30.67	75586.53125
119	137	ESmSTVPADFETDESVMr	+2	1088.47571	26.73	59698.25391
181	188	RSWDQQIK	+2	530.78113	17.18	230911.6406
231	241	DFDVYSGTPTK	+2	615.28711	21.5	39451.78906
232	241	FDVYSGTPTK	+2	557.77435	20.35	101369.6563
<b>Chymotrypsin</b>						
41	50	RPEDAEEAEHRGAE	+3	532.5733	13.22	25388.32813
76	86	ASAVEEDEmRT	+2	627.27051	14.07	14632.66504
122	135	STVPADFETDESVL	+2	755.35236	28.35	74107.63281
155	162	IKEVPRHL	+2	496.3063	17.03	601398.0625
195	207	FWDPPAEEGCDL	+2	718.2959	28.19	89290.5
199	215	PPAEEGcDLQEIHPVDL	+2	959.94598	28.46	222879.7188
209	232	EIHPVDLESAESSSEPQTSSQDDF	+2	1317.57068	26.12	20752.42773
214	232	DLESAESSSEPQTSSQDDF	+2	1029.91785	22.32	34450.32422
216	232	ESAESSSEPQTSSQDDF	+2	915.86066	18.8	94464.67969
254	263	DLEAcLTEPL	+2	580.77905	29.53	152162.375
<b>Elastase</b>						
194	204	LHFWPPAEEG	+2	649.29688	27.58	232929.7031
243	257	RHmDSQVEDEFDLEA	+2	918.8894	25.56	92016.25

Having successfully identified GST-SLBP-6xHis derived peptide sequences using protease enzymes by LC-MS/MS, it facilitated to create the inclusion list including two additional potential predicted of cleavage site *in silico* (highlighted by purple colours) shown in Table 4.2. It provided useful information for calibrating of the mass spectrometer, using precise masses of peptides obtained from bacterially expressed SLBP together with their liquid chromatography (LC) retention time, to facilitate identification of SLBP-derived peptides immuno-isolated from mammalian cells. In addition, the amount of protein required to obtain SLBP-derived peptides allowed a re-evaluation of the I-i strategy and experimental scale described in the early part of this chapter, required to obtain sufficient quantities of SLBP both for analysis of post-translational modifications in the presence and absence of replication stress, as well as to undertake a quantitative analysis of potential change in SLBP associated proteins. A further round of I-i of Flag-tagged SLBP was attempted on a significantly scale (this experiment used 10 mg of protein which less than almost 4x compared to the previous I-i coupled to mass spectrometry as described in section 4.3) using cell-cycle synchronized cells, together with a modification of the protocol whereby elution from affinity resin was followed by concentration of the eluate by centrifugal evaporation.

**Table 4.2** Inclusion list obtained from bacterially expressed GST-SLBP-6xHis (m/z = mass to charge)

Peptide position		Peptide sequences	Acquisition time (min)		MS mass
Start	End		Start	End	m/z (Da)
15	26	CDGDASPPSPAR	12.22	22.22	695.23065
52	69	GAERRPESFTTPEGPKPR	10.89	20.89	698.00427
56	69	RPESFTTPEGPKPR	11.27	21.27	893.90198
109	137	KSSSGSSDSKESMSTVPADFETDESVMR	17.85	27.85	1069.45203
109	137	KSSSGSSDSKESMSTVPADFETDESVMR	19.45	29.45	1064.12024
109	137	KSSSGSSDSKESTVPADFETDESVMR	20.74	30.74	794.34326
109	137	KSSSGSSDSKESMSTVPADFETDESVMR	21.32	31.32	1090.77917
110	137	SSSGSSDSKESMSTVPADFETDESVMR	19.82	29.82	1026.7533
110	137	SSSGSSDSKESMSTVPADFETDESVMR	18.19	28.19	1078.78882
110	137	SSSGSSDSKESMSTVPADFETDESVMR	21.53	31.53	1021.42218
161	174	HLRQPGIHPKTPNK	8.56	18.56	426.47836
178	188	YSRRSWDQQIK	12.15	22.15	516.24463
181	188	RSWDQQIK	12.7	22.7	570.76343
182	188	SWDQQIK	16.03	26.03	492.71298

HeLa cells stably transfected with Flag-tagged SLBP (as described in Chapter 3) were initially grown in culture flasks with a surface area 175 cm<sup>2</sup> (T175) in a total of 15 flasks until cells reach 80% confluence. Then Flag-tagged SLBP cells were initially synchronized by exposure to nocodazole for 12 h after that mitotic shake-off was used to detach cells prior to grown them in 100 mm dishes in the presence of 0.5 µg/ml dox for 14 h. Cells were harvested and lysate prepared, respectively. Cell lysate (10 mg in 8 ml of buffer) was incubated with 1 ml of ANTI-FLAG<sup>®</sup> M2 affinity resin overnight at 4 °C with repeated agitation prior to washed with 5 ml of TBS and elution, respectively. Eluate initially was eluted in 500 µl of altered elution buffer (10 mM Tris-HCl pH 7.4 and 30 mM NaCl) containing 300 ng/µl final concentration of 3X FLAG peptide. Following elution, the eluate (500 µl) was concentrated by centrifugal evaporation prior to SDS-PAGE and gel slice excision as before.

**A.**

**B.**

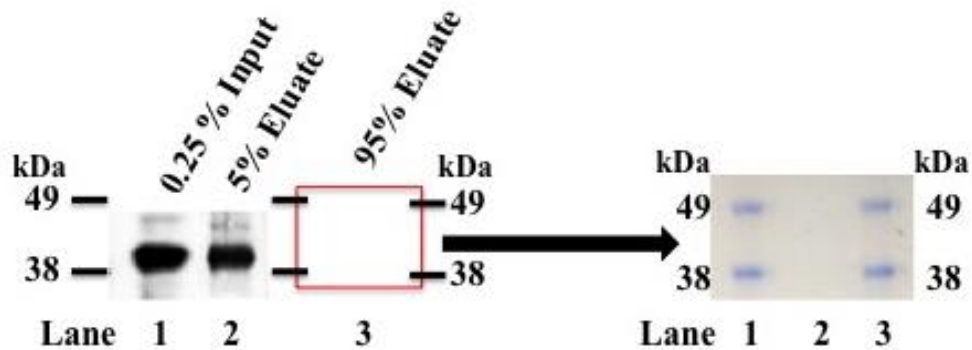


**Figure 4.12** The regions corresponding to full-length Flag-tagged SLBP were excised (red square) and stained with colloidal Coomassie blue in parallel to detect by western blotting prior to processing for enzymatic digestion

I-i analysis of Flag-tagged SLBP. The packed resin was eluted with 300 ng/ $\mu$ l final concentration of 3X FLAG peptide in 500  $\mu$ l of 10 mM Tris HCl and 30 mM NaCl. The eluate volume was reduced to dryness by centrifugal evaporation and the resulting pellet was resuspended in total volume 25  $\mu$ l (5  $\mu$ l of 5x sample loading buffer and 20  $\mu$ l of ddH<sub>2</sub>O) and (A) analysed by western blotting using the  $\alpha$ -Flag antibody. Lane 1, Input 0.25% (25  $\mu$ g), Lane 2, 5% eluate (1.25  $\mu$ l), Lane 3, 95% eluate (23.75  $\mu$ l). (B) stained with colloidal Coomassie blue (Lane 3). There is no band apparent after staining with colloidal Coomassie blue. This is probably due to limitation of detection using this staining method due to

the small amount of eluate analysis. SLBP-derived peptides extracted from gel slices were prepared for in-gel trypsin digestion and subsequently identified by mass spectrometry.

Following LC-MS/MS analysis, Flag-tagged SLBP-derived peptide sequences with trypsin digestion using inclusion list from bacterially expressed SLBP were successfully detected in mammalian system (Figure 4.13 and Table 4.3). The peptide sequences with highlighted by blue colours were included in inclusion list. However, there are some peptides were detected with different sequences from inclusion list but their retention time were covered in inclusion list.

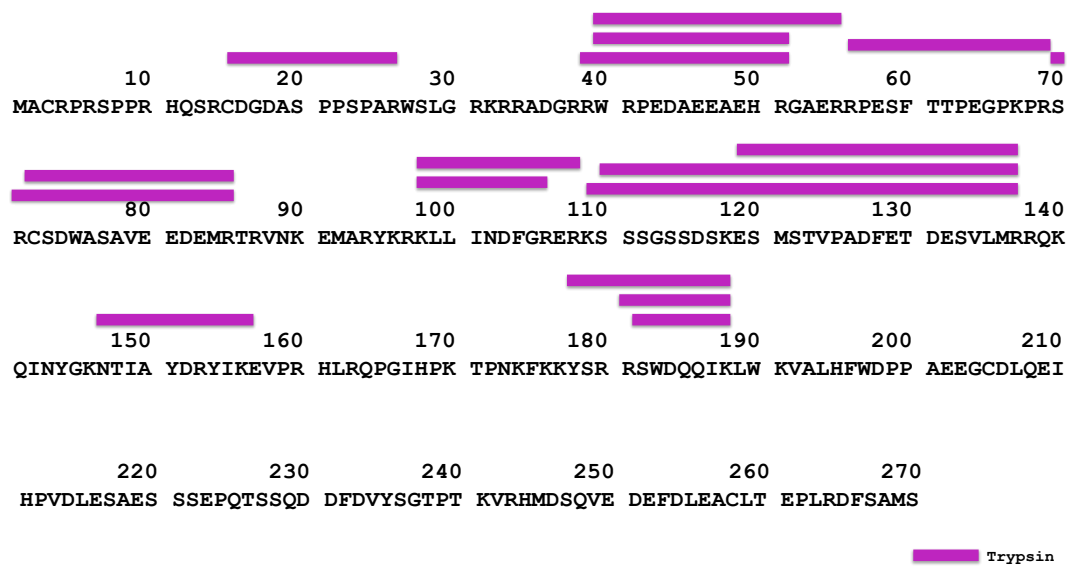


**Figure 4.13** SLBP sequence coverage with trypsin digestion of Flag-tagged SLBP in mammalian expression system using inclusion list from bacterially expressed SLBP detected by LC-MS/MS.

**Table 4.3** Identification of Flag-tagged SLBP-derived peptide sequences with trypsin digestion using inclusion list from bacterially expressed SLBP detected by LC-MS/MS (highlighted by blue colours are the peptide sequences based on inclusion list) (m/z = mass to charge). The site of with post-translational modifications by amino acids in lower-case.

Peptide position		Peptide sequences	Charge (z)	MS mass m/z (Da)	Retention time (min)	Intensity
Start	End					
15	26	CDGDAsPPsPAR	+2	695.23083	18.62	20101.2637
38	51	RWRPEDAEEAEHR	+2	840.89691	16.47	57747.5156
40	51	WRPEDAEEAEHR	+2	762.84564	17.74	97367.7031
40	55	WRPEDAEEAEHRGAER	+3	646.63361	17.49	38884.8008
56	69	RPESFtTPEGPKPR	+3	560.26996	17.3	158220.734
56	69	RPESFTTPEGPKPR	+2	799.91827	16.65	24970.7285
69	85	SRcSDWASAVEEDEMR	+3	1927.7902	23.49	41892.9688
72	85	cSDWASAVEEDEMR	+2	842.83386	25.5	238962.984
72	85	cSDWASAVEEDEmR	+2	1700.65349	23.88	307999.375
98	106	KLLINDFGR	+2	538.31689	22.21	496899.75
98	108	KLLINDFGRER	+2	454.26144	20.15	392666.156
99	106	LLINDFGR	+2	474.2692	25.25	1020594.69
99	108	LLINDFGRER	+3	411.56317	22.61	824510.25
109	137	KSSSGSSDSKESmSTVPADFETDESVMR	+3	1032.13477	25.08	46779.25
109	137	KSSSGSSDSKESmSTVPADFETDESVMR	+3	1037.46545	23.86	59009.3242
109	137	KSSSGSSDSKESmSTVPADFETDESVMr	+3	1042.79614	22.48	66919.4375
109	137	KsSSSGSSDSKESmSTVPADFETDESVMr	+3	1064.12158	25.05	69796.4766
109	137	KSSsGsSDSKESmSTVPADFETDESVMR	+3	1090.77551	27.11	16283.375
109	137	KSSsSGSSDSKESmSTVPADFETDESVMr	+3	1069.45251	23.84	202290.203
110	137	SSSGSSDSKESmSTVPADFETDESVMR	+3	989.43481	26.6	95571.8594
110	137	SSSGSSDSKESmSTVPADFETDESVMr	+3	994.76721	25.14	93637.2656
110	137	SSSGSSDSKESmSTVPADFETDESVMr	+3	1000.09845	23.93	280521.531
110	137	SSSGsSDSKESmSTVPADFETDESVMR	+3	1021.42273	27.3	28021.0801
119	137	ESMSTVPADFETDESVMR	+3	715.32349	28.87	71145.6328
119	137	ESmSTVPADFETDESVMR	+2	1080.47827	27.64	286146.375
119	137	ESmSTVPADFETDESVMr	+2	1088.47522	25.91	132510.609
147	156	NTIAYDRYIK	+2	628.8358	20.41	109203.938
178	188	YSRRsWDQQIK	+3	516.24316	18.08	62887.5313
181	188	RSWDQQIK	+2	530.78046	16.97	31771.252
182	188	swDQQIK	+2	492.71326	22.07	40506.2617

### **4.3 Discussion**

The objective of this chapter was to establish a method for the isolation of Flag-tagged SLBP and potential associated interacting proteins using an ANTI-FLAG<sup>®</sup> M2 affinity resin immuno-isolation, and to develop a method for mass spectrometry-based characterisation of SLBP. The advantage of this system is that, in principle, the addition of a small hydrophilic peptide tag to a wild-type protein minimizes the risk of disrupting protein function while enabling affinity purification by immuno-isolation using the specific, commercially available anti-Flag antibody. The moderate avidity with which the epitope is bound means that it is readily displaced by competition with a synthetic peptide, enabling the development of gentle, specific elution conditions (Technical bulletin, Sigma-Aldrich, product number A2220). These are important for subsequent analysis of SLBP post-translational modification status, together with an analysis of its interacting proteins in the HeLa cell tissue culture cell line model by LC-MS/MS.

### **4.3.1 Immuno-isolation (I-i) of Flag-tagged SLBP**

Immuno-isolation (I-i) experiments were undertaken to isolate Flag-tagged SLBP from cell lysates derived from the cell line characterised in Chapter 3. I began by using different amounts of packed resin volume (10  $\mu$ l and 20  $\mu$ l) to establish an appropriate ratio of packed resin to cell lysate necessary to immuno-isolate SLBP, as judged by western blotting detection.

There was little difference between results obtained using 10  $\mu$ l or 20  $\mu$ l of packed resin volume in terms of either depletion and recovery (Figure 4.1), although there was some variation in the apparent recovery, depending on the antibody either anti-Flag or anti-SLBP antibodies used to evaluate it. The reasons for such discrepancy are unknown. One possibility is that, as the Flag antibody clearly recognises additional polypeptides in cell lysates (Figure 4.1, lanes 2 and 6), an additional cross-reacting band was present in cell lysates at low levels at the size expected for SLBP, which was enriched using the ANTI-FLAG<sup>®</sup> M2 affinity resin.

Because there can be significant loss of gel beads on this scale, during incubation and washing steps, which might result in poor

recovery, an attempt was made to perform immuno-isolation using a fixed column format and gravity flow. This approach has a number of advantages. The depleted lysate may be efficiently collected with minimal dilution, wash steps can be monitored for loss of bound protein efficiently and effectively remove contaminating proteins from beads, without resin loss, and high recovery of antigen and co-precipitated proteins (Tomomori-Sato *et al.*, 2013). Somewhat surprisingly, affinity depletion and elution of Flag-tagged SLBP by chromatography on a small ANTI-FLAG<sup>®</sup> M2 affinity resin column (either 10 µl or 20 µl volume) was not effective in my hands (Figure 4.2). Although analysis of the flow-through material suggested that SLBP was depleted from the lysate, at least partially, under these conditions, it was not recovered either by specific elution with 3X FLAG peptide. SLBP recovery by boiling beads in SDS-PAGE sample buffer was negligible, although interpretation of these data was hampered by cross-reactivity of addition material which eluted from the column under these conditions (Figure 4.2). The most likely interpretation was that these additional bands represent IgG antibody heavy and light chains which were not covalently cross-linked to the resin.

Bands consistent with the elution of IgG heavy chains were observed as expected when beads were eluted with sample loading buffer, presumably because the reducing agent (DTT) in sample loading buffer eliminates the intermolecular disulphide bonds between immunoglobulin (IgG) heavy and light chains (Figure 4.1 and 4.2, lanes 3 and 7). However, in the experiment shown in Figure 4.3, IgG heavy chains were also observed in the depleted lysate (Figure 4.3, lanes 5 and 6, designated “flow-through”). This suggests that low levels of reducing agents in the lysate were sufficient in this experiment to disrupt the IgG and may have contributed to reduced yield.

#### **4.3.2 Mass spectrometric analysis of complex containing SLBP**

For mass spectrometric analysis, the conditions established above in Figure 4.3 (batch procedure; 10 µl of packed resin per 1 mg protein lysate) were used in a scaled up experiment to immuno-isolate SLBP and putative interacting protein complexes which were visualized by staining with colloidal Coomassie blue. All visible bands were excised from the gel, digested with trypsin, and analyzed by Liquid chromatography-tandem mass spectrometry (LC-MS/MS). Normally, proteins that are visible by colloidal Coomassie staining are usually in sufficient quantity for identification by mass spectrometry (Collins, M. personal

communication), therefore, all bands (number 1-10, Figure 4.4B) were excised and treated as described above. Surprisingly, no SLBP-derived peptides or known SLBP interacting proteins were detected. Most of proteins are keratins, heat shock proteins, ribosome-related, metabolic pathway enzymes and transcription/translation related such as heterogeneous nucleus ribonucleoproteins (HNRNP) and eukaryotic translation initiation factor (EIF). They are highly abundant proteins known to frequently contaminate proteins immunoprecipitated using Flag antibody and ANTI-FLAG<sup>®</sup> M2 affinity resin (Guo *et al.*, 2009 ; Mellacheruvu *et al.*, 2013). These authors reported all common contaminants following immunoprecipitation from whole cell lysate of HeLa and U2OS cells which included cytoskeletal proteins (actin and keratin), protein chaperones, ribosomal proteins, RNA-interacting proteins, and polypeptides involved in transcription and translation. All of these classes of protein were present in the samples analysed. However, some proteins could not be ruled out as contaminants because they might be SLBP-related during transcription and translation such as eukaryote translation initiation factor 4B and 2S1 (EIF4B and EIF2S1). This information will be described in detail in Chapter 6 which was detected following I-i of Flag-tagged SLBP.

It is unclear why SLBP was not detected at all in this experiment. SLBP has been analysed successfully by mass spectrometry previously, following immunoprecipitation using ANTI-FLAG<sup>®</sup> M2 affinity resin in order to investigate its phosphorylation sites that was targeted by Pin1 (Prolyl isomerase) coordinating the degradation of SLBP by the ubiquitin proteasome system (Krishnan *et al.*, 2012). However, its cellular abundance has not been accurately determined.

A band corresponding to the correct size for Flag-tagged SLBP was observed by western blotting of a sample of the specific eluate after concentration with the VivaSpin concentrator, however it is not clear whether this band corresponds to any of the ~50 kDa colloidal Coomassie blue-stained bands shown in Figure 4.4B. Because of the relatively large matrix volume required, this necessitated elution in a large volume (37.5 mg protein derived from dox-treated Flag-tagged SLBP expressing cells in total volume 7.5 ml and applied to 3 ml of packed resin volume and eluted with 7.5 ml PBS containing 3X FLAG peptide prior to concentration with the VivaSpin concentrator as in Figure 4.4). A VivaSpin concentrator was used to concentrate the samples by ultrafiltration in order to carry out the subsequent SDS-PAGE step. It is possible that low abundance proteins may bind disproportionately to the VivaSpin membrane and may not be recovered

efficiently. In addition, the efficiency with which peptides are recovered following tryptic in-gel digestion, is a function of substrate availability, protease concentration, time allowed for proteolysis and properties of peptides generated. In this experiment, any of the first three parameters may have been significantly sub-optimal. Trypsin, which was used to generate peptides, cleaves peptide chains to generate a C-terminal lysine or arginine, except when either is followed by proline (Granvogl and Ploscher, 2007). Given the abundance of unconstrained lysine and arginine residues, a reasonable number of SLBP-derived peptides might be expected to be recovered. It is common for only a subset of the potential tryptic peptides to be detected, and “missed cleavages” may generate peptides with significant degree of hydrophobicity, making them insoluble under the standard extraction conditions used (Hubbard, 1998). Thus, future improvements might include consideration of parallel digestion with a second protease of different specificity such as chymotrypsin to improve probability of detection and protein sequence coverage. According to literature review, it also suggested to use multi-protease protein digestion which increases proteome sequence coverage and improve the identification of post-translational modifications (Tsiatsiani and Heck, 2015).

It is important that efficient extraction of the peptides and preparation of the sample for MS is efficient, while trying to minimize the presence of salts or detergents that may adversely affect ionization. Moreover, the presence of other proteins and other impurities, and the sensitivity and performance characteristics of the mass spectrometer and its mode of ionization, mass separation, and ion detection need to be considered (Baldwin, 2004). The MS Top10 method was used in this experiment that allowed the machine only analyses the top 10 most abundant peptides in the fraction coming off the HPLC at any one time. However, in the conditions under sample complexity and purity concerned as my experiment, Top 10 method may not detect low abundance peptides which were not included in the top 10 most abundant at that time. In contrast, using Top 20 method gives much higher resolution survey scans which can greatly augment sequence related information in peptide MS/MS, as not observed by Top 10 method (Michaelski *et al.*, 2012). Therefore, it is possible that the percentages of SLBP-derived peptide coverage could improve using Top 20 or combination of two methods. The high degree of contamination, together with a potentially low abundance and recovery of SLBP by I-i together may have resulted in lack of detection of SLBP peptides.

In addition, an additional improvement would be to ensure that Flag-SLBP was excised from the polyacrylamide gel, by western blotting with anti-Flag antibody after excision of the relevant gel region. Considering this, I subsequently established an independent method to set up accurate parameters for the identification of SLBP-derived peptides by expression of SLBP as a tagged fusion (GST) protein in *E.coli* followed by affinity chromatography to obtain purified SLBP polypeptides for MS analysis.

#### **4.3.3 SLBP expression in the *E.Coli* system**

Previous analysis of SLBP have used baculovirus expression to produce human SLBP for the purpose of mass spectrometry analysis (Dominski *et al.*, 2002 ; Koseoglu *et al.*, 2008 ; Bansal *et al.*, 2013). Time constraints prevented me from using baculovirus expression to establish conditions for the analysis of SLBP by mass spectrometry. The expression of protein in *E. coli* is the easiest, quickest, cheapest and high production method of protein production (Sivashanmmugam *et al.*, 2008). However, no previous work has reported the successful expression and isolation of soluble SLBP from *E.coli*.

In my study, a GST fusion protein was constructed by inserting SLBP coding sequence with an addition 3' tag encoding 6xHis, into the

pGEX-6P-1 vector under the control of the *lac* promoter. I carried out at different temperatures (30 °C and 37 °C). The results clearly demonstrated that both temperatures expressed low protein production and it was predicted to form insoluble aggregates (inclusion bodies). Therefore, it is possible to resolubilize the protein from the inclusion bodies or improve the solubility by expressing the protein at a lower temperature. Lower culture temperature may enhance the proper export and folding protein (Donovan *et al.*, 1996). After lower temperature, the yield of SLBP was increased before and after purification with GSH compared to both culture temperatures at 30 °C and 37 °C. Although, the level of SLBP expression was not much high production, it reached my purpose to obtain SLBP purity for mass spectrometry analysis. Therefore, further experiment was to identify SLBP peptide using purified GST-SLBP-6xHis by proteolytic enzymes, trypsin, chymotrypsin and elastase following mass spectrometry.

#### **4.3.4 Bacterial expression system provides an SLBP profile by mass spectrometry**

After bacterial expression of the protein GST-SLBP-6xHis, I was able to successfully identify SLBP peptides by mass spectrometry. This confirmed that it is a sufficient abundance of SLBP with the right position of protein band on SDS-PAGE which corresponds to the protein band probed with anti-Flag antibody on western blotting. However, contaminants were still identified in the mass spectrometry data. These are difficult to avoid as they can be introduced during gel electrophoresis and cutting bands from the gel and from sample tubes, pipettes, buffers, or extraneous matter dropping into the sample (such as hair, skin, material from clothing, laboratory dust) (Baldwin, 2004).

The identification of candidate proteins was performed by searching the database with the MASCOT search engine. Peptide mapping of SLBP identifies the percentage sequence coverage after digestion by each enzyme. Trypsin digestion gave the highest total sequence coverage of SLBP compared to chymotrypsin and elastase (41%, 34% and 10%), respectively. Using *in silico* digestion (ExPasy portal with PeptideMass), the prediction of the percentage sequence coverage of SLBP is about 40-80%, depending on the input parameters such as size of masses. Therefore, for example, the low percentage sequence coverage of SLBP

using trypsin digestion, it is possible that trypsin digestion does not cleave at some positions in the protein. The specificity of any proteases is influenced by other residues in close proximity to the cleavage site, together with other factors such as local conformation, tertiary structure and experimental conditions (Siepen *et al.*, 2007). Therefore, using different digestion should improve the sequence coverage of proteins.

In summary, the success of this independent method for the identification of SLBP peptide with 45% of sequence coverage SLBP provides important insights into the strategy and scale of I-i required to obtain sufficient quantities of SLBP for both the analysis of SLBP post-translational modification status, together with an analysis of its interacting proteins in the HeLa cell tissue culture cell line model by LC-MS/MS. In particular, using inclusion list provided the calibration of the mass spectrometry experiment using the precise masses of peptides obtained from bacterially expressed SLBP together with their HPLC retention time should detect SLBP-derived peptides from mammalian expressed protein. The retention time using bacterially expressed SLBP covered the mammalian expressed Flag-tagged SLBP-derived peptide sequences (compare Table 4.3, highlighted by blue colour to Table 4.2, non-highlighted). However, some mammalian expressed SLBP-derived

peptide sequences were different sequences from inclusion list and vice versa. The reasons for this are obviously structural which affects accessible cleavage of trypsin (Hubbard, 1998).

### 4.3 References

- Baldwin, M.A. 2004. Protein identification by mass spectrometry: issues to be considered. *Mol Cell Proteomics*. 3: 1-9.
- Bansal, N., Zhang, M., Bhaskar, A., Itotia, P., Lee, E., Shlyakhtenko, L.S., Lam, T.T., Fritz, A., Berezney, R., Lyubchenko, Y.L., Stafford, W.F. and Thapar, R. 2013. Assembly of the SLIP1-SLBP complex on histone mRNA requires heterodimerization and sequential binding of slbp followed by SLIP1. *Biochemistry*, 52(3): 520-536.
- Chen, Y., Kwon, S.W., Kim, S.C. and Zhao, Y. 2005. Integrated approach for manual evaluation of peptides identified by searching protein sequence databases with tandem mass spectra. *J. Proteome Res.* 4: 998-1005.
- Domon, B. and Aebersold, R. 2006. Mass Spectrometry and Protein analysis. *Science*. 312: 212-217.
- Dominski, Z., Erkmann, J.A., Yang, X., Sanchez, R. and Marzluff, W.F. 2002. A novel zinc finger protein is associated with U7 snRNP and interacts with the stem-loop binding protein in the histone pre-mRNP to stimulate 3'-end processing. *Genes & Dev.* 16: 58-71.

- Donovan, R.S., Robinson, C.W., Glick, B.R. 1996. Optimizing inducer and culture conditions for expression of foreign proteins under the control of the lac promoter. *J Ind Microb.* 16: 145-154.
- Granvogel B, Plösch M, Eichacker LA. 2007. Sample preparation by in-gel digestion for mass spectrometry-based proteomics. *Anal Bioanal Chem.* 389(4): 991-1002.
- Guo, R., Xu, D. and Wang, W. 2009. Identification and analysis of new Proteins involved in the DNA Damage Response network of Fanconi anemia and Bloom syndrome. *Methods.* 48(1): 72-79.
- [http://web.expasy.org/peptide\\_mass/](http://web.expasy.org/peptide_mass/)
- <https://www.sigmaaldrich.com/content/dam/sigma-aldrich/docs/Sigma/Bulletin/a2220bul.pdf>
- Hubbard, S.J. 1998. The structural aspects of limited proteolysis of native proteins. *Biochim Biophys Acta* 1382(2): 191-206.
- Jaffe, J.D., Keshishian, H. Chang, B. Addona, T.A. Gillette, M.A. and Carr, S.A. 2008. Accurate Inclusion Mass Screening. *Mol Cell Proteomics.* 7(10): 1952-1962.
- Koseoglu, M.M., Graves, L.M. and Marzluff, W.F. 2008. Phosphorylation of threonine 61 by cyclin a/Cdk1 triggers degradation of stem-loop binding protein at the end of S phase. *Mol. Cell. Biol.* 28: 4469-4479.

Krishnan, N., Lam, T.T., Fritz, A. Rempinski, D., O'Loughlin, K., Minderman, H., Berezney, R. Marzluff, W.F. and Thapar. R. 2012. The Prolyl Isomerase Pin1 Targets Stem-Loop Binding Protein (SLBP) To Dissociate the SLBP-Histone mRNA Complex Linking Histone mRNA Decay with SLBP Ubiquitination. *Mol Cell Biol.* 32(21): 4306-4322.

Markham, K., Bai, Y. and Schmitt-Ulms, G. 2007. Co-immunoprecipitations revisited: an update on experimental concepts and their implementation for sensitive interactome investigations of endogenous proteins. *Anal Bioanal Chem.* 389(2): 461- 473.

Mellacheruvu, D., Wright, Z., Couzens, A., Lambert, J., St-Denis, N., Li, T., Miteva, Y., Hauri, S., Sardi, M., Low, T., Halim, V., Bagshaw, R., Hubner, N., Hakim, A., Bouchard, A., Faubert, D., Fermin, D., Dunham, W., Goudreault, M., Lin, Z., Badillo, B., Pawson, T., Durocher, D., Coulombe, B., Aebersold, R., Furga, G., Colinge, J., Heck, A., Choi, H., Gstaiger, M., Mohammed, S., Cristea, I., Bennett, K., Washburn, M., Raught, B., Ewing, R., Gingras, A.C. and Nesvizhskii, A. 2013. The CRAPome: a Contaminant Repository for Affinity Purification Mass Spectrometry Data. *Nat Methods* 10: 730-736.

- Michalski, A., Damoc, E., Lange, O., Denisov, E., Nolting, D., Müller, M., Viner, R., Schwartz, J., Remes, P., Belford, M., Dunyach, J.-J., Cox, J., Horning, S., Mann, M. and Makarov, A. 2012. Ultra High Resolution Linear Ion Trap Orbitrap Mass Spectrometer (Orbitrap Elite) Facilitates Top Down LC-MS/MS and Versatile Peptide Fragmentation Modes. *Mol Cells Proteomics*. 11: 1-11.
- Qoronfleh, M.W., Ren, L., Emery, D., Perr, M., Kaboord, B. 2003. Use of immunomatrix methods to improve protein-protein interaction detection. *J Biomed Biotechnol*. 291- 298.
- Siepen, J.A., Keevil, E.J., Knight, D. and Hubbard, S.J. 2007. Prediction of Missed Cleavage Sites in Tryptic Peptides Aids Protein Identification in Proteomics. *J Proteome Res* 6(1): 399-408.
- Tomomori-Sato, C., Sato, S., Conaway, R.C. and Conaway, J.W. 2013. Immunoaffinity Purification of Protein Complexes from Mammalian Cells. *Methods Mol. Biol*. 977: 273-287
- Tsiatsiani, L. and Heck, A.J.R. 2015. Proteomics beyond trypsin. *FEBS Journal* 282: 2612-2626.
- Willander, M. and Al-Hilli, S. 2009. Analysis of biomolecules using surface plasmons. *Methods Mol. Biol*. 544: 201-229.
- Young, K.H. 1998. Yeast two-hybrid: so many interactions, (in) so little time. *Biol Reprod*. 58(2): 302-311.

Zhao, Y. and Jensen, O.N. 2009. Modification-specific proteomics: Strategies for characterization of post-translational modifications using enrichment techniques. *Proteomics*. 9(20): 4632-4641.

# *Chapter 5*

## *Regulation of Serine 182 on cell cycle progression, SLBP expression, histone mRNA decay and SLBP stability*

### **5.1 Introduction**

The identification of SLBP-derived peptides has been successfully analysed by mass spectrometry after using a bacterial expression system generating GST-SLBP-6xHis and consequent affinity chromatography to obtain pure protein. Having established an independent method to obtain accurate HPLC and isotopic masses for SLBP-derived peptides, mass spectrometric analysis of immuno-isolated Flag-tagged SLBP was undertaken. SLBP-derived tryptic peptides were detected and, for the first time in mammalian cells, a series of phospho-modified peptides were also observed, several of which have been identified previously by other approaches. The functional significance of SLBP phosphorylation at position 182 has not been previously studied even though this site is in the RNA binding domain (RBD) of SLBP and the surrounding sequence

contains an evolutionarily conserved SRRS sequence (Thapar *et al.*, 2004).

In order to understand the function of phosphorylation at Ser182, the experiment undertaken and discussed in Chapter 5 provides evidence of phosphomimetic substitution from serine to glutamate (S182E), and the non-phosphorylatable substitution to alanine (S182A) on cell cycle progression, SLBP expression, and histone mRNA decay. Moreover, the investigation of the protein kinase responsible for the phosphorylation of S182 was identified by *in silico* computational analysis of phosphorylation site substrate preference (GPS 3.0 software). The Aurora and WEE1 kinases were two high-scoring protein kinase families both of which are known to play relevant key roles related to genetic instability in the cell cycle. (Ducat and Zheng, 2004 ; Kollareddy *et al.*, 2008).

WEE1 is the first kinase investigated to determine if it might be responsible for the phosphorylation of S182 *in vitro*. WEE1 plays an important role in regulation of the replication checkpoint, the control of DNA damage responses during S-phase as well as a role in regulating histone synthesis (Watanabe *et al.*, 1995 ; Berry and Gould, 1996 ; Booher *et al.*, 1997 ; Mahajan and Mahajan, 2013 ; Heijink *et al.*, 2015 ; Saini *et al.*, 2015). Unexpectedly, SLBP is not phosphorylated directly

by WEE1. However, the investigation of SLBP level by MK-1775, WEE1 kinase inhibitor, provides evidence to establish model that WEE1 kinase might activate Cyclin A/Cdk1 involving in T61 phosphorylation at the end of S phase and also the coordination of WEE1 and SLBP degradation.

## 5.2 Results

### 5.2.1 Identification of the phosphorylated Serine 182 in the conserved SRRS motif of SLBP

In the previous chapter, tryptic peptides derived from Flag-tagged SLBP expressed in synchronised HeLa cells were identified by LC-MS/MS. Bacterially expressed SLBP-derived peptides was used for accurate MS calibration prior to analysis of peptides derived from the mammalian expressed protein.

Phosphorylation sites at Ser20, Ser23, Thr61, Thr62, Ser110, Ser111, Ser112, Ser114, Ser120, Thr171 and Ser182 were detected after the re-analysis of data from Chapter 4. The peptide sequences of these phosphorylation sites and the annotated spectra of each of the relevant peptides are shown in Table 5.1 and diagram showing these phosphorylation sites in Figure 5.1 (see Appendix I for mass spectra). These phosphorylation sites identified here have been reported previously in PhosphoSitePlus<sup>®</sup> and PHOSIDA (phosphorylation site databases) (Hornbeck *et al.*, 2004 ; Gnad *et al.*, 2007), however, a number of these (Ser120 and Ser182) were identified in analyses of SLBP following heterologous expression in baculovirus-infected insect cells with unknown function (Bansal *et al.*, 2013).

**Table 5.1** Mass spectrometry (MS) of phospho-sites and other modifications on human SLBP expressed in HeLa cells.

Peptide position		Peptide sequences	Modifications	IonScore	m/z (Da)
start	End				
15	26	CDGDAsPPsPAR	C1 (Carbamidomethyl); S6(Phospho); S9(Phospho)	40.99	695.2307
52	69	GAERRPESFtPEGPKPR	T10 (Phospho)	11.12	698.0043
56	69	RPESFtPEGPKPR	T7 (Phospho)	52	839.902
109	137	KSSSGSSDSKESmSTVPADFETDESVMR	S12 (Phospho)	35.93	794.3433
109	137	KsSSGSSDSKESmSTVPADFETDESVMR	S3(Phospho); M13(Oxidation)	64.16	1064.12
109	137	KsSSGSSDSKESmSTVPADFETDESVMR	S2(Phospho); M13(Oxidation); M28(Oxidation)	72.94	1069.452
109	137	KsSSGSSDSKESmSTVPADFETDESVMR	S3(Phospho); S4(Phospho); M13(Oxidation)	24.03	1090.779
110	137	sSSGSSDSKESmSTVPADFETDESVMRR	S1(Phospho); M12(Oxidation); M27(Oxidation)	36.69	1078.789
110	137	SSSGsSDSKESmSTVPADFETDESVMR	S5(Phospho); M12(Oxidation)	42	1021.422
110	137	SsSSGSSDSKESmSTVPADFETDESVMR	S2(Phospho); M12(Oxidation); M27(Oxidation)	38.93	1026.753
161	174	HLRQPGIHPKtPNK	T11 (Phospho)	14.01	426.4784
178	188	YSRRsWDQQIK	S5 (Phospho)	14.42	1021.422
181	188	RsWDQQIK	S2 (Phospho)	30.17	570.7634
182	188	sWDQQIK	S1 (Phospho)	30.44	492.713

10            20            30            40            50            60            70  
 MACRPRSPPR HQSRCGDAS PPSPARWSLG RKRRADGRRW RPEDAEEAEH RGAERRPESEF **TT**PEGPKPRS

80            90            100            110            120            130            140  
 RCSDWASAVE EDEMTRVNK EMARYKRKLL INDFGRERKS **SSGSSDSKES** MSTVPADFET DESVLMRRQK

150            160            170            180            190            200            210  
 QINYGKNTIA YDRYIKEVPR HLRQPGIHPK **TP**PNKFKKYSR **RS**WDQQIKLW KVALHFDPP AEEGCDLQEI

220            230            240            250            260            270  
 HPVDLESAES SSEPQTSSQD DFDVYSGTPT KVRHMDSQVE DEFDLACLTL EPLRDFSAMS

**Figure 5.1** Diagram showing phosphorylation sites (red letters) found on human SLBP expressed in HeLa cells.

Moreover, the phosphorylation sites at Ser20 and Ser23 were identified as a phosphodegron that controls SLBP polyubiquitination (Krishnan *et al.*, 2012). Phosphorylation at Thr61 and Thr62 has been shown to trigger SLBP degradation at the end of S phase (Koseoglu *et al.*, 2008). The roles of phosphorylation sites at Ser110, Ser111, Ser112 and Ser114 are still unknown. Interestingly, I observed two phosphorylation sites (Thr171 and Ser182) within the RNA-binding domain (RBD or L-motif; residues 125-197). The L-motif of the histone mRNA binding domain of SLBP form a ternary complex with histone mRNA stem-loop and 3'hExo (Tan *et al.*, 2013). This leads to the modulation of L-motif function by posttranslational modifications (PTMs) which has been proposed to interact with proteins involved in histone pre-mRNA processing, mRNA decay, and mRNA translation (Thapar, 2015). For example, the interaction of prolyl isomerase Pin1 interacts with phosphor-Thr 171 form of the SLBP-L-motif which is necessary for recruitment of SLBP to the stem-loop to the site of histone pre-mRNA processing in the nucleus (Krishnan *et al.*, 2012). Moreover, at the end of S phase, dephosphorylation of SLBP in its RNA binding domain by Pin1 and a phosphatase PP2A remove SLBP from the 3' UTR, resulting in histone mRNA decay via exosome-mediated mRNA degradation and subsequent ubiquitination proteasomal degradation of

SLBP (Krishnan *et al.*, 2012). Although, Ser182 phosphorylation has previously been reported, its significance or functional role is unknown (Bansal *et al.*, 2013). It is possible that this Ser of the SLBP L-motif plays important biological or functional roles regulated by PTM. Therefore, I directed attention to phosphorylation at Ser182.

The identified mass spectrum of Ser182 phosphorylation in peptide sequence  $^{181}\text{RpS}\text{WDQQIK}^{188}$  is shown in Figure 5.2

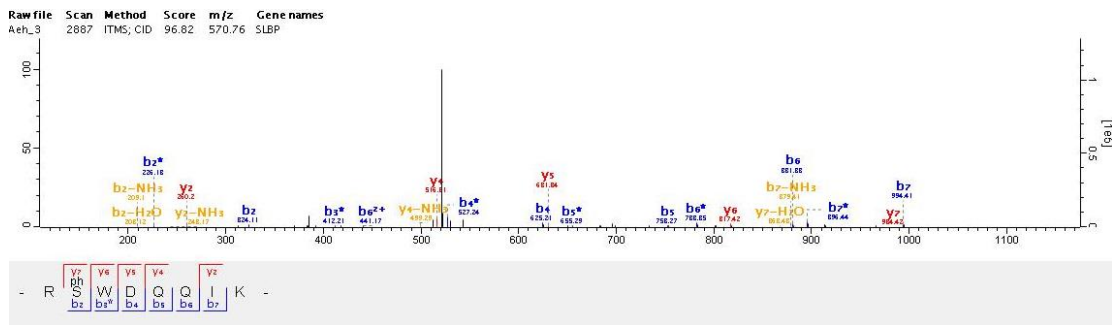


**Figure 5.2** MS/MS spectrum of a phosphorylated peptide showing a doubly-charged peak at m/z 570.76. The corresponding peptide is identified as RpSWDQQIK (181-188), of which Ser182 is phosphorylated.

In order to study the role of phosphorylation at Ser182, I undertook site-directed mutagenesis to establish a phosphomimetic substitution from serine to glutamate (S182E) and also the non-phosphorylatable substitution to alanine (S182A) using the template plasmid pCDNA5/FRT/TO/CAT-Flag-SLBP<sup>res</sup>. The Flag-SLBP<sup>res</sup> notation refers to a form of the SLBP gene containing two silent mutations in the sequence corresponding to that targeted by siRNA knockdown. These mutants were used to generate the corresponding HeLa cell line using the FLP-IN system as described in section 2.2.3.2. The cell lines identified as Flag-SLBP<sup>resS182A</sup> and Flag-SLBP<sup>resS182E</sup> were used to investigate the cell cycle progression, the duration of SLBP expression, and the efficiency of histone mRNA decay after DNA replication arrest.

### **5.2.2 S phase progression**

In order to determine whether expression of either Flag-SLBP<sup>resS182A</sup> or Flag-SLBP<sup>resS182E</sup> in the continued presence of endogenous SLBP, had an effect on progression through S-phase, cells were synchronized with 40 ng/ $\mu$ l nocodazole (Noc) for 12 h and mitotic cells were isolated by shake-off exactly as described in the experiment, figure 3.6-3.9 of Chapter 3. Cells were re-plated in presence of

doxycycline (Dox)-containing fresh medium for 5 h, after which medium was replaced with Dox-free medium. At indicated times, cells were harvested, lysates prepared, and analysed by western blotting. Cell cycle profile was analysed by flow cytometry.

As before with Flag-SLBP expressing cells (Figure 5.3), Noc treatment and subsequent release resulted in enrichment for a G1 population of cells which was similar for Flag-SLBP<sup>resS182A</sup> cells and Flag-SLBP<sup>resS182E</sup> cells (Figures 5.4 ; 5.5 ; Table 5.2). Once again, a proportion of cells were observed in S and G2 phases (Figures 5.4 ; 5.5 ; Table 5.2). Both mutant cell lines progressed through S phase as judged by flow cytometry, although a noticeable difference was observed in the approximate duration of S phase (Table 5.2) which was ~10 h long in the Flag-SLBP<sup>resS182A</sup>-expressing cell line, and ~ 14 h long in the Flag-SLBP<sup>resS182E</sup>-expressing cell line, compared to ~ 12 h for Flag-SLBP<sup>res</sup> (Figure 5.6). The timing of S phase initiation for each cell line appeared to vary, although it is not clear whether this reflects the stochastic variability associated with the G1/S transition (see below). Flag-SLBP<sup>resS182A</sup> cells appeared to transit through G2/M more quickly (12-14 h) than Flag-SLBP<sup>res</sup> cells (14-18 h) with the Flag-SLBP<sup>resS182E</sup> cells taking even longer to complete a cell cycle (18-24 h) with new G1

population of the foremost clearly visible after 14 h, compared with 18-24 h in the latter (Figures 5.4 ; 5.5 ; 5.6).

By western blotting analysis, the overall duration of expression of Flag-SLBP<sup>resS182E</sup> appeared to be longer (~11 h) than Flag-SLBP<sup>resS182A</sup> (~8 h) and similar to that of Flag-SLBP<sup>res</sup> at ~11 h (Figure 5.7A). While the profile of Flag-SLBP expression broadly coincided with the proportion of cells in S phase for Flag-SLBP<sup>resS182E</sup> cells and Flag-SLBP<sup>res</sup> cells, this did not appear to be the case for Flag-SLBP<sup>resS182A</sup> cells. In these cells, SLBP protein expression lagged behind the peak of cells transiting through S-phase, as judged by FACS analysis.

Consistent with published observations (Pines and Hunter, 1991 ; Erlandsson *et al.*, 2000) and its known role in S-phase progression and mitotic entry, levels of cyclin A increased during S phase, approaching close to maximal levels ~16 h after Noc release in Flag-SLBP<sup>res</sup> cells, Flag-SLBP<sup>resS182A</sup> and Flag-SLBP<sup>resS182E</sup> cell lines (Figure 5.7B). The Flag-SLBP<sup>resS182A</sup> cells appeared to show a slight delay in cyclin A accumulation, compared with the other 2 lines and consistent with a similar delay in SLBP accumulation (Figure 5.7). Cyclin A levels subsequently decreased within 2-4 h in Flag-SLBP<sup>resS182E</sup>-expressing cells, consistent with the known timing of cyclin A destruction just after nuclear envelope breakdown in prometaphase (den Elzen and Pines,

2001). Surprisingly, levels of cyclin A in Flag-SLBP<sup>resS182A</sup>-expressing cells (Figure 5.7B) did not appear to decrease over the time course of this experiment. The reason for this is not clear, and will require further investigation. It is possible that these cells do not enter into mitosis in schedule. Time constraints precluded the investigation of this point.

These data suggested that expression of phospho-mimetic SLBP may increase the duration of S phase, and non-phosphorylatable SLBP facilitates more rapid transit through S phase, at least when compared to the wild-type tagged protein, despite the presence of endogenous wild-type protein.

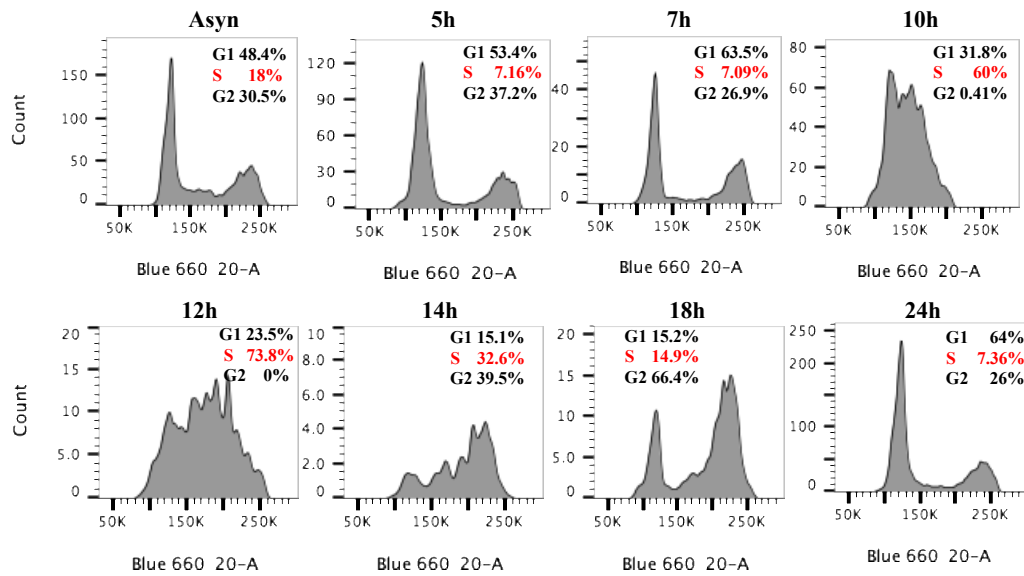


**Figure 5.3** Cell cycle progression of Flag-SLBP<sup>res</sup> cells. Flag-SLBP cells were arrested by treatment with nocodazole and subsequently released. Samples were prepared for FACS analysis by staining with propidium iodide (PI) at the indicated times after release. FACS profiles with PI staining Asynchronous (Asyn), 5, 7, 10, 12, 14, 18 and 24 h after release from nocodazole block. The percentage of cells with G1, S and G2-phases DNA content were shown. Results are representative of two independent experiments.

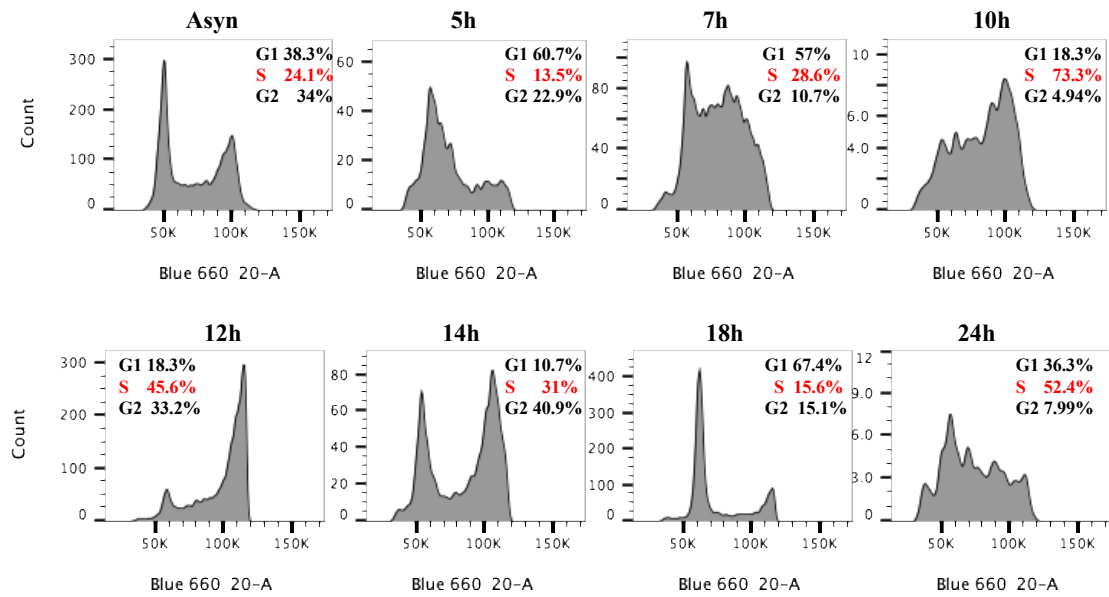


**Figure 5.4** Cell cycle progression of Flag-SLBP<sup>resS182A</sup> cells. Flag-SLBP<sup>resS182A</sup> cells were arrested by treatment with nocodazole and subsequently released. Samples were prepared for FACS analysis by staining with propidium iodide (PI) at the indicated times after release. FACS profiles with PI staining Asynchronous (Asyn), 5, 7, 10, 12, 14, 18 and 24 h after release from Noc block. The percentage of cells with G1, S and G2-phases DNA content were shown. Results are representative of two independent experiments.

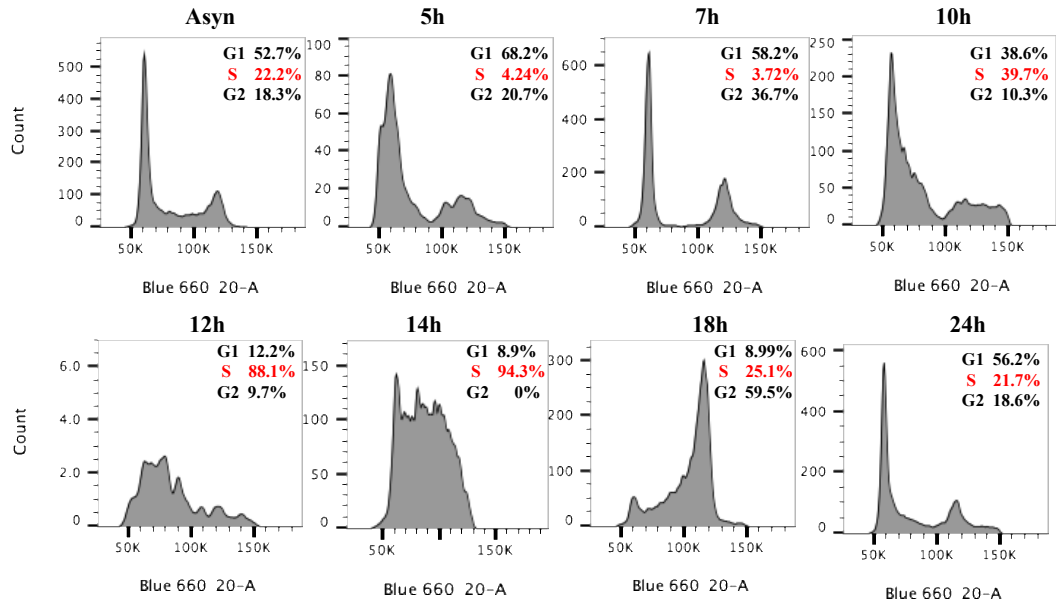


**Figure 5.5** Cell cycle progression of Flag-SLBP<sup>resS182E</sup> cells. Flag-SLBP<sup>resS182E</sup> cells were arrested by treatment with nocodazole and subsequently released. Samples were prepared for FACS analysis by staining with propidium iodide (PI) at the indicated times after release. FACS profiles with PI staining Asynchronous (Asyn), 5, 7, 10, 12, 14, 18 and 24 h after release from Noc block. The percentage of cells with G1, S and G2-phases DNA content were shown. Results are representative of two independent experiments.

**Table 5.2** Summary of the percentages of cells in the respective phases (G1, S and G2) with different time points of the cell cycle in Flag-SLBP<sup>res</sup>, Flag-SLBP<sup>resS182A</sup> and Flag-SLBP<sup>resS182E</sup>-expressing cells

Time (h)	Cells	Percentage of cells		
		G1	S	G2
Asyn	Flag-SLBP <sup>res</sup>	48.4	18	30.5
	Flag-SLBP <sup>resS182A</sup>	38.3	24.1	34
	Flag-SLBP <sup>resS182E</sup>	52.7	22.2	18.3
5	Flag-SLBP <sup>res</sup>	53.4	7.16	37.2
	Flag-SLBP <sup>resS182A</sup>	60.7	13.5	22.9
	Flag-SLBP <sup>resS182E</sup>	68.2	4.24	20.7
7	Flag-SLBP <sup>res</sup>	63.5	7.09	26.9
	Flag-SLBP <sup>resS182A</sup>	57	28.6	10.7
	Flag-SLBP <sup>resS182E</sup>	58.2	3.72	36.7
10	Flag-SLBP <sup>res</sup>	31.8	60	0.41
	Flag-SLBP <sup>resS182A</sup>	18.3	73.3	4.94
	Flag-SLBP <sup>resS182E</sup>	38.6	39.7	10.3
12	Flag-SLBP <sup>res</sup>	23.5	73.8	0
	Flag-SLBP <sup>resS182A</sup>	18.3	45.6	33.2
	Flag-SLBP <sup>resS182E</sup>	22.2	88.1	9.7
14	Flag-SLBP <sup>res</sup>	15.1	32.6	39.5
	Flag-SLBP <sup>resS182A</sup>	10.7	31	40.9
	Flag-SLBP <sup>resS182E</sup>	8.9	94.3	0
18	Flag-SLBP <sup>res</sup>	15.2	14.9	66.4
	Flag-SLBP <sup>resS182A</sup>	67.4	15.6	15.1
	Flag-SLBP <sup>resS182E</sup>	8.99	25.1	59.5
24	Flag-SLBP <sup>res</sup>	64	7.36	26
	Flag-SLBP <sup>resS182A</sup>	36.3	52.4	7.99
	Flag-SLBP <sup>resS182E</sup>	56.2	21.7	18.6

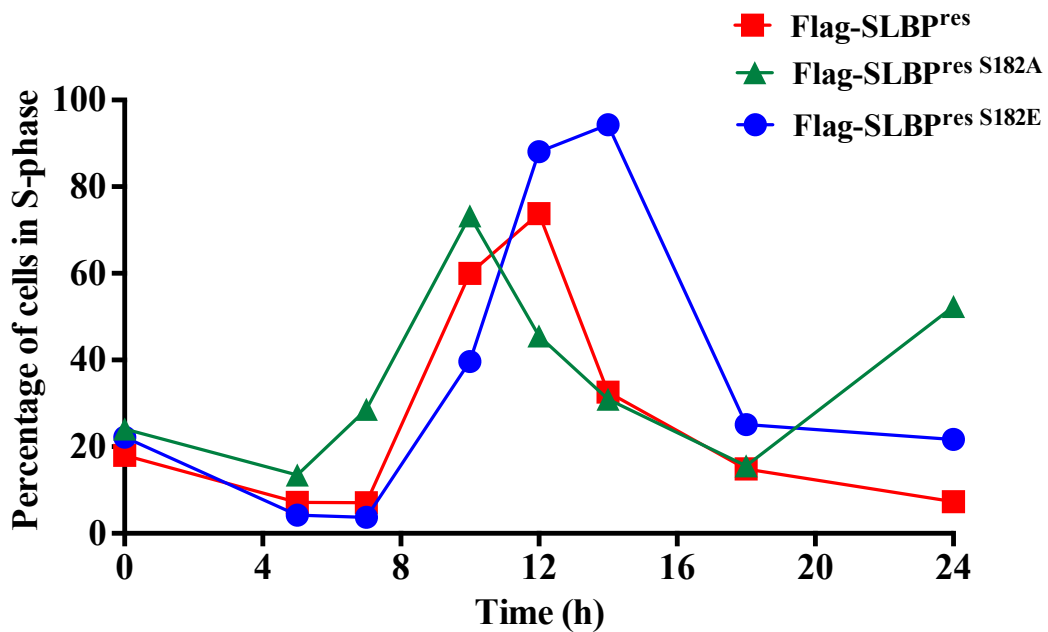


**Figure 5.6** Flag-SLBP<sup>resS182E</sup> cells display and apparent delay in S phase progression. The percentage of cells in S phase in Flag-SLBP<sup>res</sup>, Flag-SLBP<sup>resS182A</sup> and Flag-SLBP<sup>resS182E</sup> cell lines after synchronised release Noc block. The second set of data shows the same trend as the first set. However, the second set of data has incomplected time course (data not shown).

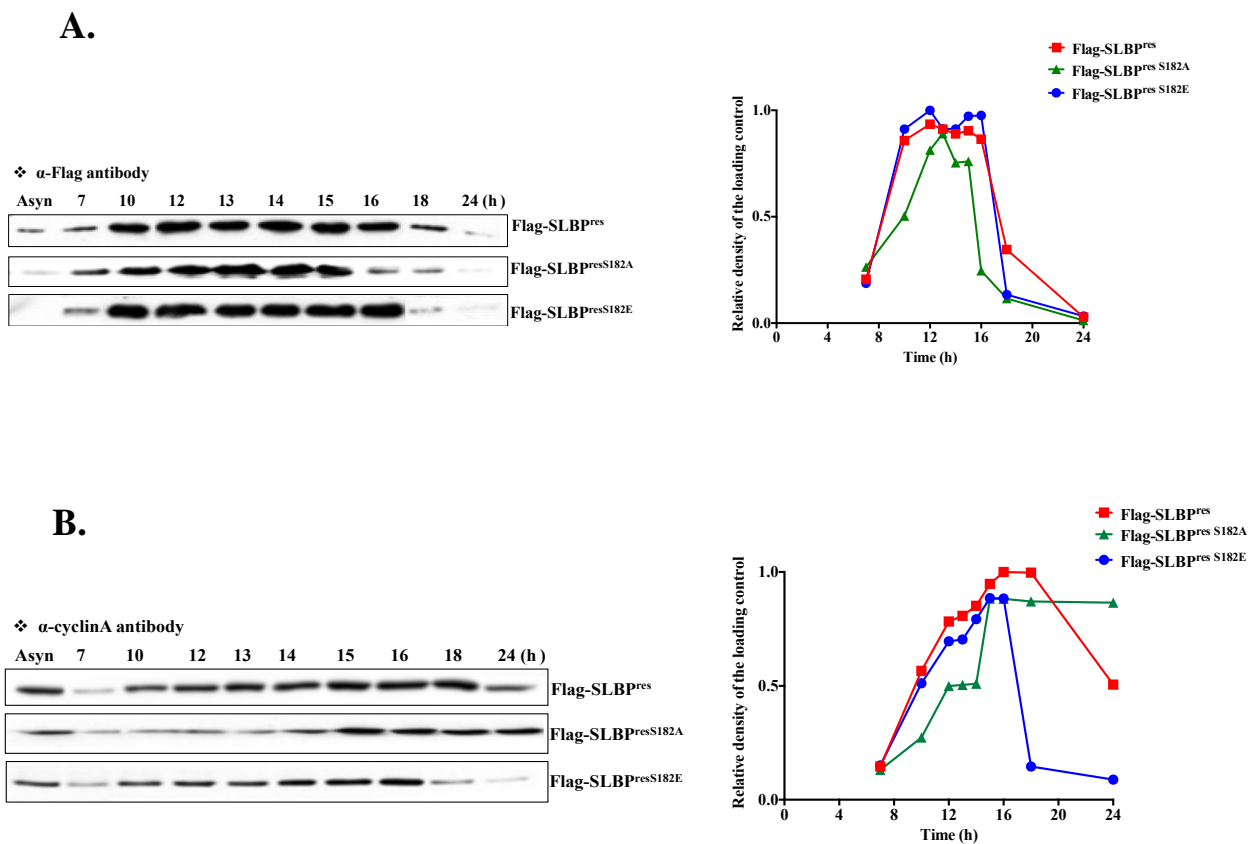


**Figure 5.7** SLBP expression is prolonged in Flag-SLBP<sup>res</sup>S182E cells compared to Flag-SLBP<sup>res</sup>S182A cells. Western blot analysis of the Flag-SLBP<sup>res</sup>, Flag-SLBP<sup>res</sup>S182A and Flag-SLBP<sup>res</sup>S182E cell lysates using  $\alpha$ -Flag (A) and  $\alpha$ -cyclin A (B) antibodies collected at indicated time after treatment with Noc and subsequently released. Graph was normalised with loading control. Results are representative of two independent experiments.

Another experiment was undertaken with an extended time courses (18, 24 and 29 h) in order to observe the relative stability of the phospho-mimetic form of SLBP compared to the wild-type protein. These three extended length experiments allows cells to progress continually through the next cell cycle. In this experiment, Flag-SLBP<sup>resS182E</sup> cells were compared solely with Flag-SLBP<sup>res</sup> cells. Cells were first treated with either non-targeting siRNA (NT) or siRNA targeting SLBP for 24 h. Then cells were synchronized with Noc as described above. Cells were harvested at 18, 24 and 29 h after release from Noc block. The level of SLBP, Flag, cyclin A and nucleolin (as loading control) proteins were analysed by western blotting (Figures 5.8A and B) and quantified (Figure 5.8C). Simultaneously, mRNAs of them were extracted from lysates in order to quantify histone mRNA level by qPCR (Figure 5.9).

The protein expression results show that, when normalised to the amount of SLBP present at 18 h after Noc release, the efficiency with which SLBP levels decrease is dramatically reduced in cells expressing Flag-SLBP<sup>resS182E</sup> compared with Flag-SLBP<sup>res</sup> (Figure 5.8C), with ~70% of protein remaining 29 h after release from Noc arrest, compared with 0-25% remaining in cells expressing Flag-SLBP<sup>res</sup>. siRNA-mediated knockdown of the endogenous protein had a small effect in

Flag-SLBP<sup>res</sup> expressing cells, reducing the efficiency with which SLBP levels decreased, with no effect on Flag-SLBP<sup>resS182E</sup> cells.

Interestingly, qPCR analysis of histone mRNA revealed that histone mRNA levels were significantly elevated in Flag-SLBP<sup>resS182E</sup> cells compared to Flag-SLBP<sup>res</sup> cells at least at 18 and 29 h after release from Noc arrest, consistent with data obtained in Figure 5.8C (Figure 5.9), and the notion that prolonged expression of SLBP results in prolonged stabilization of histone mRNA.

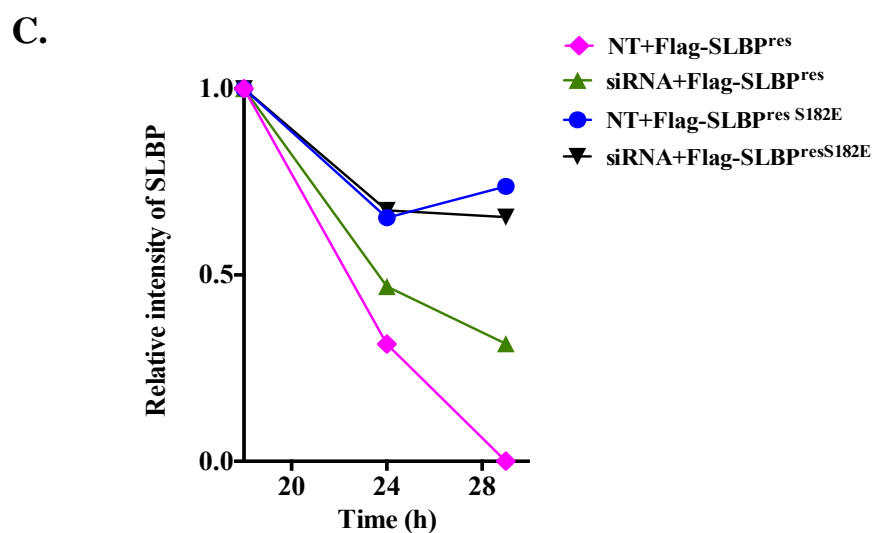
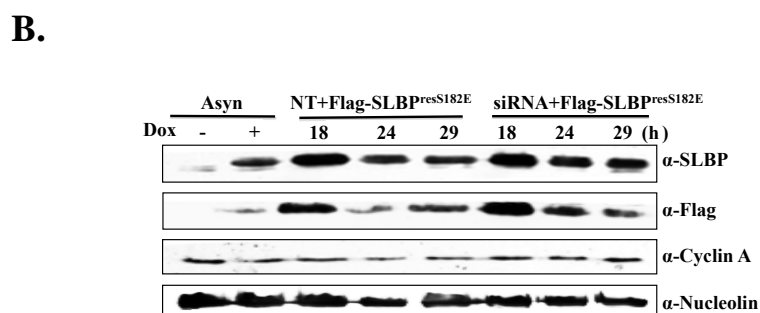
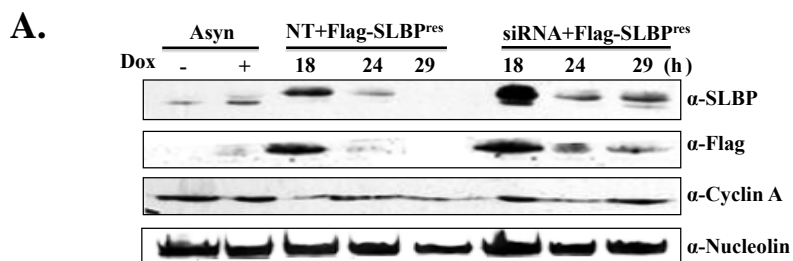


**Figure 5.8** Flag-SLBP<sup>resS182E</sup> cells slow SLBP degradation

Flag-SLBP<sup>res</sup> and Flag-SLBP<sup>resS182E</sup> Flp-In HeLa cells were exposed to non-targeting (NT) or SLBP-targeted siRNA for 24 h using the electroporation method as describe in section 2.2.3.4.1 followed by

synchronisation with Noc for 12 h. After cells were released from Noc arrest, Dox was added to cells for 5 h. Cells were subsequently harvested at 18, 24 and 29 h. The levels of SLBP, Flag, cyclin A and nucleolin were determined by western blotting with relevant antibodies. **(A)** Flag-SLBP<sup>res</sup> cells treated with NT or SLBP-targeted siRNA as indicated **(B)** Flag-SLBP<sup>resS182E</sup> cells treated with NT or siRNA-targeted siRNA as indicated **(C)** the relative intensity of indicated Flag-SLBP variant normalised to the amount of nucleolin and Flag-SLBP<sup>resS182E</sup> with NT or siRNA, determined by Image J of the anti-Flag antibody blots. The second set of data shows the same trend as the first set. However, the second set of data has incompleting time course (data not shown).

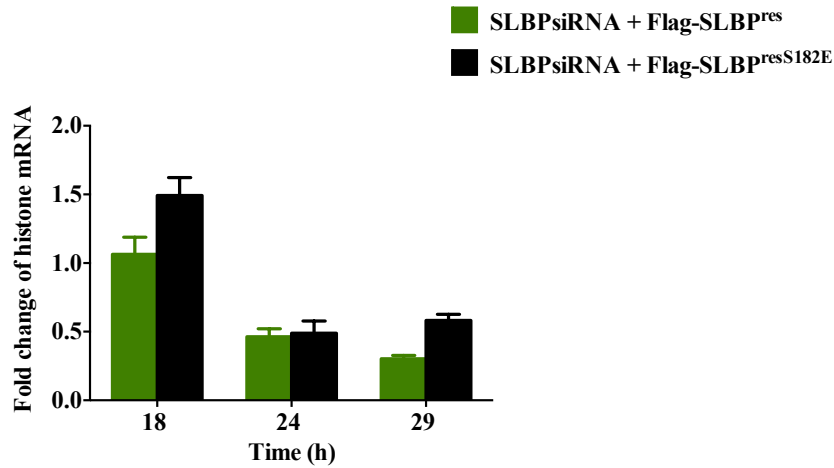


**Figure 5.9** Relative levels of histone mRNA derived from Flag-SLBP<sup>res</sup> and Flag-SLBP<sup>resS182E</sup> cells at the indicated time.

The total RNA from the cells from Figure 5.8 were extracted and reverse transcribed to cDNA as described in section 2.2.8. The level of histone cDNA was determined by subsequent qPCR as described in section 2.2.8.3. The values obtained for Flag-SLBP<sup>res</sup> cells were normalised with NT+Flag-SLBP<sup>res</sup> at 18 h and the value of Flag-SLBP<sup>resS182E</sup> was normalised with NT+ Flag-SLBP<sup>resS182E</sup> at 18 h. Each bar showed SD of three technical replicates within each condition.

### **5.2.3 Flag-SLBP<sup>resS182E</sup> - expressing cells delay histone mRNA decay after the inhibition of DNA synthesis**

The results above demonstrate that Flag-SLBP<sup>resS182E</sup> -expressing cells appear to transit through S phase more slowly than Flag-SLBP<sup>resS182A</sup> cells, and that compared to wild-type cells show a delay in SLBP degradation and retain higher levels of histone mRNA as a result of prolonged S-phase progression.

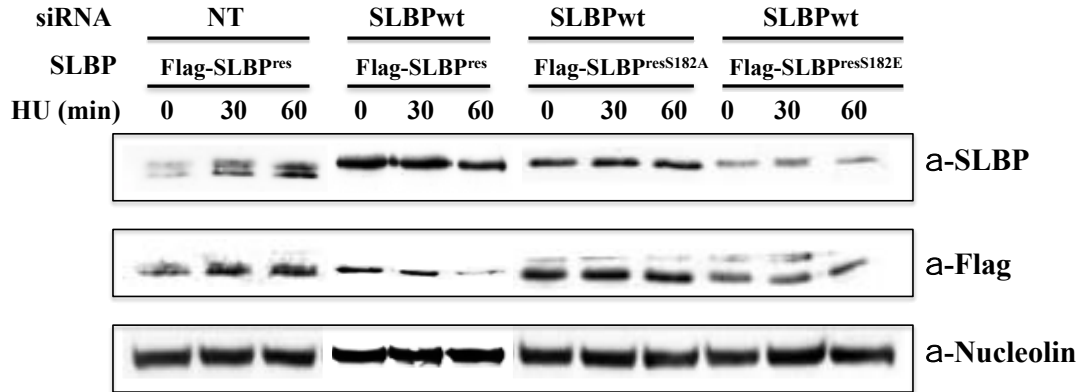
I also wished to determine whether Flag-SLBP<sup>resS182E</sup> -expressing cells were capable of efficient histone mRNA decay after the inhibition of DNA synthesis (Marzluff *et al.*, 2008). Flag-SLBP<sup>res</sup>, Flag-SLBP<sup>resS182A</sup> and Flag-SLBP<sup>resS182E</sup> cells were transfected with SLBP-targeted siRNA for 24 h in the presence of Dox. For comparison, Flag-SLBP<sup>res</sup> cells were transfected with NT siRNA for 24 h in the presence of Dox. Then cells were treated with or without 5 mM HU up to 60 min. Lysates were harvested at indicated times in order to detect SLBP expression and quantify the level of protein and mRNA by western blotting and qPCR, respectively.

To determine knockdown efficiency, the level of SLBP protein was examined by western blotting. The results showed knockdown of endogenous SLBP was > 95% in Flag-SLBP<sup>resS182A</sup>, Flag-SLBP<sup>resS182E</sup> and Flag-SLBP<sup>res</sup> cells treated with SLBP-targeted siRNA compared to

Flag-SLBP<sup>res</sup> exposed to the NT control siRNA (Figure 5.10A). Somewhat surprisingly, in Flag-SLBP<sup>resS182E</sup>-expressing cells, the levels of histone mRNA appeared to increase transiently, following imposition of replication stress (5 mM HU) before ultimately decreasing to ~10% of the original level after 60 min of exposure to HU. In contrast, Flag-SLBP<sup>resS182A</sup> expressing cells efficiently induced histone mRNA decay following HU treatment, with kinetics that were indistinguishable from Flag-SLBP<sup>res</sup>-expressing cells. Again surprisingly, the efficiency of histone mRNA decay in Flag-SLBP<sup>res</sup>-expressing cells exposed to NT siRNA was reduced compared to cells solely expressing either Flag-SLBP<sup>res</sup> or Flag-SLBP<sup>resS182A</sup>, although not to the extent of that seen with Flag-SLBP<sup>resS182E</sup>-expressing cells. The results of the two-way ANOVA and Tukey's multiple comparisons test indicated that there was a statistically significant difference of histone mRNA levels in between groups at 30 min after HU treatment ( $p = 0.0001$ ). However, there was no significant difference of histone mRNA levels in the conditions of SLBP-targeted siRNA with Flag-SLBP<sup>res</sup> compared to Flag-SLBP<sup>resS182A</sup> following HU treatment for 30 min. Moreover, SLBP-targeted siRNA with Flag-SLBP<sup>res</sup> compared to Flag-SLBP<sup>resS182E</sup> was a statistically significant difference of histone mRNA levels at 60 min after HU treatment ( $p = 0.001$ ).

Taken together, these data suggest that S182 phosphorylation may play a role in regulating the efficiency with which histone mRNA is degraded following replication stress, and that the phosphorylated form of the protein is less efficient than either wild-type protein or the unphosphorylatable form of SLBP in executing this aspect of SLBP-related function. Interestingly, expression of Flag-SLBP<sup>res</sup> in the absence of siRNA-mediated knockdown of endogenous protein also resulted in a reduction in efficiency of histone mRNA decay. As a proportion of wild-type protein must be phosphorylated, these data are not consistent with a role for phosphor-S182 in negatively regulating replication stress induced histone mRNA decay.

**A.**



**B.**

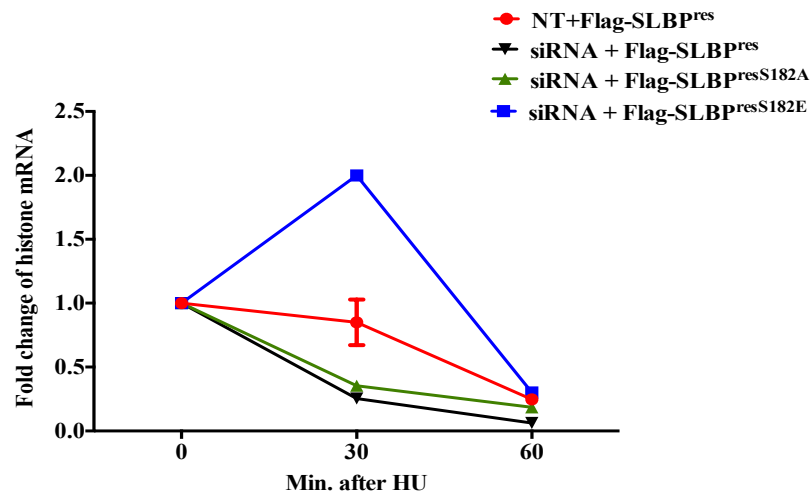


**Figure 5.10** Differential response to replication stress in cells expressing either Flag-SLBP<sup>resS182A</sup> and Flag-SLBP<sup>resS182E</sup>.

Asynchronous Flag-SLBP<sup>resS182A</sup> and Flag-SLBP<sup>resS182E</sup> stably transfected in Flp-In HeLa cells were treated with either NT or siRNA for 24 h using electroporation method. (A) Lysates were subjected to 12% SDS-PAGE and analysed by western blotting followed by probing with the indicated

antibodies, SLBP, flag and nucleolin **(B)** Histone mRNA levels after HU treatment for 30-60 min were analysed by qPCR. Statistical analysis was performed using an analysis of variance (ANOVA) with the addition of a post test using Tukey's multiple comparisons test at the 95% confidence interval for the difference. The GraphPad Prism v 6.0f (GraphPad Software, Inc., San Diego, CA, USA) was used for analysis in this study. Error bars show the standard error in the mean obtained from three independent experiments. The data shows that no significant difference was observed when cells lacking endogenous SLBP and expressing Flag-SLBP<sup>res</sup> degraded histone mRNA in response to HU treatment.

### 5.2.4 The protein kinase, WEE1 prevents premature SLBP degradation

In a first approach to investigate the identify of the protein kinase responsible for the phosphorylation of S182, an *in silico* computational analysis of phosphorylation site substrate preference (GPS 3.0 software) was used to identify candidate protein kinases which might be expected to phosphorylate S182 on the basis of the amino acid motifs surround the site of phosphorylation (Liu *et al.*, 2015). The analysis of ranked protein kinases with the potential to phosphorylate S182 is shown in Table 5.3, including peptide sequences and prediction scores.

**Table 5.3** List of Ser/Thr kinases identified using GPS 3.0 software

Position	Code	Kinase	Peptide	Score
182	S	Other/AUR/AurC	FKKYSRRS <b>S</b> WDQQIKL	10.333
182	S	Other/AUR/AurB	FKKYSRRS <b>S</b> WDQQIKL	10.093
182	S	Other/AUR	FKKYSRRS <b>S</b> WDQQIKL	9.085
182	S	Other/WEE/Myt1	FKKYSRRS <b>S</b> WDQQIKL	8
182	S	Other/WEE/Myt1/PKMYT1	FKKYSRRS <b>S</b> WDQQIKL	8
182	S	Other/WEE	FKKYSRRS <b>S</b> WDQQIKL	8
182	S	Atypical/PDHK/PDHK/PDK3	FKKYSRRS <b>S</b> WDQQIKL	7
182	S	CAMK/DAPK/DAPK/DAPK1	FKKYSRRS <b>S</b> WDQQIKL	5.7

This analysis identified two high-scoring protein kinase families both of which are known to play relevant key roles related to genetic instability in the cell cycle. The Aurora kinase family are involved in regulation of spindle morphology, chromosome alignment and cytokinesis (Ducat and Zheng, 2004 ; Kollareddy *et al.*, 2008).

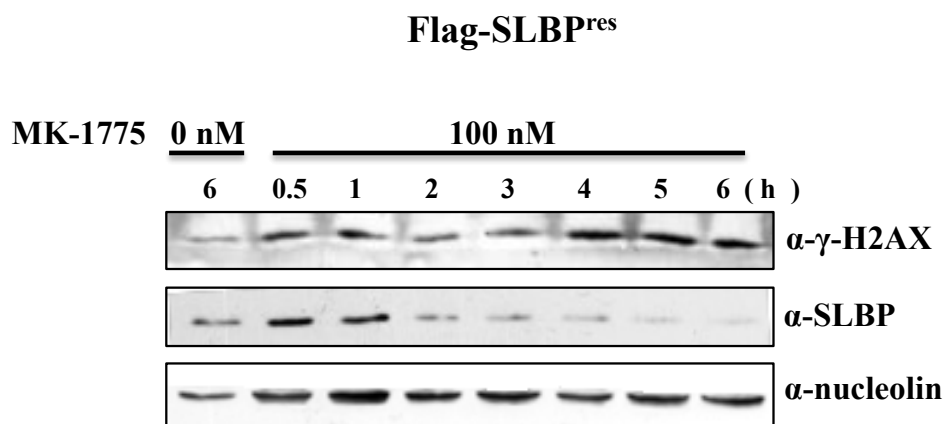
WEE1, and the related Myt1 protein kinase, plays an important role in regulation of the replication checkpoint, the control of DNA damage responses during S phase as well as a role in regulating histone synthesis (Watanabe *et al.*, 1995 ; Berry and Gould, 1996 ; Booher *et al.*, 1997 ; Mahajan and Mahajan, 2013 ; Heijink *et al.*, 2015 ; Saini *et al.*, 2015). WEE1 controls the activity of both Cdk2 and Cdk1, acting as a negative regulator of both by phosphorylation of tyrosine 15, (Parker and Piwnica-Worms, 1992 ; Watanabe, 2008) ensuring maintenance of genome integrity (Sørensen and Syljuåsen, 2012 ; Beck *et al.*, 2012). Moreover, WEE1 phosphorylation is regulated by components of the DNA replication checkpoint machinery and controls normal mitotic entry (Smythe and Newport, 1992 ; Michael and Newport, 1998; Owens *et al.*, 2010).

### **5.2.5 Inhibition of WEE1 kinase by MK-1775 reduces cellular SLBP levels**

Aurora kinases are involved in regulation of spindle morphology, chromosome alignment and cytokinesis (Ducat and Zheng, 2004 ; Kollareddy *et al.*, 2008) and in the absence of an obvious connection to the replication checkpoint were not considered for this initial analysis this with. However, WEE1, and the related Myt1 protein kinase, plays an important role in regulation of the replication checkpoint, the control of DNA damage responses during S phase as well as a role in regulating histone synthesis (Watanabe *et al.*, 1995 ; Berry and Gould, 1996 ; Booher *et al.*, 1997 ; Mahajan and Mahajan, 2013 ; Heijink *et al.*, 2015 ; Saini *et al.*, 2015). Because of the direct role for WEE1 in the coordination of S phase events, I chose to investigate whether experimental manipulation of WEE1 kinase activity affected SLBP stability *in vivo*. Asynchronous Flag-SLBP<sup>res</sup> cells which had previously been exposed to 0.5 µg/ml Dox for 5 h were either untreated (control) for 6 h, or exposed to the potent and selective WEE1 kinase inhibitor, MK-1775 (Hirai *et al.*, 2009) for the same period.

As shown in Figure 5.12, exposure of Flag-SLBP<sup>res</sup> cells to MK-1775 resulted in the progressive reduction in SLBP levels detected by western blotting, with SLBP being almost undetectable after 6 h.

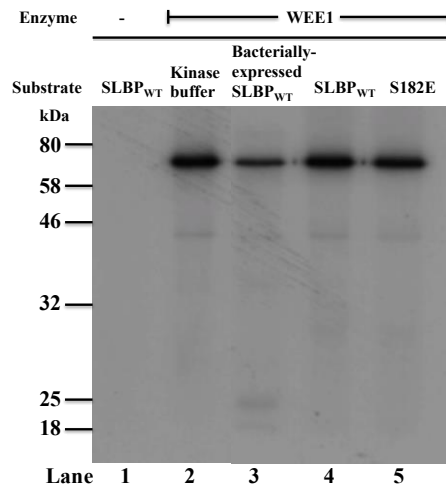
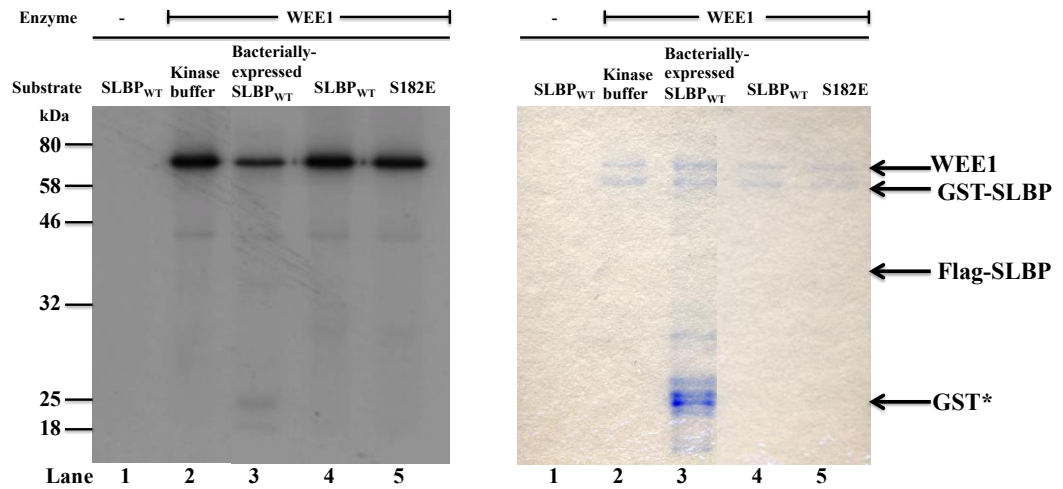
Previous work has indicated that loss of WEE1 activity *in vivo* triggers a DNA damage response involving the production of DNA double strand breaks (Domínguez-Kelly *et al.*, 2011). Consistent with this observation, cells exposed to MK-1775 showed elevated levels of gamma-H2AX ( $\gamma$ -H2AX), the biomarker for DNA double-strand breaks.



**Figure 5.11** Inhibition of WEE1 results in destabilisation of SLBP in Flag-SLBP<sup>res</sup>-expressing cells.

Flag-SLBP<sup>res</sup>-expressing cells were treated with 100 nM MK-1775 for the indicated time (0.5-6 h) in the presence of 0.5  $\mu$ g/ml Dox. Cell lysate (50  $\mu$ g of protein) were subjected to 12% SDS-PAGE and analyzed by western blotting with anti- $\gamma$ -H2AX and anti-SLBP. **NB:** Under the electrophoresis conditions used, resolution was insufficient to distinguish between endogenous and Flag-SLBP species. Anti-nucleolin was used as a loading control.

One explanation for the data presented above is that WEE1 directly phosphorylates SLBP to modulate the stability of the latter under circumstances where S phase must be prolonged as a result of DNA damage or replication stress. To investigate whether WEE1 kinase directly phosphorylates S182, I performed a protein kinase assay *in vitro* using a commercially produced source of WEE1 (in Sf21 insect cells, Millipore) together with immuno-isolated Flag-SLBP<sup>res</sup> cells (SLBPwt), Flag-SLBP<sup>resS182E</sup> cells and purified GST-SLBP as potential substrates (isolated as described in Chapter 4).

**A.****B.**

**Figure 5.12** *In vitro* WEE1 kinase assay with SLBP.

Individual proteins (Flag-SLBP<sup>res</sup> and Flag-SLBP<sup>resS182E</sup>) were obtained by immuno-isolation from cell lysate using ANTI-FLAG<sup>®</sup> M2 affinity resin (packed resin) (Sigma-Aldrich). Bacterially-expressed GST-SLBP was purified using Glutathione-agarose beads. Each kinase reaction was carried out as described in Chapter 2 using Mg[ $\gamma$ -<sup>32</sup>P]ATP at a specific activity of (10<sup>6</sup> cpm/nmol) ATP. Each reaction mixture was subjected to (A) autoradiography and (B) SDS-PAGE. The relative mobility of WEE1, GST-SLBP, and Flag-SLBP are indicated.

No phosphorylation of full-length SLBP (expected relative  $M_r$  of bacterially-expressed SLBP<sub>WT</sub> ~ 65 kDa ; expected relative  $M_r$  of Flag-SLBP ~ 38kDa) was observed in any reaction mixture containing added SLBP (Figure 5.12). That the preparation of WEE1 was capable of phosphorylation was confirmed by the presence of significant degree of autophosphorylation in all samples to which the kinase was added (Fig. 5.12 A and B, Lanes 2, 3, 4 and 5), at a relative  $M_r$  consistent with that expected for WEE1 (Parker *et al.*, 1995 ; Millipore, 2012). Weak phosphorylation of a low molecular weight species ( $M_r$  ~ 26 kDa) was observed in the sample containing added GST-SLBP (Figure 5.12 A and B, Lane 3). This likely corresponds to a truncated translation product comprised predominantly of GST, together with some N-terminal sequence of SLBP (Carl Smythe, personal communication), and may indicate adventitious phosphorylation of a C-terminal disordered region in the fusion protein.

While the experiment described above suggest that SLBP is not phosphorylated directly by WEE1, at least *in vitro*, it did not rule out the possibility that WEE1 is responsible for the phosphorylation of SLBP at S182 *in vivo*. If WEE1 is responsible for SLBP phosphorylation at S182 and its resultant stabilisation, then treating Flag-SLBP<sup>resS182E</sup>-expressing cells with MK-1775 would be expected to have limited or no effect on

levels of the expressed protein. Therefore, I examined the effect of inhibiting WEE1 on the stability of Flag-SLBP<sup>resS182E</sup> *in vivo* (Figure 5.13)

Flag-SLBP<sup>resS182E</sup>-expressing cells were treated with 100 nM MK-1775 for up to 6 h in the presence of 0.5 µg/ml Dox. Cell lysate (50 µg of protein) were subjected to 12% SDS-PAGE and analysed by western blotting with anti-γ-H2AX and anti-SLBP antibodies.

### Flag-SLBP<sup>resS182E</sup>

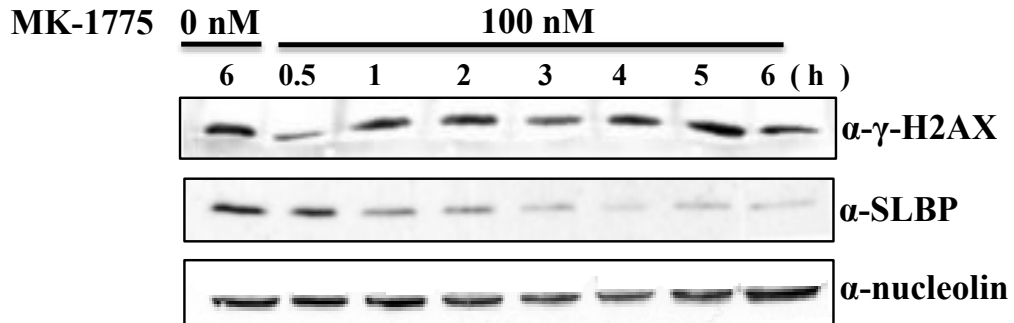


**Figure 5.13** Destabilisation of Flag-SLBP<sup>resS182E</sup> is also observed following treatment with MK-1775 *in vivo*.

Flag-SLBP<sup>resS182E</sup>-expressing cells were treated with 100 nM MK-1775 for indicated times (0.5-6 h) in the presence of 0.5  $\mu$ g/ml Dox. Cell lysate (50  $\mu$ g of protein) were subjected to 12% SDS-PAGE and analysed by western blotting with anti- $\gamma$ -H2AX and anti-SLBP antibodies. **Note:** Under the electrophoresis conditions used, resolution was insufficient to distinguish between endogenous and Flag-SLBP species. Western blotting with anti-nucleolin antibodies was used as a loading control.

The kinetics of MK-1775-induced loss of SLBP in Flag-SLBP<sup>resS182E</sup>-expressing cells was very similar to that observed for Flag-SLBP<sup>res</sup> cells (Figure 5.14), indicating that MK-1775 induced SLBP degradation is not blocked by the presence of phosphomimetic residue at position 182. This data strongly suggest that the destabilisation of SLBP resulting from WEE1 inhibition is independent of the state of S182 phosphorylation.

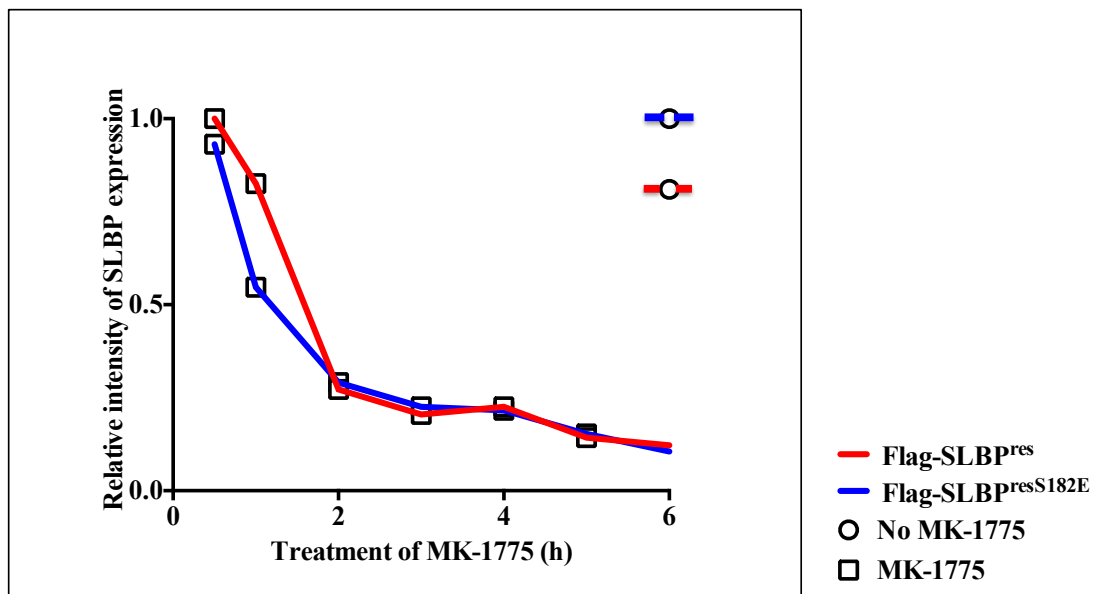


**Figure 5.14** SLBP degradation following MK-1775 treatment.

Quantitative using Image J of the level of SLBP protein in Flag-SLBP<sup>res</sup> and Flag-SLBP<sup>res S182E</sup>-expressing cells shown in Figure 5.10 and 5.12 normalised to the amount of nucleolin in each sample.

### 5.3 Discussion

Here, I have used phospho-proteomics to identify *in vivo* phosphorylation sites in human SLBP. This analysis showed for the first time that in mammalian cells, hSLBP is phosphorylated on at least 11 sites. The function of some of these sites (such as Ser110, Ser111, Ser112 and Ser114) is reasonably well understood, all these modification sites have not previously been determined using LC-MS/MS strategy. In the case of Ser182, it has been previously reported as a site of modification using an LC-MS/MS strategy, although the function of this remains the unknown (Bansal *et al.*, 2013). It lies in the RBD and present in a highly conserved SRRS sequence (Thapar *et al.*, 2004). Therefore, I directed attention to attempting to understand the role and significance of phosphorylation at Ser182.

In order to study the role of phosphorylation at Ser182, site-directed mutagenesis was undertaken to establish a phospho-mimetic substitution from serine to glutamate (S182E) and also the non-phosphorylatable substitution to alanine (S182A) in cells that enable doxycycline inducible expression of a siRNA-resistant form of the protein. Observing cells that predominantly express only the mutant form of SLBP, differences between mutants in S phase progression, and duration of SLBP expression, were observed. The kinetics of replication

stress-induced histone mRNA decay also varied dependent on the nature of the expressed form of SLBP. Bioinformatics analysis suggested that WEE1 kinase is a potential candidate to directly phosphorylate Ser182. No evidence was found to support this notion, however, treatment of cells with the WEE1 selective inhibitor MK-1775 brought about a rapid destruction of both Flag-SLBP<sup>res</sup> and Flag-SLBP<sup>resS182E</sup>, suggesting a role for the WEE1 kinase in the regulation of SLBP stability, that is likely independent of the phosphorylation state of Ser182. However, the mechanism of this regulation is still unknown.

### **5.3.1 Identification of post-translational modifications in hSLBP**

In order to determine sites of post-translational modification (PTM) on hSLBP by mass spectrometry, it was necessary to obtain a purified hSLBP preparation isolated from the model cell system. This was done by using the strategy of adding a Flag-tag to the SLBP coding sequences at N-terminus prior to its introduction into mammalian HeLa cells. In addition, the isolation was undertaken from cell preparations in S-phase by synchronization using Noc. Anti-FLAG<sup>®</sup> M2 affinity gel and 3X FLAG peptide were used to purify Flag-tagged SLBP and the efficiency of Flag-tag based protein purification was described as in Chapter 4. Despite the use of tryptic peptides derived from bacterially-

expressed hSLBP as calibration standards to ensure maximise the extent of identity of equivalent peptides from *in vivo* samples and synchronised cells were used in order to increase the yield of SLBP, the percentage of SLBP coverage following tryptic digestion was not covered more than 50%. There are three explanations of these. Firstly, it is likely of low abundance of SLBP. In my study, the amount of protein is approx. 0.475 mg by comparing with bacterially expressed SLBP-derived peptides based on western blotting data for detecting PTM by LC-MS/MS. There were no literature reviews showing the used amount of purified SLBP for LC-MS/MS analysis.

Secondly, the condition of the mass spectrometer and its mode of ionization, mass separation, and ion detection need to be considered. It is possible that some peptides were out of range of mass spectrometry detection an (See discussion in section 4.3.2, Chapter 4).

Finally, it may be relevant that additional limitations may have impacted on the protein coverage obtained using the expression system and purification method utilised here. The purification technique and expression system are important tools to keep peptide soluble which involves in the amino acid composition (Price *et al.*, 2011 ; Niu *et al.*, 2013). The amino acid composition has an effect on chemical and

physical properties of peptide in condition of solubility. As previously shown SLBP has an intrinsically disordered structure and low stability in the absence of histone mRNA stem-loop (Thapar *et al.*, 2004). A number of mass spectrometry studies into hSLBP phosphorylation for structural and sequence information have been undertaken previously using protein expressed in, and isolated from, baculovirus-infected insect cells, using Ni<sup>2+</sup> affinity and gel filtration chromatography for hSLBP purification (Zheng *et al.*, 2003 ; Borchers *et al.*, 2006 ; Bansal *et al.*, 2013). Use of relatively large amounts of protein using this approach may have resulted in the 85.2% coverage of the sequence reported by Bansal and colleagues (2013).

For FLAG-affinity purification, the Flag-tag was located at the N-terminus of SLBP. Functional studies have shown that SLBP N-terminal domain are important for translation initiation of histone mRNAs, SLBP degradation, cyclin binding and also the binding site for hSLIP1 (Sanchez and Marzluff, 2002 ; Zheng *et al.*, 2003 ; Cakmakci *et al.*, 2008 ; Bansal *et al.*, 2013). However, there was only one publication shown dSLBP expressed with C-terminal tags, which does not influence the function of SLBP (Thapar *et al.*, 2004). Thus there was potential for loss via proteolytic cleavage (and thus loss) of SLBP protein during

purification, N-terminal proteolysis affecting the DYK epitope, or aberrant folding of the FLAG tag masking the epitope, are potential reasons for reduced efficiency of the purification (Slootstra *et al.*, 1997). A recent study has suggested that post-translational modification (PTM) of FLAG-tag by sulfation abolishes the interaction between FLAG epitope and its cognate antibody, resulting in difficulties in detection and FLAG purification of secreted Flag-tagged protein (Schmidt *et al.*, 2012). Although SLBP is not a secreted protein, it is not clear whether this or other PTMs of FLAG-tag reduced the potential of the immunisolation method. The use of complimentary purification approaches such as tandem affinity purification (TAP) tag improves purification complexes from a relative small number of cells (Riguat *et al.*, 1999). Moreover, combined TAP for MS analysis has proven to efficiently allow for study proteins interacting with a given target protein (Völkel *et al.*, 2010). Thus, in order to increase the overall yield of tagged SLBP is likely to improve the overall proportion of the mammalian-expressed hSLBP protein sequence detected using mass spectrometry.

### 5.3.2 S phase progression

Expression of SLBP phosphorylation site mutants appeared to have subtle effects on cell cycle progression and the apparent length of S-phase. Both FACS analysis and analysis of SLBP expression levels suggested that the rate of progression of the entire cell population through S-phase was faster for cells co-expressing Flag-SLBP<sup>resS182A</sup> than either Flag-SLBP<sup>resS182E</sup> or Flag-SLBP<sup>res</sup> suggesting that phosphorylation of SLBP at this site affects progression through S phase. This may arise through increasing the extent of dispersion of a synchronised cell population progressing through S phase and might reflect a role for SLBP phosphorylation in participating in co-ordinated regulation of normal S phase checkpoint responses to ensure availability of histone mRNA as cells progress through S phase. Alternatively, at this stage it was also conceivable that phosphorylation plays a role in regulating directly the stabilisation mechanism of SLBP. This latter issue is addressed below. As these effects were observed in cells that also expressed normal levels of endogenous wild-type SLBP, these data suggest that these mutants may act in part as dominant negatives, preventing normal SLBP-mediated homeostasis.

The analysis of proportion of cells in S phase in the various Flag-SLBP-expressing cell lines shown in Figure 5.6, which suggested that a significant proportion of cells remained in S phase for extended periods of time in Flag-SLBP<sup>resS182E</sup> cells compared to Flag-SLBP<sup>res</sup> cells prompted a more detailed study of the stability of SLBP species both in the presence and absence of the endogenous wild-type protein. Initially this analysis was undertaken comparing Flag-SLBP<sup>resS182E</sup> with Flag-SLBP<sup>res</sup>. This was because it was clear from the data in Figures 5.3 and 5.4 that Flag-SLBP<sup>resS182E</sup>-expressing cells take significantly longer to transit through G2/M compared to either wild-type or S182A mutant cells.

Interestingly these results showed that SLBP stability was maintained for significantly longer periods in cells expressing solely Flag-SLBP<sup>resS182E</sup> than in Flag-SLBP<sup>res</sup>-expressing cells (Figure 5.8C). Consistent with these data, comparative qPCR data suggested that levels of histone mRNA were elevated in Flag-SLBP<sup>resS182E</sup> at least at some time points, than in Flag-SLBP<sup>res</sup> cells. Taken together these data suggest that one role of S182 phosphorylation may be to modulate (i.e. delay) the scheduled destruction pathway that normally brings about the SLBP destruction at the end of S phase. As is well established, destruction is

brought about by Cdk1-mediated phosphorylation of Thr61 which facilitates Casein Kinase II (CK2) mediated Thr60 phosphorylation and proteosomal degradation (Zheng *et al.*, 2003). Interestingly, S182E also appeared to induce a delayed response to replication induced stress induced histone mRNA decay, although the reason for the apparent increase in histone mRNA immediately after addition of HU is not clear. In this circumstance, the rate of decay observed with wild-type protein was very similar to that observed with the S182A mutant. These data might suggest that the dephosphorylated form of SLBP may be required for a rapid response following exposure to replication stress, while the phosphorylated form may be relevant in circumstances where histone mRNA levels are required for chromatin homeostasis or outstanding DNA replication/repair in late S- or G2-phases.

Unfortunately time constraints precluded a comparative analysis of the Flag-SLBP<sup>resS182A</sup> mutant for comparison. However, future work might be expected to examine directly the role of both mutants on the timing and molecular interactions of SLBP at the end of S phase, including the efficiency with which combinations of phosphorylation mutations (such as T60A, S182A) are degraded to understand whether one site acts dominantly over the other to alter the timing of SLBP

destruction. Although S182 phosphorylation was observed in SLBP samples obtained from synchronised cells, it is not clear whether the stoichiometry of phosphorylation at this site alters throughout S-phase. However given that this site is conserved (Thapar *et al.*, 2004) and that there are differences in S phase progression, SLBP stability and replication stress induced histone mRNA decay efficiency between cell lines expressing the various mutants compared to wild-type protein, it would be surprising if phosphorylation at this site was not involved in some aspect of regulation of SLBP function.

Interestingly, analysis of cell cycle profiles of cells expressing the various phosphorylation site mutants suggested that there were distinct differences in the efficiency with which progression through S-phase was achieved, and Fag SLBP<sup>resS182A</sup>-expressing cells are most efficient at progressing through S phase, through G2-phase and into the next cell cycle. Analysis of the capability of various mutants to efficiently process histone pre-mRNA to ensure a timely supply of histone protein was beyond the scope of this thesis. One possible explanation for the variation in S phase progression relates to the possibility that Ser182 mutations affect efficient delivery of histone protein which in turn impact on the rate of DNA replication. Recently, Broderson and

colleagues (2016) have reported an important role for CRL4<sup>WDR23</sup> mediated ubiquitination of SLBP during S-phase to ensure adequate histone supply during DNA replication. It will be interesting to establish whether phosphorylation at Ser182 has any role to play in modulating CRL4<sup>WDR23</sup> ubiquitination which occurs at residue K156.

### **5.3.3 Regulatory pathways affecting SLBP stability**

Serine 182 phosphorylation site is interesting due to the position at RNA binding domain which is an important domain for RNA binding and processing (Zhang *et al.*, 2012). Importantly, Ser182 is present in a highly conserved SRRS sequence as shown in Figure 5.15 (Thapar *et al.*, 2004). Therefore, it was important to study the molecular function of the phosphorylation at Ser182. Thus, I mainly examined whether or not the functions of phosphomimic and unphosphorylated mutations affect the biological pathway associated with SLBP and histone mRNA degradation.

182

```

HS 123 TVPADFETDESVMRRQKQINYGKNTIAYDRYIKEVPRHLRQPGIHPKTPNKFKKYSRRSWDQQIKLWKVALHFWDPP
X1 121 STHGEMETDPAVITRRQKQINYGKNTIAYDRYIKAVPRHLREPENVHPRTPNKPKKYSRRSWDQQIRLWRIALHQWDPP
SU 239 KKETAMEEDRDVLIIRQKQIDFGKNTAAYDNYLHKVRRNRRLKGGHPYTPNKPQVTSRRSWDKQIRLWRIKLHEHDDPP
CI 149 LEEVAVEEDSVLMRREKQIEYGKNTIAYDNYTREIQKHKRTK-FHPRTPKPAKSRRSWDAQVKIWRKALHNWEEY
X2 96 PDAVGYETDEATLHRRQKQIDYGKNTVGYQCYLQQVPKTERKSGVHPRTPNKSKKYSRRSWDMQIKLWRRDLHAWDDPP
CE 216 EPTLGWCTDEAVLKRRSREIDRAKEKAVYQRYTSEVPLRDRIKGGHPRTPNKLISRRSWDTQIKKWRSLYEYCGE

```

**Figure 5.15** SLBP sequence aligned with the RNA-binding domain (RBD) of *Homo sapiens* (HS), *Xenopus laevis* (X1 and X2), sea urchin (SU), *Ciona* (CI) and *Caenorhabditis elegans* (CE). The bold black letters are conserved residues and red letters are the position of S182.

Interestingly, phosphomimetic S182E has an effect on SLBP stability which was also associated with elevated levels of histone mRNA after cells treated with HU. This is the first insight into the functional differences that arise in cells which are incapable of expressing a form of SLBP, which cannot be dephosphorylated at S182. Although the precise mechanism by which the phosphorylation of SLBP at Ser182 prolongs the effect on stability SLBP, bio-informatics analysis in addition to literature reports supported WEE1 as a potential candidate. WEE1 protein is normally expressed in S and G2 phases (Featherstone and Russell, 1991 ; McGowan and Russell, 1995). WEE1 has roles both in S phase regulation and histone synthesis (Beck *et al.*, 2012 ; Mahajan and Mahajan, 2013) as well as a role in regulating the G2/M transition (Smythe and Newport, 1992). Importantly, during replication stress,

WEE1 is a crucial downstream activator after CHK1 phosphorylates and inactivates CDC25 (Saini *et al.*, 2015). WEE1 phosphorylates Cdk1 at tyrosine15 throughout S phase to prevent the G2/M transition (McGowan and Russell, 1995 ; Beck *et al.*, 2012) and also has a role in regulating the activation state of Cdk2 (Chow *et al.*, 2003) which is believed to be required for S phase progression (Figure 5.16). Interestingly, inhibition of WEE1 results in the emergence of DNA damage in newly synthesised DNA, suggesting that WEE1 plays a direct role in ensuring genomic stability during S phase progression (Beck *et al.*, 2012). As DNA damage and replication stress may be encountered unexpectedly during S phase progression, it would not be inconceivable therefore that one role of WEE1 would be to ensure that the duration in which histone mRNA is expressed may be prolonged to accommodate delays in S phase duration emerging from such DNA damage and replication stress. Moreover, exposure of Flag-SLBP<sup>res</sup> cells to MK-1775 resulted in the progressive reduction in SLBP levels detected by western blotting. WEE1 is therefore the first kinase to test that it could robustly phosphorylates SLBP at Ser182 *in vivo*.

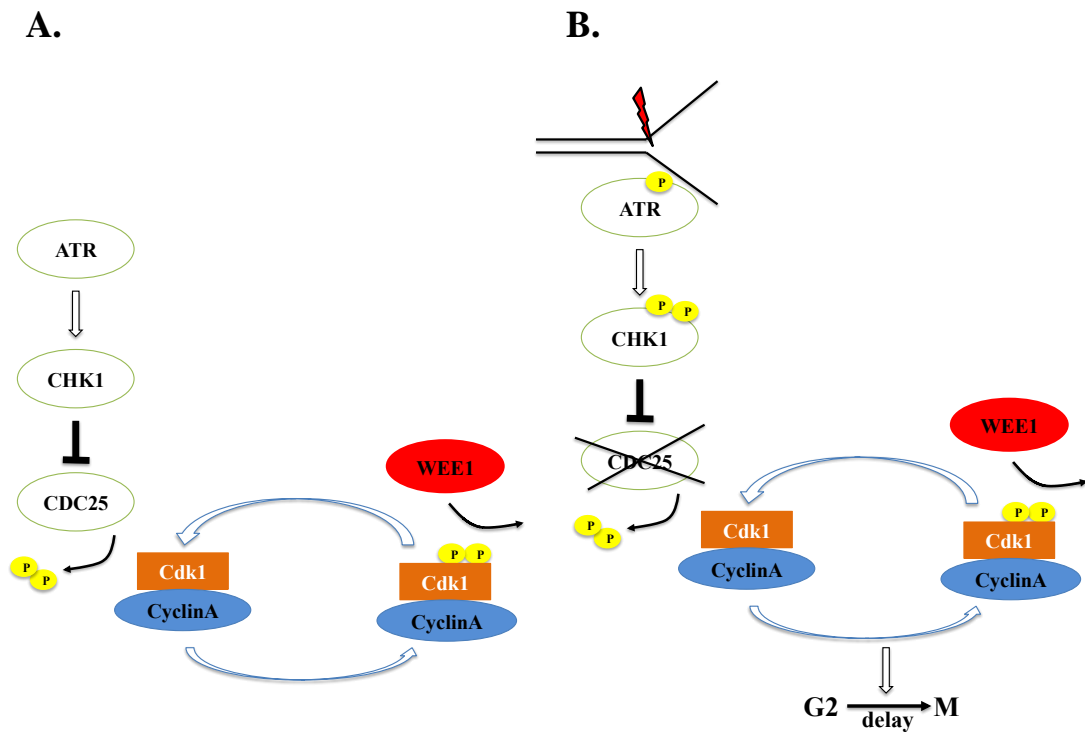


**Figure 5.16 Regulation of WEE1 during DNA replication stress**

(diagram was redrawn from Sorensen *et al.*, 2011 and Seligmann, H (Ed)). The authors and journal give permission to use this picture.

(A). During S phase, CHK1 controls CDC25 by phosphorylation. Cdk1 activity is regulated by phosphorylation and dephosphorylation. WEE1 activity is counteracted by CDC25 phosphatase. (B). During replication stress in S phase, it is sensed by ATR, which stimulates CHK1. This affects the effective activity of CDC25 and thus its capacity to activate Cdk1, while WEE1 phosphorylates Cdk1 at tyrosine15 throughout S phase to prevent the G2/M transition.

#### **5.3.4 Inhibition of WEE1 kinase by MK-1775 reduces cellular SLBP levels**

On the basis of bioinformatics analysis suggesting that Ser182 might be expected to be phosphorylated by WEE1, one hypothesis that we wished to test was whether WEE1 kinase was responsible for SLBP Ser182 phosphorylation. When asynchronous cells were treated with MK-1775, SLBP levels decreased rapidly compared to untreated cells. Assuming that MK-1775 is indeed specific for WEE1, then these results suggested that WEE1 kinase does play a role in maintaining SLBP stability.

It was an unexpected result that WEE1 did not phosphorylate S182E in *in vitro* experiments. Weak phosphorylation of a low molecular weight species ( $M_r \sim 26$  kDa) was observed in the sample containing added GST-SLBP. This likely corresponds to a truncated translation product comprised predominantly of GST, together with some N-terminal sequence of SLBP (Carl Smythe, personal communication), and may indicate adventitious phosphorylation of a C-terminal disordered region in the fusion protein. It is possible that bacterially-expressed wtSLBP along with GST-tagged protein purification might interrupt SLBP translation which leads to truncated

protein product as the consequence of codon usage during expression in *E. coli* (Zhang *et al.*, 1991).

Protein kinases execute their cellular function through the covalent attachment of an ATP-derived phosphate to one or more protein substrates. To identify a substrate for a specific kinase, it is essential that there is a sufficient substrate concentration and active kinase activity as well as the additional substrate [ $\gamma$ - $^{32}\text{P}$ ]ATP under appropriate conditions. In the experiments reported here, autophosphorylation of WEE1 was observed, suggesting that this protein kinase preparation was indeed active and functional under the conditions used. However there was less confidence in the abundance of SLBP as discussed in Chapter 4, which was not observable even using Colloidal coomassie blue stain after a protein gel electrophoresis. It is conceivable that the molecular forms of SLBP substrate utilized here were inappropriate, either because they are inappropriately folded or they lacked an additional critical macromolecule - either protein or potentially RNA, rendering the relationship between substrate and kinase insufficient for catalytic activity (Ubersax and Ferrell, 2007).

SLBP might not be in proper conformation to be receptive to phosphorylation. SLBP is unfolded in the free state having limited extended secondary structure but not a compact one. It is less stable,

easily degraded, and stabilized only in the presence of another protein or in the presence of an ordered mRNA interface (Thapar *et al.*, 2004). Therefore, the observed biochemical properties of SLBP may be simply due to this unusual feature of SLBP in the absence of a highly ordered RNA stem-loop.

Another obvious possibility is that that WEE1 is not the relevant protein kinase that targets Ser182. In addition to the high scoring Aurora kinase reported in the bio-informatics analysis, based on literature analysis, inspection of amino acid sequences surrounding Ser182 (FKKY**SRRS**WDQQIKL), also matches motifs preferred by PKA (R-X-S/T) and CK1 (S-X-X-S/T (Gnad *et al.*, 2011)) protein kinase families. The CK1 family is a highly conserved Ser/Thr protein kinase that phosphorylates key regulatory protein involved in cell cycle, transcription and translation (Schitteck and Sinnberg, 2014). Therefore, either Aurora, PKA or CK1 families might also be responsible for Ser182 phosphorylation.

An additional possibility arises from observations related to phosphorylation dependent substrate protein kinase targeting. It might be the case that phosphorylation of S182E is controlled by more than one protein kinases. Multiple examples exist where phosphorylation

both *in vivo* and *in vitro* require a previous priming phosphorylation event for efficient subsequent phosphorylation. For example, the phosphorylation of SLBP at Thr60 for SLBP degradation at the end of S phase and the phosphorylation involved in WEE1 degradation at the onset of M-phase by cyclin/cdk1 requires a priming phosphorylation by CK2 (Watanabe *et al.*, 2005 ; Koseoglu *et al.*, 2008).

Phosphorylation/dephosphorylation is a dynamic system. Therefore, it is also possible that additional, inhibitory phosphorylation sites exist that was not found in my study. For example, although I could not detect phosphorylation of S182E *in vitro*, glutamate substitution at this site prolonged SLBP degradation, with the notion that dynamic phosphorylation and dephosphorylation of this site could be important if it is phosphorylated *in vivo*.

Under the conditions of time available to complete Ph.D., I did not have enough time to further experiment in order to identify other candidate protein kinases such as Aurora (AUR) and CK1. However, there are many approaches to identifying the kinase without having to resort to bioinformatics. One way might be to utilise a luciferase based assay system. With regard to the known Cdk sites that promote SLBP destruction (Koseoglu *et al.*, 2008), I would mutate the Cdk sites such

that they were permissive for SLBP degradation (T60E) and then create SLBP mutant expressed in a cell line that expresses a reporter gene by making a luciferase (such as luciferase containing a 3' UTR stem loop). Thus, cells might be expected to generate luciferase when SLBP phosphorylated, but not when not phosphorylated. In combination with genome wide siRNA knockdown approaches, it might be possible to identify their kinase that reduces SLBP induced luciferase expression.

However, I found that cells solely expressing Flag-SLBP<sup>S182E</sup>, which presumably mimics phosphorylation at Ser182, also displayed equivalent kinetics of SLBP destabilization when exposed to the inhibitor of MK-1775. These data indicated whatever the mechanism by which WEE1 regulates the stability of SLBP, it is likely to be independent of the phosphorylation state of SLBP at Ser182. Currently, the significance of a phosphorylatable residue at position 182 in SLBP thus remains unknown.

The regulation of WEE1 and both Cdk1 and Cdk2 is a double negative regulation (Enders, 2010). Both Cdk1 and Cdk2 are inhibited when phosphorylated on tyrosine 15 which is located in the ATP binding site of the protein kinase. At the low levels of cyclin A or B, the WEE1 kinase inactivates Cdk1/Cdk2 by phosphorylating residue

Tyr15, blocking ATP binding and hydrolysis which blocks mitotic entry (Cdk1) and S phase progression (Cdk2) (Soloman, 1990).

This phosphorylation is brought about by both WEE1 and Myt1 protein kinases (Chow *et al.*, 2003) The activation of each Cdk by its cognate cyclin increases the activity of any unphosphorylated Cdk complex which is capable of phosphorylating and activating the relevant CDC25 phosphatase. Consequently, activated CDC25 can remove the inhibitory Tyr15 phosphorylation on Cdk1/2 which allows cells to undergo S phase progression (Cdk2) or mitotic entry (Cdk1) (Watanabe *et al.*, 1995 ; Okamoto and Sagata, 2007).

The mechanism by which phosphorylation at Thr61 by CyclinA/Cdk1 is believed to trigger SLBP destruction at the end of S phase is shown in Figure 5.17. An alternative explanation for the effect of MK-1775 on SLBP stability is as follows. Because WEE1 is believed to be the protein kinase responsible for the negative regulation of Cyclin A/Cdk1 during S phase (Chow *et al.*, 2003), and as increasing levels of Cyclin A/Cdk1 appear to determine precisely when SLBP destruction is triggered, it follows that any pharmacological agent that suppresses WEE1 activity is likely to result in a prematurely active Cyclin A/Cdk1. In these circumstances, prematurely activated Cyclin A/Cdk1 would be expected to bring about phosphorylation of Thr61 in SLBP and thus

reduce cellular SLBP levels, irrespective of whether S phase was completed or not (Figure 5.18). Future work will be required to establish whether or not this is indeed the case, and whether treatment of synchronised cells with MK-1775 results in a premature activation of Cyclin A/Cdk1 and, early phosphorylation of Thr61 and premature SLBP destruction. One prediction of this hypothesis would be that the supply of histone would be insufficient for ongoing DNA synthesis towards the end of S phase, and the resulting inability of cells to assemble chromatin would result in DNA and chromosome instability. Such an outcome is not inconsistent with the data obtained in other studies where WEE1 activity has been reduced using siRNA technology (Beck *et al.*, 2012).

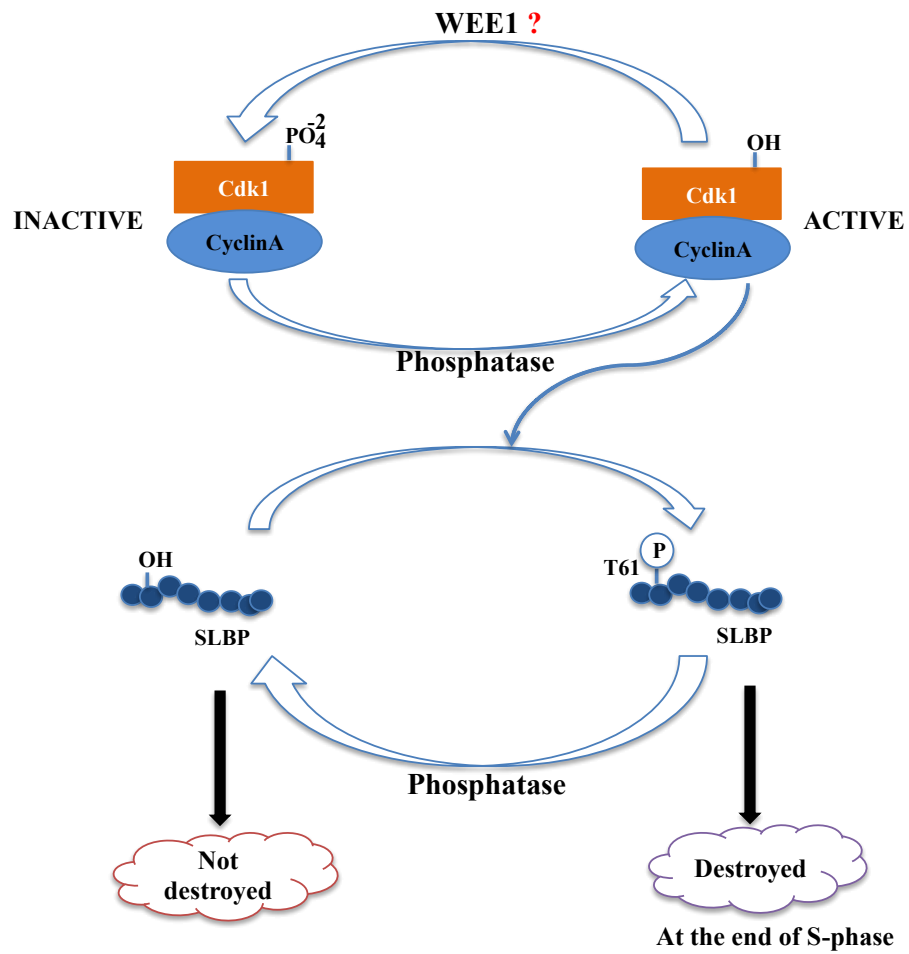


**Figure 5.17** Potential WEE1 kinase might activate cdk1 involving in T61 phosphorylation at the end of S phase.

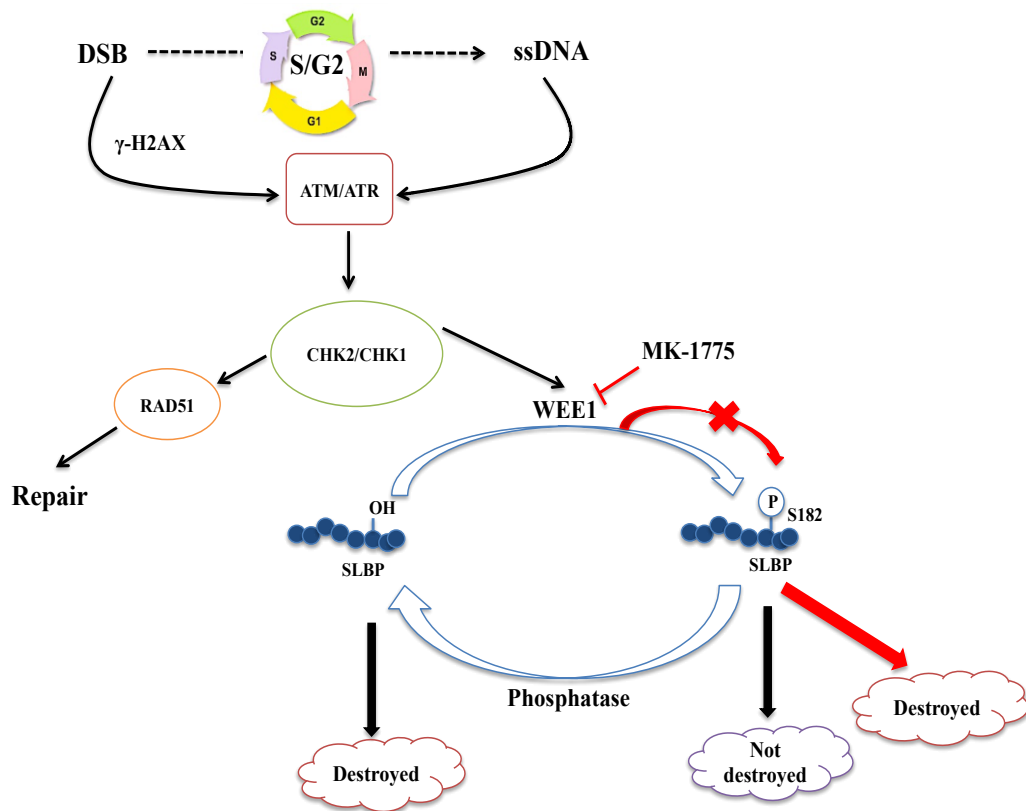


**Figure 5.18** Model for the coordination of WEE1 and SLBP degradation

Exposure of cells to double-strand breaks induce a pathway involving in ATM/ATR and CHK2/CHK1. However, WEE1 is a protein kinase that negatively regulate cell cycle progression by phosphorylating and deactivating cyclin-associated Cdks. WEE1 has been shown to phosphorylate cyclin-associated Cdk at Tyr15 during the S-G2 phase, resulting the delay of onset of mitosis. The model pathway of WEE1 and SLBP is unknown. It is an interesting mechanism somehow WEE1 inhibitor involves SLBP degradation.

It has previously been shown that the phosphorylation of Ser20 and Ser23 in SLBP acts as a phosphodegron resulting in polyubiquitination and proteasomal degradation during S phase. This involves Peptidyl-prolyl cis-trans isomerase NIMA-interacting 1 (Pin1) which facilitates the dissociation of SLBP from the SLBP-histone mRNA complex (Krishnan *et al.*, 2012). However, the kinases responsible for phosphorylation at these positions remain unknown. It is possible that there is complex interplay between phosphorylation at Ser20 and Ser23 and Ser182 which ultimately impinges on Thr61 phosphorylation. As Pin1 has also been reported to be involved in the regulation of Wee1 function, it is tempting to speculate that Pin1 might be involved in a coordinated mechanism to link cell cycle progression with the stability of critical components involved in each phase of the cycle.

Through the results provided in Chapter 5, it can be summarised that (1) there are factors that affect low percentage coverage of SLBP following tryptic digestion such as low abundance of SLBP, the conditions of mass spectrometry analysis setting, and expression system/purification method (2) S182 phosphorylation may be to modulate (i.e. delay) the scheduled destruction pathway that normally

brings about the SLBP destruction at the end of S-phase (3) WEE1 might not be the target protein kinase of S182 phosphorylation, however, it involves in SLBP stability.

## 5.4 References

- Bansal, N., Zhang, M., Bhaskar, A., Itotia, P. and Lee, E. 2013. Assembly of the SLIP1–SLBP complex on histone mRNA requires heterodimerization and sequential binding of SLBP followed by SLIP1. *Biochemistry*. 52: 520-536.
- Beck, H., Nähse-Kumpf, V., Larsen, M.S., O'Hanlon, K.A., Patzke, S., Holmberg, C., Mejlvang, J., Groth, A., Nielsen, O., Syljuåsen, R.G. and Sørensen, C.S. 2012. Cyclin-dependent kinase suppression by WEE1 kinase protects the genome through control of replication initiation and nucleotide consumption. *Mol Cell Biol*. 32(20): 4226-4236.
- Berry, L.D. and Gould, K.L. 1996. Regulation of Cdc2 activity by phosphorylation at T14/Y15. *Prog Cell Cycle Res*. 2: 99-105.
- Booher RN, Holman PS, Fattaey A. 1997. Human Myt1 is a cell cycle-regulated kinase that inhibits Cdc2 but not Cdk2 activity. *J Biol Chem*. 272: 22300-22306.
- Borchers, C.H., Thapar, R., Petrotchenko, E.V., Torres, M.P., Speir, J.P., Easterling, M., Dominski, Z. and Marzluff, W.F. 2006. Combined top-down and bottom-up proteomics identifies a phosphorylation site in stem-loop-binding proteins that contributes to high-affinity RNA binding. *Proc Natl Acad Sci U S A*. 103(9): 3094-3099.

- Brodersen, M.M., Lampert, F., Barnes, C.A., Soste, M., Piwko, W., and Peter, M. 2016. CRL4(WDR23)-Mediated SLBP Ubiquitylation Ensures Histone Supply during DNA Replication. *Mol. Cell* 62: 627-635.
- Brosch, M., Yu, L., Hubbard, T. and Choudhary, J. 2009, Accurate and Sensitive Peptide Identification with Mascot Percolator. *J Proteome Res.* 8(6): 3176-3181.
- Cakmakci, N.G., Lerner, R.S., Wagner, E.J., Zheng, L. and Marzluff, W.F. 2008. SLIP1, a factor required for activation of histone mRNA translation by the stem-loop binding protein. *Mol Cell Biol.* 28: 1182-1194.
- Chow, J.P., Siu, W.Y., Ho, H.T., Ma, K.H., Ho, C.C. and Poon, R.Y. 2003. Differential contribution of inhibitory phosphorylation of CDC2 and CDK2 for unperturbed cell cycle control and DNA integrity checkpoints. *J Biol Chem.* 278(42): 40815-40828.
- den Elzena, N. and Pinesa, J. 2001. Cyclin a is destroyed in prometaphase and can delay chromosome alignment and anaphase. *JCB* 153(1): 121-136.

- Domínguez-Kelly, R., Martín, Y., Koundrioukoff, S., Tanenbaum, M.E., Smits, V.A., Medema, R.H., Debatisse, M. and Freire, R. 2011. Wee1 controls genomic stability during replication by regulating the Mus81-Eme1 endonuclease. *J Cell Biol.* 194(4): 567-579.
- Ducat, D. and Zheng Y. 2004. Aurora kinases in spindle assembly and chromosome segregation. *Exp Cell Res.* 301(1): 60-67.
- Enders, G.H. 2010. *Cell Div.* 2010. Gauchos and ochos: a Wee1-Cdk tango regulating mitotic entry. 5(12): 1-7.
- Erlandsson, F., Linnman, C., Ekholm, S., Bengtsson, E. and Zetterberg, A. 2000. A detailed analysis of cyclin A accumulation at the G(1)/S border in normal and transformed cells. *Exp. Cell Res.* 259: 86-95.
- Featherstone, C. and Russell, P. 1991. Fission yeast p107wee1 mitotic inhibitor is a tyrosine/serine kinase. *Nature.* 349: 808-811.
- Gnad, F., Ren, S. Cox, J., Olsen, J.V., Macek, B., Oroshi, M. and Mann, M. 2007. PHOSIDA (phosphorylation site database): management, structural and evolutionary investigation, and prediction of phosphosites. *Genome Biol.* 2007: R250.

- Heijinka, A.M., Blomenb, V.A., Bisteauc, X., Degenera, F., Matsushitaa, F.Y., Kaldis, P., Fojjere, F. and van Vugta, M. A. 2015. A haploid genetic screen identifies the G1/S regulatory machinery as a determinant of Wee1 inhibitor sensitivity. *Proc Natl Acad Sci U S A.* (112)49: 15160-15165.
- Hirai, H., Iwasawa, Y., Okada, M., Arai, T., Nishibata, T., Kobayashi, M., Kimura, T., Kaneko, N., Ohtani, J., Yamanaka, K., Itadani, H., Takahashi-Suzuki, I., Fukasawa, K., Oki, H., Nambu, T., Jiang, J., Sakai, T., Arakawa, H., Sakamoto, T., Sagara, T., Yoshizumi, T., Mizuarai, S. and Kotani, H. 2009. Small-molecule inhibition of Wee1 kinase by MK-1775 selectively sensitizes p53-deficient tumor cells to DNA-damaging agents. *Mol Cancer Ther.* 8(11): 2992-3000.
- Hornbeck, P.V., Chabra, I., Kornhauser, J.M., Skrzypek, E., Zhang, B. 2004. PhosphoSite: A bioinformatics resource dedicated to physiological protein phosphorylation. *Proteomics* 4(6): 1551-1561.
- Katayama, K., Fujita, N. and Tsuruo, T. 2005. Akt/protein kinase B-dependent phosphorylation and inactivation WEE1Hu promote cell cycle progression at G2/M transition. *EMBO J.* 25(13): 5725-5737.

- Kollareddy, M., Dzubaka, P., Zhelevab, D. and Hajducha, M. 2008. Aurora kinases: structure, functions and their association with cancer. *Biomed Pap Med Fac Univ Palacky Olomouc Czech Repub.* 152(1): 27-33.
- Koseoglu, M.M., Graves, L.M. and Marzluff, W.F. 2008. Phosphorylation of threonine 61 by cyclin a/Cdk1 triggers degradation of stem-loop binding protein at the end of S phase. *Mol. Cell. Biol.* 28: 4469-4479.
- Krishnan, N., Lam, T.T., Fritz, A., Rempinski, D., O'Loughlin, K., Minderman, H., Berezney, R., Marzluff, W.F. and Thapar, R. 2012. The prolyl isomerase Pin1 targets stem-loop binding protein (SLBP) to dissociate the SLBP-histone mRNA complex linking histone mRNA decay with SLBP ubiquitination. *Mol Cell Biol.* 32(21): 4306-22.
- Liu, Z., Wang, Y., Cheng, H., Deng, W., Pan, Z., Ullah, S., Ren, J. and Xue, Y. 2015. GPS 3.0: web servers for the prediction of protein post-translational modification sites. Submitted.
- Mahajan, K. and Mahajan, N.P. 2013. WEE1 tyrosine kinase, a novel epigenetic modifier. *Trends Genet.* 29(7): 394-402.

- Marzluff, W.F., Wagner, E.J. and Duronio, R.J. 2008. Metabolism and regulation of canonical histone mRNAs: life without a poly (A) tail. *Nat. Rev. Genet.* 9: 843-854.
- McGowan, C.H. and Russell, P. 1995 Cell cycle regulation of human WEE1. *EMBO J.* 14: 2166-2175.
- Millipore (UK) Ltd. 2012. Wee1, active (Recombinant enzyme expressed in Sf21 insect cells), Item # 14-925. Lot # D12MP002NA.
- Michael, W. M. and Newport, J. 1998. Coupling of Mitosis to the Completion of S Phase Through Cdc34-Mediated Degradation of Wee1. *Science.* 282: 1886-1889.
- Niu, X., Li, N., Chen, D. and Wang, Z. 2013. Interconnection between the protein solubility and amino acid and dipeptide compositions. *Protein Pept Lett.* 20(1): 88-95.
- Okamoto, K. and Sagata, N. 2007. Mechanism for inactivation of the mitotic inhibitory kinase Wee1 at M phase. *Proc Natl Acad Sci U S A.* 104(10): 3753-3758.
- Owens, L., Simanski, S., Squire, C., Smith, A., Cartzendafner, J., Cavett, V., Caldwell Busby, J., Sato, T. and Ayad, N.G. 2010. Activation domain-dependent degradation of somatic Wee1 kinase. *J Biol Chem.* 285(9): 6761-6769.

- Parker, L.L. and Piwnica-Worms, H. 1992. Inactivation of the p34cdc2-cyclin B complex by the human WEE1 tyrosine kinase. *Science*. 257(5078): 1955-1957.
- Parker, L.L., Sylvestre, P.J., Byrnes, M.J., Liu, F., Piwnica-Worms, H. 1995. Identification of a 95-kDa WEE1-like tyrosine kinase in HeLa cells. *Proc Natl Acad Sci U S A*. 92(21): 9638-9642.
- PhosphoSite and the Phosphoproteome of Cancer, NIH-NCI. R44CA126080, 2006-2010.
- Price, W.N., Handelman, S.K., Everett, J.K., Tong, S.N., Bracic, A., Luff, J.D., Naumov, V., Acton, T., Manor, P., Xiao, R., Rost, B., Montelione, G.T. and Hunt, J.F. 2011. Large-scale experimental studies show unexpected amino acid effects on protein expression and solubility in vivo in *E. coli*. *Microb Inform and Exp* 1:6.
- Rigaut, G., Shevchenko, A. Rutz, B. Wilm, M., Mann, M. and Séraphin, B. 1999. A generic protein purification method for protein complex characterization and proteome exploration. *Nat Biotechnol* 17: 1030-1032.
- Pines, J., and Hunter, T. 1991. Human cyclins A and B1 are differentially located in the cell and undergo cell cycle-dependent nuclear transport. *J. Cell Biol.* 115: 1-17.

- Rigaut, G., Shevchenko, A., Rutz, B., Wilm, M., Mann, M., Séraphin, B. 2009. A generic protein purification method for protein complex characterization and proteome exploration. *Nat Biotechnol.* 17(10): 1030-1032.
- Schmidt, P.M., Sparrow, L.G., Attwood, R.M., Xiao, X., Adams, T.E., McKimm-Breschkin, J.L. 2012. Taking down the FLAG! How insect cell expression challenges an established tag-system. *PLoS One.* 7(6): e37779.
- Slotstra, J.W., Puijk, W.C., Ligtoet, G.J., Kuperus, D., Schaaper, W.M. and Meleen, R.H. 1997. Screening of a Small Set of Random Peptides: A New Strategy to Identify Synthetic Peptides that Mimic Epitopes. *J. Mol. Recognit.* 10: 217-224.
- Solomon, M.J., Glotzer, M., Lee, T.H., Philippe, M. and Kirschner, M.W. 1990. Cyclin activation of p34cdc2. *Cell* 63: 1013-1024.
- Saini, P., Li, Y. and Dobbelstein, M. 2015. Wee1 is required to sustain ATR/Chk1 signaling upon replicative stress. *Oncotarget.* 6(15): 13072-13087.
- Sanchez, R. and Marzluff, W.F. 2002. The stem-loop binding protein is required for efficient translation of histone mRNA in vivo and in vitro. *Mol Cell Biol.* 22: 7093-7104.

- Schitteck, B. and Sinnberg, T. 2014. Biological functions of casein kinase 1 isoforms and putative roles in tumorigenesis. *Mol Cancer*. 13: 231.
- Seligmann, H (Ed.), ISBN: 978-953-307-593-8, InTech, Available from:<http://www.intechopen.com/books/dna-replication-current-advances/faithful-dna-replication-requires-regulation-of-cdk-activity-by-checkpoint-kinases>.
- Smythe, C and Newport, J.W. 1992. Coupling of mitosis to the completion of S phase in *Xenopus* occurs via modulation of the tyrosine kinase that phosphorylates p34cdc2. *Cell*. 68(4): 787-797.
- Sørensen, C.S. and Syljuåsen, R.G. 2012. Safeguarding genome integrity: the checkpoint kinases ATR, CHK1 and WEE1 restrain CDK activity during normal DNA replication *Nucleic Acids Res*. 40(2): 477-486.
- Tan, D., Marzluff, W.F., Dominski, Z., Tong, L. 2013. Structure of histone mRNA stem-loop, human stem-loop binding protein, and 3'hExo ternary complex. *Science*. 339: 318-321.
- Thapar, R. 2014. Contribution of protein phosphorylation to binding-induced folding of the SLBP-histone mRNA complex probed by phosphorus-31 NMR. *FEBS Open Bio*. 16(4): 853-857.

- Thapar, R. 2015. Structure-specific nucleic acid recognition by L-motifs and their diverse roles in expression and regulation of the genome. *Biochim Biophys Acta*. 1849(6): 677-687.
- Thapar, R., Mueller, G.A. and Marzluff, W.F. 2004. The N-terminal domain of the *Drosophila* histone mRNA binding protein, SLBP, is intrinsically disordered with nascent helical structure. *Biochemistry*, 43: 9390-9400.
- Ubersax, J.A. and Ferrell, J.E. Jr. 2007. Mechanisms of specificity in protein phosphorylation. *Nat Rev Mol Cell Biol*. 8(7): 530-541.
- Völkel, P., Le Faou, P. and Angrand, P.O. 2010. Interaction proteomics: characterization of protein complexes using tandem affinity purification-mass spectrometry. *Biochem Soc Trans*. 38(4): 883-887.
- Watanabe, N. 2008. Wee1. UCSD-Nature Molecule Pages (<http://www.signaling-gateway.org/molecule/query?afcsid=A002371>)
- Watanabe, N., Arai, H., Iwasaki, J., Shiina, M., Ogata, K., Hunter, T and Osada, H. 2005. Cyclin-dependent kinase (CDK) phosphorylation destabilizes somatic Wee1 via multiple pathways. *Proc Natl Acad Sci U S A*. 102(33): 11663-11668.
- Watanabe, N., Arai, H., Nishihara, Y., Taniguchi, M., Watanabe, N., Hunter, T., and Osada, H. 2004. M-phase kinases induce phospho-

dependent ubiquitination of somatic Wee1 by SCFbeta-TrCP.

Proc Natl Acad Sci U S A. 101(13): 4419-4424.

Watanabe, N. Broome, M. and Hunter, T. 1995. Regulation of the human WEE1Hu CDK tyrosine 15-kinase during the cell cycle. EMBO J. 14:1878-1891.

Zhang, S.P., Zubay, G. and Goldman, E. 1991. Low-usage codons in Escherichia coli, yeast, fruit fly and primates. Gene. 105(1): 61-72.

Zheng, L., Dominski, Z., Yang, X.C., Elms, P., Raska, C.S., Borchers, C.H. and Marzluff, W.F. 2003. Phosphorylation of stem-loop binding protein (SLBP) on two threonines triggers degradation of SLBP, the sole cell cycle-regulated factor required for regulation of histone mRNA processing, at the end of S phase. Molecular and cellular biology. 23: 1590-1601.

# Chapter 6

## *Analysis of the Interactome of SLBP in response to DNA damage and replication arrest-induced histone mRNA decay*

### **6.1 Introduction**

Cellular surveillance mechanisms act as the safeguards of genome integrity in eukaryotes to reduce the risk of errors that may result either in cell death or diseases. Cell cycle checkpoints are the surveillance mechanisms that operate to regulate the timing of critical cell cycle events to ensure that cells have sufficient time to resolve aberrant DNA or chromosomal structures. One component of the cell cycle checkpoint system operates via a large network of DNA damage response (DDR) genes. Checkpoint components are predicted to comprise sensor components, in addition to signal transduction components as well as effector molecules (as described in section 1.5, Chapter 1) For example, DNA replication stress involves a series of molecules (Mazouzi *et al.*, 2014) including ATRIP, Rad17 and 9-1-1 complex which together with TOPBP1 recognises the presence of excessive amounts of the single-

stranded DNA binding protein RPA, in addition to the highly conserved signal transduction system that comprises the PIKK family members ATR and ATM, as well as their downstream amplifying protein kinases Chk1 and Chk2 (Ciccia and Elledge, 2010) (see diagram in section 1.4.2, Chapter 1). These kinases are activated by genotoxic stresses, either generated externally, such as ionising radiation or ultraviolet light induced DNA damage, or internally as a consequence of innate challenges associated with whole genome replication, leading to delays in cell-cycle progression, the activation of DNA repair pathways, or, should it become clear that genome integrity is compromised, programmed cell death (Ciccia and Elledge, 2010). It is clear that loss of checkpoint functions results in genomic instability, which is the critical factor in the initiation of many cancers.

The Smythe group in collaboration with Muller (2007), as well as Marzluff and colleagues (Kaygun and Marzluff, 2005a), have investigated histone mRNA decay as a potential target of the intra-S phase checkpoint. In support of this notion, Kaygun and Marzluff (2005a) showed that a dominant negative form of ATR was sufficient to block efficient histone mRNA decay. In contrast, Muller *et al* found that a dominant negative form of ATR was not sufficient to induce replication stress-induced histone mRNA decay which required the

presence of inhibitors of checkpoint signalling including caffeine which principally targets ATR, in addition to LY294002 which blocks DNA-PK (Muller *et al.*, 2007).

However, replication stress does not induce histone mRNA decay via destabilisation and proteolytic destruction of SLBP, as SLBP may still be detected after a prolonged period of replication stress (Kaygun and Marzluff, 2005a). Several models have been proposed to explain how checkpoint transducers such as, ATR and/or DNA-PK may regulate the stability of histone mRNA. However, the detailed mechanism by which replication stress induced histone mRNA decay is unknown. Therefore, I chose to use mass spectrometry to investigate potential changes in SLBP post-translational modification status, together with an analysis of its interacting proteins following replication stress. Flag-tagged SLBP was utilised as a bait to immuno-isolate mRNP complex for analysis by mass spectrometry.

## 6.2 Results

### 6.2.1 Triple labeling SILAC strategy

To investigate both SLBP and changes in its network of interacting proteins following replication arrest-induced histone mRNA decay, mass spectrometry analyses of Flag-tagged SLBP and associated proteins was undertaken. To do this, a stable isotopic labeled amino acids in cell culture (SILAC) approach was adopted involving 3 separate isotopically labeled media formulations-heavy (H), medium (M) and light (L), (see below). Cell lysates from each condition were subjected to the immuno-isolation protocol devised in Chapter 4. Given the distinct isotopic content as a result of incubation with SILAC amino acid-containing media, proteins obtained from each treatment show a characteristic mass difference that is detectable by mass spectrometric analyses. The ratios of M/L, H/L and H/M represent a change in protein levels in their respective conditions.

SILAC media containing either light (K0R0), medium ([D<sub>4</sub>]-lysine, [<sup>13</sup>C<sub>6</sub>]-arginine, K4R6) or heavy ([<sup>13</sup>C<sub>6</sub><sup>15</sup>N<sub>2</sub>]-lysine, [<sup>13</sup>C<sub>6</sub><sup>15</sup>N<sub>4</sub>]- arginine, K8R10) isotopes of the indicated amino acids were used for three separate growth cell incubation conditions that could be resolved and quantitated by MS. Incorporation of light, medium and

heavy amino acids was verified after cells were permitted to grow over 5 passages to ensure that all proteins were homogeneously labelled isotopically. To check this, a lysate derived from cells grown in K8R10 and K0R0 medium was mixed 1:1 ratio and ratios verified for greater than > 95% of all proteins (data not shown).

In all cases, cells were subjected to the synchronisation protocol, in which cells were treated with Noc for 12 h, released into fresh medium and after that mitotic shake-off was used to detach cells prior to grown them in dishes in the presence of 0.5 µg/ml dox for 14 h, at which point cells are in S phase, either mock-treated, or exposed to 5 mM HU for 20 min. To control for non-specific interactions, cells both exposed to HU and not (50:50 ratio), were grown in K0R0 (light) medium in the absence of Dox (Figure 6.1). Cells in the presence of Dox (and thus expressing Flag-SLBP) were either grown in K4R6 (medium) medium in the absence of HU (mock-treated), or grown in K8R10 (heavy) medium, and subsequently exposed to HU for 15 min to induce replication stress (Figure 6.1).

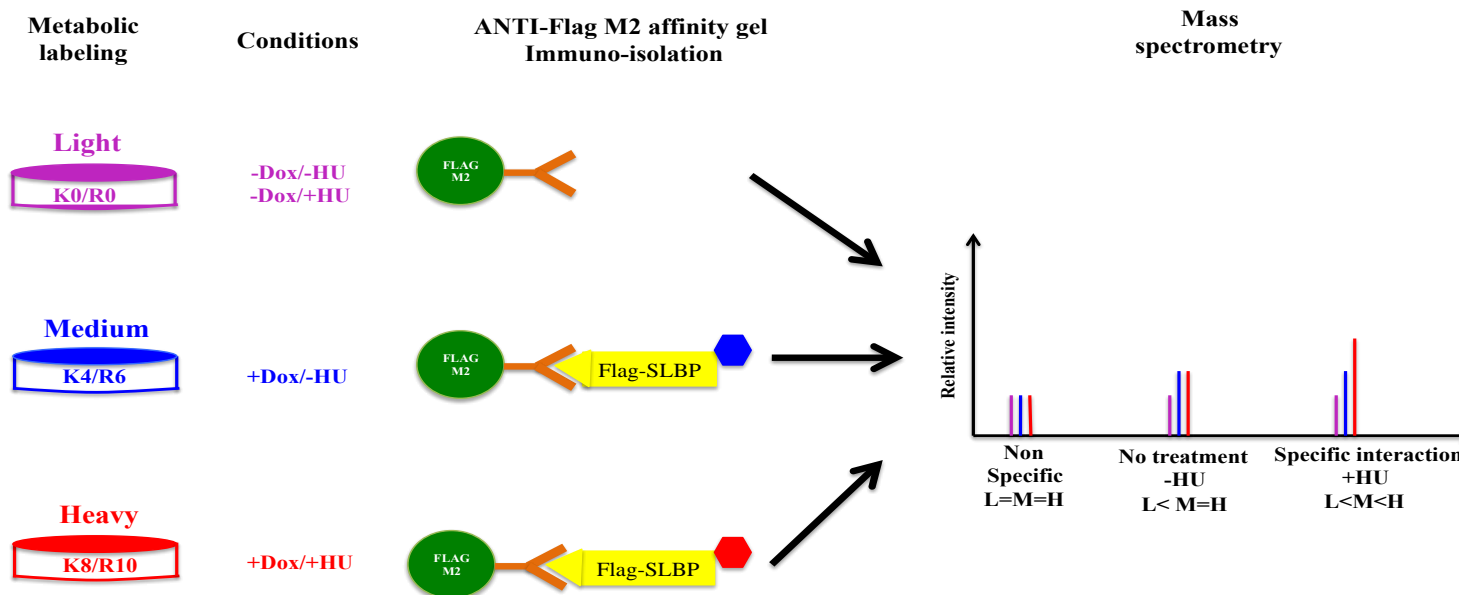


**Figure 6.1** Schematic diagram of the experimental strategy

Triple metabolic labelling SILAC strategy was used to label HeLa cells expressing Flag-tagged SLBP with three different combinations of isotope lysine and arginine. Flag-tagged SLBP stably transfected in Flp-In-HeLa cells growing in asynchronous culture were treated with 40 ng/ $\mu$ l Noc for 12 h, isolated by shake off, replated and then

treated with or without 0.5  $\mu\text{g/ml}$  Dox for 14 h. Then cells were treated with or without 5 mM HU for 20 min., harvested and immunisolated with ANTI-FLAG M2 affinity gel. Immunisolations were pooled and analyzed simultaneously by mass spectrometry. Peptides arising from each cell population were quantified by measurement of the relative intensity of light (K0/R0), medium (K4/R6), and heavy (K8/R10) peaks with MaxQuant.

In all three cases, cell lysates were prepared, each subjected to the immuno-isolation protocol described in Chapter 4, and the eluates were combined in equal proportion (by volume). Subsequently, the combined eluate comprising proteins labelled with each isotope combination were subjected to gel electrophoresis, 5 gel slices were generated, and each was subjected to in-gel digestion with trypsin as described in section 2.2.10. This experimental protocol was undertaken for three separate experiments.

### **6.2.2 Overview of identified SLBP-interacting proteins**

In total, peptides derived from 2,964 proteins were identified over all three experimental conditions after data processing using MaxQuant software (Cox and Mann, 2008). In order to calculate isotopic ratios and thus relative abundances of individual proteins, Maxquant software requires that a minimum of 2 peptides, and their isotopic variants (that is M/L, H/L and H/M) were identified for any given protein, and these criteria were fulfilled for 977 proteins.

One way to verify that true SLBP interactors are detected using this approach is to establish whether previously characterized SLBP

interacting proteins are identified in the MS analysis. I therefore selected published SLBP interactors from six databases:

IntAct (<http://www.ebi.ac.uk/intact/>),

BioGRID (<https://thebiogrid.org>),

HPRD(<http://www.hprd.org>),

APID (<http://cicblade.dep.usal.es:8080/APID/init.action>),

STRING (<http://string-db.org>),

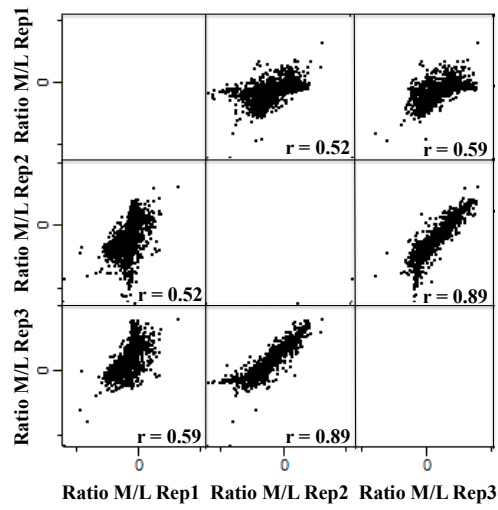
and PIPs (<http://www.compbio.dundee.ac.uk/www-pips/>).

I selected those interactions supported by more than one publication (Appendix J). The data presented here showed that 67% (12/18) of those interactors were identified (see below), indicating that the experimental set-up is capable of the analysis of the SLBP interactome, with a high level of sensitivity.

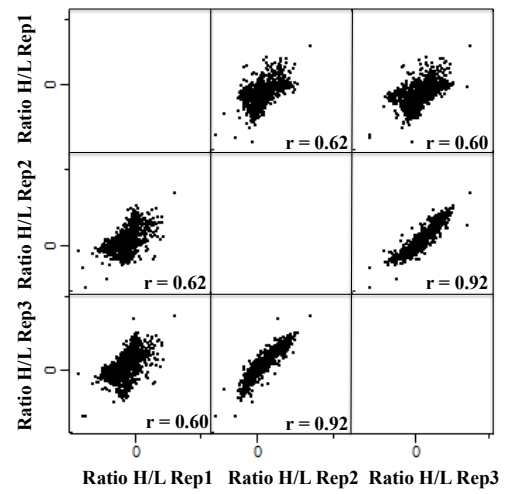
### **6.2.3 Identification of SLBP-bound proteins by quantitative mass spectrometry**

Determination of the sets of ratios describe above allows for the normalisation of the data, to allow comparison between experimental conditions and between biological replicates. To determine equivalence of the ratio distributions between biological replicates, I calculated Pearson's correlation coefficient ( $r$ ) between replicates. While high values were obtained for all three sets of ratios between replicates 2 and 3, (M/L, H/L and H/M correlations of 0.89, 0.92 and 0.53, respectively), very poor correlation was observed with replicate 1 (Figure 6.2), suggesting poor performance in this replicate (non-linear correlation). This data indicates that the distribution of population values in the three biological replicates varies between individual experiments which may have the effect of increasing both false positive and false negative identification of candidate interaction partner proteins. However, stringent criteria threshold and restricted filtering data to reduce contaminants were applied and will be discussed in more detail in the sections that follow.

A.



B.



C.

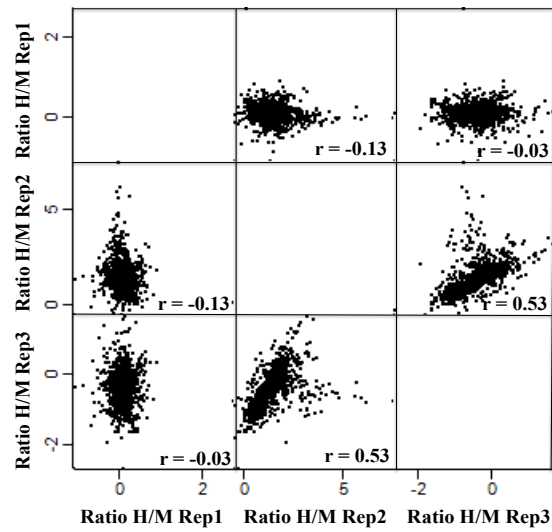


**Figure 6.2** The comparison of the three independent biological replicates of  $\log_2$  SILAC ratios (A) M/L, (B) H/L and (C) H/M for each experiment.

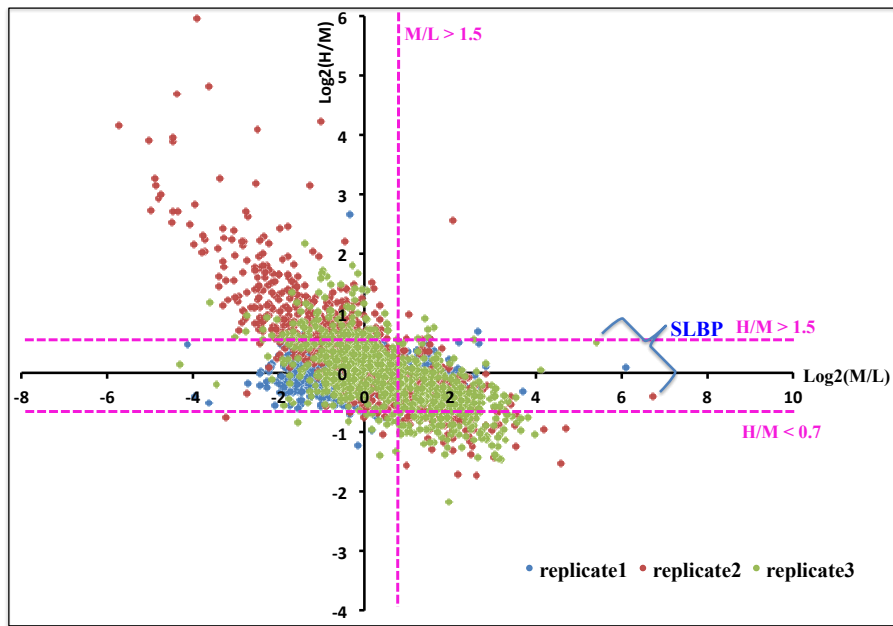


**Figure 6.3** Analysis of protein interaction dynamics occurring between no HU and HU conditions.

Scatter-plots were plotted with  $\text{Log}_2(\text{M/L})$  on the x axis versus  $\text{Log}_2(\text{H/M})$  ratios on the y axis of all proteins quantified by MaxQuant in the three biological replicates of each SLBP-interacting proteins. The dotted pink lines show a threshold cutoff 0.5 fold change. Proteins identified with H/M ratios between 1.5 and 0.7 ( $0.5 > \log_2 \text{H/M} > -0.5$ ) were categorised as unchanging. Proteins whose association is increased in response to replication stress are expected to have H/M ratios more than 1.5 ( $\log_2 \text{H/M} > 0.5$ ) while proteins whose association is decreased in response to replication stress show H/M ratios lower than 0.7 ( $\log_2 \text{H/M} < -0.5$ ). Blue, red and green spots represent quantified proteins in replicate 1, 2 and 3, respectively.

In order to display the specificity of the interaction between identified proteins and SLBP (M/L ratio) together with any changes resulting from imposition of replication stress (H/M ratio), a plot of  $\log_2(M/L)$  versus  $\log_2(H/M)$  values was produced for all 977 proteins in all three replicate experiments (Figure 6.3).

SLBP was enriched between 40 and 100 fold in all three replicates (Figure 6.3). Although the level of SLBP does not change upon HU treatment (Kaygun and Mazluff, 2005a), the H/M ratios obtained for SLBP varied between 1.5 and 0.7 ( $-0.5 < \log_2 H/M < 0.5$ ). Consequently, proteins identified with H/M ratios between 1.5 and 0.7 ( $0.5 > \log_2 H/M > -0.5$ ) were categorised as unchanging under the conditions of the experiment.

Thus proteins whose association is increased in response to replication stress are expected to have H/M ratios more than 1.5 ( $\log_2 H/M > 0.5$ ) while proteins whose association is decreased in response to replication stress show H/M ratios lower than 0.7 ( $\log_2 H/M < -0.5$ ) (Figure 6.3). Proteins that show M/L ratios lower than 1 are likely to be mostly non-specific contaminants. The threshold value of the M/L ratio used here was 1.5 ( $\log_2 M/L > 0.5$ ). This is an arbitrary figure and proteins close to this threshold may either be contaminants or falsely discarded interaction partners. To minimise the number of proteins

mis-categorised in this way, candidate proteins were only identified if shown to be enriched in at least two of three independent biological replicates.

Consequently, the I-i-MS experiment identified 299 proteins interactors of SLBP consisting of 3 categories with respect to status following replication stress: increased association (4 proteins), unchanged association (213 proteins) and decreased association (82 proteins) as shown in Table 6.1-6.3 (categorised protein names by alphabetical order were shown in Appendix K).

I failed to observe some previously reported SLBP interactors such as MIF4G domain-containing protein (*MIF4GD* or *SLIP1*) (von Moeller *et al.*, 2013), CBP80/20-dependent translation initiation factor (*CTIF*) (Choe *et al.*, 2013) and zinc finger protein 473 (*ZNF473* or *ZFP100*) (Dominski *et al.*, 2002). However previously reported SLBP interactors such as nuclear cap-binding protein subunit 1 (*NCBP1* or *CBP80*), nuclear cap-binding protein subunit 2 (*NCBP2* or *CBP20*) (Choe *et al.*, 2013) were identified. In addition, components (UPF1,UPF2 and UPF3B) of the nonsense mediated decay pathway, at least one of which (UPF1) has been previously implicated in replication stress induced histone mRNA decay (Kaygun and Marzluff, 2005b ; Mueller *et al.*, 2007) were identified. Moreover, immuno-isolation-MS

experiments led to identification of a number of novel SLBP-interactors, both under steady-state conditions as well as following replication stress. Most notable among these are proteins involved in mRNA export, translation initiation, DNA repair, nuclear exosome complex, RNA helicases and histone mRNA processing.

**Table 6.1** Proteins (4 proteins) whose association with SLBP increases following replication stress. The  $\log_2(M/L)$  and  $\log_2(H/M)$  of 3 biological replicates were shown.

Protein names	Gene names	Log <sub>2</sub> (M/L) rep1	Log <sub>2</sub> (M/L) rep2	Log <sub>2</sub> (M/L) rep3	Log <sub>2</sub> (H/M) rep1	Log <sub>2</sub> (H/M) rep2	Log <sub>2</sub> (H/M) rep3
	THO complex subunit 4	ALYREF	1.09309	0.977097	1.63882	0.0361869	0.571628
THO complex subunit 1	THOC1	2.67446	1.55189	1.48923	0.494774	0.571628	0.614851
THO complex subunit 5 homolog	THOC5	2.63483	1.03759	0.0961269	0.699285	0.970486	0.729009
THO complex subunit 6 homolog	THOC6	1.55567	1.34908	1.43039	0.586308	0.404685	0.920446

**Table 6.2** Proteins (213 proteins) whose association with SLBP unchanged following replication stress. The  $\log_2(M/L)$  and  $\log_2(H/M)$  of 3 biological replicates were shown.

Protein names	Gene names	Log <sub>2</sub> (M/L) rep1	Log <sub>2</sub> (M/L) rep2	Log <sub>2</sub> (M/L) rep3	Log <sub>2</sub> (H/M) rep1	Log <sub>2</sub> (H/M) rep2	Log <sub>2</sub> (H/M) rep3
AFG3-like protein 2	AFG3L2	0.933195	0.986884	1.20132	0.283329	0.00129789	-0.0763716
UPF0568 protein C14orf166	C14orf166	1.24099	0.50518	1.49866	0.0508847	0.312781	-0.11416
Uncharacterized protein C17orf85	C17orf85	1.80826	2.82995	2.25707	-0.270991	-0.0131887	-0.0242231
Chromatin target of PRMT1 protein	CHTOP	0.667211	1.67152	1.7473	0.0583859	0.182184	0.19333
Casein kinase I isoform alpha	CSNK1A1	1.19219	1.41072	1.86477	-0.2446	-0.398246	-0.427886
Casein kinase II subunit alpha; Casein kinase II subunit alpha 3	CSNK2A1 CSNK2A3	0.831148	1.0552	1.38571	-0.226662	0.0542234	0.0528332
Casein kinase II subunit alpha	CSNK2A2	0.854315	0.924936	1.71826	-0.263438	0.00374607	0.123666
ATP-dependent RNA helicase DDX1	DDX1	2.18568	1.15556	1.62985	0.064469	0.0282862	-0.224907
Probable ATP-dependent RNA helicase DDX17	DDX17	1.47379	2.03471	2.12334	0.131326	-0.263057	-0.24127
ATP-dependent RNA helicase DDX3X/DDX3Y	DDX3X DDX3Y	1.4653	1.75241	1.72809	0.0639171	-0.200647	-0.285724
Probable ATP-dependent RNA helicase DDX5	DDX5	1.30836	2.44241	2.55893	-0.0168476	-0.420144	-0.392118
ATP-dependent RNA helicase DDX50	DDX50	0.951812	2.28182	2.34628	0.346985	-0.0495465	-0.0723159
Putative pre-mRNA-splicing factor ATP-dependent RNA helicase DHX15	DHX15	1.35659	1.10333	1.18669	0.0295589	0.0457225	0.00877379
H/ACA ribonucleoprotein complex subunit4	DKC1	1.05415	1.8532	1.83289	-0.0810338	-0.174198	-0.247748
Eukaryotic translation initiation factor 4E	EIF4E	1.03175	2.1775	2.55589	-0.125022	-0.092048	-0.194873
Protein FAM98B	FAM98B	1.55964	1.29519	1.58183	0.0575542	-0.140046	-0.27275
Fragile X mental retardation protein 1	FMR1	1.42164	1.9863	2.22716	0.49057	0.0654344	-0.222397
Fragile X mental retardation syndrome-related protein1	FXR1	1.23192	1.70443	2.26987	0.384492	0.00331442	-0.333025
Glycogen synthase kinase-3 beta	GSK3B	0.721504	0.963326	1.63352	0.0204844	0.090447	-0.474573
Histone H1x	H1FX	0.677801	3.42559	3.36401	-0.0540777	-0.387544	-0.48655
KRR1 small subunit processome component homolog	KRR1	0.570171	1.81287	2.10145	-0.0194189	0.405992	0.247442
Leucine-rich repeat-containing protein 47	LRRC47	1.09119	1.25978	1.64805	-0.203851	-0.149809	-0.222902
Enscosin	MAP7	0.787014	0.814919	1.25532	0.159371	-0.398684	-0.492078
DNA replication licensing factor MCM5	MCM5	1.8974	0.76511	0.780142	-0.150897	-0.102775	0.0241777
Nuclear cap-binding protein subunit 2	NCBP2	2.00418	1.68086	1.25151	-0.10538	-0.339017	0.167615
PHD finger protein 6	PHF6	0.796764	1.18307	1.39402	-0.207378	-0.490051	-0.251419
Polymerase delta-interacting protein 3	POLDIP3	1.53998	2.23312	2.00781	-0.290092	-0.186311	0.156138
Pre-mRNA-splicing factor 38B	PRPF38B	1.2458	1.47228	0.848077	-0.00154454	0.00173014	0.160662
RNA-binding protein 27	RBM27	0.996316	0.779386	1.42013	-0.156563	-0.240486	-0.450124
Protein RCC2	RCC2	2.06143	1.3041	2.32147	-0.080988	-0.204084	-0.425346
Ribonuclease P protein subunit p30	RPP30	1.2441	0.831472	1.87527	-0.0276897	0.0824301	-0.0684682
tRNA-splicing ligase RtcB homolog	RTCB	1.30527	1.51395	1.69728	0.0980152	-0.46943	-0.313154
Splicing factor 1	SF1	1.52381	0.901031	0.503145	0.17645	0.24732	0.296898
Histone RNA hairpin-binding protein	SLBP	6.09748	6.74524	5.41799	0.0865121	-0.391475	0.508327
Lamina-associated polypeptide 2, isoforms beta/gamma	TMPO	0.722029	0.890563	1.2337	-0.0561762	-0.203851	-0.475355
Probable tRNA pseudouridine synthase 2	TRUB2	0.857344	0.815739	1.55046	-0.00826141	-0.066926	-0.263889
Regulator of nonsense transcripts 2	UPF2	2.09721	1.02418	0.758644	-0.0273367	-0.162267	-0.227135
Regulator of nonsense transcripts 3B	UPF3B	1.34965	2.31362	1.80112	-0.0109337	-0.170475	-0.405968
WD repeat-containing protein 82	WDR82	0.511772	0.982583	1.38211	-0.114285	0.258217	-0.0400518
X-ray repair cross-complementing protein 5	XRCC5	1.99393	2.6294	2.75399	0.196103	-0.347748	-0.212451
X-ray repair cross-complementing protein 6	XRCC6	1.56959	2.49349	2.98246	0.134221	-0.250491	-0.207778
RAC-beta serine/threonine-protein kinase	AKT2	0.674189	-0.152227	0.637007	0.068602	-0.374599	0.0233263
Mitotic checkpoint protein BUB3	BUB3	0.776104	0.380175	0.870661	-0.10355	-0.037799	0.0750534
Caldesmon	CALD1	0.824646	-0.641581	0.900799	-0.104682	1.17332	-0.00272928
Cell division cycle 5-like protein	CDC5L	1.39999	1.41765	2.22786	0.0492126	-0.463987	-0.904251
Cleavage and polyadenylation specificity factor subunit 7	CPSF7	0.959102	1.10755	1.33743	-0.18641	-0.515027	-0.440381
Cold shock domain-containing protein E1	CSDE1	1.24007	0.986884	0.87342	-0.00978573	-0.596798	-0.355848
Cleavage stimulation factor subunit 1	CSTF1	1.10923	0.41792	0.612871	-0.450006	-0.306359	-0.00718809
ATP-dependent RNA helicase DDX42	DDX42	0.741747	-0.640569	0.967685	0.015212	0.333309	-0.389338
Ras GTPase-activating protein-binding protein1	G3BP1	1.2022	1.52777	2.74562	-0.0903267	-0.209545	-0.514944
Histone H1.5	HIST1H1B	1.07711	2.21198	3.30132	0.11023	-0.405623	-0.796937
Histone H2B; Histone H2B type 1-L; Histone H2B type 1-M; Histone H2B type 1-H; Histone H2B type 2-F; Histone H2B type 1-C/E/G/I; Histone H2B type 1-D; Histone H2B type F-S; Histone H2B type 1-K	HIST1H2BN HIST1H2BL HIST1H2BM HIST1H2BH HIST2H2BF HIST1H2BC HIST1H2BD H2BFS HIST1H2BK	0.991463	0.0458623	0.83374	0.179766	0.190046	-0.0680447
Histone H4	HIST1H4A	1.48109	-0.197749	0.721416	0.317188	0.751635	0.35682
Histone H2A type 2-C; Histone H2A type 2-A; Histone H2A type 1-J; Histone H2A type 1-H; Histone H2A.J; Histone H2A type 1-D; Histone H2A type 1;	HIST2H2AC HIST2H2AA3 HIST1H2AJ HIST1H2AH H2AFJ HIST1H2AD HIST1H2AG	1.04663	0.373063	1.80814	0.213627	0.134615	-0.248913

Protein names	Gene names	Log2(M/L) rep1	Log2(M/L) rep2	Log2(M/L) rep3	Log2(H/M) rep1	Log2(H/M) rep2	Log2(H/M) rep3
BTB/POZ domain-containing protein KCTD17	KCTD17	2.00978	2.62779	1.47804	-0.245232	-1.73663	-0.336045
BTB/POZ domain-containing protein KCTD2	KCTD2	1.71282	2.46336	1.47799	-0.252862	-1.16188	-0.339984
Far upstream element-binding protein 2	KHSRP	0.659194	-0.140142	0.731965	-0.183638	0.733788	0.0374524
Mannosyl-oligosaccharide glucosidase	MOGS	0.590913	-0.0099192	0.778293	-0.160798	-0.752413	-0.285354
Nuclear cap-binding protein subunit 1	NCBP1	2.32507	3.52682	2.83554	-0.0427688	-0.702609	0.169412
Negative elongation factor E	NELFE	0.673285	2.07029	1.8788	-0.155036	-0.778705	-0.451051
Non-POU domain-containing octamer-binding protein	NONO	0.532267	0.395063	1.18707	0.179384	-0.122727	-0.376732
6-phosphofructo-2-kinase/fructose-2,6-bisphosphatase 3	PFKFB3	1.63473	0.187134	0.591871	0.0792927	0.10541	-0.374729
Phosphorylated adapter RNA export protein	PHAX	3.70896	4.69805	4.12027	-0.311327	-0.923195	0.0518593
PHD and RING finger domain-containing protein 1	PHRF1	1.41878	0.254715	0.680504	0.0319598	0.655319	0.434455
26S proteasome non-ATPase regulatory subunit 4	PSMD4	1.35688	0.0315363	0.945458	-0.0647967	0.630499	-0.428139
Polypyrimidine tract-binding protein 1	PTBP1	2.06167	1.96525	2.5363	0.0282862	-0.550402	-0.428449
RNA-binding protein 6	RBM6	0.774671	0.776104	1.60796	-0.286181	-0.562018	-0.560728
60S ribosomal protein L11	RPL11	0.629566	-0.0839668	0.780394	0.0835197	0.234624	0.0170667
40S ribosomal protein S20	RPS20	0.881351	0.108491	0.717912	-0.0411054	-0.0504277	-0.260567
SWI/SNF-related matrix-associated actin-dependent regulator of chromatin subfamily A member 5	SMARCA5	0.719402	1.77871	1.78379	0.104873	-0.378626	-0.506619
Survival motor neuron protein	SMN1	0.804301	0.873026	1.9637	-0.38694	0.0633648	-0.592723
Signal recognition particle 14 kDa protein	SRP14	0.792439	0.637935	-0.121518	-0.183359	-0.323805	-0.65102
Serrate RNA effector molecule homolog	SRRT	1.62307	2.21614	2.04862	-0.0704514	-0.820031	-0.0726344
SURP and G-patch domain-containing protein 1	SUGP1	0.516116	1.55149	1.25338	0.067088	0.466444	0.572599
Splicing factor U2AF 65 kDa subunit	U2AF2	0.843662	0.212507	0.665484	-0.147969	0.213378	0.16337
Pre-mRNA-splicing regulator WTAP	WTAP	0.938173	0.510557	0.243425	0.0897694	-0.175941	0.139731
Zinc finger CCH-type antiviral protein 1	ZC3HAV1	1.05942	1.9539	1.52361	-0.00310513	-0.355116	-0.687985
Double-stranded RNA-specific adenosine deaminase	ADAR	0.424385	0.962956	1.11703	0.239642	-0.16707	-0.175224
ATP synthase subunit gamma	ATP5C1	-0.477081	0.535754	1.40261	-0.23703	0.0888201	-0.29612
CD2 antigen cytoplasmic tail-binding protein 2	CD2BP2	0.222063	0.734829	1.34073	0.0357646	0.0409626	-0.449828
Cytoskeleton-associated protein 4	CKAP4	0.377401	1.75886	2.42728	-0.246995	-0.401616	-0.324365
CDKN2A-interacting protein	CDKN2AIP	0.413919	1.53844	1.94744	0.0192037	-0.210596	-0.266871
Protein CMSS1	CMSS1	0.419647	1.28291	2.29025	0.0540844	0.312317	0.0396999
2,3-cyclic-nucleotide 3-phosphodiesterase	CNP	0.013498	0.656176	1.20126	-0.0377693	0.156655	0.197614
Coatomer subunit epsilon	COPE	-0.293076	0.926455	1.60654	0.172359	0.381726	0.227248
Carnitine O-palmitoyltransferase 1	CPT1A	-0.0699061	0.617769	0.827087	-0.139522	-0.0558912	-0.197087
DDRGK domain-containing protein 1	DDRGK1	-1.24451	0.668755	0.851439	0.0462816	0.0732718	-0.188266
Dolichol-phosphate mannosyltransferase subunit 1	DPM1	0.0517201	0.754888	1.81852	-0.0289256	0.183836	-0.317157
Eukaryotic initiation factor 4A-I	EIF4A1	0.0497701	0.659194	1.3305	-0.0175339	-0.227236	-0.320901
Eukaryotic initiation factor 4A-III	EIF4A3	-0.614094	0.511468	0.562768	0.287709	0.0229004	0.0551957
Engulfment and cell motility protein 2	ELMO2	-0.984046	0.772139	0.66175	0.403704	0.0382958	-0.0248247
Emerin	EMD	-1.29577	0.509746	0.693498	-0.0164974	0.359071	0.272023
Erlin-1	ERLIN1	-1.0233	1.1046	1.37585	-0.393956	-0.217038	-0.103705
Exosome complex component RRP42	EXOSC7	0.201508	1.00036	1.96824	0.405557	-0.312921	-0.420762
Constitutive coactivator of PPAR-gamma-like protein 1	FAM120A	0.153416	0.888071	1.44652	-0.0609992	-0.165807	-0.457534
Phenylalanine--tRNA ligase alpha subunit	FARSA	-0.0830037	1.24068	1.24227	-0.209795	-0.249393	-0.423642
40S ribosomal protein S30	FAU	0.336055	0.815903	2.60144	0.0926134	-0.312258	-0.324642
Flap endonuclease 1	FEN1	-0.242243	1.92888	2.71257	-0.0918173	-0.486469	-0.395872
Flap FRG1	FRG1	0.495491	1.88823	0.675816	0.292311	-0.104821	0.0280033
Far upstream element-binding protein 3	FUBP3	-0.330247	1.00375	1.84266	-0.0293083	-0.177457	-0.343238
Guanine nucleotide-binding protein-like 3	GNL3	-0.191623	2.85422	2.57913	0.203264	-0.213571	-0.381517
Trifunctional enzyme subunit alpha	HADHA	-0.0345149	0.549521	0.823179	0.251325	0.199625	-0.125652
Histone deacetylase 1	HDAC1	0.148609	0.899562	1.85072	-0.110417	0.114234	-0.242908
Histone deacetylase 2	HDAC2	0.140648	1.0439	1.27852	-0.171076	-0.431501	-0.3311
Heterogeneous nuclear ribonucleoprotein A0	HNRNPA0	0.205768	1.26015	1.56438	0.238175	-0.129718	-0.0421597
Heterogeneous nuclear ribonucleoprotein A1;	HNRNPA1;	0.304745	0.682573	2.36	0.0196308	0.00432164	-0.470589
Heterogeneous nuclear ribonucleoprotein A1-like 2	HNRNPA1L2						
Heterogeneous nuclear ribonucleoprotein A3	HNRNPA3	0.165172	1.24787	1.99121	0.0881415	-0.364125	-0.379826
Heterogeneous nuclear ribonucleoprotein A/B	HNRNPAB	-0.0557412	1.07827	1.92649	0.00863037	-0.360916	-0.435593
Heterogeneous nuclear ribonucleoprotein F	HNRNPF	-0.0150243	0.989648	1.68733	0.0190613	-0.0469657	-0.383417
Heterogeneous nuclear ribonucleoprotein K	HNRNPK	0.333882	1.29237	1.94103	0.0254541	-0.19798	-0.415153
Heterogeneous nuclear ribonucleoprotein L	HNRNPL	-0.10019	1.39446	1.88131	0.0285691	-0.321171	-0.401501
Heterogeneous nuclear ribonucleoprotein M	HNRNPM	0.370388	1.64847	1.96466	0.188781	-0.139299	-0.395739
Heterogeneous nuclear ribonucleoprotein R	HNRNPR	0.316725	1.57405	1.7291	0.0982848	-0.142115	-0.0853131
Heterogeneous nuclear ribonucleoprotein U-like protein 2	HNRNPUL2	-0.190108	0.569977	0.844868	-0.0240324	-0.169599	-0.211414
Insulin-like growth factor 2 mRNA-binding protein 3	IGF2BP3	-0.0308403	2.12178	2.15623	0.0655723	-0.176838	-0.14038
Transcription factor jun-B	JUNB	-0.115723	1.25369	1.34318	0.166715	-0.109997	-0.352437
Importin subunit alpha-1	KPNA2	-0.573209	0.777199	0.950842	0.312317	-0.0324182	-0.0986291
Importin subunit alpha-7	KPNA6	-0.0373103	0.699374	0.9568	-0.260843	-0.105954	-0.352381
Galectin-3; Galectin	LGALS3	-0.141351	0.566766	0.823342	-0.277027	-0.494475	0.498455
Lamin-B1	LMBN1	-0.0928786	0.817951	1.29854	-0.362789	0.182311	0.057277
Leucine-rich repeat-containing protein 59	LRRCS9	0.149389	0.983313	2.01685	0.0724488	-0.0789141	-0.435963
Melanoma-associated antigen D2	MAGED2	-0.00414652	0.685178	1.24239	-0.168009	0.279412	0.0378742
39S ribosomal protein L3, mitochondrial	MRPL3	-0.257977	0.753005	0.558072	0.00877379	-0.347839	0.0777899
28S ribosomal protein S22, mitochondrial	MRPS22	0.374066	0.964288	1.71444	-0.116848	0.381283	0.124328
28S ribosomal protein S27, mitochondrial	MRPS27	0.351515	1.55748	2.09062	-0.0838291	-0.351148	-0.28179
28S ribosomal protein S34, mitochondrial	MRPS34	0.481919	1.42578	1.85052	-0.00492797	0.0315363	-0.012359
28S ribosomal protein S9, mitochondrial	MRPS9	-0.127116	0.896543	0.922426	0.0628125	-0.255512	-0.164044
Metastasis-associated protein MTA2	MTA2	0.308244	1.01321	1.40196	-0.0890218	-0.455851	-0.47911
Nucleolar protein 56	NOP56	0.299948	1.81422	1.88565	0.372952	0.113701	-0.0804692
Nucleolar protein 58	NOP58	0.425137	1.68872	2.04194	0.242206	0.111699	-0.114863
PCI domain-containing protein 2	PCID2	0.190678	1.56106	1.35986	0.0149266	0.0149266	0.490262
PDZ and LIM domain protein 7	PDLIM7	0.436908	0.815166	1.11043	-0.173807	0.132643	0.0772429
Protein arginine N-methyltransferase 1	PRMT1	0.119157	0.598746	0.850319	-0.0662008	-0.0362152	0.143785
U4/U6small nuclear ribonucleoprotein Ppp31	PRPF31	0.388465	1.44334	2.21956	-0.106063	-0.134003	-0.345564
Glutamyl-peptidyl cyclotransferase-like protein	QPCTL	0.231432	0.877823	0.856388	0.00115371	0.0695647	-0.000302979
Histone-binding protein RBBP7	RBBP7	-0.144744	0.532068	1.08038	-0.134889	-0.34828	-0.155791
RNA-binding protein 14	RBM14	0.332164	1.45875	1.36126	-0.00695607	0.365133	-0.0440921
Splicing factor 45	RBM17	0.0837921	1.56652	1.39693	0.230818	0.0736831	0.251083
RNA-binding protein 4;	RBM4;						
RNA-binding protein 4B	RBM4B	0.118891	1.63059	1.65627	-0.00228126	-0.036304	0.017922
RNA-binding motif protein, X chromosome;	RBMX;						
RNA binding motif protein, X-linked-like-1	RBMXL1	-1.15985	0.743644	0.752064	0.299948	-0.47682	-0.342616
RNA 3-terminal phosphate cyclase-like protein	RCL1	0.305795	1.67338	2.25145	0.0549179	-0.387714	-0.46037
RE1-silencing transcription factor	REST	0.0870554	1.22416	0.72465	0.0859685	-0.491389	-0.2932
Replication factor C subunit 3	RFC3	0.0946415	1.32077	2.07073	0.207768	-0.479915	-0.465699
Replication factor C subunit 4	RFC4	-0.0648571	1.66125	2.09983	0.242328	-0.490456	-0.177751
Replication factor C subunit 5	RFC5	-0.217122	1.03766	1.16434	0.235237	-0.280159	0.0490731

Protein names	Gene names	Log2(M/L) rep1	Log2(M/L) rep2	Log2(M/L) rep3	Log2(H/M) rep1	Log2(H/M) rep2	Log2(H/M) rep3
Phosphorylated adapter RNA export protein	PHAX	3.70896	4.69805	4.12027	-0.311327	-0.923195	0.0518593
26S proteasome non-ATPase regulatory subunit4	PSMD4	1.35688	0.0315363	0.945458	-0.0647967	0.630499	-0.428139
Polypyrimidine tract-binding protein 1	PTBP1	2.06167	1.96525	2.5363	0.0282862	-0.550402	-0.428449
RNA-binding protein 6	RBM6	0.774671	0.776104	1.60796	-0.286181	-0.282018	-0.560728
60S ribosomal protein L11	RPL11	0.629566	-0.0839668	0.780394	0.0835197	0.234624	0.0170667
40S ribosomal protein S20	RPS20	0.881351	0.108491	0.717912	-0.0411054	-0.0504277	-0.260567
SWI/SNF-related matrix-associated actin-dependent regulator of chromatin subfamily A member 5	SMARCA5	0.719402	1.77871	1.78379	0.104873	-0.378626	-0.506619
Survival motor neuron protein	SMN1	0.804301	0.873026	1.9637	-0.38694	0.0633648	-0.592723
Signal recognition particle 14 kDa protein	SRP14	0.792439	0.637935	-0.121518	-0.183359	-0.323805	-0.65102
Serrate RNA effector molecule homolog	SRRT	1.62307	2.21614	2.04862	-0.0704514	-0.820031	-0.0726344
SURP and G-patch domain-containing protein 1	SUGP1	0.516116	1.55149	1.25338	0.067088	0.466444	0.572599
Splicing factor U2AF 65 kDa subunit	U2AF2	0.843662	0.212507	0.665484	-0.147969	0.213378	0.16337
Pre-mRNA-splicing regulator WTAP	WTAP	0.938173	0.510557	0.243425	0.0897694	-0.175941	0.139731
Zinc finger CCHC-type antiviral protein 1	ZC3HAV1	1.05942	1.9539	1.52361	-0.00310513	-0.355516	-0.687985
Double-stranded RNA-specific adenosine deaminase	ADAR	0.424385	0.962956	1.11703	0.239642	-0.16707	-0.175224
ATP synthase subunit gamma	ATP5C1	-0.477081	0.617769	0.535754	1.40261	0.0888201	-0.29612
CD2 antigen cytoplasmic tail-binding protein 2	CD2BP2	0.222063	0.734829	1.34073	0.0357646	0.0409626	-0.449828
Cytoskeleton-associated protein 4	CKAP4	0.377401	1.75886	2.42728	-0.246995	-0.401616	-0.324365
CDKN2A-interacting protein	CDKN2AIP	0.413919	1.53844	1.94744	0.0192037	-0.210596	-0.266871
Protein CMSS1	CMSS1	0.419647	1.28291	2.29025	0.0540844	0.312317	0.0396999
2,3-cyclic-nucleotide 3-phosphodiesterase	CNP	0.013498	0.656176	1.20126	-0.0377693	0.156655	0.197614
Coatamer subunit epsilon	COPE	-0.293076	0.926455	1.60654	0.172359	0.381726	0.227248
Carnitine O-palmitoyltransferase 1	CPT1A	-0.0699061	0.617769	0.827087	-0.139522	-0.0558912	-0.197087
DDRKG domain-containing protein 1	DDRKG1	-1.24451	0.668755	0.851439	0.0462816	0.0732718	-0.188266
Dolichol-phosphate mannosyltransferase subunit 1	DPM1	0.0517201	0.754888	1.81852	-0.0289256	0.183836	-0.317157
Eukaryotic initiation factor 4A-1	EIF4A1	0.0497701	0.659194	1.3305	-0.0175339	-0.227236	-0.320901
Eukaryotic initiation factor 4A-III	EIF4A3	-0.614094	0.511468	0.562768	0.287709	0.0229004	0.0551957
Engulfment and cell motility protein 2	ELMO2	-0.984046	0.772139	0.66175	0.403704	0.0382958	-0.0248247
Emerin	EMD	-1.29577	0.509746	0.693498	-0.0164974	0.359071	0.272023
Erlin-1	ERLIN1	-1.0233	1.1046	1.37585	-0.393956	-0.217038	-0.103705
Exosome complex component RRP42	EXOSC7	0.201508	1.00036	1.96824	0.405557	-0.312921	-0.420762
Constitutive coactivator of PPAR-gamma-like protein 1	FAM120A	0.153416	0.888071	1.44652	-0.0609992	-0.165807	-0.457534
Phenylalanine--tRNA ligase alpha subunit	FARSA	-0.0830037	1.24068	1.24227	-0.209795	-0.249393	-0.423642
40S ribosomal protein S30	FAU	0.336055	0.815903	2.60144	0.0926134	-0.312258	-0.324022
Flap endonuclease 1	FEN1	-0.242243	1.92888	2.71257	-0.0918173	-0.486469	-0.395872
Protein FRG1	FRG1	0.495491	1.88823	0.675816	0.292311	-0.104821	0.0280033
Far upstream element-binding protein 3	FUBP3	-0.330247	1.00375	1.84266	-0.0293083	-0.177457	-0.343238
Guanine nucleotide-binding protein-like 3	GNL3	-0.191623	2.85422	2.57913	0.203264	-0.213571	-0.381517
Trifunctional enzyme subunit alpha	HADHA	-0.0345149	0.549521	0.823179	0.251325	0.199625	-0.125652
Histone deacetylase 1	HDAC1	0.148609	0.899562	1.85072	-0.110417	0.114234	-0.242908
Histone deacetylase 2	HDAC2	0.140648	1.0439	1.27852	-0.171076	-0.431501	-0.3311
Heterogeneous nuclear ribonucleoprotein A0	HNRNPA0	0.205768	1.26015	1.56438	0.238175	-0.129718	-0.0421597
Heterogeneous nuclear ribonucleoprotein A1;	HNRNPA1;						
Heterogeneous nuclear ribonucleoprotein A1-like 2	HNRNPA1L2	0.304745	0.682573	2.36	0.0196308	0.00432164	-0.470589
Heterogeneous nuclear ribonucleoproteinA3	HNRNPA3	0.165172	1.24787	1.99121	0.0881415	-0.364125	-0.379826
Heterogeneous nuclear ribonucleoprotein A/B	HNRNPAB	-0.0557412	1.07827	1.92649	0.00863037	-0.369016	-0.435593
Heterogeneous nuclear ribonucleoprotein F	HNRNPF	-0.0150243	0.989648	1.68733	0.0190613	-0.0469657	-0.383417
Heterogeneous nuclear ribonucleoprotein K	HNRNPK	0.333882	1.29237	1.94103	0.0254541	-0.19798	-0.415153
Heterogeneous nuclear ribonucleoprotein L	HNRNPL	-0.10019	1.39446	1.88131	0.0285691	-0.321171	-0.401501
Heterogeneous nuclear ribonucleoproteinM	HNRNPM	0.370388	1.64847	1.96466	0.188781	-0.139299	-0.395739
Heterogeneous nuclear ribonucleoprotein R	HNRNPR	0.316725	1.57405	1.7291	0.0982848	-0.142115	-0.0853131
Heterogeneous nuclear ribonucleoprotein U-like protein 2	HNRNPUL2	-0.190108	0.569977	0.844868	-0.0240324	-0.169599	-0.211414
Insulin-like growth factor 2 mRNA-binding protein 3	IGF2BP3	-0.0308403	2.12178	2.15623	0.0655723	-0.176838	-0.14038
Transcription factor jun-B	JUNB	-0.115723	1.25369	1.34318	0.166715	-0.109997	-0.352437
Importin subunit alpha-1	KPNA2	-0.573209	0.777199	0.950842	0.312317	-0.0324182	-0.0986291
Importin subunit alpha-7	KPNA6	-0.0373103	0.699374	0.9568	-0.260843	-0.105954	-0.352381
Galectin-3;Galectin	LGALS3	-0.141351	0.566766	0.823342	-0.277027	-0.494475	0.498455
Lamin-B1	LMNB1	-0.0928786	0.817951	1.29854	-0.362789	0.182311	0.057277
Leucine-rich repeat-containing protein 59	LRRC59	0.149389	0.983313	2.01685	0.0724488	-0.0789141	-0.435963
Melanoma-associated antigen D2	MAGED2	-0.00414652	0.685178	1.24239	-0.168009	0.279412	0.0378742
39S ribosomal protein L3, mitochondrial	MRPL3	-0.257977	0.753005	0.558072	0.00877379	-0.347839	0.0777899
28S ribosomal protein S22, mitochondrial	MRPS22	0.374066	0.964288	1.71444	-0.116848	0.381283	0.124328
28S ribosomal protein S27, mitochondrial	MRPS27	0.351515	1.55748	2.09062	-0.0838291	-0.351148	-0.28179
28S ribosomal protein S34, mitochondrial	MRPS34	0.481919	1.42578	1.85052	-0.00492797	0.0315363	-0.012359
28S ribosomal protein S9, mitochondrial	MRPS9	-0.127116	0.896543	0.922426	0.0628125	-0.255512	-0.164044
Metastasis-associated protein MTA2	MTA2	0.308244	1.01321	1.40196	-0.0890218	-0.455851	-0.47911
Nucleolar protein 56	NOP56	0.299948	1.81422	1.88565	0.372952	0.113701	-0.0804692
Nucleolar protein 58	NOP58	0.425137	1.68872	2.04194	0.242206	0.111699	-0.114863
PCI domain-containing protein 2	PCID2	0.190678	1.56106	1.35986	0.289008	0.0149266	0.490262
PDZ and LIM domain protein 7	PDLIM7	0.436908	0.815166	1.11043	-0.173807	0.132643	0.0772429
Protein arginine N-methyltransferase 1	PRMT1	0.119157	0.598746	0.850319	-0.0662008	-0.0362152	0.143785
U4/U6small nuclear ribonucleoprotein Prp31	PRPF31	0.388465	1.44334	2.21956	-0.106063	-0.13603	-0.345564
Glutamyl-peptide cyclotransferase-like protein	QCCTL	0.231432	0.877823	0.856388	0.00115371	0.0695647	-0.000302979
Histone-binding protein RBBP7	RBBP7	-0.144744	0.532068	1.08038	-0.134889	-0.34828	-0.155791
RNA-binding protein 14	RBM14	0.332164	1.45875	1.36126	-0.00695607	0.365133	-0.0440921
Splicing factor 45	RBM17	0.0837921	1.56652	1.39693	0.230818	0.0736831	0.251083
RNA-binding protein 39	RBM39	-0.0214529	1.61513	1.58135	0.0862402	-0.0936789	-0.174898
RNA-binding protein 4;	RBM4;						
RNA-binding protein 4B	RBM4B	0.118891	1.63059	1.65627	-0.00228126	-0.036304	0.017922
RNA-binding motif protein, X chromosome;	RBMX;						
RNA-binding motif protein, X-linked-like-1	RBMXL1	-1.15985	0.743644	0.752064	0.299948	-0.47682	-0.342616
RNA 3-terminal phosphate cyclase-like protein	RCL1	0.305795	1.67338	2.25145	0.0549179	-0.387714	-0.46037
RE1-silencing transcription factor	REST	0.0870554	1.22416	0.72465	0.0859685	-0.491389	-0.2932
Replication factor C subunit 3	RFC3	0.0946415	1.32077	2.07073	0.207768	-0.479915	-0.465699
Replication factor C subunit 4	RFC4	-0.0648571	1.66125	2.09983	0.242328	-0.490456	-0.177751
Replication factor C subunit 5	RFC5	-0.217122	1.03766	1.16434	0.235237	-0.280159	0.0490731

**Table 6.3** Proteins (82 proteins) whose association with SLBP decreases

following replication stress. The  $\log_2(M/L)$  and  $\log_2(H/M)$  of 3 biological replicates were shown.

Protein names	Gene names	Log2(M/L) rep1	Log2(M/L) rep2	Log2(M/L) rep3	Log2(H/M) rep1	Log2(H/M) rep2	Log2(H/M) rep3
ATP-binding cassette sub-family F member 1	ABCF1	0.993493	1.27095	3.10378	-0.267132	-0.701131	-1.24171
Actin-like protein 6A	ACTL6A	0.29901	1.85204	2.42282	0.173895	-0.655717	-0.574326
Aspartyl/asparaginyl beta-hydroxylase	ASPH	0.683113	1.08454	1.35265	-0.138235	-0.713947	-0.710307
ATPase family AAA domain-containing protein 3A	ATAD3A	0.0257376	2.19027	2.58628	0.128161	-0.634039	-0.686313
Ataxin-2-like protein	ATXN2L	0.710966	0.690909	0.984261	-0.071012	-0.537592	-0.996196
Ribosome biogenesis proteinBMS1homolog	BMS1	0.67726	1.86592	2.01981	-0.116927	-0.890198	-0.666439
Caprin-1	CAPRN1	2.60179	1.53082	2.56769	-0.0314595	-0.948391	-0.878799
Cytoskeleton-associated protein 5	CKAP5	0.75745	1.85012	1.37662	0.0229004	-1.18148	-1.20078
Carboxymethylenebutenolidase homolog	CMBL	0.485736	0.993566	0.827413	-0.748796	-1.54738	-0.994183
Nucleolar RNA helicase 2	DDX21	1.05873	2.36991	2.83261	0.016211	-0.821381	-0.876387
Probable ATP-dependent RNA helicase DDX47	DDX47	0.782409	2.98714	3.01623	-0.0562362	-0.982477	-0.883635
Probable ATP-dependent RNA helicase DDX6	DDX6	1.44747	2.07632	2.3822	0.142217	-0.82309	-0.600424
Putative ATP-dependent RNA helicase DDX30	DDX30	0.987685	1.90068	2.28084	0.00805652	-0.547953	-0.584674
ATP-dependent RNA helicase DHX36	DHX36	0.684998	1.42637	1.7398	0.00705191	-0.756575	-0.623154
ATP-dependent RNA helicase A	DHX9	0.416948	0.918615	1.65668	0.0427844	-0.80826	-0.947167
DnaJ homolog subfamily A member 3, mitochondrial	DNAJA3	0.328147	2.21636	1.96706	-0.229179	-0.760577	-0.561409
Developmentally-regulated GTP-binding protein1	DRG1	0.746571	2.42862	2.49339	-0.224857	-1.05224	-0.90417
Probable rRNA-processing protein EBP2	EBNA1BP2	-0.0196676	3.54164	3.29992	0.0843364	-1.23253	-1.12664
Eukaryotic translation initiation factor 2	EIF2S1	0.750949	1.05436	1.8324	-0.0923709	-0.603299	-0.558878
Eukaryotic translation initiation factor 2 subunit 2	EIF2S2	0.93885	2.07738	3.15189	-0.125463	-1.10995	-1.43901
Eukaryotic translation initiation factor 2 subunit 3	EIF2S3 EIF2S3L	1.24294	1.93708	2.54955	-0.202207	-1.04922	-1.13343
Eukaryotic translation initiation factor 3 subunit E	EIF3E	-0.209278	0.70496	2.03372	-0.167231	-0.554167	-0.892848
Eukaryotic translation initiation factor 3 subunit H	EIF3S3; EIF3H	-0.772407	1.45654	2.0588	-0.0132905	-0.697266	-0.853475
Eukaryotic initiation factor 4A-II	EIF4A2	1.07998	2.17961	2.97807	0.116365	-1.70925	-1.22267
Eukaryotic translation initiation factor 4 gamma 1	EIF4G1	0.487898	1.68916	2.43435	-0.132483	-0.676503	-0.80138
Eukaryotic translation initiation factor 5B	EIF5B	0.555914	0.885028	1.88554	-0.116364	-0.807149	-1.36587
Exosome complex component RRP4	EXOSC2	0.232661	0.991898	2.2047	-0.0250596	-0.789935	-0.52197
Exosome complex component RRP41	EXOSC4	0.563158	1.51243	1.80244	0.0227584	-0.662337	-0.522323
Exosome complex component MTR3	EXOSC6	0.000432815	1.59034	2.09748	0.184979	-0.843862	-0.516532
pre-rRNA processing protein FTSJ3	FTSJ3	-0.0653401	1.76791	2.47298	0.130008	-0.875513	-0.782198
Ras GTPase-activating protein-binding protein 2	G3BP2	1.09228	2.37446	2.26147	0.0429245	-0.594683	-0.637626
Gem-associated protein 5	GEMIN5	0.406537	1.46957	2.05513	0.00388999	-1.10321	-0.873397
Glioma tumor suppressor candidate region gene 2 protein	GLTSCR2	0.140909	3.40667	2.67154	-0.229568	-0.527533	-0.594617
Putative oxidoreductase GLYR1	GLYR1	1.94235	4.57634	3.06781	-0.0330971	-1.53061	-1.40916
G-rich sequence factor 1	GRSF1	0.59846	1.91659	2.60604	-0.129339	-1.11282	-0.764469
Nucleolar GTP-binding protein 1	GRTPBP4	0.0597706	3.30118	3.15714	0.334568	-0.636055	-0.578068
Vigilin	HDLBP	0.857105	2.05287	2.29152	0.0143553	-1.30134	-1.25822
Inhibitor of nuclear factor kappa-B kinase-interacting protein	IKBIP	-0.212584	3.01781	2.48238	0.0900404	-1.41227	-0.943278
Interleukin enhancer-binding factor 2	ILF2	0.345964	2.04736	2.31307	0.00230651	-0.853006	-0.578736
Interleukin enhancer-binding factor 3	ILF3	0.810649	1.74252	1.32866	0.0329472	-0.604148	-0.72922
BTB/POZ domain-containing protein KCTD5	KCTD5	1.34596	1.51435	1.68648	-0.106343	-0.756965	-0.526203
KH domain-containing, RNA-binding, signal transduction-associated protein 1	KHDRBS1	1.51546	2.63448	2.72179	-0.0497107	-0.553617	-0.672864
La-related protein 4	LARP4	0.689925	0.908044	1.28765	-0.170995	-0.562495	-0.807528
Microtubule-associated protein;Microtubule-associated protein 4	MAP4	1.98535	1.60374	2.87741	-0.0685439	-0.785005	-1.06664
Protein LYRIC	MTDH	0.356707	3.5036	3.08217	0.351967	-0.894751	-0.763758
Myb-binding protein 1A	MYBBP1A	0.158725	1.7586	1.92471	0.15769	-0.631667	-0.774009
N-acetyltransferase 10	NAT10	0.327687	1.84844	2.83952	0.00360232	-0.858227	-1.11397
Nucleolin	NCL	0.573181	1.86271	3.16712	0.139601	-0.615641	-1.03753
Nucleolar protein 14	NOP14	0.809497	0.548634	1.64547	0.0200577	-0.621111	-1.17358
Probable 28S rRNA (cytosine(4447)-C(5))-methyltransferase	NOP2	0.00532815	2.26027	2.87149	0.339023	-0.794783	-1.12674
rRNA (cytosine(34)-C(5))-methyltransferase	NSUN2	0.438932	0.856309	1.72238	0.116498	-0.633815	-0.989192
Nuclear fragile X mental retardation-interacting protein 2	NUFIP2	1.23799	2.22983	2.09478	-0.102744	-0.681006	-0.594857
Protein odr-4 homolog	ODR4	-0.434286	1.00087	1.15853	-0.177751	-0.581886	-0.722586
Poly [ADP-ribose] polymerase 1	PARP1	1.56589	0.929034	1.63166	-0.253773	-0.808917	-0.877712
Protein polyhromo-1	PBRM1	-0.156048	1.1501	2.64934	0.233029	-0.679873	-1.41231
Pre-mRNA-processing factor 19	PRPF19	0.80331	2.32328	2.42148	0.116098	-0.697055	-0.57626
Polymerase I and transcript release factor	PTRF	0.279531	2.15445	2.13622	-0.591353	-0.670865	-0.518288
60S ribosomal protein L10a	RPL10A	0.0617071	1.31499	3.11347	0.286171	-0.529156	-1.07585
60S ribosomal protein L23a	RPL23A	0.259062	1.54992	2.05408	-0.0342489	-0.523442	-0.635943
60S ribosomal protein L27	RPL27	0.042084	0.971737	1.42277	0.0127833	0.0619835	-0.205414
60S ribosomal protein L3	RPL3	0.280362	3.08819	3.34696	0.141564	-0.890252	-0.703055
60S ribosomal protein L30	RPL30	0.00647761	1.53481	2.36569	0.293488	-0.681932	-1.06873
60S ribosomal protein L36	RPL36	-0.227168	1.3003	1.94561	0.264837	-0.698974	-1.11791
60S ribosomal protein L4	RPL4	0.490159	3.15262	3.55937	0.10809	-0.852016	-0.847544
60S ribosomal protein L8	RPL8	0.0174944	3.04937	3.96689	0.263515	-0.616945	-1.03792
Ribosome-binding protein 1	RRBP1	0.180403	2.12241	3.06176	-0.146579	-0.845417	-1.36665
Ribosomal L1 domain-containing protein 1	RSL1D1	0.43808	4.19456	3.8339	0.0511633	-0.939925	-0.757428

Protein names	Gene names	Log2(M/L) rep1	Log2(M/L) rep2	Log2(M/L) rep3	Log2(H/M) rep1	Log2(H/M) rep2	Log2(H/M) rep3
SWI/SNF-related matrix-associated actin-dependent regulator of chromatin subfamily E member 1	SMARCE1	0.441377	2.0234	2.86439	0.0607391	-0.798742	-1.05284
Signal recognition particle subunit SRP68	SRP68	-0.0111954	2.58193	3.6589	0.0352017	-0.610874	-0.772629
Signal recognition particle subunit SRP72	SRP72	0.237074	2.46106	2.73851	-0.118022	-0.824929	-1.1083
SRSF protein kinase 1	SRPK1	1.25223	2.5291	2.45004	-0.0141207	-0.771495	-0.693248
FACT complex subunit SSRP1	SSRP1	1.0297	2.23011	2.38593	0.366924	-0.850923	-0.844277
Erythrocyte band 7 integral membrane protein	STOM	-0.846402	1.3278	1.80033	0.204016	-0.600708	-0.844872
Transducin beta-like protein 2	TBL2	-0.185901	3.11323	3.33871	0.187641	-0.656899	-0.702093
Mitochondrial import inner membrane translocase subunit TIM44	TIMM44	-0.928924	1.30065	0.782996	-0.208294	-0.629121	-0.521308
DNA topoisomerase 1	TOP1	1.81991	2.49976	3.20408	-0.207195	-1.38105	-1.46849
Regulator of nonsense transcripts 1	UPF1	-0.0985365	1.07806	1.81672	-0.0141644	-0.852954	-1.07595
Y-box-binding protein 3	YBX3	0.305795	2.55213	2.60559	0.0863761	-0.945249	-0.552728
Zinc finger CCCH domain-containing protein 15	ZC3H15	1.2307	2.83968	2.36603	-0.116895	-0.881135	-0.696307
Zinc finger CCCH domain-containing protein 18	ZC3H18	0.269871	1.5654	1.15225	0.289716	-1.2769	-0.619315

#### 6.2.4 Functional analysis

The Cytoscape plugin ClueGO integrates Gene Ontology (GO) terms, Kyoto Encyclopedia of Genes and Genomes (KEGG) information and BioCarta data to generate functionally grouped gene ontology and pathway annotation networks (Bindea *et al.*, 2009 ; Lopes *et al.*, 2010). Default settings for the biological process category were used to analyse the three categories of enriched proteins and only pathway connections which showed statistical significance ( $p < 0.05$ ) (Huang *et al.*, 2007) are displayed.

The group of up-regulated proteins, ALYREF, THOC1, THOC5 and THOC6 are well-established components of the TREX complex which is involved in multiple steps of transcription, 3' end formation and nuclear export (Katathira, 2012). (Figure 6.4). Interestingly, ALYREF, THOC1 and THOC5 have also been implicated in replication fork processing and connect with genome instability (Wellinger *et al.*, 2006 ; Dominguez-Sanchez *et al.*, 2011 ; Heath *et al.*, 2016) and at least one of these components (THOC5) is a known target of the DNA damage checkpoint regulator ATM (Ramachandran *et al.*, 2011).

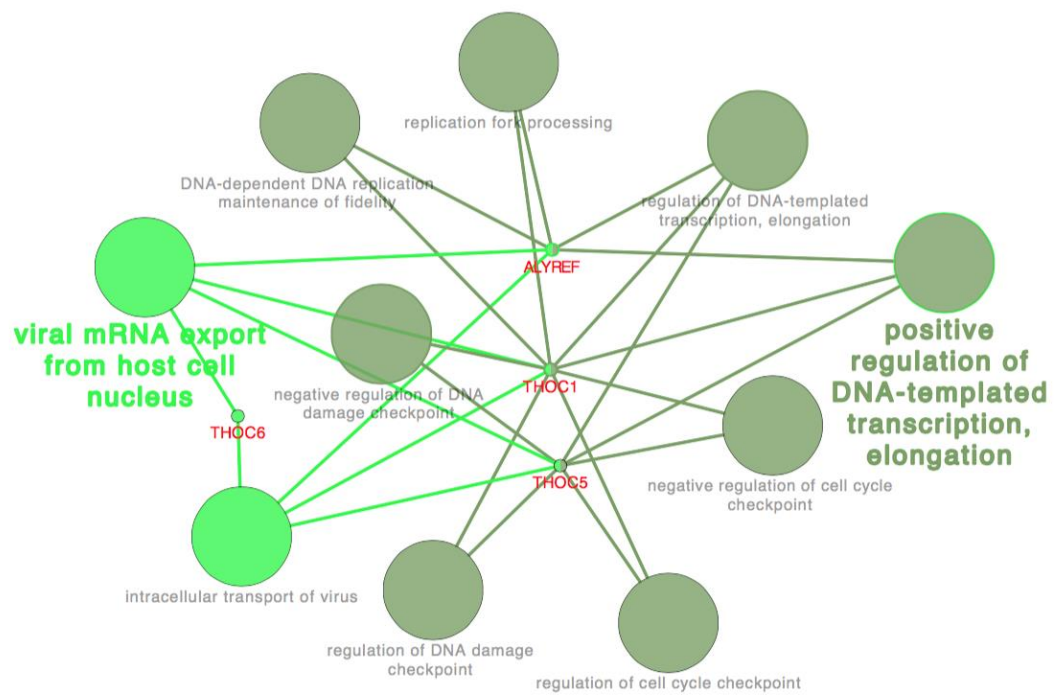


**Figure 6.4** The biological role of up-regulated genes visualised with ClueGO (kappa score:  $\geq 0.4$ ).

In the group of down-regulated proteins, the group leading terms involved regulatory pathways associated with translation initiation complex formation, translation, nuclear-transcribed mRNA catabolic processes, ribonucleoprotein complex assembly, regulation of mRNA stability, assembly of the 60S ribosome subunit and DNA damage recognition in global genome nucleotide excision repair (GG-NER) (Figure 6.5).

In the group of stable-regulated proteins, there were 20 group-leading pathways as shown in Figure 6.6. The roles of stable-regulated genes are in the pathways of mRNA processing, transcription, post-transcriptional processing and translation. However, there are also proteins involved in epigenetic modification, nucleosome assembly, non-coding RNA (ncRNA) metabolic processing, telomere maintenance and ribonucleoprotein complex assembly.

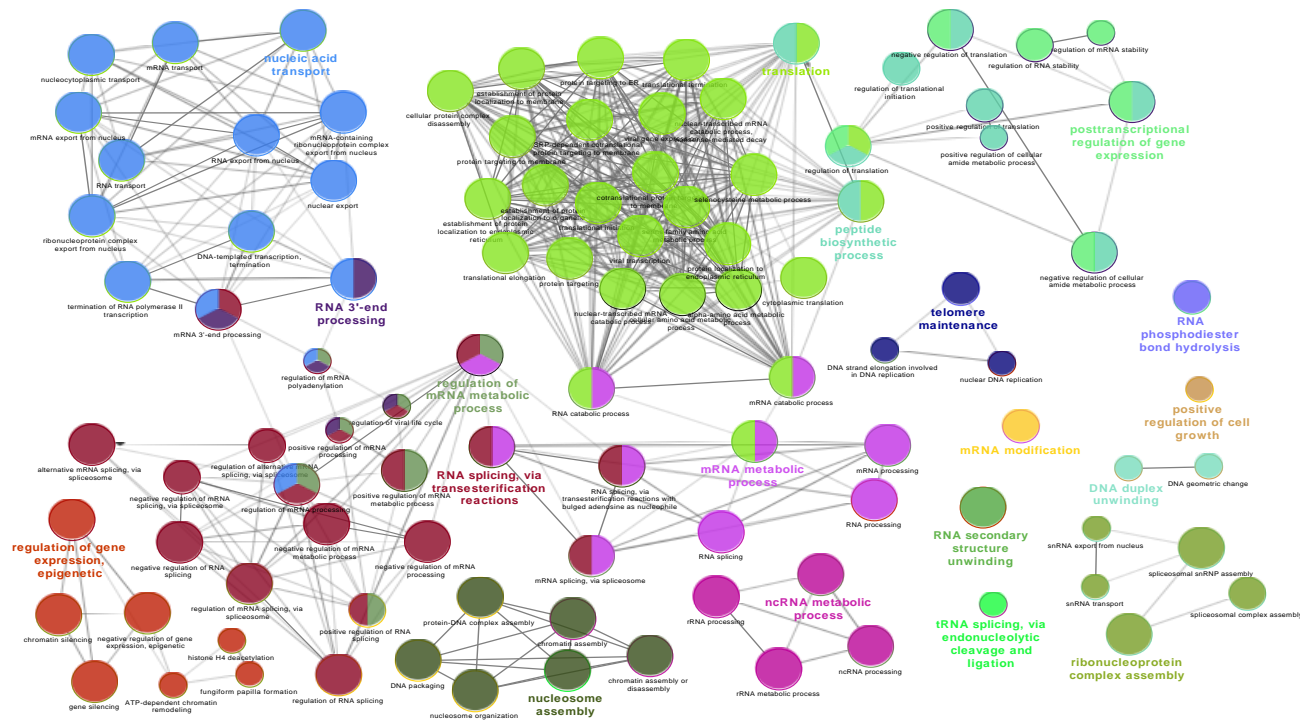


**Figure 6.5** The biological role of stable-regulated proteins visualised with ClueGO (kappa score:  $\geq 0.4$ )



### **6.2.5 Interactome analysis based literature reviews**

As previously mentioned, my study aimed to discover potential interacting proteins of SLBP which might improve the understanding of molecular pathway of histone mRNA decay, following imposition of replication stress. In order to accurately determine all of proteins in each category, all of proteins were reviewed together with keyword “DNA damage response (DDR)” by searching on PubMed database (Table 6.4).

**Table 6.4** Proteins involve in DDR found in this study

<b>Protein names</b>	<b>Pathways involved</b>	<b>References</b>
XRCC5, XRCC6, PARP1, DHX9, RCC2, HDAC1, HDAC2, NONO, PHRF1	NHEJ	Taccioli <i>et al.</i> , 1994 Walker <i>et al.</i> , 2001 Zhou <i>et al.</i> , 2010 Miller <i>et al.</i> , 2010 Krietsch <i>et al.</i> , 2012 Chang, <i>et al.</i> , 2015
RBM14	DNA-PK-dependent NHEJ pathway	Kai, 2016
hnRNPUL, SERBP1, CtIP PARP1, RBMX	HR	Polo <i>et al.</i> , 2012 Hong <i>et al.</i> , 2013 Ahn <i>et al.</i> , 2015 Adamson <i>et al.</i> , 2012
MYBBP1A, NAT10, GLTSCR2	p53	Kuroda <i>et al.</i> , 2011 Liu <i>et al.</i> , 2016 Lee <i>et al.</i> , 2012

### **6.2.6 Post-translational modification of SLBP detected by mass spectrometry**

In addition to undertaking a protein-protein interaction analysis, the availability of isotopically labelled Flag-tagged SLBP from mock as well as HU-treated cells enabled the analysis of changes in SLBP phosphorylation stoichiometry following this treatment. In this experiment the peptides containing sites previously observed at Thr62, Thr171 and Ser182 were not observed. However, in this analysis, two high-confidence sites (high-confidence identity, posterior error probability [PEP], < 0.01) were identified (shown in red in Figure 6.7) in addition to 3 other sites with medium PEP (shown in blue). Importantly all of these sites have been reported previously on the PhosphoSitePlus database ([www.phosphosite.org](http://www.phosphosite.org)) with a high number of records assigned using only MS, suggesting that these modification sites are commonly present on SLBP. Importantly the isotopic labelling data indicates that phosphorylation at Ser20 and Ser23 is significantly up-regulated in response to hydroxyurea treatment (Table 6.5). There was no change in stoichiometry at positions 61. However, phosphorylation at Ser110 and Ser115 was not shown the same changes at the different retention time.

These data indicate clearly that SLBP undergoes a significant increase in phosphorylation at residues 20 and 23, and probably 114 and 115, in response to replication stress.

```

      10          20          30          40          50          60          70
MACRPRSPPR HQSRCGDGAS PPSSPARWSLG RKRRADGRRW RPEDAEEAEH RGAERRPESEF TTPEGPKPRS

      80          90          100         110          120          130          140
RCSDWASAVE EDEMTRVNK EMARYKRKLL INDFGRERKS SSGSSDSKES MSTVPADFET DESVLMRRQK

      150         160          170          180          190          200          210
QINYGKNTIA YDRYIKEVPR HLRQPGIHPK TPNKFKKYSR RSWDQQIKLW KVALHFWDDP AEEGCDLQEI

      220         230          240          250          260          270
HPVDLESAES SSEPQTSSQD DFDVYSGTPT KVRHMDSQVE DEFDLEACLT EPLRDFSAMS

```

**Figure 6.7** SLBP sequence coverage with phosphorylation sites of Flag-tagged SLBP in mammalian expression system detected by SILAC based-LC-MS/MS.

**Table 6.5** Identification of SLBP phosphorylation and unphosphorylation sites in the presence of SILAC conditions (highlighted by red colours are phosphorylated residues).

Peptide position		MS/MS scan no.	Retention time	Position of Phosphorylation site	Peptide sequences	Intensity		
Start	End					L	M	H
15	26	5688	22.046	20 and 23	CDGDA <sup>S</sup> PP <sup>S</sup> PAR	N/A	N/A	754730
15	26	3263	13.328	20 or 23	CDGDA <sup>S</sup> PP <sup>S</sup> PAR	N/A	N/A	199030
56	69	2306	13.275	61	RPESFTTPEGPKPR	592390	33800000	28746000
56	69	1996	10.822	61	RPESFTTPEGPKPR (unphosphorylated)	8013500	383770000	502210000
109	137	6029	26.438	110	K <sup>S</sup> SSGSSDSKESMSTVPADFETDESVMIR	N/A	3561300	2755900
109	137	6921	58.214	110	K <sup>S</sup> SSGSSDSKESMSTVPADFETDESVMIR	N/A	6944900	9121900
109	137	21590	82.645	110	K <sup>S</sup> SSGSSDSKESMSTVPADFETDESVMIR	N/A	N/A	567590
110	137	7181	30.112	115	SSSGS <sup>S</sup> DSKESMSTVPADFETDESVMIR	N/A	1969400	2012100
110	137	8277	33.43	115	SSSGS <sup>S</sup> DSKESMSTVPADFETDESVMIR	N/A	N/A	1021200
110	137	21887	83.774	115	SSSGS <sup>S</sup> DSKESMSTVPADFETDESVMIR (unphosphorylated)	0	287500	259710

## **6.3 Discussion**

Quantitative mass spectrometry using stable isotope labeling of amino acids in cell culture (SILAC) is a powerful technique in order to study the protein interactomes. Changes in interactome composition as a function of different biological conditions could offer insights into biological states, complementing analyses of molecular mechanism of the protein of interest. Therefore, this approach was applied to investigate changes in SLBP-interacting proteins directly and indirectly under DNA damage and replication stress-induced histone mRNA decay. It was also hoped to discover new protein members of the SLBP interactomes which may help to understand this DDR pathway.

### **6.3.1 Intrinsic strengths and limitations of immuno-isolation-mass spectrometry (I-i-MS)**

Immuno-isolation (I-i) is a term using in this study in order to isolate Flag-tagged SLBP and SLBP-interacting proteins from whole cell lysates using ANTI-FLAG<sup>®</sup> M2 Affinity gel, to facilitate the isolation and analysis of SLBP, and in particular SLBP-protein interactions. However, I-i is a subset term of affinity-purification (AP). Compared to other methods used to define protein-protein interactions such as yeast two-hybrid, I-i coupled to MS has four major advantages. First, it can be

performed under near physiological conditions, in the relevant organism and cell type. Second, it does not affect post-translational modifications which are often important for the organization and/or activity of complexes. Third, it can be used to study dynamic changes in the composition of protein complexes in combination with SILAC. Finally, MS can detect every abundant protein present in the immuno-isolation (Gingras *et al.*, 2007).

The I-i approach coupled to MS does have limitations particularly regarding the issues of false positive and false negative identifications. False positives deal with the lack of specificity in the presence of contaminants proteins due to non-specific binding such as common contaminants (for examples, actin and tubulin) which are often present in immuno-isolated protein samples, in addition to a set of proteins that are known to interact with affinity matrices (such as Flag-antibody resins) (Gingras *et al.*, 2007 ; Dunham *et al.*, 2012).

In this study, the experimental design allowed me to distinguish between proteins associated with Flag-SLBP (i.e. in the presence of Dox) in the absence and presence of replication stress, and proteins associated with the matrix identified from cell lysates not expressing Flag-SLBP (in the absence of Dox). The use of quantitative proteomics using SILAC helps to distinguish true interactors from background

contaminants. In this work, high thresholds both for increased and decreased association were used, in order to identify proteins whose abundance change significantly in response to replication stress. Protein identifications were also only included if they were hits in at least two of three independent biological replicates.

Unfortunately, the correlation coefficient of SILAC ratios was low in replicate 1 compared with replicates 2 and 3. However, the data arising from replicate 1 was not eliminated as to do so would impact the statistical confidence of results. Unfortunately, given the time constraints, there was not enough time to repeat this replicate again. That multiple biological replicates were undertaken nonetheless increases confidence that identified proteins are true interactors as they were observed twice or more.

This study is the first to report SLBP-interacting proteins under normal and replication stress conditions using SILAC-based MS. There is a paucity of previously documented SLBP-interacting proteins under replication stress conditions with the possible exception of UPF1 (Kaygun and Marzluff, 2005a ; Kaygun and Marzluff, 2005b). However, the validity of this experiment is confirmed by the identification of 67% of known protein SLBP interactions identified in six databases.

In the case of false negatives, there are four factors likely contribute to the lack of detection of known interactors. Firstly, the proteins might not have interacted under the tested conditions. Secondly, the nature and N-terminal location of the Flag-tag might have disrupted interactions when this form of the protein was expressed in the model cell line. Thirdly, the conditions of the I-i may have been too harsh to preserve the interaction. Lastly, a potential problem resides with the relative abundances of a tagged bait and the amount of prey in the cell sample (Gingras *et al.*, 2007 ; Bonetta, 2010). The detection of low-abundance interactors of SLBP may be challenging given the nature of SLBP itself. Native SLBP is an intrinsically disordered protein, lacking a stable three-dimensional structure (Thapar *et al.*, 2004a ; Thapar *et al.*, 2004b ; Zhang *et al.*, 2012). It is conceivable that SLBP structural flexibility may result in loss of some interactors that require a specific conformation for stable interaction (Thapar, 2014). Thus, using *in vivo* cross-linking combined with I-i is an option in the future to enrich SLBP-interacting proteins and minimise false negatives in this type of experiment.

There are several points that should be kept in mind when interpreting the SLBP-interacting proteins in all 3 categories. The presented results do not distinguish between direct and indirect interactions, and thus identified proteins might interact indirectly with SLBP, via one or more bridging molecules. In the work presented here, ribonuclease (RNase) was deliberately not added in the I-i experiment. This was to ensure that a comprehensive list of SLBP associated proteins were identified that would include ribonucleoprotein components. It is conceivable that RNAase treatment would reduce the complexity of the SLBP interactome enabling analysis solely of proteins that interact directly with SLBP and possibly eliminate additional false positive contaminants. This was not done for the reasons given above. Finally, it is conceivable that some protein-protein interactions detected in a cell lysate may occur as a consequence of artifact arising from the generation of the lysate, and may not actually occur *in vivo* if the relevant proteins never co-localize within the cell. It follows that the validation of SLBP-interacting proteins should be in the next step for comprehensive insight into the biological functions of this protein both during normal and replication stress induced conditions.

### 6.3.2 Overview GO analysis

Using all three independent biological replicates, the SILAC approach used here allowed the identification of 997 proteins in which isotopic ratios corresponding M/L, H/L and H/M could be quantified. By plotting the distribution of the  $\log_2$  isotopic ratios on a scatter-plot graph, this enabled the identification of proteins that associate non-specifically with the matrix ( $\log_2\text{M/L} < 0.5$ ; 121 proteins), together with proteins whose association with SLBP increases ( $\log_2\text{H/M} > 0.5$ ; 4 proteins), decreases ( $\log_2\text{H/M} < 0.5$ ; 82 proteins) or stays largely unchanged ( $0.5 > \log_2\text{H/M} > -0.5$ ); 213 proteins).

To date, no studies of the SLBP-interactome in the presence of HU-induced histone mRNA decay has been presented. Most studies have been focused on identification of RNA binding protein (RBP) targets, RNA-protein interaction by using RNA immunoprecipitation (RIP), UV crosslinking and immunoprecipitation (CLIP), enhanced CLIP (eCLIP), photoactivatable-ribonucleoside-enhanced CLIP (PAR-CLIP) and individual-nucleotide-resolution CLIP (iCLIP) (Ule *et al.*, 2005 ; Konig *et al.*, 2010 ; Ascano *et al.*, 2011 ; van Nostrand *et al.*, 2016). However, this substantial information will be useful a framework for SLBP- or other RBP-protein interaction database in the future.

With the data provided here when DNA damage and replication stress response, protein alters between different cell compartments especially nucleolar proteins in Cajal bodies (CBs) and nucleolus. In general, both Cajal bodies (CBs) and the nucleolus are involved in the production of non-poly(A)-tailed RNAs, including histone mRNAs, small nuclear RNAs (snRNAs), and small nucleolar ribonucleoproteins (snoRNAs) (Boulon *et al.*, 2007). Interestingly, most of the SLBP interacting proteins described here are associated with either CBs and nucleoli in the cellular response to replication stress.

#### **6.3.2.1. Up-regulated proteins**

Export of histone mRNA into the cytoplasm requires the transcription export complex (TREX) in addition to the export receptor TAP (Erkman *et al.*, 2005 ; Lei *et al.*, 2011). TREX complex comprised of the components listed in Table 6.6 is an evolutionary conserved multi-protein complex that plays a major role in the functional coupling of different steps during mRNA biogenesis, including mRNA transcription, processing, mRNP maturation and nuclear export (Katahira, 2012 ; Heath *et al.*, 2016). The RNA export factors, including the TREX complex (THOC1, THOC2, THOC3, ALYREF, THOC5, THOC6, THOC7, spliceosome RNA helicase DDX39B (UAP56), CHTOP,

POLDIP3, ZC3H11A and UAP56-interacting factor (UIF) bind the cap-binding protein (CBC) complex comprising CBP80/20, also referred to as nuclear cap-binding protein (NCBP) 1 and 2) (Ohno *et al.*, 2000 ; Cheng *et al.*, 2006) as part of the assembly of an export competent mRNP. CBP80/20 (or NCBP1/2) rather than EIF4E are believed to be bound to histone mRNA when histone mRNA degradation is initiated (Choe *et al.*, 2013).

**Table 6.6** Composition of the TREX complex

<b>Protein name</b>	<b>Role</b>
<b>THO subunits</b>	
THOC1	Core subunit of THO subcomplex
THOC2	Core subunit of THO subcomplex
THOC3	Core subunit of THO subcomplex
THOC5	Export co-adaptor
THOC6	Metazoa-specific subunit
THOC7	Metazoa-specific subunit
<b>TREX subunits</b>	
UAP56 (DDX39B)	DEAD-type box helicase, splicing factor
DDX39A	Putative EJC-associated protein
ALYREF	Export adaptor, EJC-associated protein
UIF	Export adaptor, EJC-associated protein
LUZP4	Export adaptor, EJC-associated protein
CHTOP	Export adaptor, EJC-associated protein
CIP29 (SARNP)	ATP-dependent interaction with UAP56
POLDIP3	ATP-dependent interaction with UAP56
ZC3H11A	ATP-dependent interaction with UAP56

<b>TREX-associated proteins</b>	
NXF1 (TAP)	RNA export receptor
NXT1	Required for NXF1 stabilisation and mRNA export
ZC3H18	NEXT complex component
SRRT	CBC effector in RNA 3' processing
C17orf85 (NCBP3)	Involved in RNA export upon viral infection
NCBP1 (CBP80)	Transcription elongation, RNA export and stability

Why might there be increased association between components of the TREX complex and SLBP under conditions of replication stress? One possibility is that the increased association reflects an additional step in the mechanism of replication stress induced histone mRNA decay that up-regulates the steady state levels of histone mRNPs for export to induce rapid degradation of the histone mRNA which occurs in the cytoplasm. Thus the increased association of these proteins with SLBP following replication stress may reflect the notion that the intra S-phase checkpoint targets the process of RNP assembly and the export of mature RNAs from the nucleus, in addition to affecting cytoplasmic SLBP associated proteins.

However, a significant number of proteins involved in this pathway (Table 6.7) such as THOC2, chromatin target of PRMT1 protein (CHTOP), polymerase delta-interacting protein3 (POLDIP3) and Zinc finger CCCH domain-containing protein 11A (ZC3H11A) were not found to increase in association with SLBP following HU treatment.

**Table 6.7** The Log<sub>2</sub>H/M ratios of composition of the TREX complex found in this study

<b>Protein name</b>	<b>Log<sub>2</sub>H/M rep.1</b>	<b>Log<sub>2</sub>H/M rep.2</b>	<b>Log<sub>2</sub>H/M rep.3</b>
<b>Up-regulated proteins</b>			
THOC1	0.49	0.57	0.61
ALYREF	0.03	0.57	0.75
THOC5	0.69	0.97	0.72
THOC6	0.58	0.4	0.92
<b>Stable-regulated protein</b>			
THOC2	0.51	0.48	0.15
CHTOP	0.05	0.18	0.19
POLDIP3	-0.29	0.18	0.15
ZC3H11A	0.22	-0.19	-0.23

The relative lack of enrichment of these components may be due to technical limitations associated with selected stability of some components of the TREX complex. However, it is also entirely possible that the subset of the TREX complex found associated with SLBP represents a novel replication stress-induced sub-complex which facilitates histone mRNA decay. For example, in yeast, deletion of specific THO/TREX components increases genome instability via R-loop formation during transcription, resulting in loss of genomic integrity (Huertas and Aguilera, 2003 ; Bermejo *et al.*, 2012 ; Montecucco and Biamonti, 2013).

While the data in this study support the notion that THOC5 (in addition to other TREX components) associates with SLBP under conditions of replication stress, its ability to bind to target mRNAs in response to DNA damage mediated is reportedly reduced following phosphorylation by the checkpoint kinase, ATM (Ramachandran *et al.*, 2011). Disruption of THOC1 function has also been implicated in loss of genomic integrity. Mutants in THOC1 accumulate DNA damage as measured by increases in the level of phosphorylated histone H2AX (Li *et al.*, 2007). Thus further work will be required to establish the precise nature and composition of this complex as well as its functional implications in the cellular response to replication stress.

It is becoming increasingly evident that rapid responses to physiological stress conditions involve the synthesis, processing and export of synthesized mRNA (Holcik and Sonenberg, 2005). Interestingly, several previous studies have identified RNA binding proteins involved in different steps of mRNP assembly and maturation, as targets of the DNA damage or replication checkpoint kinases ATM (ataxia telangiectasia mutated) and ATR (ATM-Rad3 related). (Matsuoka *et al.*, 2007; Paulsen *et al.*, 2009; Hurov *et al.*, 2010 ; Montecucco *et al.*, 2013).

In particular, a large-scale proteomic study assessing protein expression changes in the DNA damage response (DDR) revealed enrichment in RNA processing proteins, indicating that RNA metabolism and DNA repair pathways functionally intersect. In addition genetic screens have identified a range of RNA processing factors including RBPs in the DNA damage response (Paulsen *et al.*, 2009 ; Lackner *et al.*, 2011 ; Kai, 2016).

Together these data, in addition to the data presented here, suggest that there is a complex interplay between the cellular response to replication stress, and the machinery involved in progress from transcription to translation. However, the role played by mRNA processing factors in the cellular response to endogenous and exogenous

sources of DNA damage is still largely unexplored and will require considerable additional dissection.

### **6.3.2.2 Stable and down-regulated proteins**

Under normal circumstances, SLBP associated with the histone stem loop would be expected to interact with the processes of histone gene expression, mRNA maturation, RNP assembly, nuclear export, translation and mRNA turnover. Replication stress induced histone mRNA decay is dependent both on the presence of SLBP and on ongoing translation. Consequently it is unsurprising that, in the experimental set up utilized in this screen proteins associated with histone mRNP assembly and biogenesis, as well as ribosomal components and the products of histone translation were abundant components associated with I-i of SLBP.

Following pre-mRNA processing, RNP assembly and nuclear export, translational initiation involves the engagement of capped mRNA with components of the 40S subunit of the ribosome before the recruitment of the 60S component and assembly of a functional ribosome. Categories of proteins that were specifically down-regulated in response to replication stress included 8 protein components of the 60S ribosomal complex (Figure 6.8) as well as 12 translation initiation

factors (Figure 6.9). In contrast, none of the 11 heterogeneous ribonucleoproteins (hnRNPs) identified were down-regulated (Figure 6.10), nor were any of the 11 identified components of the 40S ribosomal subunit (Figure 6.11). These data are consistent with the initiation of a cellular response to selectively down-regulate histone protein production in response to replication stress via a suppression of the ribosome assembly pathway, at the point of recruitment of the 60S subunit. Despite these changes, surprisingly, there was no observable change in the abundance of any of the 18 histone protein variants (Figure 6.12) associated with SLBP following 20 min of replication stress. While this time period was chosen, as it is approximately the length of time required for decay of ~50% of replication dependent histone mRNA following replication stress, it is presumably insufficient to effect a significant change in histone protein production rate.

**60 S ribosomal proteins  
(Ribosomal large subunit biogenesis)**

RPL11 (-)  
RPL3(d)  
RPL4(d)  
RPL8 (d)  
RPL10A(d)  
RPL23A(d)  
RPL27(d)  
RPL30(d)  
RPL36(d)

**Figure 6.8** The component of 60S ribosomal proteins in response to replication stress (d stands for down-regulation and – stands for stable regulation)

**Eukaryotic translation initiation factor**

EIF2A (d)  
EIF2B (d)  
EIF2G (d)  
EIF3E (d)  
EIF3H (d)  
EIF4A1 (d)  
EIF4A2 (d)  
EIF4F (d)  
EIF4GI (d)  
EIF4G1 (d)  
EIF4G2 (d)  
EIF5B (d)  
EIF4E (-)  
EIF4A1 (-)  
EIF4A3 (-)

**Figure 6.9** The component of translation initiation factor in response to replication stress (d stands for down-regulation and – stands for stable regulation)

**Heterogeneous nuclear ribonucleoproteins**

HNRNPA0 (-)  
HNRNPA1 (-)  
HNRNPA1L2 (-)  
HNRNPA3 (-)  
HNRNPAB (-)  
HNRNPF (-)  
HNRNPK (-)  
HNRNPL (-)  
HNRNPM (-)  
HNRNPR (-)  
HNRNPUL2 (-)

**Figure 6.10** The component of heterogeneous nuclear ribonucleoprotein (hnRNPs) in response to replication stress (– stands for stable regulation)

**40 S ribosomal proteins  
(Ribosomal large subunit biogenesis)**

RPS2 (-)  
RPS3 (-)  
RPS3A(-)  
RPS6 (-)  
RPS9 (-)  
RPS15A(-)  
RPS16 (-)  
RPS18 (-)  
RPS20 (-)  
RPS25 (-)  
FAU (-)

**Figure 6.11** The component of 40S ribosomal proteins in response to replication stress (– stands for stable regulation)

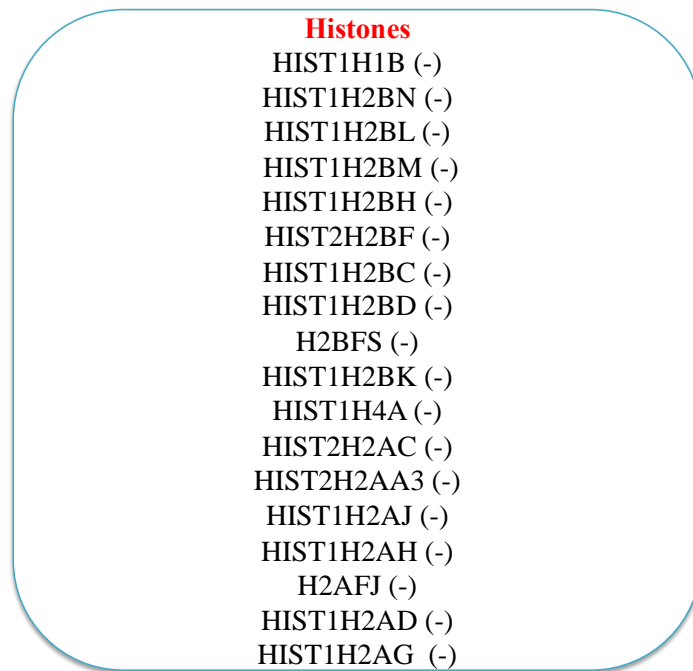


**Figure 6.12** The component of histone protein variants in response to replication stress (– stands for stable regulation)

### **6.3.3 The role of known mRNA decay factors in histone mRNA degradation**

Another major category of proteins whose SLBP-associated abundance decreased following HU treatment was components of the exosome, the multi-protein intracellular complex capable of degrading RNA. Components EXOSC2, EXOSC4, EXOSC7 and MTR3 (Januszyk and Lima, 2014) all of which are members of the cytoplasmic exosomal complex and have 3'-5' exoribonuclease activity, were significantly reduced. These data are consistent with the notion that that replication stress induces significant cytoplasmic exosomal degradation of histone mRNA within 20 min of HU exposure, resulting in a decreased abundance of the exosomal components. As these data were obtained via an SLBP immuno-isolation approach, they are not consistent with models that propose that SLBP dissociation is required for histone mRNA decay. Although significant levels of the nuclear 5'-3' exonuclease XRN2 was also detected in SLBP isolates, there was no significance change in its levels under these conditions. XRN2 is the conserved homolog of XRN1 that is recruited to facilitate pre-mRNA 3'-processing and terminates RNA polymerase II transcription by degrading the downstream RNA in nucleus (Kaneko *et al.*, 2007 ; Brannan *et al.*, 2012). However it also plays a role in mRNA decay (Brannan *et al.*,

2012). These data may imply that it is involved in normal pre-mRNA processing, and/or it plays a limited role in replication stress induced mRNA decay, although given that it is a processive exonuclease, it is also conceivable that it retains the capability to interact indirectly with SLBP via its cognate histone mRNA, while the process of degradation is underway.

CBP80/20 are the components of the cap-binding complex (CBC) that binds to 5'cap 7-methylguanosine (7mG) and recruits the enzymes and cofactors to the transcript which mediate further processing, export and translation (Gonatopoulos-pournatzis and Cowling, 2014). Choe *et al* (2012) have reported that histone mRNA may be found associated either with the cap binding proteins CBP80/20 (also known as NCBP1/2) or eukaryotic translation initiation factor eIF4E, but that rapid degradation of histone mRNA following inhibition of DNA replication preferentially occurs on CBP80/20 associated histone mRNA. Although both CBP80, and CBP20, in addition to eIF4E were detected in this experiment, no significant change in either cap binding configurations was observed. These data suggest that the difference in efficiency of histone mRNA decay occurs independently of the interaction between CBC components and SLBP, despite the known role of decapping (via Dcp1/Dcp2) in the process of histone mRNA decay (Coller *et al.*,

2001 ; Kaygun and Marzluff, 2005b). As SLBP was identified in a yeast two hybrid screen as a CBP80/20-dependent translation (CT) initiation factor interacting protein, this result may not be unexpected.

The interactomic analysis also identified additional interaction partners of the CBC - arsenic-resistance protein 2 (ARS2) and zinc finger CCCH domain-containing protein 18 (ZC3H18) - which have been linked to the role of the nuclear RNA exosome in transcription termination (Andersen *et al.*, 2013). The CBC associates with ARS2 to form CBC-ARS2 (CBCA) for transcription termination and together with nuclear exosome targeting complex (NEXT) which contains superkiller viralicidic activity 2-like 2 (SK2L2 or MTR4), the putative RNA binding protein RBM7, and the Zn-knuckle protein ZCCHC8, forms CBC-NEXT (CBCN) for exosome targeting (Lubas *et al.*, 2011). Both CBCA and CBCN interact with ZC3H18 to form NEXT complex aiding in the exosomal degradation of promoter-upstream transcripts (PROMPTS) (Preker *et al.*, 2008).

Additional proteins down-regulated in response to DNA damage and replication stress induced histone mRNA decay were DEAH-Box Helicase 9 (DHX9) which is involved in resolving intra-molecular triplex nucleic acid structures thus preventing genomic instability (Jain *et al.*, 2013) and Y-Box Binding Protein (YBX3) which has a role in

mRNA stability (Eliseeva *et al.*, 2011). In addition to helicases discussed above, a full list of helicases showing reduced association, in addition to those which did not change is shown in Figure 6.13. The significance of these changes is currently unknown.

<b>DExH/D box RNA helicase</b>	
DDX1 (-)	DDX21 (d)
DDX17 (-)	DDX47 (d)
DDX3X (-)	DDX6 (d)
DDX3Y (-)	DHX9 (d)
DDX42 (-)	DHX30 (d)
DDX5 (-)	DHX36 (d)
DDX50 (-)	
DHX15 (-)	

**Figure 6.13** The component of helicases in response to replication stress (d stands for down-regulation and – stands for stable regulation)

#### **6.3.4 UPF1 associates with SLBP following imposition of replication stress**

Kaygun and Marzluff (2005a) were the first to suggest that Upf1, the core RNA helicase involved in nonsense mediated decay also plays a role in replication stress induced histone mRNA decay, and demonstrated a modest increase in the association between SLBP and UPF1 following imposition of replication stress. Consequently there are two working models proposed to explain how UPF1 mediates histone mRNA decay.

(1). Upf1 binds to the decapping complex (Dcp1/Dcp2) and the Xrn1 5'-3' exoribonuclease, which are involved in degrading mRNA from its 5' end (Kaygun and Marzluff, 2005b).

(2). The recruitment of Upf1 stimulates the specific recruitment of the terminal uridylyl transferases (TUTases) which oligouridylate to 3' mRNA end. The U6 snRNA-associated Sm-like protein (Lsm 1-7) complex binds this tails and recruits decapping complex (Dcp1/Dcp2) to remove the 5' cap of the mRNA (Coller *et al.*, 2001). Then mRNA is degraded from 5'-3' by the Xrn1 exoribonuclease or degraded from 3' - 5' exonuclease by exosome components (Mitchell *et al.*, 1997).

With the exception of components of the exosome, almost none of these proteins were identified in this interactomic experiment. However, a notable exception to this was the identification of UPF1. Somewhat surprisingly, a significant decrease in abundance was observed in response to replication stress, in direct contrast to results reported by Kaygun and Marzluff (2005a), who used cells over-expressing both components to detect an increased level of co-immunoprecipiating complex. Although Kaygun and Marzluff (2005a), reported that other components of the nonsense mediated decay pathway were not involved in replication stress induced histone mRNA decay, the analysis undertaken here also identified the presence of components UPF2 and UPF3 associated with SLBP, although interestingly, the relative levels did not decrease in response to replication stress. Taken together, these data confirm that SLBP does interact with UPF1, and possibly other components of the NMD machinery, although precise details of mechanism remain to be elucidated.

### **6.3.5 SLBP-interacting proteins involved in DDR**

Somewhat surprisingly, the SLBP interactome also contained a large number of proteins, which, although their levels did not change in response to replication stress, are nonetheless well-established components of replication pathways, or DNA damage response components associated with replication fork stalling and its consequences.

DNA replication components identified include the replicative helicase subunit MCM5, in addition to the replication factor C (RFC) subunits 1,3, 4 and 5. MCM5 is part of the MCM2-7 complex which acts as the major DNA replicative helicase during replication (Bochman and Schwacha, 2009). RFC1, RFC2, RFC3, RFC4 and RFC5 form a heteropentamer complex that interacts with proliferating cell nuclear antigen (PCNA) and enables the binding of its N-terminal DNA-binding domain to duplex DNA. This mechanism is essential in the recognition of non-primer template DNA structures during replication and/or repair (Mossi *et al.*, 1997).

One of the key consequences of replication stress, whether it occurs endogenously as a result of the competition between replication and transcription, the presence of fragile sites, or as a result of exogenous genotoxic stress, involves replication fork arrest, stalling, and

then distinct restart pathways that depend on the extent of DNA damage arising from these events. Such responses include both homologous recombination induced replication restart, as well as both HR and NHEJ associated mechanisms to address double strand breaks repair arising from replication fork stalling (Shrivastav *et al.*, 2008). Most of these responses are known or are believed to respond to checkpoint signalling pathways activated in response to replication stress.

SLBP immuno-isolates were enriched in X-ray repair cross-complementing protein 5 (XRCC5/ Ku70) and X-ray repair cross-complementing protein 6 (XRCC6/Ku80), two proteins involved in DNA double-strand break (DSB) repair by non-homologous end joining (NHEJ) (Taccioli *et al.*, 1994 ; Walker *et al.*, 2001) Importantly, both Ku70 and Ku80 are known to activate the PIKK DNA activated protein kinase (DNA-PK) (Lovejoy and Cortez, 2009 ; Fell and Schild-Poulter, 2015) which has been implicated in the mechanism by which replication stress induced histone mRNA decay is activated (Muller *et al.*, 2007). Also enriched were a number of proteins previously identified as partners of Ku 70/80, including: the poly(ADP-ribose) polymerase I (PARP1), ATP-dependent RNA helicase 9 (DHX9) and protein RCC2 (RCC2) (Zhou *et al.*, 2010). PARP1 is one of the first proteins to be recruited and activated through its binding to the free DNA ends after the

generation of DSBs. Upon activation, PARP1 recruits DNA and RNA binding proteins such as non-POU domain-containing octamer-binding protein (NONO). NONO is known to stimulate NHEJ and represses homologous recombination (HR) (Krietsch *et al.*, 2012) and participates in mediating the DDR including the activation of the PIKK ATR. ATR is also implicated in the mechanism by which replication stress induced histone mRNA decay is activated (Muller *et al.*, 2007; Kaygun and Marzluff, 2005a).

Additional enriched proteins included RNA-binding motif protein, X chromosome (RBMX) binds to PARP1 to promote HR (Adamson *et al.*, 2012). RNA-binding protein 14 (RBM14) interacts with XRCC6 in controlling the DNA-PK-dependent NHEJ pathway (Kai, 2016). Moreover, histone modifying enzymes such as histone deacetylase 1 and 2 (HDAC1 and HDAC2) (Miller *et al.*, 2010) and PHD and RING finger domain-containing protein 1 (PHRF1) (Chang, *et al.*, 2015) that function in promoting DSB repair by NHEJ were also enriched. Interestingly, HDAC1 is directly involved in the recruitment of the Rad9-HUS1-Rad1 DNA binding clamp which in turn directly activates the ATR PIKK (Cai *et al.*, 2000).

Fragile X mental retardation protein 1 (FMR1 or FMRP) was also enriched in SLBP immuno-isolates. FMR1 is recruited to chromatin in

response to replication stress following the phosphorylation of the histone, H2AX mediated by ATR kinase (Alpatov *et al.*, 2014 ; Zhang *et al.*, 2014). FMR1 forms heterodimers with FXR1 (autosomal homolog FXR1 fragile X related 1) and associates with nuclear fragile X mental retardation-interacting protein 2 (NUFIP2) which was also enriched here. This complex is known to engage directly with the micro RNAs (miRNA) induced silencing complex (RISC) which can lead to the degradation or translational regulation of the respective RNA molecule (Gessert *et al.*, 2010). It is possible that DNA damage and replication arrest-induced histone mRNA decay might require FMR1 through chromatin association connected to DDR regulating genome stability. However, the detailed molecular mechanism of FMR-dependent DDR in response to replication stress still needs further investigation.

All of the proteins identified in this segment have been previously linked to DNA damage signalling consistent with a block in DNA synthesis, stalled replication fork and collapse into DNA double-strand break (DSBs). Taken together, the extent and range of SLBP associated proteins that have functions in replication and replication stress, suggest that histone mRNA surveillance and its regulation may be closely associated with these processes in the nuclear compartment.

### **6.3.6 SLBP phosphorylation and protein kinases immuno-isolated with SLBP**

SLBP function is known to be regulated by phosphorylation and a number of phosphorylation sites have been reported and characterised (Koseoglu, M.M. 2007 ; Zhang *et al.*, 2014). Previously, phosphorylation at Ser20 and Ser23 has been implicated as a Pin1 mediated phosphodegron that controls SLBP polyubiquitination and subsequently proteasomal degradation at the end of S-phase, although other phosphorylation sites in the C-terminus of the protein were also implicated in the interaction with Pin1 (Krishnan *et al.*, 2012). Importantly, the identification of those phosphide sites in that study were not performed in synchronised cells, nor were stoichiometries determined. Thus, the significance of that data is not clear. The data obtained here clearly show that phosphorylation at these sites only become significantly elevated following imposition of replication stress. As it is known that SLBP is not degraded during replication stress, it is very unlikely that phosphorylation at these sites do act as a phosphodegron as reported (Krishnan *et al.*, 2012). At least two hypotheses can be proposed. The first is that replication stress induced phosphorylation at residues 20 and 23 (in addition to 114 and 115) results in Pin1 mediated disassociation of SLBP from histone mRNA,

allowing for the rapid destruction of the latter. The alternative is that replication stress brings about the dissociation of Pin1 from the N-terminal region of SLBP enabling access to the sites by an unidentified protein kinase. Irrespective of the details of the mechanism, it will be of great importance to establish the identity of the protein kinase responsible for phosphorylation of Ser20 and Ser23.

Because of the catalytic nature of protein kinases and thus their transient interaction with multiple substrates, it would not necessarily be expected that relevant kinases might be detected in immuno-isolation interactomic experiments such as that undertaken here. Nonetheless SLBP I-i was enriched for two isoforms of casein kinase (CK2) as well as casein kinase 1. In addition both Glycogen synthase kinase-3 (GSK3) (Cohen and Frame, 2001) and Aurora A kinase (Gavriilidis *et al.*, 2015) were also found. Casein kinase 2 is functionally implicated in the destruction of SLBP at the end of S-phase, as it is responsible for phosphorylation of Thr60, after a priming phosphorylation at Thr61 by Cyclin A/Cdk1. Mutations in these residues result in a failure to bring about efficient degradation of SLBP at the end of S phase.

Interestingly, Aurora A kinase was also identified. The principle known function of Aurora A is related to the control of mitotic progression, including the coordination of spindle assembly, regulation of spindle assembly checkpoint, and control of cytokinesis (Ducat and Zheng, 2004). To date, no role for Aurora A has been found during interphase. For this reason, despite the fact that bio-informatics analysis suggested that it was a likely possible kinase with the capability of phosphorylating Ser182, this experiment was not undertaken. Given the data reported here, future experiments should be undertaken to test this possibility.

The significance of the presence of GSK3 associated with SLBP is unclear at present. However, it is of note that this kinase is required for the destruction of the S phase cyclin E via the ubiquitin pathway (Duronio and Xiong, 2013). Its role, if any in the mechanisms regulating SLBP homeostasis remain to be determined.

### 6.3.7 A potential role for C17orf85 in histone mRNA homeostasis

In response to DNA damage and replication arrest, histone mRNA decay is initiated to prevent the production of excess of histone proteins (Muller *et al.*, 2007). Part of the mechanism by which this occurs appears to involve an interaction between the nonsense mediated decay component UPF1 and SLBP (Kaygun and Marzluff, 2005;Muller *et al.*, 2007). In addition, the PIKK checkpoint kinases ATR and DNA-PK are also implicated in this mechanism as inhibition of both results in inefficient histone mRNA decay. Because UPF1 is rich in serine/threonine-glutamine clusters (S/TQ domain) (Fiolini *et al.*, 2012), which are the preferred substrate motifs for this family of protein kinases, and which appear to be required for its RNA decay function, hyperphosphorylation of UPF1 is suspected of being one mechanism by which the checkpoint signaling pathway engages with the histone decay machinery.

However recently, a novel mRNA cap binding protein (previously referred to as C17orf85 but renamed nuclear cap-binding protein subunit 3 (NCBP3)) has been identified and shown to interact with CBP 80/20 (Gebhardt *et al.*, 2015). Interestingly, NCBP3 was found to be associated with SLBP in addition to CBP80/20. Intriguingly, NCBP3 has been shown to be an *in vivo* substrate for the

checkpoint kinase Chk1 that acts downstream of ATR (Blasius *et al.*, 2011). Taken together these data suggest that a multi-protein complex comprising SLBP, CBP80/20 and BCBP2 is a target for checkpoint phosphorylation. The functional consequences of Chk1 phosphorylation on this complex may provide new insights in to the mechanism of histone mRNA decay.

In summary, Immuno-isolation mass spectrometry-coupled SILAC approach enabled me to extend novel knowledge on the interactome of SLBP upon DNA damage and replication arrest-induced histone mRNA decay by providing a global view of connection network of RNA metabolism and DNA repair. However, mechanistic models for building effective covering all the functions of SLBP will be a long and arduous process.

In light of these findings as a whole, it is clear that SLBP is a key part to modulate histone mRNA processing through a direct interaction with stem-loop and some proteins as mentioned above, and also through an indirect association along with other RBPs impact on many steps of gene expression such as nuclear export complexes. Moreover, in agreement with previous findings, my study confirms that RBPs coordinate the functional regulation with a diverse set of proteins of RNA molecule, including SLBP (Anko and Neugebauer, 2012).

Moreover, the participation of DNA repair proteins and RNA binding proteins in complexes are dynamically modulated in response to DNA damage by activating DNA repair pathways. This study is the first report that novel CHK1 substrate ‘C17orf85’ activates ATR in response to DNA damage and replication arrest-induced histone mRNA decay. However, it needs to be confirmed by further experiments. Taken together, these data provide the groundwork for a system-wide modeling of the effects of DNA damage and replication arrest-induced histone mRNA decay on other biological processes.

## 6.4 References

- Adamson, B., Smogorzewska, A., Sigoillot, F.D., King, R.W. and Elledge, S.J. 2012. A genome-wide homologous recombination screen identifies the RNA-binding protein RBMX as a component of the DNA damage response. *Nat Cell Biol.* 14(3): 318–328.
- Ahn1, J-W, Kim, S. Na, W. Baek, S-J, Kim, J-H, Min, K, Yeom, J. Kwak, H., Jeong, S., Lee, C., Kim, S-Y and Choi, C.Y. 2015. SERBP1 affects homologous recombination-mediated DNA repair by regulation of CtIP translation during S phase. *Nucleic Acids Res.* 43(13): 6321-6333.
- Alpatov, R., Lesch, B.J., Nakamoto-Kinoshita, M., Blanco, A., Chen, S. , Stutzer, A., Armache, K.J., Simon, M.D., Xu, C., Ali, M., Murn, J., Priscic, S. Kutateladze, T.G., Vakoc, C.R., Min, J., Kingston, R.E. Fischle, W., Warren, S.T., Page, D.C. and Shi, Y. 2014. A Chromatin-Dependent Role of the Fragile X Mental Retardation Protein FMRP in the DNA Damage Response. *Cell.* 157: 869-888.
- Andersen, J.S., Lam, Y.W., Leung, A.K.L., Ong, S., Lyon, C.E., Lamond, A.I. and Mann, M. 2005. Nucleolar proteome dynamics. *Nature* 433: 77-83.

- Andersen, P.R., Domanski, M., Kristiansen, M.S., Storrvall, H., Ntini, E., Verheggen, C., Schein, A., Bunkenborg, J., Poser, I., Hallais, M., Sandberg, R., Hyman, A., LaCava, J., Rout, M.P., Andersen, J.S., Bertrand, E. and Jensen, T.H. 2013. The human cap-binding complex is functionally connected to the nuclear RNA exosome. *Nat Struct Mol Biol.* 20(12): 1367-1376.
- Änkö, M.I. and Neugebauer, K.M. 2012. RNA–protein interactions in vivo: global gets specific. *Trends Biochem Sci.* 37: 255–262.
- Ascano, M., Hafner, M., Cekan, P., Gerstberger, S. and Tuschl, T. 2012. Identification of RNA-protein interaction networks using PAR-CLIP. *Wiley Interdiscip Rev RNA.* 3(2):159-177.
- Ashburner, M., Ball, C.A., Blake, J.A., Botstein, D., Butler, H., Cherry, J.M., Davis, A.P., Dolinski, K., Dwight, S.S., Eppig, J.T., Harris, M.A., Hill, D.P., Issel-Tarver, L., Kasarskis, A., Lewis, S., Matese, J.C., Richardson, J.E., Ringwald, M., Rubin, G.M. and Sherlock, G. 2000. Gene ontology: tool for the unification of biology. The Gene Ontology Consortium. *Nat Genet.* 25: 25-29.

- Bansal, N., Zhang, M., Bhaskar, A., Itotia, P., Lee, E., Shlyakhtenko, L. S., Lam, T. T., Fritz, A., Berezney, R., Lyubchenko, Y. L., Stafford, W.F. and Thapar, R. 2013. Assembly of the SLIP1-SLBP complex on histone mRNA requires heterodimerization and sequential binding of SLBP followed by SLIP1. *Biochemistry*. 52: 520-536.
- Baroni, T.E., Chittur, S.V., George, A.D. and Tenenbaum, S.A. 2008. Advances in RIP-chip analysis: RNA-binding protein immunoprecipitation-microarray profiling. *Methods Mol Biol*. 419: 93-108.
- Bermejo, R., Lai, M. S. and Foiani, M. 2012. Preventing replication stress to maintain genome stability: resolving conflicts between replication and transcription. *Mol. Cell* 45: 710-718.
- Bindea, G., Mlecnik, B., Hackl, H., Charoetong, P., Tosolini, M., Kirilovsky, A., Fridman, W.H., Pages, F., Trajanoski, Z. and Galon, J. 2009. ClueGO: a Cytoscape plug-in to decipher functionally grouped gene ontology and pathway annotation networks. *Bioinformatics*. 25(8): 1091-1093.

- Blasius, M., Forment, J.V., Thakkar, N., Wagner, S.A., Choudhary, C. and Jackson, S.P. 2011. A phospho-proteomic screen identifies substrates of the checkpoint kinase Chk1. *Genome Biology*. 12: R78.
- Bochman, M.L. and Schwacha, A. 2009. The Mcm Complex: Unwinding the Mechanism of a Replicative Helicase. *Microbiol Mol Biol Rev*. 73(4): 652-683.
- Bonetta, L. 2010. Protein–protein interactions: Interactome under construction. *Nature*. 468: 851–854.
- Bono, F., Ebert, J., Lorentzen, E. and Conti, E. 2006. The crystal structure of the exon junction complex reveals how it maintains a stable grip on mRNA. *Cell*. 126(4): 713-725.
- Boulon, S., Westman, B.J., Hutten, S., Boisvert, F.M. and Lamond, A.I. 2010. The nucleolus under stress. *Mol Cell*. 40(2): 216-227.
- Brannan, K., Kim, H., Erickson, B., Glover-Cutter, K., Kim, S., Fong, N., Kiemele, L., Hansen, K., Davis, R., Lykke-Andersen, J. and Bentley, D.L. 2012. mRNA decapping factors and the exonuclease Xrn2 function in widespread premature termination of RNA polymerase II transcription. *Mol Cell*. 46(3): 311-324.

- Cai, R.L., Yan-Neale, Y., Cueto, M.A., Xu, H. and Cohen, D. 2000. HDAC1, a histone deacetylase, forms a complex with Hus1 and Rad9, two G2/M checkpoint Rad proteins. *J Biol Chem.* 275(36): 27909-27916.
- Chang, C-F., Chu, P-C., Wu, P-Y., Yu, M-Y., Lee, J-Y. Tsai, M-D. and Chang, M-S. 2015. PHRF1 promotes genome integrity by modulating non-homologous end-joining. *Cell Death Dis.* 6: 1-11.
- Cheng, H., Dufu, K., Lee, C.S., Hsu, J.L., Dias, A. and Reed, R. 2006. Human mRNA export machinery recruited to the 5' end of mRNA. *Cell* 127: 1389-1400.
- Choe, J., Kim, K.M., Park, S., Lee, Y.K., Song, O.K., Kim, M.K., Lee, B.G., Song, H.K. and Kim, Y.K. 2010. Rapid degradation of replication-dependent histone mRNAs largely occurs on mRNAs bound by nuclear cap-binding proteins 80 and 20. *Nucleic Acids Res.* 41(2): 1307-1318.
- Ciccia, A. and Elledge, S.J. 2010. The DNA Damage Response: Making it safe to play with knives. *Mol Cell.* 40(2): 179-204.
- Cohen, P. and Frame, S. 2001. The renaissance of GSK3. *Nat. Rev. Mol. Cell Biol.* 2: 769-776.

- Coller, J.M., Tucker, M., Sheth, U., Valencia-Sanchez, M.A., Parker, R. 2001. The DEAD box helicase, Dhh1p, functions in mRNA decapping and interacts with both the decapping and deadenylase complexes. *RNA* 7: 1717–1727.
- Das, S., Saha, U. and Das, B. 2014. Cbc2p, Upf3p and eIF4G are components of the DRN (Degradation of mRNA in the Nucleus) in *Saccharomyces cerevisiae*. *FEMS Yeast Res.* 14: 922-932.
- Domínguez-Sánchez, M.S., Barroso, S., Gómez-González, B., Luna, R. and Aguilera, A. 2011. Genome Instability and Transcription Elongation Impairment in Human Cells Depleted of THO/TREX. *PLoS Genet.* 7(12): e1002386
- Dominski, Z., Erkmann, J.A., Yang, X., Sanchez, R., Marzluff, W.F. 2002. A novel zinc finger protein is associated with U7 snRNP and interacts with the stem-loop binding protein in the histone pre-mRNP to stimulate 3'-end processing. *Genes & Dev.* 16: 58-71.
- Ducat, D. and Zheng, Y. 2004. Aurora kinases in spindle assembly and chromosome segregation. *Exp. Cell Res.* 301: 60-67.
- Dunham, W.H., Mullin, M. and Gingras, A.C. 2012. Affinity-purification coupled to mass spectrometry: basic principles and strategies. *Proteomics.* 12(10): 1576-1590.

- Duronio, R.J. and Xiong, Y. 2013. Signaling Pathways that Control Cell Proliferation. *Cold Spring Harb Perspect Biol.* 5(3): a008904.
- Eliseeva, I.A., Kim, E.R., Guryanov, S.G., Ovchinnikov, L.P., and Lyabin, D.N. (2011). REVIEW Y Box Binding Protein 1 (YB1) and Its Functions. *Biochemistry(Moscow).* 76: 1402-1433.
- Erkman, J.A., Wagner, E.J., Dong, J., Zhang, Y., Kutay, U. and Marzluff, W.F. 2005. Nuclear Import of the Stem-Loop Binding Protein and Localization during the Cell Cycle. *Mol Biol Cell.* 16(6): 2960-2971.
- Fell, V.L. and Schild-Poulter, C. 2015. The Ku heterodimer: Function in DNA repair and beyond. *Mutat Res.* 763: 15-29.
- Fiorini, F., Bonneau, F. and Le Hir, H. 2012. Biochemical characterization of the RNA helicase UPF1 involved in nonsense-mediated mRNA decay. *Methods Enzymol.* 511: 255-274.
- Gavriilidis, P., Giakoustidis, A. and Giakoustidis, D. 2015. Aurora Kinases and Potential Medical Applications of Aurora Kinase Inhibitors: A Review. *J Clin Med Res.* 7(10): 742-751.

- Gebhardt, A., Habjan, M., Benda, C., Meiler, A., Haas, D.A., Hein, M.Y. Mann, A., Mann, M., Habermann, B. and Pichlmair, A. 2015. mRNA export through an additional cap-binding complex consisting of NCBP1 and NCBP3. *Nat. Commun.* 6: 1-13.
- Gingras, A-C., Gstaiger, M. Raught, B. and Aebersold, R. 2007. Analysis of protein complexes using mass spectrometry. *Nat. Rev. Mol. Cell Biol.* 8: 645-654.
- Gonatopoulos-Pournatzis, T. and Cowling, V.H. 2014. Cap-binding complex (CBC). *457 (2): 231-242.*
- Harding, H. P., Zhang, Y., Bertolotti, A., Zeng, H. & Ron, D. 2000. Perk is essential for translational regulation and cell survival during the unfolded protein response. *Mol. Cell.* 5: 897-904.
- He, Q. and Ge, W. 2014. FMRP: A new chapter with chromatin. *Protein Cell.* 5(12): 885-888.
- Heath, C.G., Viphakone, N. and Wilson, S.A. 2016. The role of TREX in gene expression and disease. *Biochem. J.* 473: 2911-2935.
- Holcik, M. and Sonenberg, N. 2005. Translational control in stress and apoptosis. *Nature.* 6: 318-327. 7: 529-539.
- Hong, Z., Jiang, J., Ma, J., Dai, S., Xu, T., Li, H. and Yasui, A. 2013. The role of hnRPU1 involved in DNA damage response is related to PARP1. *PLoS ONE* 8(4): 1-10.

Houseley, J., LaCava, J. and Tollervey, D. 2006. RNA-quality control by the exosome. *Nat Rev Mol Cell Biol.* 7(7): 529-539.

<http://cicblade.dep.usal.es:8080/APID/init.action>

<http://www.compbio.dundee.ac.uk/www-pips/>

<http://www.ebi.ac.uk/intact/>

<http://www.hprd.org>

<http://string-db.org>

<https://thebiogrid.org>

Huang, D.W., Sherman, B.T., Tan, Q., Collins, J.R., Alvord, W.G., Roayaei, J., Stephens, R., Baseler, M.W., Lane, H.C. and Lempicki, R.A. 2007. The DAVID Gene Functional Classification Tool: a novel biological module-centric algorithm to functionally analyze large gene lists. *Genome Biol.* 8(9): R183.

Huertas, P. and Aguilera, A. 2003. Cotranscriptionally formed DNA:RNA hybrids mediate transcription elongation impairment and transcription-associated recombination. *Mol. Cell.* 12: 711-721.

Jackson, R.J., Hellen, C.U. and Pestova, T.V. 2010. The mechanism of eukaryotic translation initiation and principles of its regulation. *Nat Rev Mol Cell Biol.* 11(2): 113-127.

- Jain, A., Bacolla, A., Del Mundo, I.M., Zhao, J., Wang, G., Vasquez, K.M. 2013. DHX9 helicase is involved in preventing genomic instability induced by alternatively structured DNA in human cells. *Nucleic Acids Res.* 41(22): 10345-10357.
- Januszyk, K. and Lima, C.D. 2014. The eukaryotic RNA exosome. *Curr Opin Struct Biol.* 24: 132-140.
- Kai, M. 2016. Roles of RNA-binding proteins in DNA damage response. *Int. J. Mol. Sci.* 17(310): 1-9.
- Kaneko, S., Rozenblatt-Rosen, O., Meyerson, M., Manley, J.L. 2007. The multifunctional protein p54nrb/PSF recruits the exonuclease XRN2 to facilitate pre-mRNA 3' processing and transcription termination. *Genes Dev* 21: 1779-1789.
- Katahira, J. 2012. mRNA export and the TREX complex. *Biochim Biophys Acta.* 1819(6): 507-513.
- Kaygun, H., Marzluff, W.F. 2005a. Regulated degradation of replication-dependent histone mRNAs requires both ATR and Upf1. *Nat Struct Mol Biol.* 12(9): 794-800.
- Kaygun, H. and Marzluff, W.F. 2005b. Upf1 regulates mammalian histone mRNA decay. *RNA.* 1(7): 567-574.

- Kaygun, H. and Marzluff, W.F. 2005c. Translation termination is involved in histone mRNA degradation when DNA replication is inhibited. *Mol Cell Biol.* 25(16): 6879-6888.
- König, J., Zarnack, K., Rot, G., Curk, T., Kayikci, M., Zupan, B., Turner, D.J., Luscombe, N.M. and Ule, J. 2010. iCLIP reveals the function of hnRNP particles in splicing at individual nucleotide resolution. *Nat Struct Mol Biol.* 17(7): 909-915.
- Koseoglu, M.M.2007. Cell cycle regulation of the stem loop binding protein: A key regulator in histone mRNA metabolism. (Doctoral thesis, University of North Carolina at Chapel Hill, the US). Retrieved from <https://cdr.lib.unc.edu/record/uuid:eb053416-6d94-4b5e-853b-7cfc7f494238>
- Krietsch, J., Caron, M.C., Gagné, J.P., Ethier, C., Vignard, J., Vincent, M., Rouleau, M., Hendzel, M.J., Poirier, G.G. and Masson, J.Y. 2012. PARP activation regulates the RNA-binding protein NONO in the DNA damage response to DNA double-strand breaks. *Nucleic Acids Res.* 40(20): 10287-10301.

- Krishnan, N., Lam, T.T., Fritz, A., Rempinski, D., O'Loughlin, K., Minderman, H., Berezney, R., Marzluff, W.F. and Thapar, R. 2012. The prolyl isomerase Pin1 targets stem-loop binding protein (SLBP) to dissociate the SLBP-histone mRNA complex linking histone mRNA decay with SLBP ubiquitination. *Mol Cell Biol.* 32(21): 4306-22.
- Kuroda, T., Murayama, A., Katagiri, N., Ohta, Y., Fujita, E., Masumoto, H., Ema, M., Takahashi, S., Kimura, K. and Yanagisawa, J. 2011. RNA content in the nucleolus alters p53 acetylation via MYBBP11A. *30: 1054-1066.*
- Lee, S., Kim, J.Y., Kim, Y.J., Seok, K.O., Kim, J.H., Chang, Y.J., Kang, H.Y., Park, J.H. 2012. Nucleolar protein GLTSCR2 stabilizes p53 in response to ribosomal stresses. *Cell Death Differ.* 19(10): 1613-1622.
- Lei, H., Dias, A.P. and Reed, R. 2011. Export and stability of naturally intronless mRNAs require specific coding region sequences and the TREX mRNA export complex. *Proc Natl Acad Sci U S A.* 108(44): 17985-17990.
- Li, Y., Lin, A.W., Zhang, X., Wang, Y., Wang, X. and Goodrich, D.W. 2007. Thoc1 as a potential molecular target for cancer therapy. *MEDICINA (Buenos Aires).* 67 (Supl. II): 13-19.

- Liu, X., Tan, Y., Zhang, C., Zhang, Y., Zhang, L., Ren, P., Deng, H., Luo, J., Ke, Y. and Du, X. 2016. NAT10 regulated p53 activation through acetylating p53 at K120 and ubiquitinating Mdm2. *EMBO Rep.* 17(3): 349-366.
- Lopes, C.T., Franz, M., Kazi, F., Donaldson, S.L., Morris, Q. and Bader, G.D. 2010. Cytoscape Web: an interactive web-based network browser. *Bioinformatics.* 26(18): 2347-2348.
- Lovejoy, C.A. and Cortez, D. 2009. Common mechanisms of PIKK regulation. *DNA Repair (Amst).* 8(9): 1004-1008.
- Lubas, M., Andersen, P.R. Schein, A. Dziembowski, A., Kudla, G., Jensen, T.H. 2015. The Human Nuclear Exosome Targeting Complex Is Loaded onto Newly Synthesized RNA to Direct Early Ribonucleolysis. *Cell Rep.* 10(2): 178-192.
- Mazouzi, A., Velimezi, G. and Loizou, J.I. 2014. DNA replication stress: Causes, resolution and disease. *Exp Cell Res.* 329(15): 85-93.
- Milek, M., Wyler, E. and Landthaler, M. 2012. Transcriptome-wide analysis of protein-RNA interactions using high-throughput sequencing. *Semin Cell Dev Biol.* 23(2): 206-212.

- Miller, K.M., Tjeertes, J.V., Coates, J., Legube, G., Polo, S.E., Britton, S. and Jackson, S.P. 2010. Human HDAC1 and HDAC2 function in the DNA-damage response to promote DNA nonhomologous end-joining. *Nat. Struct. Mol. Biol.* 17: 1144-1151.
- Mitchell, P. and Tollervey, D. 2000. mRNA stability in eukaryotes. *Curr. Opin. Genet. Dev.* 10: 193–198.
- Montecucco, A. and Biamonti, G. 2013. Pre-mRNA processing factors meet the DNA damage response. *Front Genet.* 4: 1-14.
- Mossi R, Jonsson ZO, Allen BL, Hardin SH, Hubscher U: Replication factor C interacts with the C-terminal side of proliferating cell nuclear antigen. *J Biol Chem* 1997, 272:1769-1776.
- Muller, B., Blackburn, J., Feijoo, C., Zhao, X. and Smythe, C. 2007. DNA-activated protein kinase functions in a newly observed S phase checkpoint that links histone mRNA abundance with DNA replication. *J Cell Biol* 179: 1385–1398.
- Narita, T., Yung, T.M.C., Yamamoto, J., Tsuboi, Y., Tanabe, H., Tanaka, K., Yamaguchi, Y. and Handa, H. 2007. NELF Interacts with CBC and Participates in 3' End Processing of Replication-Dependent Histone mRNAs. *Mol Cell.* 26: 349-365.

- Nicholson, P. and Müller, B. 2008. Post-transcriptional control of animal histone gene expression--not so different after all. *Mol Biosyst.* 4(7): 721-725.
- Ohno, M., Segref, A., Bachi, A., Wilm, M. and Mattaj, I.W. 2000. PHAX, a mediator of U snRNA nuclear export whose activity is regulated by phosphorylation. *Cell.* 101: 187-198.
- Polo, S.E., Blackford, A.N., Chapman, J.R., Baskcomb, L., Gravel, S., Rusch, A., Thomas, A., Blundred, R., Smith, P., Kzhyshkowska, J., Dobner, T., Taylor, A.M., Turnell, A.S., Stewart, G.S., Grand, R.J. and Jackson, S.P. 2012. Regulation of DNA-end resection by hnRNPU-like proteins promotes DNA double-strand break signaling and repair. *Mol Cell.* 45(4): 505-516.
- Preker, P., Nielsen, J., Kammler, S., Lykke-Andersen, S., Christensen, M.S., Mapendano, C.K., Schierup, M.H., Jensen, T.H., Rudra, D. and Warner, J. R. 2008. RNA exosome depletion reveals transcription upstream of active human promoters. *Science* 322(5909): 1851-1854.
- Saavedra, C., Tung, K. S., Amberg, D. C., Hopper, A. K. and Cole, C. N. 1996. Regulation of mRNA export in response to stress in *Saccharomyces cerevisiae*. *Genes Dev.* 10: 1608-1620.

- Shrivastav, M., De HarO, L.P. and Nickoloff, J.A. 2008. Regulation of DNA double-strand break repair pathway choice. *Cell Res.* 18: 134-147.
- Siomi, M.C., Zhang, Y., Siomo, H. and Dreyfuss, G. 1996. Specific Sequences in the fragile X syndrome protein FMR1 and the FXR proteins mediate their binding to 60S ribosomal subunits and the interactions among them. *16(7): 3825-3832.*
- Taccioli, G.E., Gottlieb, T.M., Blunt, T., Priestley, A., Demengeot, J., Mizuta, R., Lehmann, A.R., Alt, F.W., Jackson, S.P. and Jeggo, P.A. 1994. Ku80: product of the XRCC5 gene and its role in DNA repair and V(D)J recombination. *Science.* 265: 1442–1445.
- Takemura, R., Inoue, Y. and Izawa, S. 2004. Stress response in yeast mRNA export factor: reversible changes in Rat8p localization are caused by ethanol stress but not heat shock. *J. Cell Sci.* 117: 4189-4197.
- Thapar, R. 2014. Contribution of protein phosphorylation to binding-induced folding of the SLBP-histone mRNA complex probed by phosphorus-31 NMR. *FEBS Open Bio.* 16(4): 853-857.
- Thapar, R., Marzluff, W.F. and Redinbo, M.R. 2004a. Electrostatic contribution of serine phosphorylation to the Drosophila SLBP-histone mRNA complex. *Biochemistry.* 43(29): 9401-9412.

- Thapar, R., Mueller, G.A. and Marzluff, W.F. 2004b. The N-terminal domain of the *Drosophila* histone mRNA binding protein, SLBP, is intrinsically disordered with nascent helical structure. *Biochemistry*. 43(29): 9390-400.
- Traven, A. and Heierhorst, J. 2005. SQ/TQ cluster domains: concentrated ATM/ATR kinase phosphorylation site regions in DNA-damage-response proteins. *Bioessays*. 27(4): 397-407.
- Ule, J., Jensen, K., Mele, A. and Darnell, R.B. 2005. CLIP: a method for identifying protein-RNA interaction sites in living cells. *Methods*. 37(4): 376-386.
- Van Nostrand, E.L., Pratt, G.A., Shishkin, A.A., Gelboin-Burkhart, C., Fang, M.Y., Sundararaman, B., Blue, S.M., Nguyen, T.B., Surka, C., Elkins, K., Stanton, R., Rigo, F., Guttman, M. and Yeo, G.W. 2016. Robust transcriptome-wide discovery of RNA binding protein binding sites with enhanced CLIP (eCLIP). *Nat Methods*. 1-9.
- von Moeller, H., Lerner, R., Ricciardi, A., Basquin, C., Marzluff, W.F. and Conti, E. 2013. Structural and biochemical studies of SLIP1-SLBP identify DBP5 and eIF3g as SLIP1-binding proteins. *Nucleic Acids Res*. 41(16): 7960-7971.

Walker, J.R., Corpina, R.A., Goldberg, J. 2001. Structure of the Ku heterodimer bound to DNA and its implications for double-strand break repair. *Nature*. 412: 607-614.

Wang, X., Zhao, B.S., Roundtree, I.A., Lu, Z., Han, D., Ma, H., Weng, X., Chen, K., Shi, H. and He, C. 2015. N(6)-methyladenosine Modulates Messenger RNA Translation Efficiency. *Cell*. 161(6): 1388-1399.

Warner, J. R. 1999. The economics of ribosome biosynthesis in yeast. *Trends Biochem. Sci.* 24: 437-440.

WebGestalt <http://bioinfo.vanderbilt.edu/webgestalt/>

Wellinger, R.E., Prado, F. and Aguilera, A. 2006. Replication fork progression is impaired by transcription in hyperrecombinant yeast cells lacking a functional THO complex. *Mol Cell Biol*. 26(8): 3327-3334.

[www.pantherdb.org](http://www.pantherdb.org)

[www.phosphosite.org](http://www.phosphosite.org)

Zhang, J., Tan, D., DeRose, E.F., Perera, L., Dominski, Z., Marzluff, W.F., Tong, L. and Hall, T.M. 2014. Molecular mechanisms for the regulation of histone mRNA stem-loop-binding protein by phosphorylation. *Proc Natl Acad Sci U S A*. 111(29): E2937-46.

- Zhang, M., Lam, T.T., Tonelli, M., Marzluff, W.F. and Thapar, R. 2012. Interaction of the histone mRNA hairpin with stem-loop binding protein (SLBP) and regulation of the SLBP-RNA complex by phosphorylation and proline isomerization. *Biochemistry*. 51(15): 3215-3231.
- Zhang, W., Cheng, Y., Li, Y., Chen, Z., Jin, P., and Chen, D. 2014. A feed-forward mechanism involving *Drosophila* fragile X mental retardation protein triggers a replication stress-induced DNA damage response. *Hum Mol Genet*. 23(19): 5188-5196.
- Zhou, F., Cardoza, J.D. Ficarro, S.B., Adelmant, G.O., Lazaro, J-B. and Marto, J.A. 2010. Online Nanoflow RP-RP-MS Reveals Dynamics of Multi-component Ku Complex in Response to DNA Damage. *J Proteome Res*. 9(12): 6242-6255.

# Chapter 7

## *Concluding discussion and future perspectives*

### **7.1 Introduction**

Histone mRNA decay (HD) is the surveillance process which ensures that histone is rapidly degraded following completion of DNA replication at the end of S-phase. Strict coordination between histone protein production and DNA replication is essential for the correct packaging of newly replicated DNA, as imbalances can lead to deleterious effects such as genomic instability.

Interestingly, histone mRNA decay is controlled by the presence of a stem-loop structure at the 3'-untranslated of histone mRNA and a protein HBP/SLBP (Hairpin/stem-loop binding protein) which specifically binds to histone mRNA. SLBP is a unique RNA-binding protein that contains a novel RNA-binding domain (RBD). RBD is the only region of SLBP conserved among diverse metazoans (*Caenorhabditis elegans*, *Drosophila* and vertebrates). SLBP expression is regulated during the cell cycle and required for multiple aspects of the regulation of histone mRNA homeostasis such as pre-mRNA transcription, processing, cleavage, translation, and degradation (Zheng

*et al.*, 2003). Moreover, HD is one functional target of an intra S-phase checkpoint activated when DNA synthesis is inhibited, ensuring that histone mRNA is rapidly destroyed when global DNA replication is blocked. However, replication stress-induced HD does not induce SLBP destruction (Muller *et al.*, 2007).

Therefore, the main goals in this thesis were to investigate the mechanism of DNA damage and replication arrest-induced histone mRNA decay by focusing on SLBP as the key player of histone mRNA stem-loop.

The data described in this thesis showed that

1. Inducible Flag- and HA-tagged SLBP protein is expressed in a regulated manner similar to that of endogenous SLBP throughout cell cycle progression.

2. The regulated timing of both the translation and the destruction of the Flag- and HA-tagged SLBP occurs normally in these cell line models.

3. A mutated form of SLBP (SLBP<sup>res</sup>) utilising redundancy in the genetic code to express wild-type protein sequence is resistant to siRNA-induced knockdown of endogenous protein. Flag-SLBP<sup>res</sup>, which does not generate alternatively spliced forms of SLBP is capable of facilitating histone mRNA decay after the inhibition of DNA replication.

4. The expression of a siRNA-resistant SLBP restores S-phase progression after knocking down endogenous SLBP.

5. Using an inclusion list of SLBP-derived peptide masses obtained from bacterially expressed GST-SLBP-6xHis enabled the identification and characterisation of immuno-isolated SLBP using shotgun proteomics with an overall SLBP sequence coverage of 45%.

6. SLBP was found by mass spectrometry to be phosphorylated in vivo at multiple sites including the novel site Ser182. This site is in the RNA binding domain (RBD) of SLBP.

7. The expression of phospho-mimetic SLBP (S182E) may increase the duration of S-phase, and non-phosphorylatable SLBP (S182A) facilitates more rapid transit through S-phase.

8. Flag-SLBP<sup>resS182E</sup>-expressing cells delay histone mRNA decay after the inhibition of DNA synthesis.

9. Inhibition of WEE1 kinase by MK-1775 rapidly reduces cellular SLBP levels and therefore, WEE1 prevents premature SLBP degradation.

10. A role for the WEE1 kinase in the regulation of SLBP stability is likely independent of the phosphorylation state of Ser182.

11. In addition to histone mRNA decay as a mechanism for replication stress induced reduction in histone protein production, there

is a cellular mechanism which blocks SLBP associated ribosomal assembly. Histone mRNA decay occurs via the exosome mediated degradation although the subcellular location is unclear.

12. UPF1, UPF2 and UPF3b are associated with SLBP, and following replication stress, Upf1 levels, but not Upf2 or 3, decrease.

13. Phosphorylation at Ser20 and Ser23, and Ser114/115 is up-regulated in response to HU treatment, but there is no change in stoichiometry at Ser111, Ser112 or Ser117.

14. SLBP is found associated with a newly identified component (C17orf85 (NCBP3)), of the cap-binding complex. As NCBP3 is a Chk1 substrate, this represents a possible novel mechanism by which replication stress may regulate histone mRNA stability and expression.

## **7.2 The potential of Flp-In<sup>TM</sup> T-Rex<sup>TM</sup> system for analysis of SLBP in a model cell line**

According to data presented in Chapter 3, it is clear that inducible expression of exogenous Flag-tagged SLBP using the Flp-In<sup>TM</sup> T-Rex<sup>TM</sup> system in HeLa cells is a successful model for further molecular analysis of SLBP function. (1) Both translation and the destruction of the Flag and HA-tagged SLBP occurs normally in Flp-In HeLa cells, and thus tagged SLBP expression is correctly limited to S phase.

(2) The progression through the cell cycle was not affected by ectopic expression of Flag- or HA-tagged SLBP. (3) Knock-down of endogenous SLBP and subsequently expression of Flag- and HA-SLBP<sup>res</sup> facilitates histone mRNA decay at the same rate as normal cells under conditions of DNA damage and replication stress, supporting the notion that the exogenously expressed protein is regulated as the endogenous protein. As the exogenously expressed protein is not capable of undergoing splicing, the data do not support a role for SLBP splice variants in the acute phase of replication stress induced histone mRNA decay.

### **7.3 Successful establishment of an approach for immuno-isolation**

#### **(I-i) of Flag-tagged SLBP for mass spectrometry**

In summary, the success of this independent method for the identification of SLBP peptides with 45% of sequence coverage of SLBP provides important insights into the strategy and scale of immuno-isolation required to obtain sufficient quantities of SLBP for both the analysis of SLBP post-translational modification status, together with an LC-MS/MS analysis of its interacting proteins in the HeLa cell tissue culture cell line model. In particular, use of an inclusion list enabled the

calibration of the mass spectrometer using the precise masses of peptides obtained from bacterially expressed SLBP together with their HPLC retention time to detect SLBP-derived peptides from an in vivo mammalian source.

Inevitably, there were differences in the specific peptides identified in the analysis of mammalian SLBP compared to the bacterial protein. This issue arises as a result of one of the common limitations of shotgun proteomics for the analysis of proteins derived from complex samples, and is related to the ability of the MS methodology to identify specific peptides in particular combinations of complex mixtures. The variation in specific peptide identification arises because MS peptide identification occurs dynamically and is dependent on the complexity of sample content, and the related peptide abundance presented at any one time to the mass spectrometer. Because these parameters inevitably differ between samples produced from distinct sources, there will always be variation in the identification of specific peptides depending on their relative abundance in the context of other peptides present in the sample mixture.

For example, a number of mass spectrometry studies into hSLBP phosphorylation for structural and sequence information have been undertaken previously using protein expressed in, and isolated from,

baculovirus-infected insect cells, using Ni<sup>2+</sup> affinity and gel filtration chromatography for hSLBP purification (Zheng *et al.*, 2003 ; Borchers *et al.*, 2006 ; Bansal *et al.*, 2013). Use of relatively large amounts of purified protein using this approach will have contributed to the 85.2% coverage of SLBP sequence reported by Bansal and colleagues (2013).

In the work presented here, coverage of the mammalian SLBP protein was significantly lower (45%) than values obtained with purified protein. This is a consequence of the difference in the nature and associated complexity of the material under analysis. In the work presented here, SLBP immuno-isolates not only contained SLBP, but also a large number of co-immunoprecipitating proteins. Analysis of these more complex mixtures inevitably reduces the extent of coverage of specific proteins, and thus limits the depth of analysis possible. Despite this issue, significant analysis of SLBP post-translational status was identified in association with changes in interactomic content, using the adopted approach.

#### **7.4 The role of Ser182 phosphorylation in SLBP function**

In the work presented here, I have shown SLBP is phosphorylated *in vivo* on Ser182 and that expression of a Ser182 phospho-mimetic mutant increases the duration of SLBP expression together with a consequent increase in the duration of histone mRNA expression. In comparison, expression of a non-phosphorylatable mutant at this site reduces the duration of SLBP expression. Additionally, a phospho-mimetic mutant at this site reduced the efficiency of histone mRNA decay following the inhibition of DNA synthesis, compared to either wild-type protein or an unphosphorylatable mutant.

WEE1 was identified as a potential candidate kinase for S182 phosphorylation given that it has roles both in S phase regulation and histone synthesis (Beck *et al.*, 2012 ; Mahajan and Mahajan, 2013) as well as a role in regulating the G2/M transition (Smythe and Newport, 1992). Importantly, during replication stress, WEE1 is a crucial downstream activator after CHK1 phosphorylates and inactivates CDC25 (Saini *et al.*, 2015). WEE1 phosphorylates Cdk1 at tyrosine15 throughout S phase to prevent the G2/M transition (McGowan and Russell, 1995 ; Beck *et al.*, 2012). It also has an analogous role in regulating the activation state of Cdk2 (Chow *et al.*, 2003) required for

S phase progression, by regulating the activation state and thus S phase substrate range during S phase.

In experiments undertaken here, SLBP was not phosphorylated by WEE1 kinase *in vitro*, suggesting that WEE1 is not the physiological kinase responsible for Ser182 phosphorylation. These data must be interpreted with caution as it may be the case that phosphorylation of SLBP at Ser182 by its cognate kinase requires the *in vivo* configuration of SLBP, which may not have been the case in the experiments undertaken here.

The bioinformatic analysis of kinases capable of Ser182 phosphorylation also included Aurora kinase A. Although there is limited information in the literature regarding the capability of Aurora A to undertake Ser182 phosphorylation, the data obtained here suggesting its enrichment in SLBP I-i preparations suggest that it is conceivably the relevant kinase in this case.

#### **7.4.1 Effects of WEE 1 inhibition on SLBP expression**

In this work, I found that inhibition of WEE1 kinase by MK-1775 reduces cellular SLBP levels, independently of S182 phosphorylation status. While these results do not inform an understanding of the significance of Ser182 phosphorylation, they do support the hypothesis

that WEE1 activity levels are important regulators of SLBP expression levels. As SLBP expression at the end of S-phase is believed to be regulated by CyclinA/Cdk2, the data presented here, together with known literature results, suggest that WEE1 inhibition results in premature activation of CyclinA/Cdk2, resulting in turn of premature activation of the SLBP destruction pathway. This hypothesis will require further testing, but may well help to explain aspects of genome instability observed in cells exposed to Wee1 inhibition.

### **7.5 SLBP acts a multi-helper in histone mRNA homeostasis**

The function of SLBP in the homeostatic regulation of histone protein production is an exciting and topical subject. It has important functions in multiple aspects of histone mRNA metabolism including: histone gene expression, mRNA maturation, RNP assembly, nuclear export, translation and mRNA turnover. In this thesis, evidence indicated that SLBP is involved in multiple aspects of histone mRNA homeostasis in nucleus and cytoplasm under the condition of DNA damage and replication arrest via TREX complex involvement in export, degradation via exosome complex and DNA damage via DDR as shown in Figure 7.1. However, caution has to be taken as most of the putative functions and interactions of SLBP have to be further confirmed.

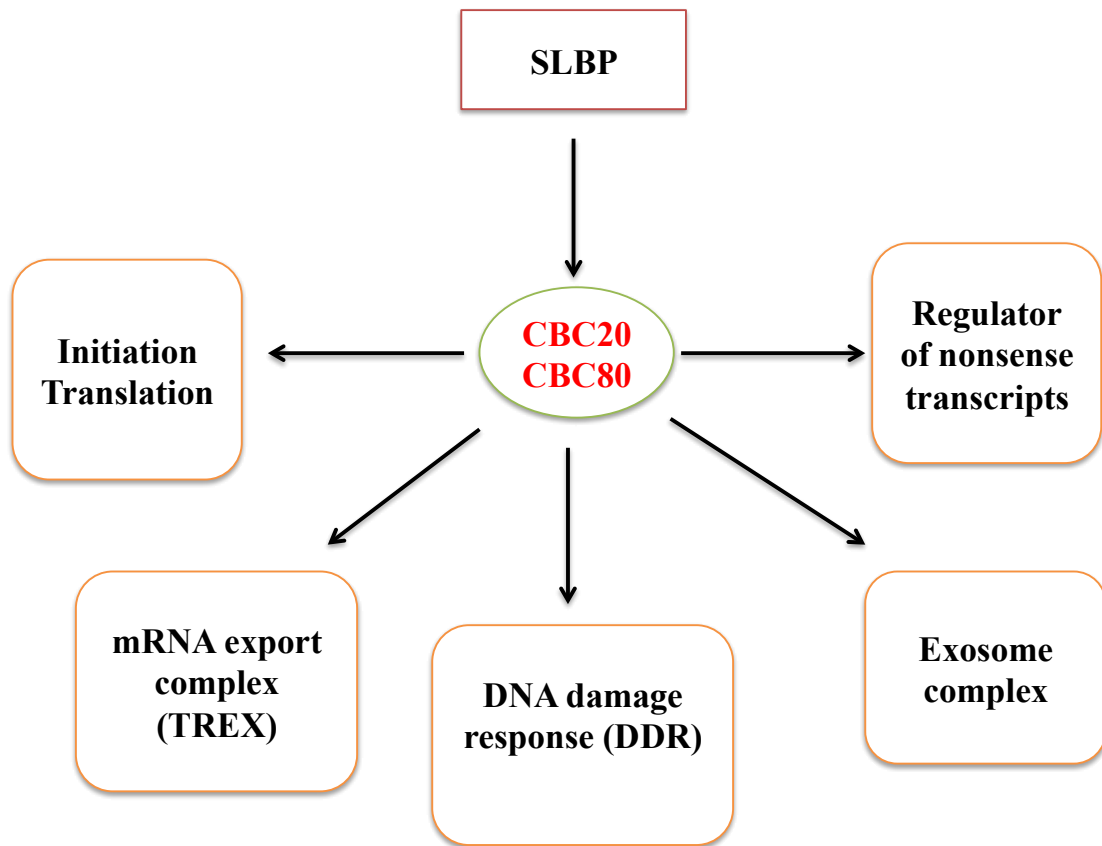


**Figure 7.1** Overall of SLBP-interactome analysis associated with many functions in response to DNA replication stress.

## **7.6 Phosphorylation of Ser20 and Ser23 play a critical role of SLBP degradation under DNA replication stress**

Evidence in this study has identified the interesting notion that phosphorylation at these sites only become significantly elevated following imposition of replication stress. As it is known that SLBP is not degraded during replication stress, it is very unlikely that phosphorylation at these sites do act as a phosphodegron as reported (Krishnan *et al.*, 2012). Therefore, at least two hypotheses can be proposed. The first is that replication stress induced phosphorylation at residues 20 and 23 (in addition to 114 and 115) results in Pin1 mediated disassociation of SLBP from histone mRNA, allowing for the rapid destruction of the latter. The alternative is that replication stress brings about the dissociation of Pin1 from the N-terminal region of SLBP enabling access to the sites by an unidentified protein kinase. Interestingly, two isoforms of casein kinase (CK2), Glycogen synthase kinase-3 (GSK3) and Aurora A kinase were enriched in response to DNA replication stress. These observations may be relevant for the identification of the kinase responsible for phosphorylation of Ser20 and Ser23 under DNA replication stress. However, this identification, and its consequences will require future analysis in this system using

synchronised cell experiments to identify the significance of Ser 20/23 in induction of replication stress induced histone mRNA decay.

## 7.7 Future perspectives

There are many remaining challenging for the future for complete understanding of details of SLBP interactions in S phase progression.

Those objectives are

1. To further confirm SILAC- based MS analysis of SLBP under DNA replication stress in presence and absence of RNAase treatment to establish the nature of direct and indirect SLBP interacting components.
2. To fully establish whether treatment of synchronised cells with WEE1 inhibitor, MK-1775 results in a premature activation of Cyclin A/Cdk1 and, early phosphorylation of Thr61 and thus premature SLBP destruction.
3. To fully establish the identity of the protein kinase responsible for phosphorylation of Ser20 and Ser23.
4. To elucidate the precise mechanism between observed SLBP-interacting proteins and their functions in response to DNA replication stress.

## **7.8 Final Conclusion**

This work highlights the notion that SLBP is a fundamental multi-helper protein involved in regulating histone mRNA homeostasis. It also provides new evidence about the functions of S182 phosphorylation on cell cycle progression, SLBP expression, histone mRNA decay and SLBP stability. Importantly, the induced signal in response to DNA replication stress involving Ser20 and Ser23 phosphorylation, which presumably involves Pin1 mediated disassociation of SLBP from histone mRNA will be important for the understanding of replication stress induced histone mRNA decay.

This is a pioneering research area providing insight into the molecular mechanisms relating to the interaction between SLBP-containing protein complexes that mediate histone homeostasis after inhibition of DNA replication. As such, it builds on the basic knowledge of contemporary fundamental cell biology in this area.

## 7.9 References

- Bansal, N., Zhang, M., Bhaskar, A., Itotia, P. and Lee, E. 2013. Assembly of the SLIP1–SLBP complex on histone mRNA requires heterodimerization and sequential binding of SLBP followed by SLIP1. *Biochemistry*. 52: 520-536.
- Beck, H., Nähse-Kumpf, V., Larsen, M.S., O'Hanlon, K.A., Patzke, S., Holmberg, C., Mejlvang, J., Groth, A., Nielsen, O., Syljuåsen, R.G. and Sørensen, C.S. 2012. Cyclin-dependent kinase suppression by WEE1 kinase protects the genome through control of replication initiation and nucleotide consumption. *Mol Cell Biol*. 32(20): 4226-4236.
- Brosch, M., Yu, L., Hubbard, T. and Choudhary, J. 2009, Accurate and Sensitive Peptide Identification with Mascot Percolator. *J Proteome Res*. 8(6): 3176-3181.
- Chow, J.P., Siu, W.Y., Ho, H.T., Ma, K.H., Ho, C.C. and Poon, R.Y. 2003. Differential contribution of inhibitory phosphorylation of CDC2 and CDK2 for unperturbed cell cycle control and DNA integrity checkpoints. *J Biol Chem*. 278(42): 40815-40828.

- Hubbard, S.J. 1998. The structural aspects of limited proteolysis of native proteins. *Biochim Biophys Acta* 1382(2): 191-206.
- Krishnan, N., Lam, T.T., Fritz, A., Rempinski, D., O'Loughlin, K., Minderman, H., Berezney, R., Marzluff, W.F. and Thapar, R. 2012. The prolyl isomerase Pin1 targets stem-loop binding protein (SLBP) to dissociate the SLBP-histone mRNA complex linking histone mRNA decay with SLBP ubiquitination. *Mol Cell Biol.* 32(21): 4306-22.
- Mahajan, K. and Mahajan, N.P. 2013. WEE1 tyrosine kinase, a novel epigenetic modifier. *Trends Genet.* 29(7): 394-402.
- McGowan, C.H. and Russell, P. 1995 Cell cycle regulation of human WEE1. *EMBO J.* 14: 2166-2175.
- Muller, B., Blackburn, L., Feijoo, C., Zhao, X. and Smythe, C. 2007. DNA- activated protein kinase functions in a newly observed S phase checkpoint that links histone mRNAs abundance with DNA replication. *JCB.* 179(7): 1385-1398.
- Niu, X., Li, N., Chen, D. and Wang, Z. 2013. Interconnection between the protein solubility and amino acid and dipeptide compositions. *Protein Pept Lett.* 20(1): 88-95.

- Price, W.N., Handelman, S.K., Everett, J.K., Tong, S.N., Bracic, A., Luff, J.D., Naumov, V., Acton, T., Manor, P., Xiao, R., Rost, B., Montelione, G.T. and Hunt, J.F. 2011. Large-scale experimental studies show unexpected amino acid effects on protein expression and solubility in vivo in *E. coli*. *Microb Inform and Exp* 1:6.
- Rattray, A.M.J., Nicholson, P. and Müller, B. 2013. Replication stress-induced alternative mRNA splicing alters properties of the histone RNA-binding protein HBP/SLBP: a key factor in the control of histone gene expression. *Biosci Rep.* 33(5): e00066.
- Saini, P., Li, Y. and Dobbstein, M. 2015. Wee1 is required to sustain ATR/Chk1 signaling upon replicative stress. *Oncotarget.* 6(15): 13072-13087.
- Smythe, C and Newport, J.W. 1992. Coupling of mitosis to the completion of S phase in *Xenopus* occurs via modulation of the tyrosine kinase that phosphorylates p34cdc2. *Cell.* 68(4): 787-797.
- Thapar, R., Mueller, G.A. and Marzluff, W.F. 2004. The N-terminal domain of the *Drosophila* histone mRNA binding protein, SLBP, is intrinsically disordered with nascent helical structure. *Biochemistry*, 43: 9390-9400.

Wagner, E.J., Berkow, A. and Marzluff, W.F. Expression of an RNAi-resistant SLBP restores proper S-phase progression. *Biochem Soc Trans.* 33(Pt 3): 471-473.

Zheng, L., Dominski, Z., Yang, X.C., Elms, P., Raska, C.S., Borchers, C.H., and Marzluff, W.F. 2003. Phosphorylation of stem-loop binding protein (SLBP) on two threonines triggers degradation of SLBP, the sole cell cycle-regulated factor required for regulation of histone mRNA processing, at the end of S phase. *Mol. Cell. Biol.* 23: 1590-1601.

## Appendix A. Recipes

Buffers	Components
Blocking buffer	5% (w/v) Skimmed milk or BSA in TBS or TBST
<b>Affinity purification buffer (Buffer A-C)</b>	
Buffer A	2.3 M sucrose 50 mM Tris-HCl pH 7.5 10 mM EDTA 1 mM PMSF
Buffer B	50 mM Tris-HCl pH 7.5 1 mM DTT 100 mM KCl 1 mM EDTA 1 mM PSMF
Buffer C	10 mM Hepes pH 8.0 1 mM DTT 1x proteinase inhibitor tablet
Cell freezing medium	10% DMSO 90% FBS

<b>Buffers</b>	<b>Components</b>
Colloidal Coomassie blue stain	0.1% Coomassie Brilliant Blue R-250 50% methanol 10% glacial acetic acid
Destaining solution	40% methanol 10% glacial acetic acid
Dilution buffer	0.5% BSA 0.2% Tween 20 in PBS
6x DNA loading buffer	0.25% (w/v) bromophenol blue 0.25% (w/v) xylene cyanol FF 30% (v/v) glycerol
IFA buffer	10 mM HEPES pH 7.4 150 mM NaCl 4% serum 0.1% sodium azide
Luria-Bertani (LB) liquid medium (1L)	10 g tryptone 5 g yeast extract 10 g NaCl
PI staining solution	20 µg/ml propidium iodide 200 µg/ml Rnase in ice-cold PBS
Stripping buffer	25 mM Glycine, pH 2.5 and 2% SDS

<b>Buffers</b>	<b>Components</b>
5x Lysis buffer	100 mM Tris-acetate pH 7.5 5 mM EGTA 5 mM EDTA 50 mM sodium $\beta$ -glycerophosphate 25 mM sodium pyrophosphate 250 mM sodium fluoride 2.4 M sucrose Add just before use to 1x lysis buffer 0.2 mM sodium ortho-vanadate 0.2 mM PMSF 1x proteinase inhibitor
2x SDS-PAGE loading buffer	100 mM Tris Cl (pH 6.8) 4% SDS 20% glycerol 200 mM DTT
10x SDS-PAGE running buffer (1L)	30 g Tris-base pH 8.3 144 g glycine 10 g SDS

Buffers	Components
<b>In-gel digestion buffer (Solution buffer 1-8)</b>	
Solution buffer 1	200 mM ABC 40% CAN
Solution buffer 2	50 mM ABC
Solution buffer 3	50 mM ABC 50% CAN
Solution buffer 4	40 mM ABC 9% CAN
Solution buffer 5	100% CAN
Solution buffer 6	5% formic acid
Solution buffer 7	50% CAN 5% formic acid
Solution buffer 8	1mM HCl
Super Optimal Broth media (SOB) (1L)	2% w/v tryptone 0.5% w/v Yeast extract 10 mM NaCl 2.5 mM KCl ddH <sub>2</sub> O to 1000 mL 10 mM MgCl <sub>2</sub> 10 mM MgSO <sub>4</sub>

<b>Buffers</b>	<b>Components</b>
Super Optimal broth with Catabolite repression media (SOC) (1 L)	1 L SOB 20 mM glucose
1x Tris-acetate EDTA (TAE)	40 mM Tris-acetate 20 mM acetic acid and 0.5 mM EDTA (pH 8.0)
1x Tris-buffered saline (TBS)	50 mM Tris-Cl, pH 7.5 150 mM NaCl
1x Tris-buffered saline tween (TBST)	50 mM Tris-Cl, pH 7.5 150 mM NaCl 0.5% (v/v) Tween-20
Wash buffer	0.5% BSA in PBS

## Appendix B. List of antibodies

<b>Antibody</b>	<b>Species</b>	<b>Raised against</b>	<b>Suppliers</b>	<b>Product Code</b>	<b>Dilution</b>
Anti-BrdU	Goat	React with BrdU in single stranded DNA	Abcam	AB6326	Flow Cytometry: 1mg/ml
Anti-Cyclin A	Mouse	Human cyclin A	Abcam	AB38	WB: 5 $\mu$ g/ml
Anti-Cyclin E	Rabbit	Human, mouse, rat, Chinese Hamster cyclin A	Abcam	AB7959	WB: 1:1000
Anti-Flag	Mouse	Flag Tag	Sigma	F1804	WB: 1:1000 IP: 1 $\mu$ g/mg protein
Anti-goat HRP	Goat	Goat IgG	Santa Cruz	SC-2020	WB: 1:5000
Anti-His	Goat	His Tag	AbD Serotec	AHP1656	

					WB: 1:500
<b>Antibody</b>	<b>Species</b>	<b>Raised against</b>	<b>Suppliers</b>	<b>Product Code</b>	<b>Dilution</b>
Anti-mouse HRP	Mouse	Mouse IgG	Santa Cruz	SC-2060	WB: 1:5000
Anti-SLBP	Mouse	Human SLBP	Santa Cruz	SC-101140	WB: 1:500
Anti-nucleolin	Mouse	Human nucleolin	Santa Cruz	SC-17826	WB: 1:10000

## Appendix C. List of oligonucleotides

Names	Sequence 5'-3'
Flag-tagged SLBP <b>Forward</b>	GCACTTAAGATGGATTACAAGGATGACGATGACAAGCTGGCCTGCCGCCCGCGAAGC
Flag-tagged SLBP <b>Reverse</b>	TCGACTCGAGTTAGCTCATGGCTGAGAAGTCTC
Flag-tagged SLBP <sup>res</sup> - <b>Forward</b>	CCTCATCAATGACTTTGGAAGGGAGCGAAAATCATCATCAGGAAGTT
Flag-tagged SLBP <sup>res</sup> - <b>Reverse</b>	AACTTCCTGATGATGATTTTCGCTCCCTTCCAAAGTCATTGATGAGG

Subcloning of human SLBP into pCI-neo- <b>Forward</b>	GCAGAATTCATGGCCTGCCGCCCGCGAAGC
<b>Names</b>	<b>Sequence 5'-3'</b>
GAPDH - <b>Forward</b>	TCGCTCTCTGCTCCTCCTGTTC
GAPDH - <b>Reverse</b>	CGACCAAATCCGTTGACTCCGACC
Histone - <b>Forward</b>	GGTAAAGCGCCACGCAAGCA
Histone - <b>Reverse</b>	GGCGGTAACGGTGAGGCTTT
SLBP-RNA Primer	GAGGGTTCTTTCCTTTTTATTTTTGCAATATCCCATACAAAAGCA
SLBP siRNA - <b>Forward</b>	GAGAGAGAAAUCAUCACUU

SLBP siRNA – <b>Reverse</b>	GAUGAUGAUUUUCUCUCUCUU
<b>Names</b>	<b>Sequence 5’-3’</b>
Subcloning of human SLBP into pCMV-tag2a- <b>Forward</b>	AATTGAATTCCATGGCCTGCCGCCCGCGAAGC
Subcloning of human SLBP into pCMV-tag2a- <b>Reverse</b>	TCGACTCGAGTTAGCTCATGGCTGAGAAGTC

A non-targeting siRNA (Thermo Scientific D-001810-01) was used as a negative control.

## Appendix D. List of plasmids

<b>Plasmids</b>	<b>Origin</b>	<b>Antibiotic resistant</b>
pCDNA5/FRT/TO/CAT	Invitrogen	Ampicillin
pCDNA5/FRT/TO/CAT-Flag-SLBP	This study	Ampicillin
pCDNA5/FRT/TO/CAT- Flag-SLBP <sup>res</sup>	This study	Ampicillin
pCI-Neo-SLBP	This study	Ampicillin
pCMV-Tag 2A-Flag-SLBP	This study	Kanamycin
pOG44	Invitrogen	Ampicillin



## Appendix F. Flag-tagged SLBP cDNA sequence

GAT TAC AAG GAT GAC GAT GAC AAG atggcctgcc gcccgcggaag cccgccgagg  
31 catcagagcc gctgcgacgg tgacgccagc ccgccgtccc ccgcgcgatg gagcctggga  
91 cggaagcgca gagccgacgg caggcgctgg aggcccgaag acgccgagga ggcagagcac  
151 cgcggcgccg agcgcagacc cgagagcttt accactcctg aaggccctaa accccgttcc  
211 agatgctctg actgggcaag tgcagttgaa gaagatgaaa tgaggaccag agttaacaaa  
271 gaaatggcaa gatataaaag gaaactcctc atcaatgact ttggaagaga gagaaaatca  
331 tcatcaggaa gttctgattc aaaggagtct atgtctactg tgccggctga ctttgagaca  
391 gatgaaagtg tcctaatgag gagacagaag cagatcaact atgggaagaa cacaattgcc  
451 tacgatcgtt atattaaaga agtcccaaga caccttcgac aacctggcat tcatcccaag  
511 acccctaata aatttaagaa gtatagtcga cgttcatggg accagcaaat caaactctgg  
571 aaggtggctc tgcatttttg ggatcctcca gcggaagaag gatgtgattt gcaagaaata  
631 caccctgtag accttgaatc tgcagaaagc agctccgagc cccagaccag ctctcaggat  
691 gactttgatg tgtactctgg cacaccacc aaggtgagac acatggacag tcaagtggag  
751 gatgagtttg atttggaagc ttgtttaact gaacccttga gagacttctc agccatgagc  
811 taa

## Appendix G. HA-tagged SLBP cDNA sequence

TAC CCA TAC GAT GTT CCA GAT TAC GCT atggcctgcc gcccgcgaag cccgccgagg  
31 catcagagcc gctgcgacgg tgacgccagc ccgccgtccc ccgcgcgatg gagcctggga  
91 cggaagcgca gagccgacgg caggcgctgg aggcccgaag acgccgagga ggcagagcac  
151 cgcggcgccg agcgcagacc cgagagcttt accactcctg aaggccctaa accccgttcc  
211 agatgctctg actgggcaag tgcagttgaa gaagatgaaa tgaggaccag agttaacaaa  
271 gaaatggcaa gatataaaag gaaactcctc atcaatgact ttggaagaga gagaaaatca  
331 tcatcaggaa gttctgattc aaaggagtct atgtctactg tgccggctga ctttgagaca  
391 gatgaaagtg tcctaatgag gagacagaag cagatcaact atgggaagaa cacaattgcc  
451 tacgatcggt atattaaaga agtcccaaga caccttcgac aacctggcat tcatcccaag  
511 acccctaata aatttaagaa gtatagtcga cgttcatggg accagcaaat caaactctgg  
571 aagggtggctc tgcatttttg ggatcctcca gcggaagaag gatgtgattt gcaagaaata  
631 caccctgtag accttgaatc tgcagaaagc agctccgagc cccagaccag ctctcaggat  
691 gactttgatg tgtactctgg cacaccacc aagggtgagac acatggacag tcaagtggag  
751 gatgagtttg atttggaagc ttgtttaact gaacccttga gagacttctc agccatgagc  
811 taa

## Appendix H.

**Table 1H.** Protein identified by LC-MS/MS in the large-scale I-i

Flag-tagged SLBP by ANTI-FLAG<sup>®</sup> M2 affinity resin.

(Highlighted by yellow colours are also identified in the IP by Flag antibody and ANTI-FLAG<sup>®</sup> M2 affinity resin from whole cell lysate of HeLa and U2OS cells.)

(Highlighted by green colour is Ig heavy chain.)

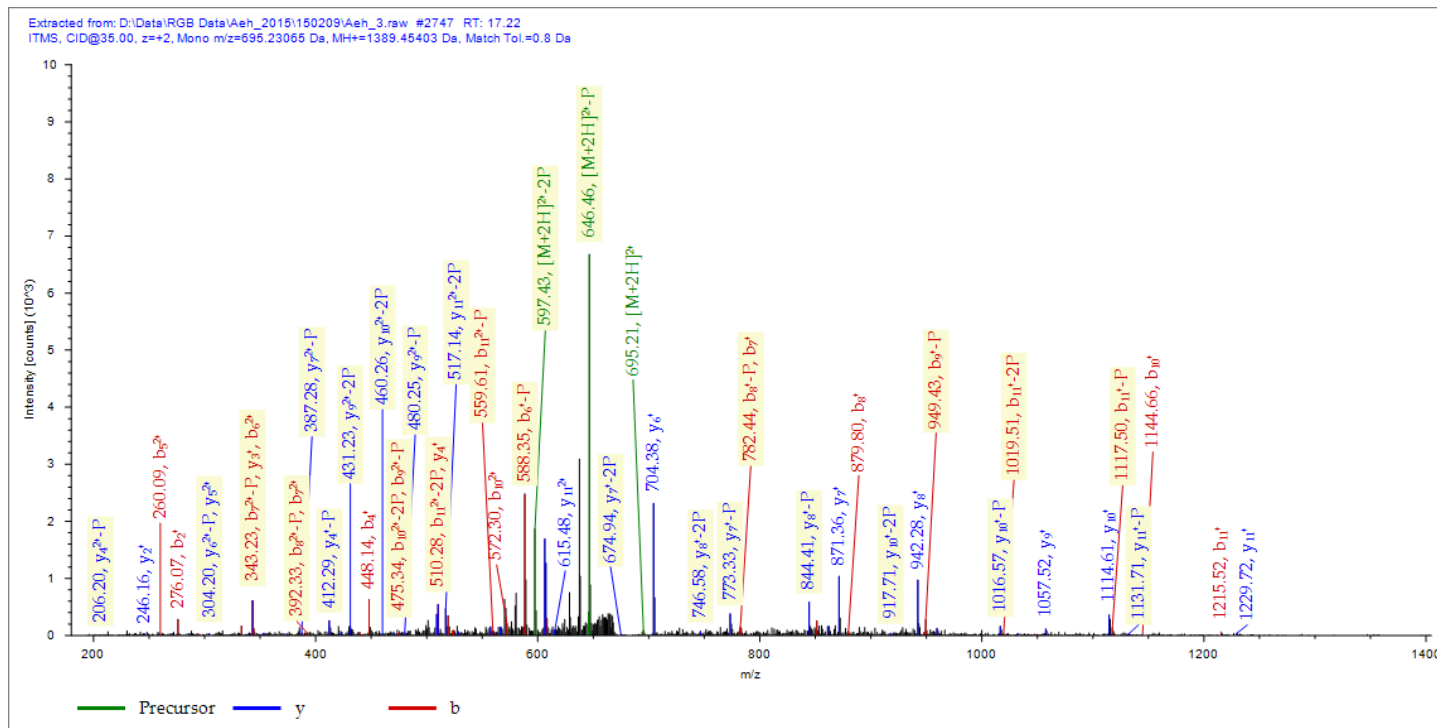
Accession numbers	Protein names	Gene Names
P62333	26S protease regulatory subunit 10B	PSMC6
P08195	4F2 cell-surface antigen heavy chain	SLC3A2
P05388	60S acidic ribosomal protein	RPLP0
P52209	6-phosphogluconate dehydrogenase, decarboxylating	PGD
P11021	78 kDa glucose-regulated protein	HSPA5
Q01518	Adenylyl cyclase-associated protein 1	CAP1
P06733	Alpha-enolase	ENO1
P04083	Annexin A1	ANXA1
P07355	Annexin A2	ANXA2
P12429	Annexin A3	ANXA3
P08133	Annexin A6	ANXA6
P00505	Aspartate aminotransferase, mitochondrial	GOT2
P27797	Calreticulin	CLAR
P81605	Dermcidin	DCD
Q9NY33	Dipeptidyl peptidase	DPP3
P27695	DNA-(apurinic or apyrimidinic site) lyase	APEX1
Q9UJU6	Drebrin-like protein	DBNL
P19474	E3 ubiquitin-protein ligase TRIM21	TRIM21
P29692	Elongation factor 1-delta	EEF1D
P26641	Elongation factor 1-gamma	EEFIG
P05198	Eukaryotic translation initiation factor 2 subunit 1	EIF2S1
P23588	Eukaryotic translation initiation factor 4B	EIF4B
P15311	Ezrin	EZR
P52907	F-actin-capping protein subunit alpha-1	CAPZA1
P04075	Fructose-bisphosphate aldolase A	ALDOA
Q13630	GDP-L-fucose synthase	TSTA3
P06744	Glucose-6-phosphate isomerase	GPI
P14314	Glucosidase 2 subunit beta	PRKCSH

Accession numbers	Protein names	Gene Names
Q9UBQ7	Glyoxylate reductase/hydroxypyruvate reductase	GRHPR
Q9Y2T3	Guanine deaminase	GDA
P08107	Heat shock 70 kDa protein 1A/1B	HSPA1B
P08238	Heat shock protein HSP 90-beta	HSP90AB1
P51991	Heterogeneous nuclear ribonucleoprotein A3	HNRNPA3
P52272	Heterogeneous nuclear ribonucleoprotein M	HNRNPM
O60506	Heterogeneous nuclear ribonucleoprotein Q	SYNCRIP
O43390	Heterogeneous nuclear ribonucleoprotein R	HNRNPR
P50502	Hsc70-interacting protein	ST13
Q15181	Inorganic pyrophosphatase	PPA1
P13645	Keratin, type I cytoskeletal 10	KRT10
P02533	Keratin, type I cytoskeletal 14	KRT14
P35527	Keratin, type I cytoskeletal 9	KRT9
P04264	Keratin, type II cytoskeletal 1	KRT1
P04259	Keratin, type II cytoskeletal 6B	KRT6B
Q16719	Kynureninase	KYNU
P20700	Lamin-B1	LMNB1
P09960	Leukotriene A-4 hydrolase	LTA4H
P00338	L-lactate dehydrogenase A chain	LDHA
P05455	Lupus La protein	SSB
Q15046	Lysine--tRNA ligase	KARS
P40925	Malate dehydrogenase	MDH1
P40926	Malate dehydrogenase	MDH2
Q9BQA1	Methylosome protein 50	WDR77
P26038	Moesin	MSN
Q15233	Non-POU domain-containing octamer-binding protein	NONO
P19338	Nucleolin	NCL
Q02790	Peptidyl-prolyl cis-trans isomerase FKBP4	FKBP4
P00558	Phosphoglycerate kinase 1	PGK1
O43660	Pleiotropic regulator 1	PLRG1
Q13310	Polyadenylate-binding protein 4	PABPC4
P02545	Prelamin-A/C	LMNA
Q9UQ80	Proliferation-associated protein 2G4	PA2G4
P48147	Prolyl endopeptidase	PREP
O14744	Protein arginine N-methyltransferase 5	PRMT5
P30101	Protein disulfide-isomerase A3	PDIA3
P13667	Protein disulfide-isomerase A4	PDIA4
P07237	Protein disulfide-isomerase	P4HB
P55735	Protein SEC13 homolog	SEC13
O00764	Pyridoxal kinase	PDXK

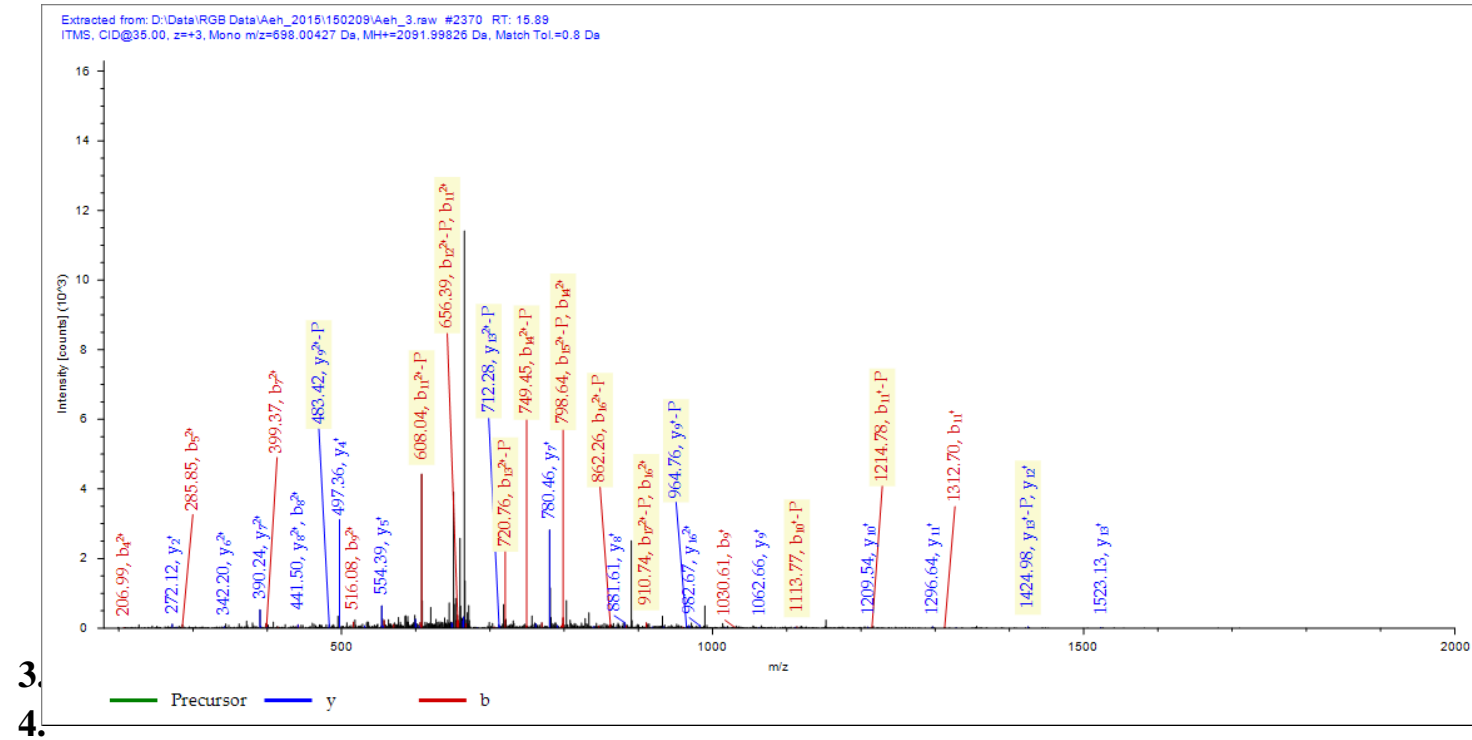
Accession numbers	Protein names	Gene Names
P50395	Rab GDP dissociation inhibitor beta	GDI2
P18754	Regulator of chromosome condensation	RCC1
Q14257	Reticulocalbin-2	RCN2
Q9H6T3	RNA polymerase II-associated protein 3	RPAP3
Q15019	Septin-2	SEPT2
P52788	Spermine synthase	SMS
Q15427	Splicing factor 3B subunit 4	SF3B4
Q14247	Src substrate cortactin	CTTN
P38646	Stress-70 protein	HSPA9
P55809	Succinyl-CoA:3-ketoacid coenzyme A transferase 1	OXCT1
P50990	T-complex protein 1 subunit theta	CCT8
Q86W42	THO complex subunit 6 homolog	THOC6
P26639	Threonine--tRNA ligase, cytoplasmic	TARS
P37837	Transaldolase	TALDO1
P29401	Transketolase	TKT
P07951	Tropomyosin beta chain	TPM2
Q9UHD9	Ubiquilin-2	UBQLN2
Q9BUA3	Uncharacterized protein C11orf84	C11orf84
Q6UXN9	WD repeat-containing protein 82	WDR82
P13010	X-ray repair cross-complementing protein 5	XRCC5
P12956	X-ray repair cross-complementing protein 6	XRCC6
P16989	Y-box-binding protein 3	YBX3

# Appendix I. The annotated spectra of the relevant peptides at the phosphorylation sites

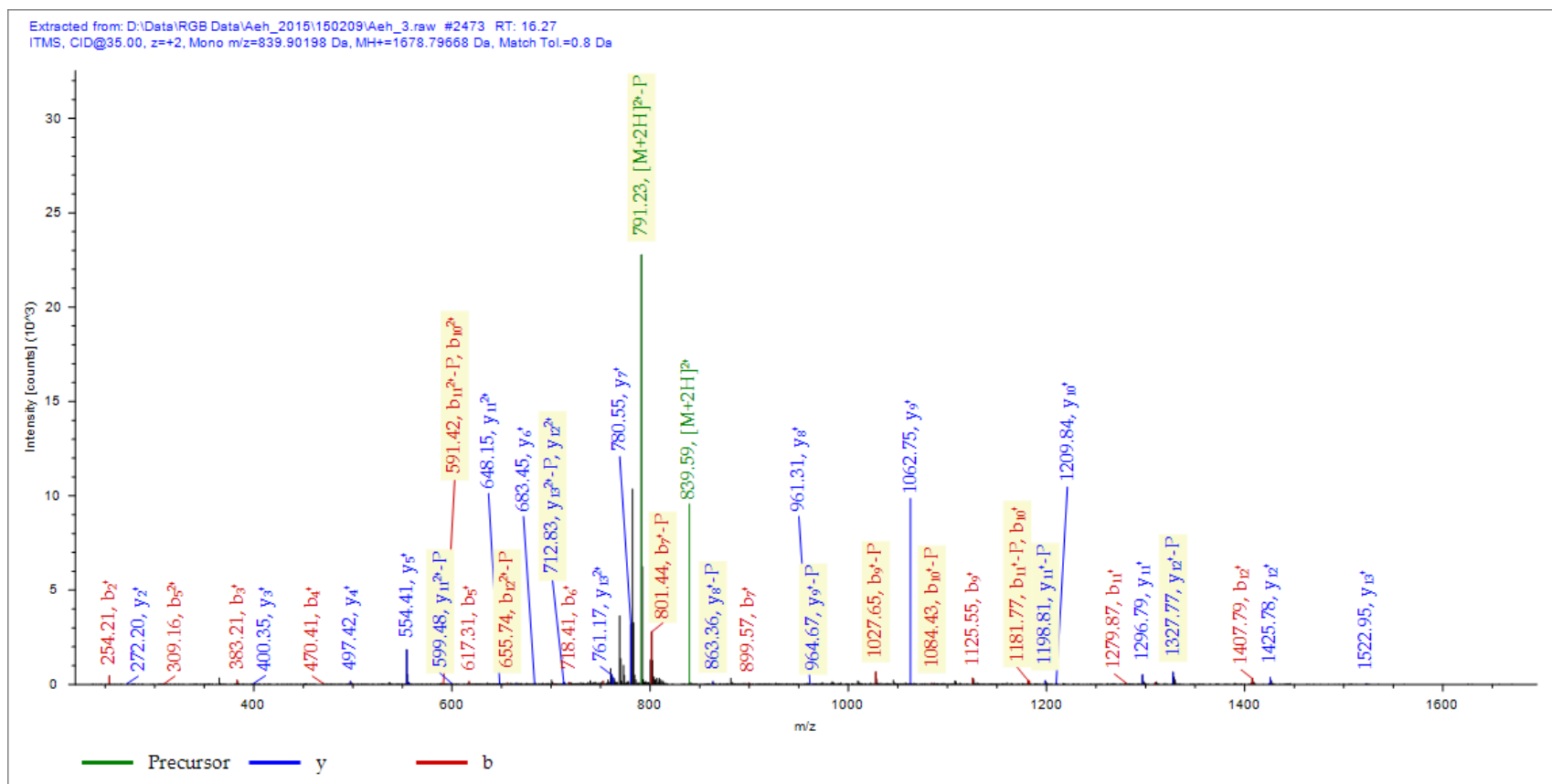
## 1. CDGDAsPPsPAR



## 2. GAERRPESFtTPEGPKPR

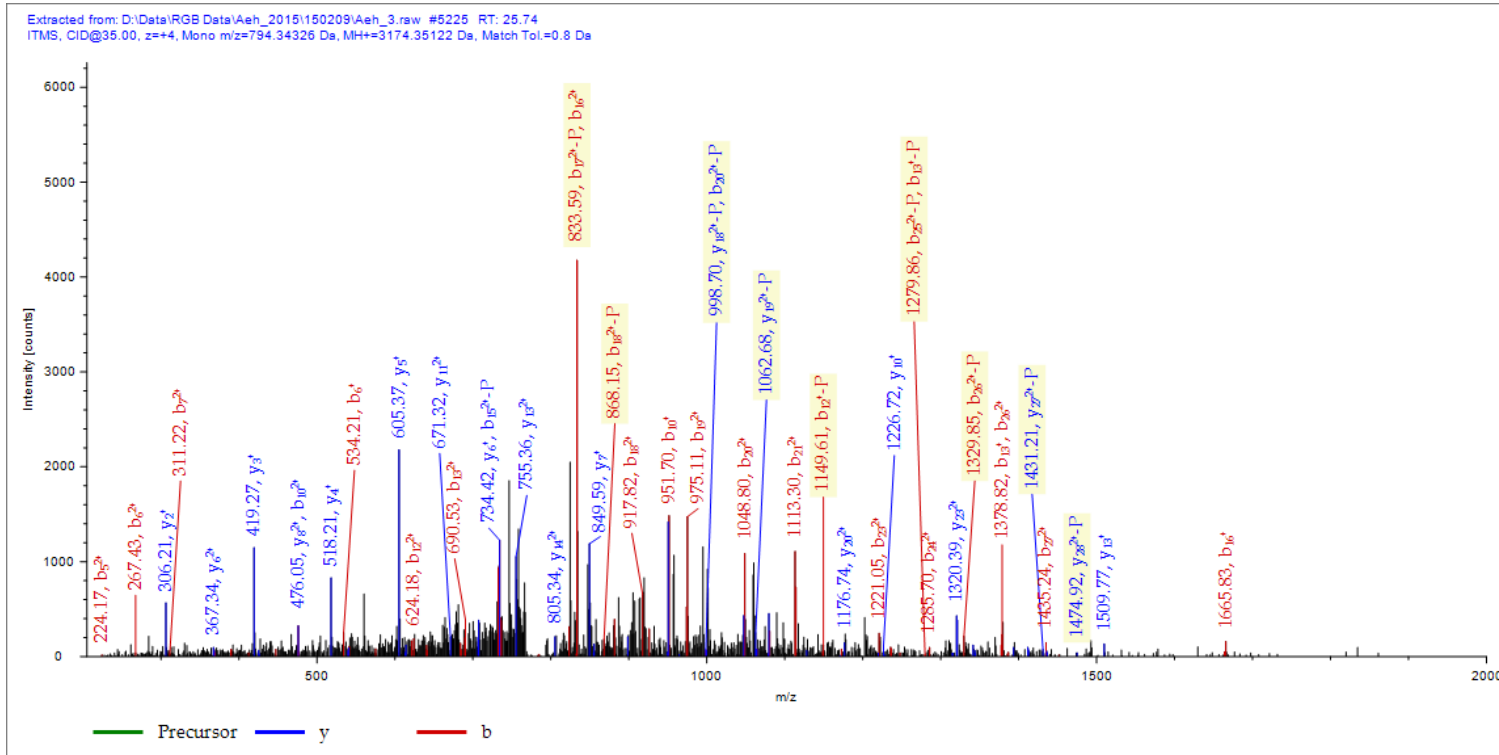


### 3. RPESFTtPEGPKPR

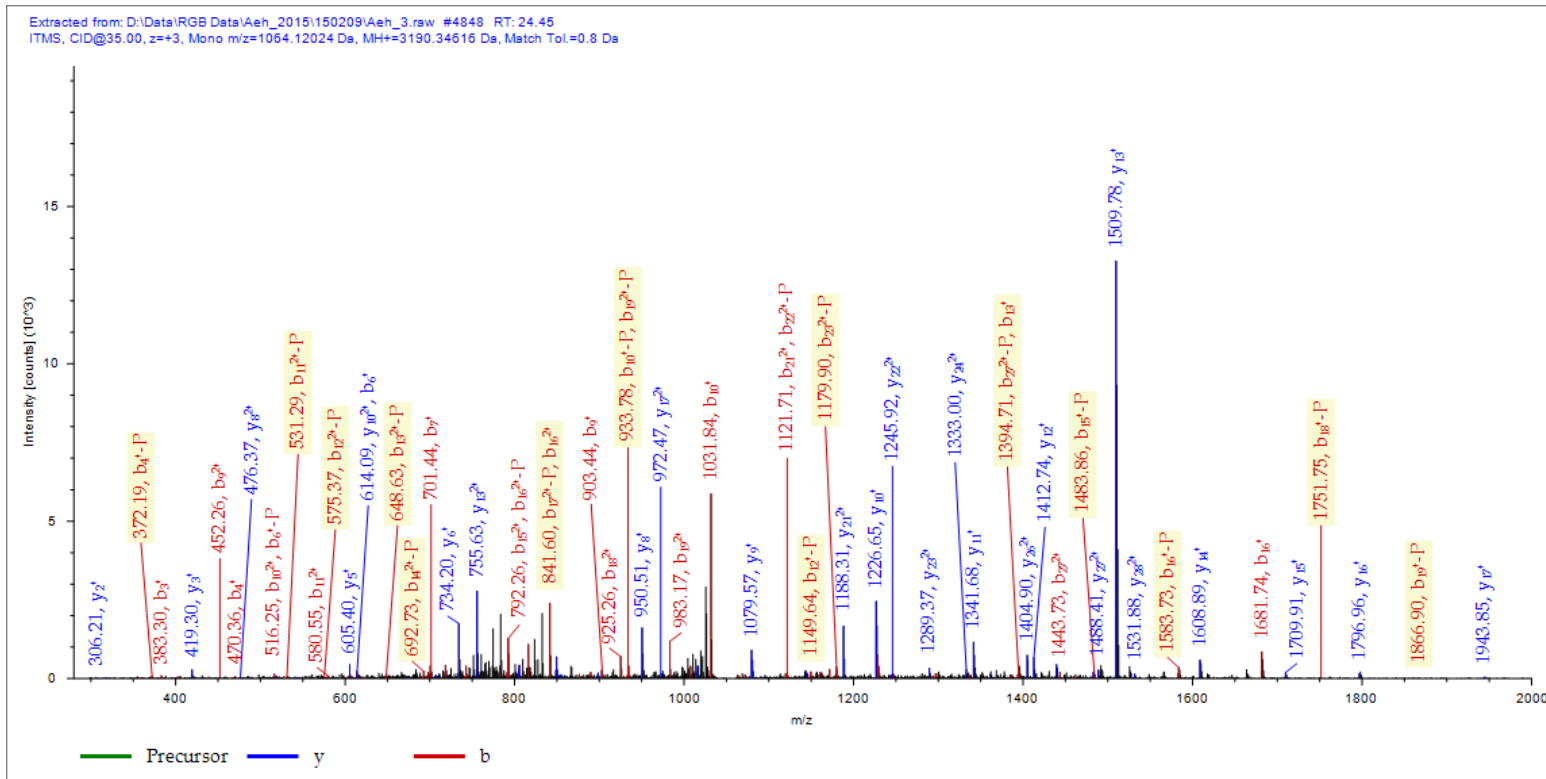


S

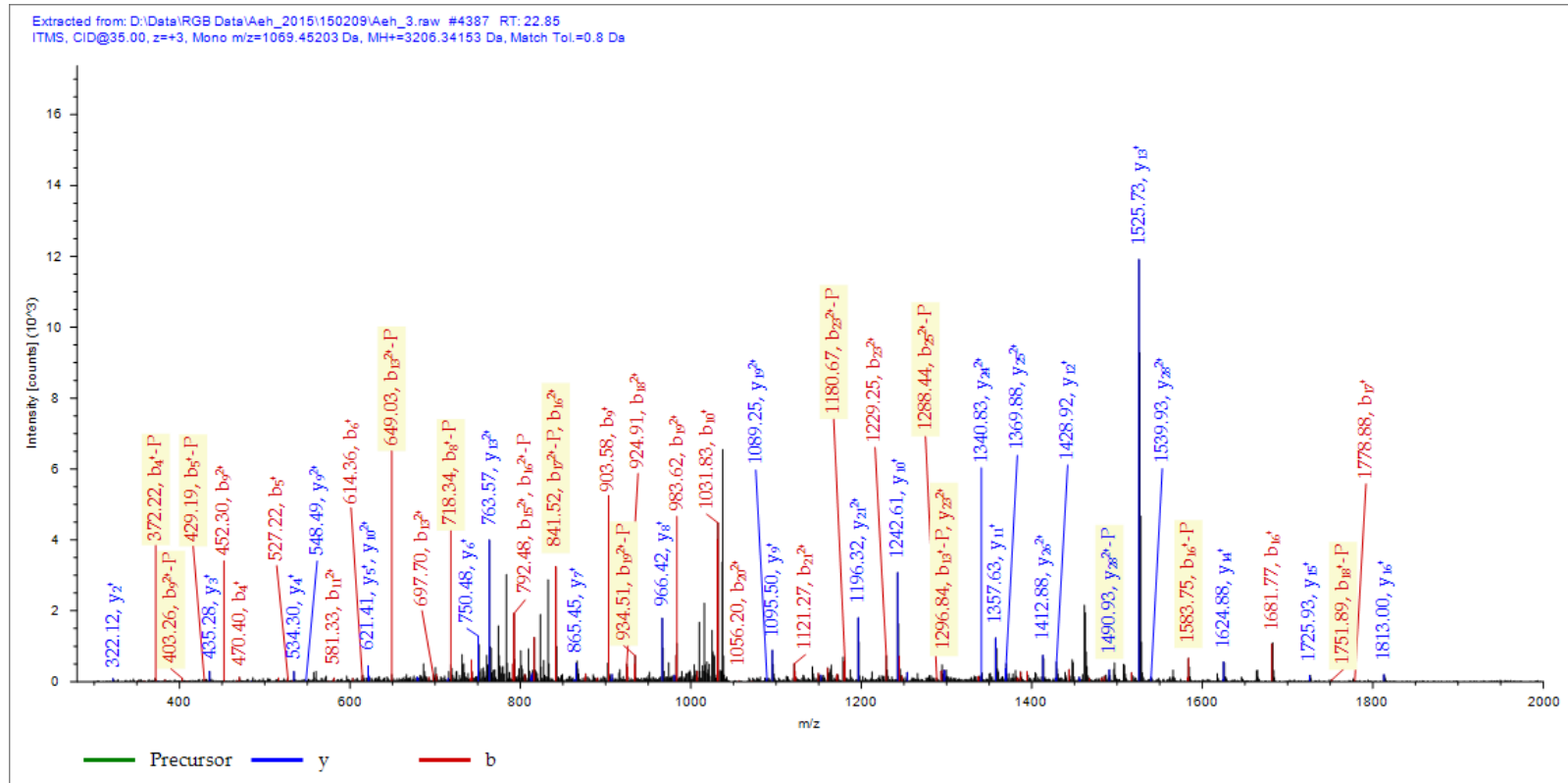
#### 4. DSKEsMSTVPADFETDESVMR



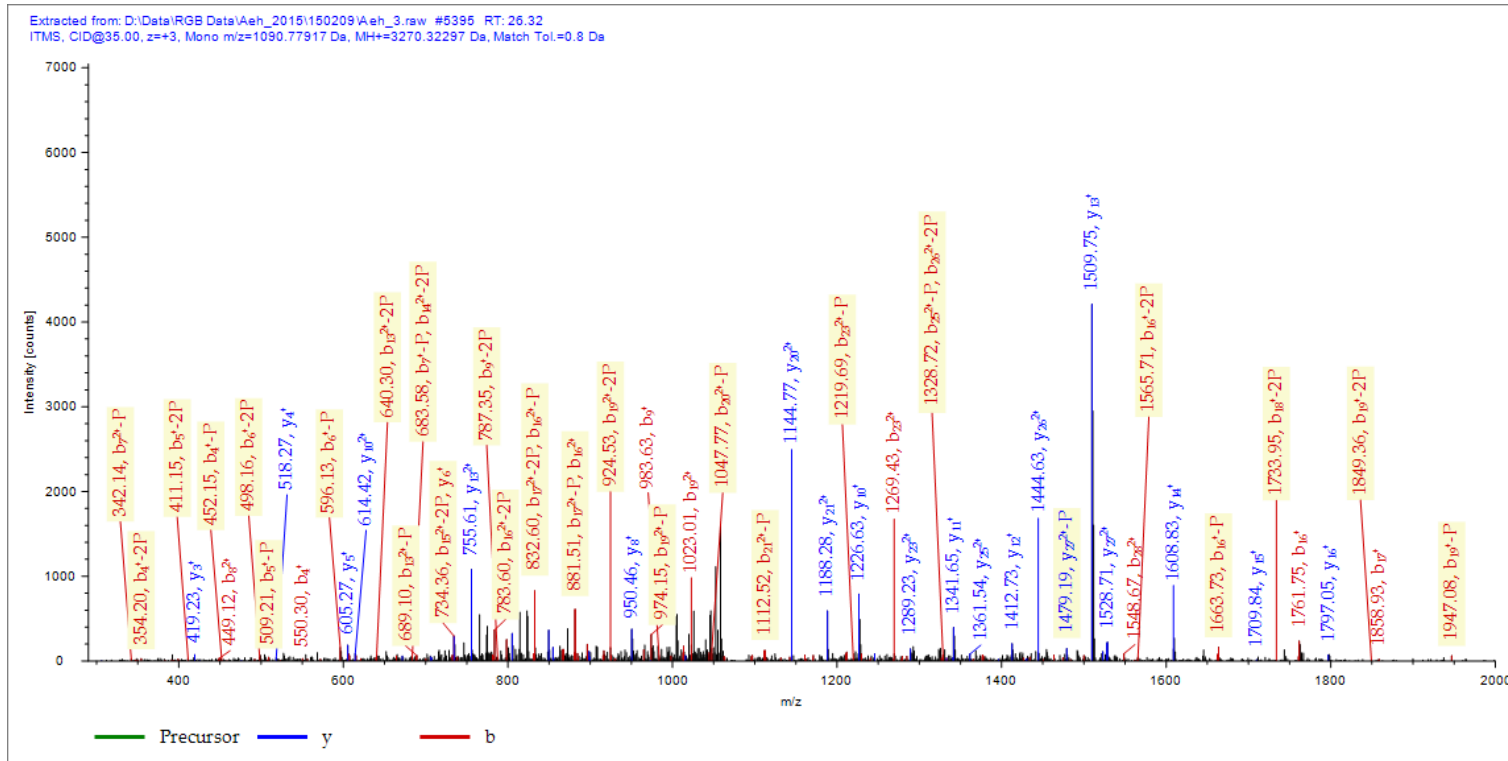
## 5. KSsSGSSDSKESmSTVPADFETDESVMR



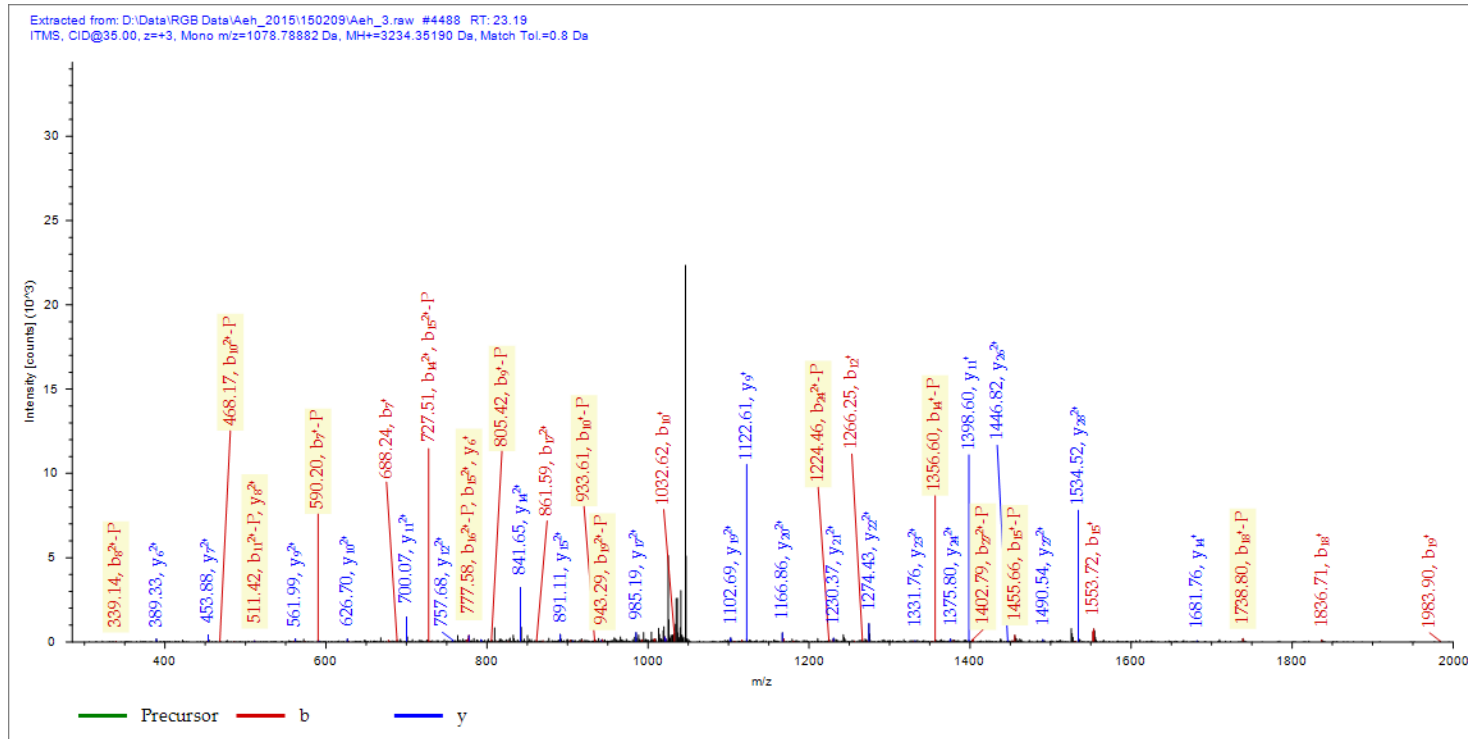
## 6. KsSSGSSDSKESmSTVPADFETDESVLmR



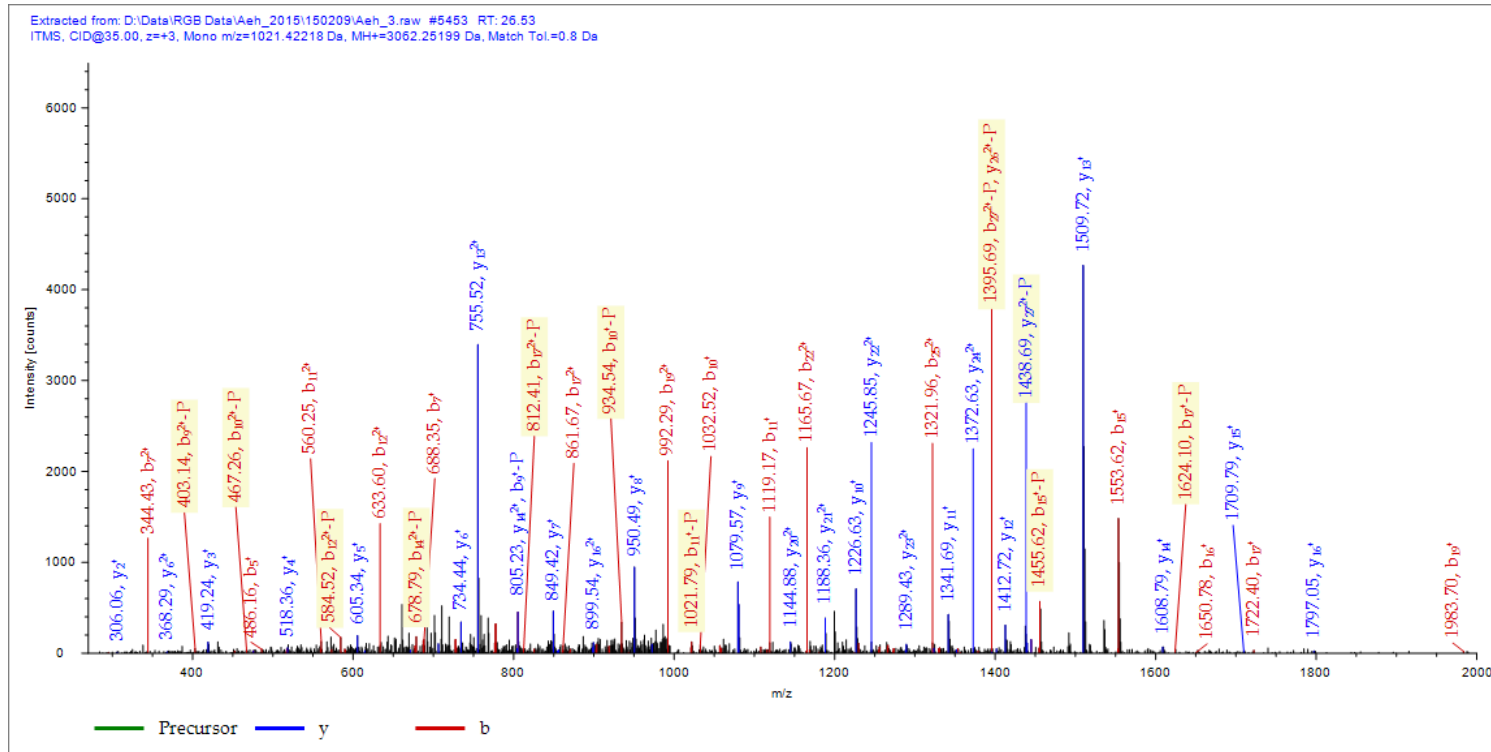
## 7. KSssGSSDSKESmSTVPADFETDESVMR



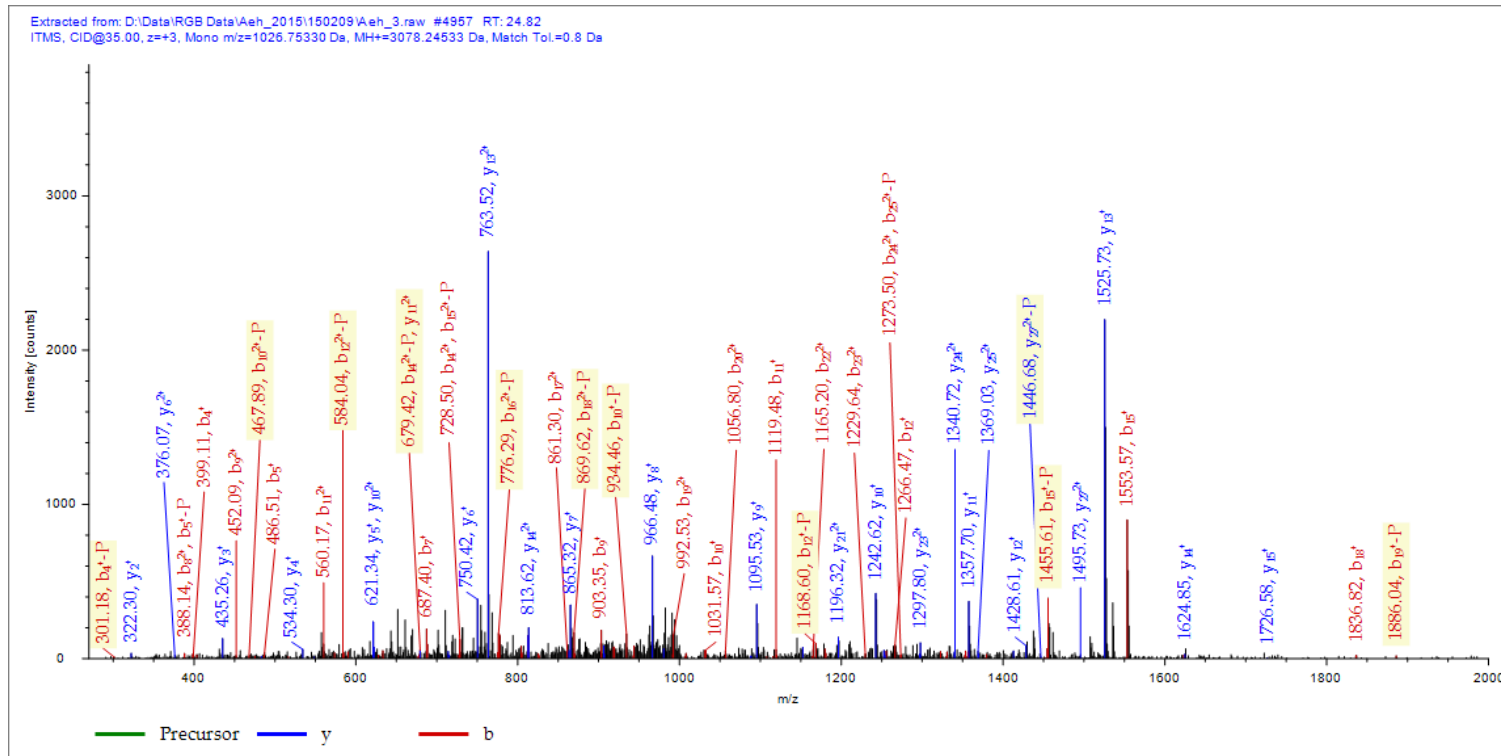
## 8. sSSGSSDSKESmSTVPADFETDESVLmRR



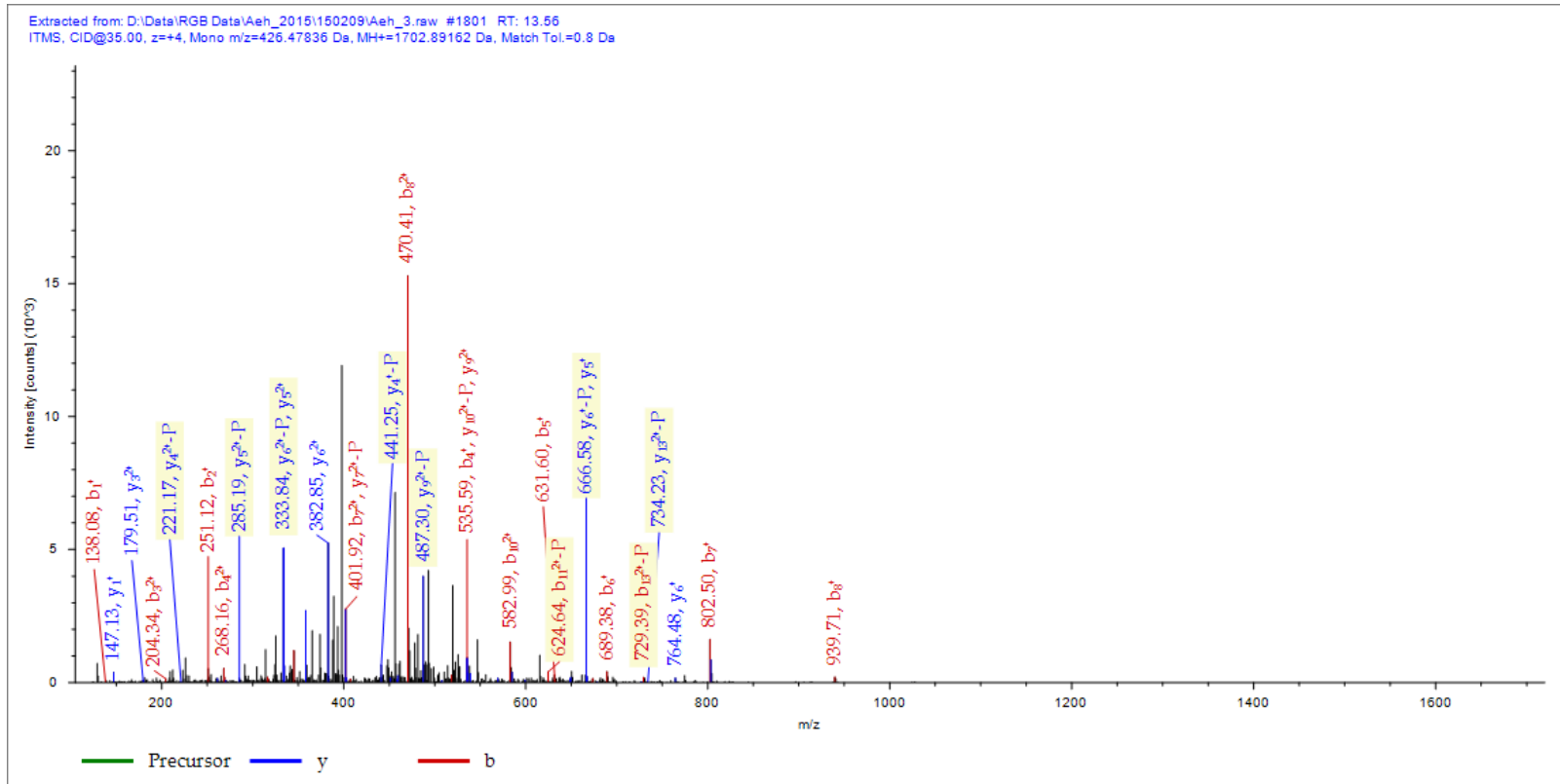
## 9. SSSG<sub>s</sub>SDSKES<sub>m</sub>STVPADFETDES<sub>V</sub>L<sub>m</sub>R



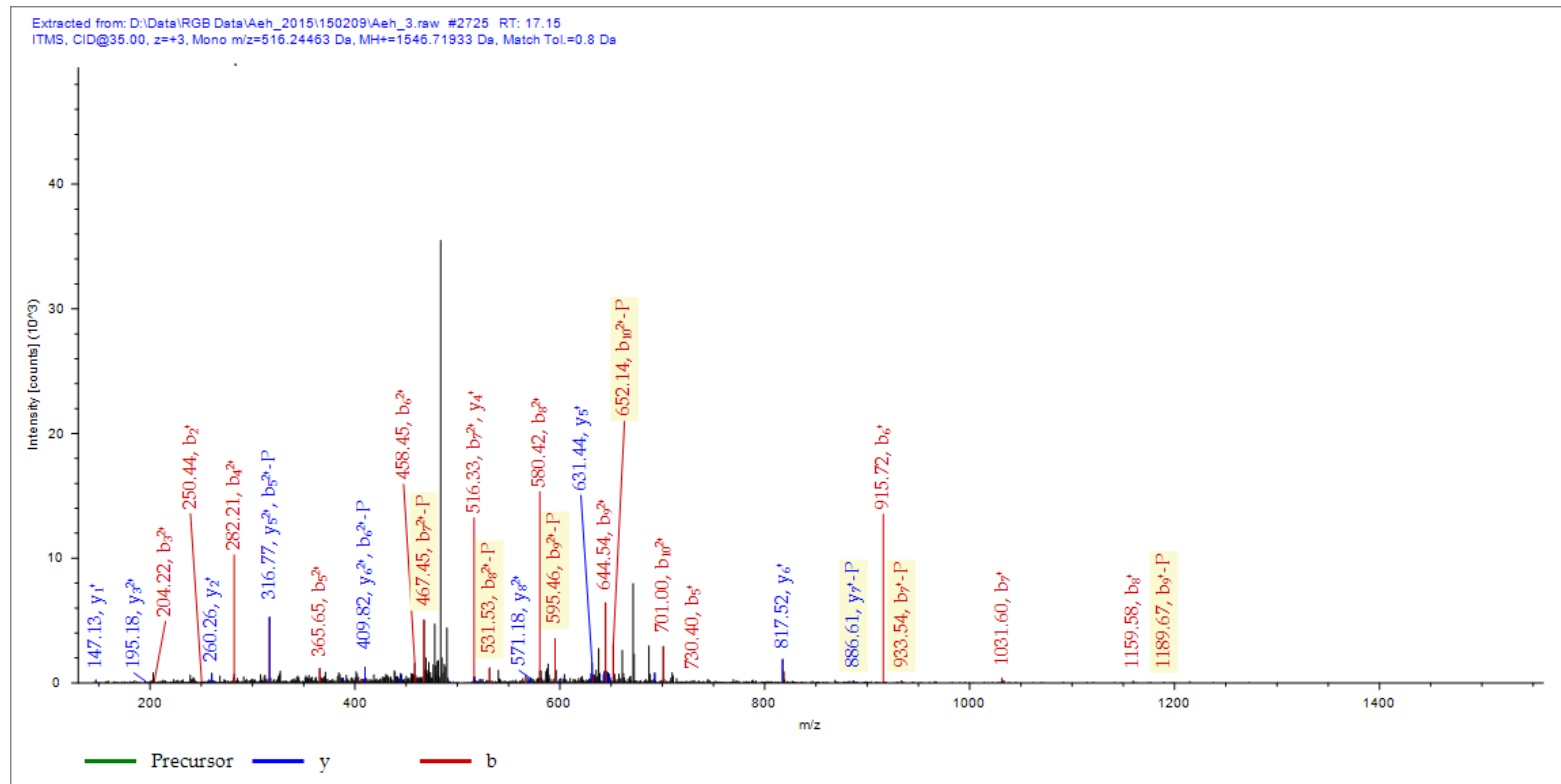
# 10.SsSGSSDSKESmSTVPADFETDESVMR



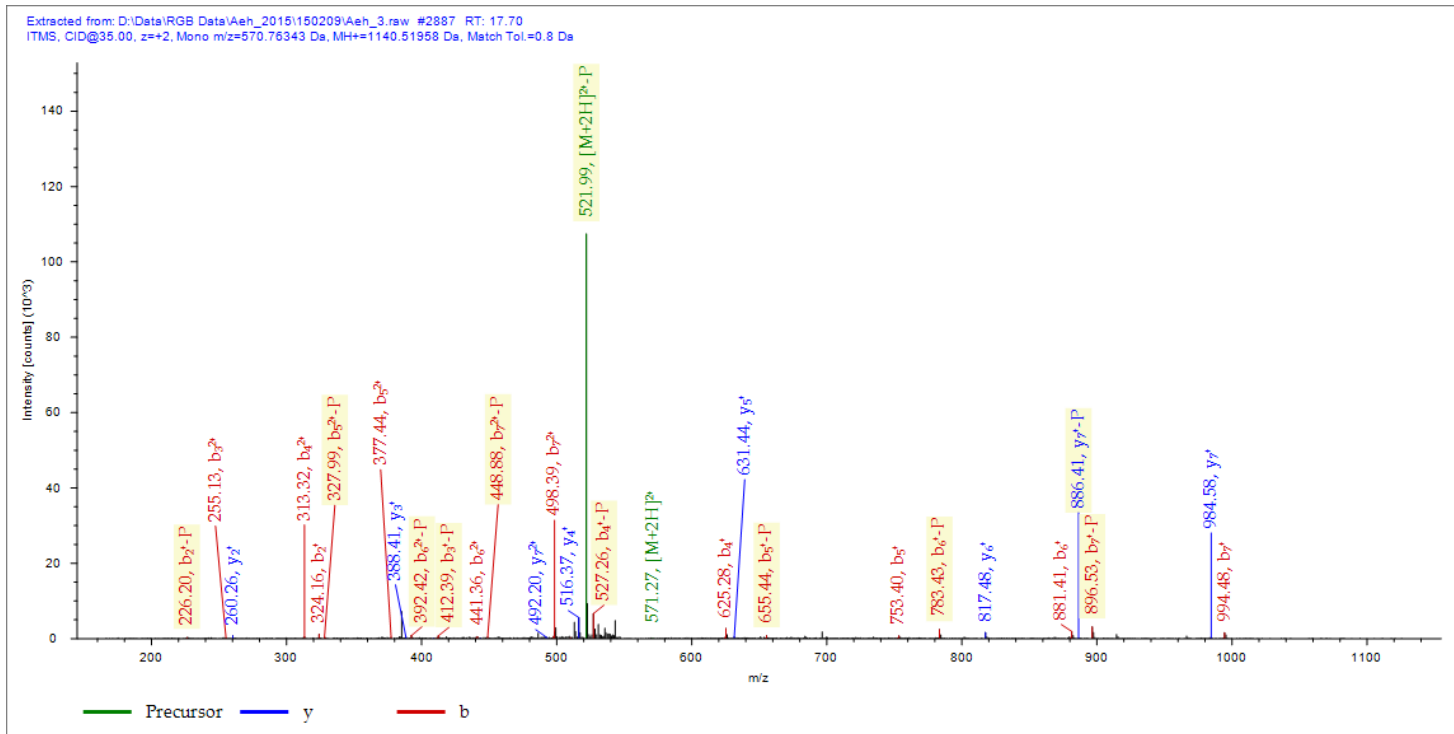
# 11.HLRQPGIHPKtPNK



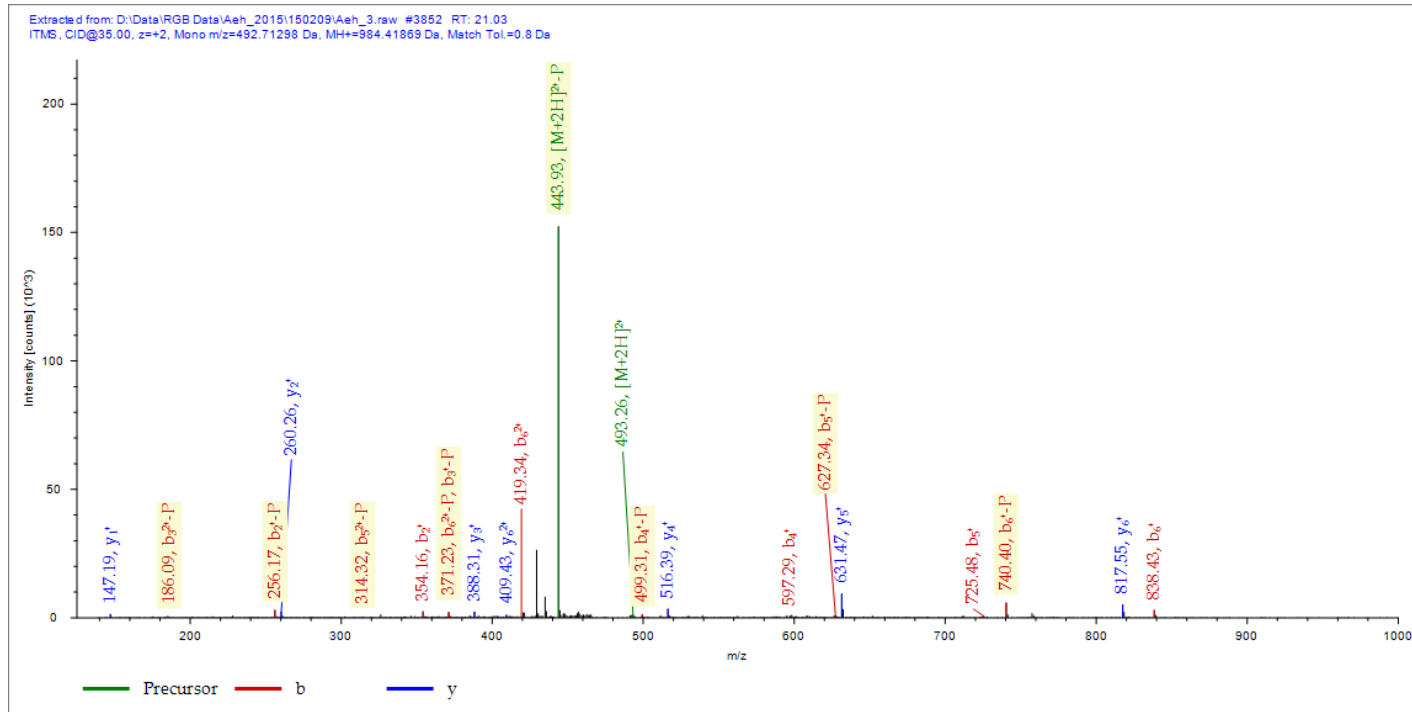
## 12.YSRRsWDQIQK



### 13.RsWDQIQK



# 14. sWDQIQK



**Appendix J.** Published SLBP-interacting protein in six databases

<b>Database name</b>	<b>Known SLBP interacting proteins</b>	<b>Found proteins on my study</b>
IntAct	ZNF473, CDK4, CDK6, TACC3, Desi1	CDK4, CDK6, TACC3
BioGRID	CDK4, CDK6, ERI1, GSTM3 HIST1H2BG, P4HA3, UPF1, ZFC3H1, XNF473	CDK4, CDK6, ERI1, GSTM3 HISTH2BG
HPRD	USP8, ZNF473, LSM10, ERI1	LSM10, ERI1
APID	MIF4GD	–
STRING	ERI1, ZNF473, LSM10, MIF4GD LSM11, SNRPB, EIF4E, SNRPG NASP, SNRPD3	ERI1, LSM10, LSM11, SNRPB EIF4E, SNRPG, NASP, SNRPD3
PIPs	EIF3S2, EIF3S4, EIF3S10	–

## Appendix K. List of categorised protein names by alphabetical order

**Table K1.** Proteins whose association with SLBP is unchanged following replication stress

ADAR	CSTF1	FAM120A	HIST1H2BK	H2BFS	MRPS9	RBBP7	RPL23	SF3A2	UPF3B
AFG3L2	C14orf166	FARSA	HIST1H2BL	IGF2BP3	MTA2	RBM4	RPL26	SLAIN2	USP39
AKAP8L	C17orf85	FAU	HIST1H2BM	IK	NCBP1	RBM4B	RPL27A	SLBP	U2AF2
AKT2	DDRGK1	FEN1	HIST1H2BN	JUNB	NCBP2	RBM6	RPL31	SLC25A13	VIM
ATP5C1	DDX1	FMR1	HIST1H4A	KCTD17	NELFE	RBM14	RPL35A	SLC25A24	WDR82
BUB3	DDX17	FRG1	HIST2H2AA3	KCTD2	NONO	RBM17	RPL36A	SMARCA5	WTAP
CALD1	DDX3X	FUBP3	HIST2H2AC	KHSRP	NOP56	RBM27	RPL36AL	SMN1	XRCC5
CDC5L	DDX3Y	FXR1	HIST2H2BF	KPNA2	NOP58	RBM39	RPN1	SMU1	XRCC6
CDKN2AIP	DDX5	GNL3	HNRNPH2	KPNA6	PA2G4	RBMX	RPP30	SNRNP70	XRN2
CD2BP2	DDX42	GSK3B	HNRNPA0	KRR1	PCID2	RBMXL1	RPS2	SNW1	YBX1
CHTOP	DDX50	G3BP1	HNRNPA1	LGALS3	PDLIM7	RCC2	RPS3	SRFBP1	YTHDF2
CKAP4	DHX15	HADHA	HNRNPA1L2	LMNB1	PFKFB3	RCL1	RPS3A	SRP14	ZBTB24
CMSS1	DKC1	HDAC1	HNRNPA3	LRRC47	PHAX	REST	RPS6	SRRT	ZC3HAV1
CNP	DPM1	HDAC2	HNRNPAB	LRRC59	PHF6	RFC3	RPS9	SRSF9	ZC3H11A
COPE	EIF4A1	HIST1H1B	HNRNPF	MAGED2	PHRF1	RFC4	RPS15A	SUGP1	ZNF622
CPSF7	EIF4A3	HIST1H2AD	HNRNPK	MAP7	POLDIP3	RFC5	RPS16	SYNCRIP	
CPT1A	EIF4E	HIST1H2AG	HNRNPL	MCM5	PRMT1	RPL6	RPS18	TAMM41	
CSDE1	ELMO2	HIST1H2AH	HNRNPM	MOGS	PRPF31	RPL7	RPS20	THOC2	
CSNK1A1	EMD	HIST1H2AJ	HNRNPR	MRPL3	PRPF38B	RPL11	RPS25	TOMM34	
CSNK2A1	ERLIN1	HIST1H2BC	HNRNPUL2	MRPS22	PSMD4	RPL17	RTCB	TMPO	
CSNK2A2	EXOSC7	HIST1H2BD	H1FX	MRPS27	PTBP1	RPL19	SCCPDH	TRUB2	
CSNK2A3	FAM98B	HIST1H2BH	H2AFJ	MRPS34	QPCTL	RPL22	SF1	UPF2	

**Table K2.** Proteins whose association with SLBP decreases following replication stress

ABCF1	EIF2S2	IKBIP	PTRF	TIMM44
ACTL6A	EIF2S3	ILF2	RPL10A	TOP1
ASPH	EIF2S3L	ILF3	RPL23A	UPF1
ATAD3A	EIF3E	KCTD5	RPL27	YBX3
ATXN2L	EIF3S3	KHDRBS1	RPL3	ZC3H15
BMS1	EIF4A2	LARP4	RPL30	ZC3H18
CAPRIN1	EIF4G1	MAP4	RPL36	
CKAP5	EIF5B	MTDH	RPL4	
CMBL	EXOSC2	MYBBP1A	RPL8	
DDX21	EXOSC4	NAT10	RRBP1	
DDX47	EXOSC6	NCL	RSL1D1	
DDX6	FTSJ3	NOP14	SERBP1	
DHX30	G3BP2	NOP2	SMARCE1	
DHX36	GEMIN5	NSUN2	SRP68	
DHX9	GLTSCR2	NUFIP2	SRP72	
DNAJA3	GLYR1	ODR4	SRPK1	
DRG1	GRSF1	PARP1	SSRP1	
EBNA1BP2	GTPBP4	PBRM1	STOM	
EIF2S1	HDLBP	PRPF19	TBL2	